

# Sarcomeric modifiers of hypertrophy in hypertrophic cardiomyopathy (HCM)

by

Liezl Margaretha Bloem

*Dissertation presented for the degree of Doctor of Philosophy in Medical Sciences  
(Medical Biochemistry) in the Faculty of Medicine and Health Sciences  
At Stellenbosch University*



Promoter: Prof JC Moolman-Smook  
Co-promoter: Prof L van der Merwe

March 2013

## **DECLARATION**

By submitting this thesis/dissertation electronically, I declare that the entirety of the work contained therein is my own, original work, that I am the sole author thereof (save to the extent explicitly otherwise stated), that reproduction and publication thereof by Stellenbosch University will not infringe any third party rights and that I have not previously in its entirety or in part submitted it for obtaining any qualification.

March 2013

Copyright © 2013 Stellenbosch University

All rights reserved

*To my parents*

## ABSTRACT

Left ventricular hypertrophy (LVH) is an independent predictor of cardiovascular morbidity and all-cause mortality. Significantly, it is considered a modifiable cardiovascular risk factor as its regression increases overall survival and reduces the frequency of adverse cardiac events. A clear understanding of LVH pathogenesis is thus imperative to facilitate improved risk stratification and therapeutic intervention.

Hypertrophic cardiomyopathy (HCM), an inherited cardiac disorder, is a model disease for elucidating the molecular mechanisms underlying LVH development. LVH, in the absence of increased external loading conditions, is its quintessential clinical feature, resulting from mutations in genes encoding sarcomeric proteins. The LVH phenotype in HCM exhibits marked variability even amongst family members who carry the same disease-causing mutation. Phenotypic expression is thus determined by the causal mutation and additional determinants including the environment, epigenetics and modifier genes.

Thus far, factors investigated as potential hypertrophy modifiers in HCM have been relatively removed from the primary stimulus for LVH; and the few studies that have been replicated yielded inconsistent results. We hypothesized that the factors that closely interact with the primary stimulus of faulty sarcomeric functioning, have a greater capacity to modulate it, and ultimately the LVH phenotype in HCM. Plausible candidate modifiers would include factors relating to the structure or function of the sarcomere, including known HCM-causal genes; and the enzymes that function in sarcomere-based energetics. Indeed, the literature highlights the relevance of sarcomeric proteins,  $Ca^{2+}$ -handling and myocardial energetics in the development of LVH in HCM.

This study, therefore, set out to evaluate the hypertrophy-modifying capacity of such factors by means of family-based genetic association testing in 27 South African HCM families in which one of three unique HCM-causing founder mutations segregates. Moreover, the single and combined effects of 76 variants within 26 candidate genes encoding sarcomeric or sarcomere-associated proteins were investigated.

The study identified a modifying role in the development of hypertrophy in HCM for each of the candidate genes investigated with the exception of the metabolic protein-encoding gene, *PRKAG1*. More specifically, single variant association analyses identified a modifying role for variants within

the genes *MYH7*, *TPM1* and *MYL2*, which encode proteins of the sarcomere, as well as the genes *CPT1B*, *CKM*, *ALDOA* and *PRKAB2*, which encode metabolic proteins. Haplotype-based association analyses identified combined modifying effects for variants within the genes *ACTC*, *TPM1*, *MYL2*, *MYL3* and *MYBPC3*, which encode proteins of the sarcomere, as well as the genes *CD36*, *PDK4*, *CKM*, *PFKM*, *PPARA*, *PPARG*, *PGC1A*, *PRKAA2*, *PRKAG2* and *PRKAG3*, which encode metabolic proteins. Moreover, a number of variants and haplotypes showed statistically significant differences in effect amongst the three HCM founder mutation groups.

The HCM-modifier genes identified were prioritised for future studies according to the number of significant results obtained for the four tests of association performed. The genes *TPM1* and *MYBPC3*, which encode sarcomeric proteins, as well as the genes *PFKM* and *PRKAG2*, which encode metabolic proteins, were identified as stronger candidates for future studies as they delivered multiple significant results for various statistical tests.

This study makes a novel contribution to the field of hypertrophy research as it tested the hypothesis that structural or energy-related factors located within the sarcomere may act as modifiers of cardiac hypertrophy in HCM, and succeeded in identifying a modifying role for many of the candidate genes selected. The significant results include substantial single and within-gene-context variant effects; and identified sizeable variation in the risk of developing LVH owing to the compound effect of the modifier and the individual founder mutations. Collectively, these findings enhance the current understanding of genotype/phenotype correlations and may, as consequence, improve patient risk stratification and choice of treatment. Moreover, these findings emphasize the potential for modulation of disease by further elucidation of some of the avenues identified.

## OPSOMMING

Linker ventrikulêre hipertrofie (LVH) is 'n onafhanklike voorspeller van kardiovaskulêre morbiditeit en van mortaliteit weens alle oorsake. Van belang is dat dit 'n wysigbare kardiovaskulêre risiko faktor is, aangesien die afname daarvan algehele oorlewing verhoog en die frekwensie van nadelige kardiaale voorvalle verlaag. 'n Duidelike begrip van LVH patogeneese is dus noodsaaklik om verbeterde risiko stratifikasie en terapeutiese intervensie te fasiliteer.

Hipertrofiese kardiomiopatie (HKM), 'n oorerflike hart-siekte, is 'n model-siekte vir die uitpluis van die molekulêre meganismes onderliggend aan die ontwikkeling van LVH. LVH, in die afwesigheid van verhoogde eksterne lading, is die kern kliniese simptome van HKM en die gevolg van mutasies in die gene wat kodeer vir sarkomeriese proteïene. Die LVH fenotipe in HKM toon merkbare veranderlikheid selfs in familie-lede wat dieselfde siekte-veroorsakende mutasie dra. Die fenotipe word dus bepaal deur die siekte-veroorsakende mutasie asook addisionele determinante insluitend die omgewing, epigenetika en modifierende gene.

Potensiële hipertrofie-modifiseerders wat tot dusver bestudeer is, is betreklik verwyder van die primêre stimulus vir LVH en die paar studies wat gerepliseer is, het teenstrydige resultate gelewer. Ons hipoteseer dat die faktore wat in noue interaksie met die primêre stimulus van foutiewe sarkomeriese funksionering is, 'n groter kapasiteit het om dit en uiteindelik die LVH fenotipe in HKM, te moduleer. Aanneemlike kandidaat-modifiseerders sou insluit faktore wat betrekking het tot die struktuur en funksie van die sarkomeer insluitend HKM-oorsaaklike gene en die ensieme wat funksioneer in sarkomeer-gebaseerde energetika. Die literatuur beklemtoon inderdaad die relevansie van sarkomeriese proteïene,  $Ca^{2+}$ -hantering en miokardiese energetika in die ontwikkeling van LVM in HKM.

Hierdie studie het beoog om die hipertrofie-modifierende kapasiteit van sulke faktore te evalueer deur middel van familie-gebaseerde genetiese assosiasie toetse in 27 Suid-Afrikaanse HKM families waarin een van drie unieke HKM-stigter mutasies segregeer. Verder was die enkel en gekombineerde effekte van 76 variante binne 26 kandidaat gene wat kodeer vir sarkomeer en sarkomeer-geassosieerde proteïene, ondersoek.

Hierdie studie het 'n modifierende rol in die ontwikkeling van hipertrofie in HKM geïdentifiseer vir elk van die kandidaat gene wat ondersoek is, met uitsluiting van die *PRKAG1*, wat kodeer vir 'n

metaboliese proteïene. Meer spesifiek, enkel variant assosiasie analyses het 'n modifiserende rol geïdentifiseer vir variante in die gene *MYH7*, *TPM1* en *MYL2*, wat kodeer vir sarkomeriese proteïene, asook die gene *CPT1B*, *CKM*, *ALDOA* en *PRKAB2*, wat kodeer vir metabolise proteïene. Haplotype-gebaseerde assosiasie-analises het gekombineerde modifiserende effekte geïdentifiseer vir variante in die gene *ACTC*, *TPM1*, *MYL2*, *MYL3* en *MYBPC3*, wat kodeer vir strukturele proteïene van die sarkomeer asook die gene *CD36*, *PDK4*, *CKM*, *PFKM*, *PPARA*, *PPARG*, *PGC1A*, *PRKAA2*, *PRKAG2* en *PRKAG3*, wat kodeer vir metabolise proteïene. Verder het 'n aantal variante en haplotipes statisties betekenisvolle verskille in effek tussen die drie HKM-stigter mutasie groepe getoon.

Die HKM-modifiserende gene wat geïdentifiseer is, is verder geprioritiseer vir toekomstige studies volgens die aantal beduidende resultate wat vir die vier assosiasie toetse verkry is. Die gene *TPM1* and *MYBPC3*, wat kodeer vir sarkomeriese proteïene, asook die gene *PFKM* and *PRKAG2*, wat kodeer vir metaboliese proteïene, is geïdentifiseer as sterker kandidate vir verdere studies omdat veelvuldige beduidende resultate vir die verskeie statistiese toetse deur hulle gelewer is.

Hierdie studie maak 'n nuwe bydrae tot die veld van hipertrofie navorsing omdat dit die hipotese dat strukturele en energie-verwante faktore, wat binne die sarkomeer geposisioneer is, potensieel as modifiseerders van kardiaal hipertrofie in HKM kan optree, ondersoek het. Dit slaag ook daarin om 'n modifiserende rol vir baie van die geselekteerde kandidaatgene te identifiseer. Die beduidende resultate sluit in aansienlike enkel en binne-geen-konteks variant-effekte en aansienlike variasie in die risiko vir LVH ontwikkeling verskuldig aan die gekombineerde effek van modifiseerder en individuele stigter mutasies. Gesamentlik verbeter hierdie bevindinge die huidige begrip van genotipe/fenotipe korrelasies en dit mag tot gevolg hê verbeterde pasiënt risiko stratifikasie en keuse van behandeling. Verder beklemtoon hierdie bevindinge die potensiaal vir siekte modulering deur verdere uitpluis van sekere van hierdie geïdentifiseerde navorsingsrigtings.

## ACKNOWLEDGEMENTS

I would like to express my sincerest gratitude to the following institutions and individuals:

The **HCM families**, for their participation in the project.

The **Department of Biomedical Sciences, University of Stellenbosch** for providing the opportunity and infrastructure required to complete this study.

The **National Research Foundation, Prof Paul van Helden**, and the **University of Stellenbosch** for financial support.

My promoter **Prof Hanlie Moolman-Smook**. Thank you for giving me the opportunity to embark on this PhD journey and for your guidance and patience throughout my study. The experience has afforded me not only great scientific knowledge but invaluable life lessons.

My co-promoter **Prof Lize van der Merwe**. Thank you for your invaluable contribution to both the statistical component and write up of the study. Also, thank you for sharing your unique sense of humour.

**Dr Craig Kinnear**, for being both a friend and excellent scientist always generously sharing your knowledge and expertise.

**Mrs Lundi Korkie**, for literally tending to wounds, sharing wise words and providing technical support.

**Prof Valerie Corfield**, for emphasizing the importance of confident communication and a holistic approach to science.

**Ms Glenda Durrheim**, for your support and assistance with the language aspects of my thesis.

**Ms Ina le Roux**, for your support and technical assistance.

**Dr Nadia Carstens**, for your friendship and patiently repeating the statistical explanations.

**Ms Martmari Botha and Hannique Human**. Thank you for holding my hand...

**Dr Carmen Swanepoel**. The first friend I made at university many years ago and still a much cherished friend today. Thank you for always listening.

My lab neighbours **Dr Moredreck Chibi** and **Ms Candice Honing** for your support and stimulating, humorous conversation.

**My MAGIC lab friends**. From lab winter games to wine clubs, thank you for making the working environment a very special.

**Karen and Fano**, for always reminding me of the bigger picture and encouraging me to believe in myself.

**Amanda and Pieter**. Thank you for supporting me on all possible levels at a time when I needed it most. You are exemplary role models both professionally and personally.

**Charl**. Thank you for motivating me over the final goal post and sharing with me special people and places. Most importantly, thank you for encouraging me to live fearlessly.

Finally, to my dear parents **Eric and Beulah Bloem**. Attaining my PhD is a very special accomplishment which was made possible by your dedication to my education. Thank you for all the sacrifices you have made.



## TABLE OF CONTENTS

LIST OF ABBREVIATIONS.....	x
LIST OF FIGURES.....	xx
LIST OF TABLES.....	xxvi
CHAPTER 1.....	1
CHAPTER 2.....	28
CHAPTER 3.....	69
CHAPTER 4.....	172
THESIS REFERENCES.....	221
APPENDIX I.....	252

**LIST OF ABBREVIATIONS**

%	Percentage
(w/v)	Weight/volume
*	Stop codon
$\Delta$	Deletion
$\Delta G_{\sim\text{ATP}}$	Free energy of ATP hydrolysis
$^{\circ}\text{C}$	Degrees Celsius
2D	Two dimensional
3' UTR	3' untranslated region
3D	Three dimensional
$-\log_{10}$	Negative logarithm base 10
$\alpha$	Alpha
$\beta$	Beta
$\gamma$	Gamma
$\mu\text{l}$	Microlitre
A (Ala)	Alanine
A (nucleotide)	Adenine
ABI	Applied biosystems incorporated
ACC	Acetyl-CoA carboxylase
<i>ACE</i>	Angiotensin-converting enzyme gene
<i>ACTC1</i>	$\alpha$ -cardiac actin gene
<i>ACTN2</i>	$\alpha$ -actinin 2 gene
<i>ACTN3</i>	$\alpha$ -actinin 3 gene
ADP	Adenosine diphosphate
<i>AGL</i>	Amylo-1,6-glucosidase gene
aIVS	Anterior interventricular septum
aIVSmit	Anterior interventricular septum thickness at the mitral valve
aIVSpap	Anterior interventricular septum thickness at the papillary level
<i>AKT1</i>	RAC-alpha serine/threonine-protein kinase gene
<i>ALDOA</i>	Aldolase A, fructose-bisphosphate gene
AMP	Adenosine monophosphate
AMPK	AMP-activated protein kinase
ANKRD1	Cardiac ankyrin repeat protein

ATP	Adenosine triphosphate
AV	Aortic valve
AW	Anterior wall
AWapx	Anterior wall thickness at the supra-apex level
AWmit	Anterior wall thickness at the mitral valve
AWpap	Anterior wall thickness at the papillary level
BB-CK	Brain-type creatine kinase
bp	Base pairs
BP	Blood pressure
bpm	Beats per minute
<i>BRAF1</i>	V-RAF murine sarcoma viral oncogen homolog B1 gene
BSA	Body surface area
C (Cys)	Cysteine
C (nucleotide)	Cytosine
Ca <sup>2+</sup>	Calcium
CBM	Carbohydrate-binding molecule
CBS	Cystathionine $\beta$ -synthase motifs
<i>CD36</i>	CD36 antigen (FAT) gene
CEPH	Centre d'Etude du Polymorphisme Humain
CEU	Utah residents with ancestry from northern and western Europe
CFC	Cardiofaciocutaneous
CHB	Han Chinese in Beijing
CHD	Coronary heart disease
CJD	Creutzfeldt-Jakob disease
CK	Creatine kinase
<i>CKB</i>	Creatine kinase, brain gene
<i>CKM</i>	Creatine kinase, muscle gene
cM	Centi-Morgans
cMRI	Cardiac magnetic resonance imaging
c-MyBP-C	Cardiac myosin-binding protein-C
CO <sub>2</sub>	Carbon dioxide
CPT1	Carnitine palmitoyl transferase I
<i>CPT1B</i>	Carnitine palmitoyl transferase 1B, muscle gene
CPT2	Carnitine palmitoyl transferase II

Cr	Creatine
<i>CSRP3</i>	Muscle LIM protein gene
cTNT	Cardiac troponin T
CWT	Cumulative wall thickness
D (Asp)	Aspartic acid
D'	Normalised disequilibrium coefficient
DBP	Diastolic BP
DCM	Dilated cardiomyopathy
del	Deletion
DHAP	Dihydroxyacetone phosphate
DNA	Deoxyribonucleic acid
<i>DTNA</i>	$\alpha$ -dystrobrevin gene
dup	Duplication
E (Glu)	Glutamic acid
EDTA	Ethylene-diamine-tetra-acetic acid
eEF2	Eukaryote elongation factor-2
ELC	Essential myosin light chain
F (Phe)	Phenylalanine
FA	Fatty acid
FAD	Flavin adenine dinucleotide
FAO	Fatty acid oxidation
FAT/CD36	Fatty acid translocase transmembrane protein
FBPase	Fructose 1,6-bisphosphatase
FFI	Fatal familial insomnia
<i>FXN</i>	Frataxin gene
G (Gly)	Glycine
G (nucleotide)	Guanine
g	Gram
G3P	Glyceraldehyde 3-phosphate
<i>GAA</i>	Glucosidase alpha acid gene
<i>GLA</i>	$\alpha$ -galactosidase A gene
GLUT1	Glucose transporter family members 1

GLUT4	Glucose transporter family members 4
GSD	Glycogen storage disease
GSDVII	Type VII GSD
H (His)	Histidine
H <sup>+</sup>	Hydrogen
HCM	Hypertrophic cardiomyopathy
<i>hdp</i> <sup>2</sup>	<i>Held-up</i> <sup>2</sup>
HF	Heart failure
Hg	Mercury
HOPE	Heart Outcomes Prevention Evaluation
HR	Heart rate
HWE	Hardy-Weinberg Equilibrium
Hz	Hertz
I (Ile)	Isoleucine
I/D	Insertion/deletion
IBD	Identical by descent
IL-1 $\beta$	Interleukin-1 $\beta$
IMM	Inner mitochondrial membrane
IVS (IVS32del25nt)	Intronic variant sequence
IVS	Interventricular septum
IVSapx	Interventricular septum thickness at the supra-apex level
IW	Inferior wall
IWmit	Inferior wall thickness at the mitral valve
IWpap	Inferior wall thickness at the papillary level
<i>JPH2</i>	Junctophilin-2 gene
JPT	Japanese in Tokyo
K (Lys)	Lysine
K <sup>+</sup>	Potassium
kb	Kilobases
<i>KRAS2</i>	Kirsten rat sarcoma viral oncogen homolog gene

L (Leu)	Leucine
LA	Left atrium
LACS	Long chain acyl-CoA synthetase
<i>LAMP2</i>	Lysosome-associated membrane protein 2 gene
<i>LBD3</i>	LIM binding domain 3 gene
LCFA	Long chain fatty acid
LCFA-CoA	LCFA-coenzyme A
LD	Linkage disequilibrium
LDU	Linkage disequilibrium unit
Leopard	Mnemonic for syndrome with clinical characteristics of lentigines, electrocardiographic conduction abnormalities, ocular hypertelorism, pulmonary hypertension, abnormal genitalia, retarded growth, deafness
LPL	lipoprotein lipase
LV	Left ventricle
LVH	Left ventricular hypertrophy
LVIDd	Left ventricular internal dimension at end-diastole
LVM	Left ventricular mass
LVNC	Left ventricular noncompaction
LVOT	Left ventricular outflow tract
LVWT	Left ventricular wall thickness
LW	Lateral wall
LWapx	Lateral wall thickness at the supra-apex level
LWmit	Lateral wall thickness at the mitral valve
LWpap	Lateral wall thickness at the papillary level
M (Met)	Methionine
m <sup>2</sup>	Per square meter
MAFs	Minor allele frequencies
MAP	Mean arterial pressure
<i>MAP2K1</i>	Mitogen-activated protein kinase kinase 1 gene
<i>MAP2K2</i>	Mitogen-activated protein kinase kinase 2 gene
MB-CK	Combined creatine kinase isoform
MC	Mutation carrier
MCD	Malonyl-CoA decarboxylase
MGB	Minor groove binder
MHC	Myosin heavy chain

MI	Myocardial infarction
min	Minute
mIVST	Maximal interventricular septum thickness
mIVSTmit	Maximal interventricular septum thickness at the mitral valve
mIVSTpap	Maximal interventricular septum thickness at the papillary level
ml	Millilitre
MLCK	Myosin light chain kinase
MLP	Muscle LIM protein
mLVWT	Maximal left ventricular wall thickness
mLVWTapx	Maximal left ventricular wall thickness at the supra-apex level
mLVWTmit	Maximal left ventricular wall thickness at the mitral valve
mLVWTpap	Maximal left ventricular wall thickness at the papillary level
mm	Millimetres
MM-CK	Myofibrillar/muscle-type creatine kinase
MPV	Mean platelet volume
mPWT	Maximal posterior wall thickness
mRNA	Messenger ribonucleic acid
MRS	Magnetic resonance imaging
MtCK	Mitochondrial creatine kinase
mtDNA	Mitochondrial DNA
MTF-A	Mitochondrial transcription factor A
MV	Mitral valve
<i>MYBPC3</i>	Cardiac myosin-binding protein C gene
<i>MYH6</i>	$\alpha$ -myosin heavy chain gene
<i>MYH7</i>	$\beta$ -myosin heavy chain gene
MyHC	Myosin heavy chain
<i>MYL2</i>	Ventricular regulatory myosin light chain gene
<i>MYL3</i>	Ventricular essential myosin light chain gene
<i>MYOZ2</i>	Myozenin 2 gene
N (Asn)	Asparagine
Na <sup>+</sup>	Sodium
Na <sup>+</sup> /K <sup>+</sup> -ATPase	Sodium-potassium pump
NAC	N-acetylcysteine
NAD <sup>+</sup>	Nicotinamide adenine dinucleotide
NC	Non-carrier

NFQ	Non-fluorescent quencher
ng	Nanograms
nt	Nucleotide
NTC	Non-template control
NTG	Non-transgenic
O <sub>2</sub>	Oxygen
OMM	Outer mitochondrial membrane
P (Pro)	Proline
p	Short arm of chromosome
PC1	First principle component score
PCA	Principal component analysis
PCr	Phosphocreatine
PCR	Polymerase chain reaction
PDH	Pyruvate dehydrogenase complex
PDK	Pyruvate dehydrogenase kinase
<i>PDK4</i>	Pyruvate dehydrogenase kinase, isozyme 4 gene
PE	Phenylephrine
PFK1	Phosphofructokinase-1
PFK2	Phosphofructokinase 2
<i>PFKM</i>	Phosphofructokinase, muscle gene
<i>PGC1A</i>	Peroxisome proliferator-activated receptor gamma, coactivator 1 alpha gene
pIVS	Posterior interventricular septum
pIVSmit	Posterior interventricular septum thickness at the mitral valve
pIVSpap	Posterior interventricular septum thickness at the papillary level
PKA	Protein kinase A
PKC	Protein kinase C
PKG	Protein kinase G
<i>PLN</i>	Phospholamban gene
PM	Plasma membrane
pmol	Picomole
<i>PPARA</i>	Peroxisome proliferator-activated receptor alpha gene
<i>PPARG</i>	Peroxisome proliferator-activated receptor gamma gene
PPARs	Peroxisome proliferator-activated receptors



<i>PRKAA1</i>	Protein kinase, AMP-activated, alpha 1 catalytic subunit gene
<i>PRKAA2</i>	Protein kinase, AMP-activated, alpha 2 catalytic subunit gene
<i>PRKAB1</i>	Protein kinase, AMP-activated, beta 1 non-catalytic subunit gene
<i>PRKAB2</i>	Protein kinase, AMP-activated, beta 2 non-catalytic subunit gene
<i>PRKAG1</i>	Protein kinase, AMP-activated, gamma 1 non-catalytic subunit gene
<i>PRKAG2</i>	Protein kinase, AMP-activated gamma 2 non-catalytic subunit gene
<i>PRKAG3</i>	Protein kinase, AMP-activated, gamma 3 non-catalytic subunit gene
<i>PRNP</i>	Prion protein gene
<i>PTPN11</i>	Protein-tyrosine phosphatase non-receptor-type 11 gene
PW	Posterior wall
PWapx	Posterior wall thickness at the supra-apex level
PWmit	Posterior wall thickness at the mitral valve
PWpap	Posterior wall thickness at the papillary level
PWTd	Posterior wall thickness at end-diastole
Q (Gln)	Glutamine
q	Long arm of chromosome
Q1	First quartile
Q3	Third quartile
QTDT	Quantitative transmission disequilibrium test
QTL	Quantitative trait loci
R (Arg)	Arginine
$r^2$	Square of the correlation coefficient
RAAS	Renin-angiotensin aldosterone system
RLC	Regulatory myosin light chain
RVOT	Right ventricular outflow tract
S (Ser)	Serine
SB	di-sodium tetraborate decahydrate
SBP	Systolic BP
SCD	Sudden cardiac death
SCFA	Short-chain fatty acid
SDS	Sequence detection software
sec	Seconds
SERCA	Sarcoplasmic reticulum $Ca^{2+}$ -ATPase

SHR	Spontaneously hypertensive rat
SNP	Single nucleotide polymorphism
<i>SOS1</i>	Son of sevenless homolog 1 gene
SR	Sarcoplasmic reticulum
SWTd	Intraventricular septum thickness at end-diastole
T (nucleotide)	Thymine
T (Thr)	Threonine
<i>TAZ</i>	Tarfazzin gene
TCA	Tricarboxylic acid
<i>TCAP</i>	Telethonin gene
T <sub>m</sub>	Melting temperature
Tm2	Tropomyosin-2
Tn	Troponin
TnC	Troponin C
TNF- $\alpha$	Tumor necrosis factor- $\alpha$
TnI	Troponin I
<i>TNNC1</i>	Cardiac troponin C gene
<i>TNNI3</i>	Cardiac troponin I gene
<i>TNNT2</i>	Cardiac troponin T gene
TnT	Troponin T
TOR	Target-of-rapamycin
<i>TPM1</i>	$\alpha$ -tropomyosin gene
tRNA	Transfer RNA
TSC	Tuberous sclerosis complex
<i>TTN</i>	Titin gene
UCT	University of Cape Town
V (Val)	Valine
v	Version
V	Volts
<i>VCL</i>	Vinculin/metavinculin gene
vs	Versus

W (Trp)	Tryptophan
WPW	Wolff-Parkinson-White syndrome
WT	Wild-type
<i>wupA</i>	Troponin I gene (fly model)
X	Termination codon
Y (Tyr)	Tyrosine
YRI	Yoruba in Ibadan

## LIST OF FIGURES

### Chapter 1

Figure 1.1 Gross and microscopic findings of hypertrophic cardiomyopathy.....	<b>3</b>
Figure 1.2 Diagrammatic representation of the myocardial-contraction apparatus i.e. the sarcomere, indicating the components of the thick, intermediate and thin myofilaments.....	<b>6</b>
Figure 1.3 Pathways involved in myocardial energetics.....	<b>19</b>
Figure 1.4 Reactions of the tricarboxylic acid cycle.....	<b>20</b>
Figure 1.5 The electron transport chain and oxidative phosphorylation.....	<b>21</b>
Figure 1.6 The creatine kinase (CK) shuttle.....	<b>22</b>

### Chapter 2

Figure 2.1 Graphic representation of the left ventricle indicating the three levels of the heart muscle at which the wall thickness measurements were taken.....	<b>31</b>
Figure 2.2 Diagrammatic representation of the left ventricle segments assessed by echocardiography.....	<b>32</b>
Figure 2.3 The genomic structure of <i>ACTC1</i> and the physical locations of SNPs selected throughout this gene.....	<b>42</b>
Figure 2.4 The genomic structure of <i>MYH7</i> and the physical locations of SNPs selected throughout this gene.....	<b>42</b>
Figure 2.5 The genomic structure of <i>TNNT2</i> and the physical locations of SNPs selected throughout this gene.....	<b>43</b>
Figure 2.6 The genomic structure of <i>TNNI3</i> and the physical locations of SNPs selected throughout this gene.....	<b>44</b>
Figure 2.7 The genomic structure of <i>TPM1</i> and the physical locations of SNPs selected throughout this gene.....	<b>44</b>
Figure 2.8 The genomic structure of <i>MYL2</i> and the physical locations of SNPs selected throughout this gene.....	<b>45</b>
Figure 2.9 The genomic structure of <i>MYL3</i> and the physical locations of SNPs selected throughout this gene.....	<b>45</b>
Figure 2.10 The genomic structure of <i>MYBPC3</i> and the physical locations of SNPs selected throughout this gene. ....	<b>46</b>

Figure 2.11 The genomic structure of <i>ACTN3</i> and the physical locations of SNPs selected throughout this gene.....	<b>46</b>
Figure 2.12 Diagram of the candidate genes relating to myocardial energetics.....	<b>47</b>
Figure 2.13 The genomic structure of <i>CD36</i> and the physical locations of SNPs selected throughout this gene.....	<b>48</b>
Figure 2.14 The genomic structure of <i>CPT1B</i> and the physical locations of SNPs selected throughout this gene.....	<b>48</b>
Figure 2.15 The genomic structure of <i>PDK4</i> and the physical locations of SNPs selected throughout this gene.....	<b>49</b>
Figure 2.16 The genomic structure of <i>CKM</i> and the physical locations of SNPs selected throughout this gene.....	<b>49</b>
Figure 2.17 The genomic structure of <i>CKB</i> and the physical locations of SNPs selected throughout this gene.....	<b>50</b>
Figure 2.18 The genomic structure of <i>ALDOA</i> and the physical locations of SNPs selected throughout this gene.....	<b>50</b>
Figure 2.19 The genomic structure of <i>PFKM</i> and the physical locations of SNPs selected throughout this gene.....	<b>51</b>
Figure 2.20 The genomic structure of <i>PPARA</i> and the physical locations of SNPs selected throughout this gene.....	<b>51</b>
Figure 2.21 The genomic structure of <i>PPARG</i> and the physical locations of SNPs selected throughout this gene.....	<b>52</b>
Figure 2.22 The genomic structure of <i>PGCIA</i> and the physical locations of SNPs selected throughout this gene.....	<b>52</b>
Figure 2.23 The genomic structure of <i>PRKAA1</i> and the physical locations of SNPs selected throughout this gene.....	<b>54</b>
Figure 2.24 The genomic structure of <i>PRKAA2</i> and the physical locations of SNPs selected throughout this gene.....	<b>54</b>
Figure 2.25 The genomic structure of <i>PRKAB1</i> and the physical locations of SNPs selected throughout this gene.....	<b>54</b>
Figure 2.26 The genomic structure of <i>PRKAB2</i> and the physical locations of SNPs selected throughout this gene.....	<b>55</b>
Figure 2.27 The genomic structure of <i>PRKAG1</i> and the physical locations of SNPs selected throughout this gene.....	<b>55</b>
Figure 2.28 The genomic structure of <i>PRKAG2</i> and the physical locations of SNPs selected throughout this gene.....	<b>55</b>

Figure 2.29 The genomic structure of <i>PRKAG3</i> and the physical locations of SNPs selected throughout this gene.....	<b>55</b>
Figure 2.30 Overview of the ABI TaqMan® SNP Validated genotyping assay hybridisation- and fluorophore-based PCR chemistry that allows for allelic discrimination.....	<b>57</b>
Figure 2.31 Graph of estimated mLVWT by mutation group and rs3729838 genotype.....	<b>66</b>
 <b>Chapter 3</b>	
Figure 3.1 The <i>CD36</i> rs10268417 genotypes.....	<b>74</b>
Figure 3.2 PCR amplification of the 25bp deletion in the <i>MYBPC3</i> gene.....	<b>75</b>
Figure 3.3 The p-values for tests of association between single SNPs in <i>ACTC1</i> and individual hypertrophy traits.....	<b>89</b>
Figure 3.4 The p-values for tests of association between <i>ACTC1</i> haplotypes and individual hypertrophy traits.....	<b>90</b>
Figure 3.5 The p-values for tests of association between single SNPs in <i>MYH7</i> and individual hypertrophy traits.....	<b>92</b>
Figure 3.6 The p-values for tests of association between <i>MYH7</i> haplotypes and individual hypertrophy traits.....	<b>93</b>
Figure 3.7 The p-values for tests of association between single SNPs in <i>TNNT2</i> and individual hypertrophy traits.....	<b>95</b>
Figure 3.8 The p-values for tests of association between <i>TNNT2</i> haplotypes and individual hypertrophy traits.....	<b>96</b>
Figure 3.9 The p-values for tests of association between single SNPs in <i>TNNI3</i> and individual hypertrophy traits.....	<b>98</b>
Figure 3.10 The p-values for tests of association between <i>TNNI3</i> haplotypes and individual hypertrophy traits.....	<b>99</b>
Figure 3.11 The p-values for tests of association between single SNPs in <i>TPM1</i> and individual hypertrophy traits.....	<b>102</b>
Figure 3.12 The p-values for tests of association between <i>TPM1</i> haplotypes and individual hypertrophy traits.....	<b>103</b>
Figure 3.13 The p-values for tests of association between single SNPs in <i>MYL2</i> and individual hypertrophy traits.....	<b>105</b>

Figure 3.14 The p-values for tests of association between <i>MYL2</i> haplotypes and individual hypertrophy traits.....	<b>106</b>
Figure 3.15 The p-values for tests of association between single SNPs in <i>MYL3</i> and individual hypertrophy traits.....	<b>108</b>
Figure 3.16 The p-values for tests of association between <i>MYL3</i> haplotypes and individual hypertrophy traits.....	<b>109</b>
Figure 3.17 The p-values for tests of association between single SNPs in <i>MYBPC3</i> and individual hypertrophy traits.....	<b>111</b>
Figure 3.18 The p-values for tests of association between <i>MYBPC3</i> haplotypes and individual hypertrophy traits.....	<b>112</b>
Figure 3.19 The p-values for tests of association between single SNPs in <i>ACTN3</i> and individual hypertrophy traits.....	<b>114</b>
Figure 3.20 The p-values for tests of association between <i>ACTN3</i> haplotypes and individual hypertrophy traits.....	<b>115</b>
Figure 3.21 The p-values for tests of association between single SNPs in <i>CD36</i> and individual hypertrophy traits.....	<b>117</b>
Figure 3.22 The p-values for tests of association between <i>CD36</i> haplotypes and individual hypertrophy traits.....	<b>118</b>
Figure 3.23 The p-values for tests of association between single SNPs in <i>CPT1B</i> and individual hypertrophy traits.....	<b>120</b>
Figure 3.24 The p-values for tests of association between <i>CPT1B</i> haplotypes and individual hypertrophy traits.....	<b>121</b>
Figure 3.25 The p-values for tests of association between single SNPs in <i>PDK4</i> and individual hypertrophy traits.....	<b>123</b>
Figure 3.26 The p-values for tests of association between <i>PDK4</i> haplotypes and individual hypertrophy traits.....	<b>124</b>
Figure 3.27 The p-values for tests of association between single SNPs in <i>CKM</i> and individual hypertrophy traits.....	<b>126</b>
Figure 3.28 The p-values for tests of association between <i>CKM</i> haplotypes and individual hypertrophy traits.....	<b>127</b>
Figure 3.29 The p-values for tests of association between single SNPs in <i>CKB</i> and individual hypertrophy traits.....	<b>130</b>

Figure 3.30 The p-values for tests of association between <i>CKB</i> haplotypes and individual hypertrophy traits.....	<b>131</b>
Figure 3.31 The p-values for tests of association between single SNPs in <i>ALDOA</i> and individual hypertrophy traits.....	<b>133</b>
Figure 3.32 The p-values for tests of association between <i>ALDOA</i> haplotypes and individual hypertrophy traits.....	<b>134</b>
Figure 3.33 The p-values for tests of association between single SNPs in <i>PFKM</i> and individual hypertrophy traits.....	<b>136</b>
Figure 3.34 The p-values for tests of association between <i>PFKM</i> haplotypes and individual hypertrophy traits.....	<b>137</b>
Figure 3.35 The p-values for tests of association between single SNPs in <i>PPARA</i> and individual hypertrophy traits.....	<b>139</b>
Figure 3.36 The p-values for tests of association between <i>PPARA</i> haplotypes and individual hypertrophy traits.....	<b>140</b>
Figure 3.37 The p-values for tests of association between single SNPs in <i>PPARG</i> and individual hypertrophy traits.....	<b>142</b>
Figure 3.38 The p-values for tests of association between <i>PPARG</i> haplotypes and individual hypertrophy traits.....	<b>143</b>
Figure 3.39 The p-values for tests of association between single SNPs in <i>PGCIA</i> and individual hypertrophy traits.....	<b>146</b>
Figure 3.40 The p-values for tests of association between <i>PGCIA</i> haplotypes and individual hypertrophy traits.....	<b>147</b>
Figure 3.41 The p-values for tests of association between single SNPs in <i>PRKAA1</i> and individual hypertrophy traits.....	<b>150</b>
Figure 3.42 The p-values for tests of association between <i>PRKAA1</i> haplotypes and individual hypertrophy traits.....	<b>151</b>
Figure 3.43 The p-values for tests of association between single SNPs in <i>PRKAA2</i> and individual hypertrophy traits.....	<b>153</b>
Figure 3.44 The p-values for the tests of association between <i>PRKAA2</i> haplotypes and individual hypertrophy traits.....	<b>154</b>
Figure 3.45 The p-values for tests of association between single SNPs in <i>PRKAB1</i> and individual hypertrophy traits.....	<b>156</b>



Figure 3.46 The p-values for tests of association between <i>PRKAB1</i> haplotypes and individual hypertrophy traits.....	<b>157</b>
Figure 3.47 The p-values for tests of association between single SNPs in <i>PRKAB2</i> and individual hypertrophy traits.....	<b>159</b>
Figure 3.48 The p-values for tests of association between <i>PRKAB2</i> haplotypes and individual hypertrophy traits.....	<b>160</b>
Figure 3.49 The p-values for tests of association between single SNPs in <i>PRKAG1</i> and individual hypertrophy traits.....	<b>162</b>
Figure 3.50 The p-values for tests of association between <i>PRKAG1</i> haplotypes and individual hypertrophy traits.....	<b>163</b>
Figure 3.51 The p-values for tests of association between single SNPs in <i>PRKAG2</i> and individual hypertrophy traits.....	<b>165</b>
Figure 3.52 The p-values for tests of association between <i>PRKAG2</i> haplotypes and individual hypertrophy traits.....	<b>166</b>
Figure 3.53 The p-values for tests of association between single SNPs in <i>PRKAG3</i> and individual hypertrophy traits.....	<b>169</b>
Figure 3.54 The p-values for tests of association between <i>PRKAG3</i> haplotypes and individual hypertrophy traits.....	<b>170</b>

**LIST OF TABLES****Chapter 1**

Table 1.1 Summary of HCM susceptibility genes grouped according to HCM subtype.....	<b>4</b>
Table 1.2 Summary of HCM Phenocopies listed according to chromosome locus.....	<b>7</b>

**Chapter 2**

Table 2.1 Composition of the study population of the South African HCM-families.....	<b>29</b>
Table 2.2 Echocardiographically derived hypertrophy traits used to characterise the extent and distribution of the cardiac hypertrophy.....	<b>33</b>
Table 2.3 Candidate modifier genes selected for investigation.....	<b>35</b>
Table 2.4 Details of the SNPs selected for genotyping.....	<b>39</b>
Table 2.5 Primer details and cycling conditions for screening of the 25 bp deletion in the <i>MYBPC3</i> gene.....	<b>58</b>

**Chapter 3**

Table 3.1 Basic characteristics of the study cohort.....	<b>70</b>
Table 3.2 The SNPs chosen for investigation in this study and their minor allele frequencies (MAF) in the CEU and YRI populations.....	<b>71</b>
Table 3.3 Cohort-specific descriptives: Hardy-Weinberg equilibrium test p-values and minor allele frequencies for the SNPs investigated.....	<b>76</b>
Table 3.4 Pair-wise LD structure for <i>PRKAA2</i> .....	<b>79</b>
Table 3.5 Pair-wise LD structure for <i>TNNT2</i> .....	<b>80</b>
Table 3.6 Pair-wise LD structure for <i>PPARG</i> .....	<b>80</b>
Table 3.7 Pair-wise LD structure for <i>PGC1A</i> .....	<b>81</b>
Table 3.8 Pair-wise LD structure for <i>PRKAA1</i> .....	<b>81</b>
Table 3.9 Pair-wise LD structure for <i>CD36</i> .....	<b>81</b>
Table 3.10 Pair-wise LD structure for <i>PRKAG2</i> .....	<b>82</b>

Table 3.11 Pair-wise LD structure for <i>MYBPC3</i> .....	<b>82</b>
Table 3.12 Pair-wise LD structure for <i>ACTN3</i> .....	<b>83</b>
Table 3.13 Pair-wise LD structure for <i>PRKAB1</i> .....	<b>83</b>
Table 3.14 Pair-wise LD structure for <i>MYH7</i> .....	<b>84</b>
Table 3.15 Pair-wise LD structure for <i>CKB</i> .....	<b>84</b>
Table 3.16 Pair-wise LD structure for <i>TPM1</i> .....	<b>85</b>
Table 3.17 Pair-wise LD structure for <i>CKM</i> .....	<b>85</b>
Table 3.18 Pair-wise LD structure for <i>PPARA</i> .....	<b>85</b>
Table 3.19 The PC1 score defined in terms of its weighted composition: the weight of each wall thickness measurement.....	<b>86</b>
Table 3.20 The environmental and heritability estimates detailed as estimated percentage contribution to trait variance as well as the p-values for heritability.....	<b>87</b>
Table 3.21 The p-values obtained for the analysis of interaction between mutation group and single SNPs in <i>ACTC1</i> .....	<b>89</b>
Table 3.22 The p-values obtained for the analysis of interaction between mutation group and <i>ACTC1</i> haplotypes.....	<b>90</b>
Table 3.23 The p-values obtained for the analysis of interaction between mutation group and single SNPs in <i>MYH7</i> .....	<b>92</b>
Table 3.24 The p-values obtained for the analysis of interaction between mutation group and <i>MYH7</i> haplotypes.....	<b>93</b>
Table 3.25 The p-values obtained for the analysis of interaction between mutation group and single SNPs in <i>TNNT2</i> .....	<b>95</b>
Table 3.26 The p-values obtained for the analysis of interaction between mutation group and <i>TNNT2</i> haplotypes.....	<b>96</b>
Table 3.27 The p-values obtained for the analysis of interaction between mutation group and single SNPs in <i>TNNI3</i> .....	<b>98</b>
Table 3.28 The p-values obtained for the analysis of interaction between mutation group and <i>TNNI3</i> haplotypes.....	<b>99</b>
Table 3.29 The p-values obtained for the analysis of interaction between mutation group and single SNPs in <i>TPM1</i> .....	<b>102</b>

Table 3.30 The p-values obtained for the analysis of interaction between mutation group and <i>TPM1</i> haplotypes.....	<b>103</b>
Table 3.31 The p-values obtained for the analysis of interaction between mutation group and single SNPs in <i>MYL2</i> .....	<b>105</b>
Table 3.32 The p-values obtained for the analysis of interaction between mutation group and <i>MYL2</i> haplotypes.....	<b>106</b>
Table 3.33 The p-values obtained for the analysis of interaction between mutation group and single SNPs in <i>MYL3</i> .....	<b>108</b>
Table 3.34 The p-values obtained for the analysis of interaction between mutation group and single haplotypes in <i>MYL3</i> .....	<b>109</b>
Table 3.35 The p-values obtained for the analysis of interaction between mutation group and single SNPs in <i>MYBPC3</i> .....	<b>111</b>
Table 3.36 The p-values obtained for the analysis of interaction between mutation group and individual haplotypes in <i>MYBPC3</i> .....	<b>112</b>
Table 3.37 The p-values obtained for the analysis of interaction between mutation group and single SNPs in <i>ACTN3</i> .....	<b>114</b>
Table 3.38 The p-values obtained for the analysis of interaction between mutation group and <i>ACTN3</i> haplotypes.....	<b>115</b>
Table 3.39 The p-values obtained for the analysis of interaction between mutation group and single SNPs in <i>CD36</i> .....	<b>117</b>
Table 3.40 The p-values obtained for the analysis of interaction between mutation group and individual haplotypes in <i>CD36</i> .....	<b>118</b>
Table 3.41 The p-values obtained for the analysis of interaction between mutation group and single SNPs in <i>CPT1B</i> .....	<b>120</b>
Table 3.42 The p-values obtained for the analysis of interaction between mutation group and <i>CPT1B</i> haplotypes.....	<b>121</b>
Table 3.43 The p-values obtained for the analysis of interaction between mutation group and single SNPs in <i>PDK4</i> .....	<b>123</b>
Table 3.44 The p-values obtained for the analysis of interaction between mutation group and <i>PDK4</i> haplotypes.....	<b>124</b>
Table 3.45 The p-values obtained for the analysis of interaction between mutation group and single SNPs in <i>CKM</i> . ....	<b>126</b>
Table 3.46 The p-values obtained for the analysis of interaction between mutation group and <i>CKM</i> haplotypes.....	<b>128</b>

Table 3.47 The p-values obtained for the analysis of interaction between mutation group and single SNPs in <i>CKB</i> .....	<b>130</b>
Table 3.48 The p-values obtained for the analysis of interaction between mutation group and <i>CKB</i> haplotypes.....	<b>131</b>
Table 3.49 The p-values obtained for the analysis of interaction between mutation group and single SNPs in <i>ALDOA</i> .....	<b>133</b>
Table 3.50 The p-values obtained for the analysis of interaction between mutation group and <i>ALDOA</i> haplotypes.....	<b>134</b>
Table 3.51 The p-values obtained for the analysis of interaction between mutation group and single SNPs in <i>PFKM</i> .....	<b>136</b>
Table 3.52 The p-values obtained for the analysis of interaction between mutation group and <i>PFKM</i> haplotypes.....	<b>137</b>
Table 3.53 The p-values obtained for the analysis of interaction between mutation group and single SNPs in <i>PPARA</i> .....	<b>139</b>
Table 3.54 The p-values obtained for the analysis of interaction between mutation group and <i>PPARA</i> haplotypes.....	<b>140</b>
Table 3.55 The p-values obtained for the analysis of interaction between mutation group and single SNPs in <i>PPARG</i> .....	<b>142</b>
Table 3.56 The p-values obtained for the analysis of interaction between mutation group and single haplotypes in <i>PPARG</i> .....	<b>144</b>
Table 3.57 The p-values obtained for the analysis of interaction between mutation group and single SNPs in <i>PGCIA</i> .....	<b>146</b>
Table 3.58 The p-values obtained for the analysis of interaction between mutation group and single haplotypes in <i>PGCIA</i> .....	<b>148</b>
Table 3.59 The p-values obtained for the analysis of interaction between mutation group and single SNPs in <i>PRKAA1</i> .....	<b>150</b>
Table 3.60 The p-values obtained for the analysis of interaction between mutation group and single haplotypes in <i>PRKAA1</i> .....	<b>151</b>
Table 3.61 The p-values obtained for the analysis of interaction between HCM founder mutation group and single SNPs in <i>PRKAA2</i> .....	<b>153</b>
Table 3.62 The p-values obtained for the analysis of interaction between mutation group and <i>PRKAA2</i> haplotypes.....	<b>154</b>
Table 3.63 The p-values obtained for the analysis of interaction between mutation group and single SNPs in <i>PRKAB1</i> .....	<b>156</b>

Table 3.64 The p-values obtained for the analysis of interaction between mutation group and <i>PRKAB1</i> haplotypes.....	<b>157</b>
Table 3.65 The p-values obtained for the analysis of interaction between mutation group and single SNPs in <i>PRKAB2</i> .....	<b>159</b>
Table 3.66 The p-values obtained for the analysis of interaction between mutation group and <i>PRKAB2</i> haplotypes.....	<b>160</b>
Table 3.67 The p-values obtained for the analysis of interaction between mutation group and single SNPs in <i>PRKAG1</i> .....	<b>162</b>
Table 3.68 The p-values obtained for the analysis of interaction between mutation group and <i>PRKAG1</i> haplotypes.....	<b>163</b>
Table 3.69 The p-values obtained for the analysis of interaction between mutation group and single SNPs in <i>PRKAG2</i> .....	<b>165</b>
Table 3.70 The p-values obtained for the analysis of interaction between mutation group and individual haplotypes in <i>PRKAG2</i> .....	<b>167</b>
Table 3.71 The p-values obtained for the analysis of interaction between mutation group and single SNPs in <i>PRKAG3</i> .....	<b>169</b>
Table 3.72 The p-values obtained for the analysis of interaction between mutation group and haplotypes in <i>PRKAG3</i> .....	<b>170</b>
Table 3.73 Allelic effects of variants predicting a significant increase in hypertrophy in the current cohort.....	<b>171</b>
Table 3.74 The distribution of the number of ‘pro-LVH’ alleles in MC and NC individuals.....	<b>171</b>
<b>Chapter 4</b>	
Table 4.1 Priority list of genes for future studies.....	<b>216</b>

## CHAPTER ONE

### INTRODUCTION

---

#### 1.1 Left ventricular hypertrophy

Left ventricular hypertrophy (LVH) is predictive of cardiovascular morbidity and all-cause mortality, independent of other disease risk factors, e.g. age and gender, and its progression is associated with an increased risk of heart failure (HF), stroke, myocardial infarction (MI), coronary heart disease (CHD), arrhythmias and sudden cardiac death (SCD) (Koren *et al.*, 1991;Levy *et al.*, 1990a;Mathew *et al.*, 2001;Schillaci *et al.*, 2000;Messerli *et al.*, 1984;Wolf *et al.*, 1991;Kannel *et al.*, 1970;Kannel & Schatzkin, 1985;Levy *et al.*, 1987;Dahlof *et al.*, 2002).

The value of LVH as a modifiable cardiovascular risk factor is apparent from studies linking its regression, achieved via antihypertensive therapy, to increased overall survival and a reduced frequency of adverse cardiac events; these beneficial effects were independent of blood pressure (BP) and drug choice (Devereux *et al.*, 2004;Okin *et al.*, 2004). The Heart Outcomes Prevention Evaluation (HOPE) trial is one such study where electrocardiographic LVH regression was associated with reduced risk of death, MI, stroke and HF (Mathew *et al.*, 2001).

However, there are limitations to the antihypertensive treatment of LVH, as is evident from the lack of correlation between the level of BP reduction and LVH regression, as well as from instances where LVH is seen even in normotensive individuals (Koren *et al.*, 1991). This highlights the involvement of other non-hemodynamic factors in the development of LVH (Schunkert *et al.*, 1994;Levy *et al.*, 1988).

To eventually facilitate improved therapeutic intervention and risk stratification, an increased understanding of LVH pathogenesis is thus imperative. That genetic factors can modify LVH risk is evident from the literature. Research motivating such genetic contributions include twin studies highlighting the influence of heritable factors on left ventricular mass (LVM), which is an indicator of LVH (Adams *et al.*, 1985;Verhaaren *et al.*, 1991), and association of the angiotensin-converting enzyme (*ACE*) gene, seemingly independent of BP-control, with increased risk of LVH (Schunkert *et al.*, 1994). However, identification of genetic markers of LVH against the backdrop of complex disorders, in which LVH is just one of many features, is challenging. Hypertrophic cardiomyopathy (HCM), an inherited cardiac disorder, with LVH as its primary clinical feature, is considered a

model disease for elucidating the molecular mechanisms underlying cardiac hypertrophy development and progression (Watkins *et al.*, 1995c).

## 1.2 Hypertrophic cardiomyopathy

HCM is a heritable myocardial disorder estimated to occur in 1 of 500 young adults (Maron *et al.*, 1995; Willard & Ginsburg, 2009). It is clinically defined by unexplained LVH, i.e. LVH occurring in the absence of other hypertrophy triggers, such as hypertension, whilst the histopathological features include myocyte hypertrophy and extensive myocytic and myofibrillar disarray, as well as interstitial fibrosis (Refer to Figure 1.1). In addition, HCM patients are at risk of SCD, whether or not they manifest any of the other clinical symptoms, including arrhythmias, dyspnea, palpitations and syncope (Seidman & Seidman, 2001; Chung *et al.*, 2003; Marian, 2002; Reviewed by Marian, 2010).

The hypertrophic phenotype in HCM is most frequently asymmetric, typically including the interventricular septum (IVS), and ultimately resulting in a decreased left ventricular cavity size (Chung *et al.*, 2003; Seidman & Seidman, 2001; Willard & Ginsburg, 2009). Nonetheless, the disease exhibits extreme variability, including that of the age of onset, disease progression, occurrence of SCD and spectrum and extent of symptoms, and most noticeably, also the degree and location of hypertrophy (Seidman & Seidman, 2001; Wigle *et al.*, 1995; Maron, 2002; Spirito & Maron, 1989). Moreover, the disease heterogeneity can range from clinically and morphologically unaffected with an asymptomatic course and normal longevity, to severe dysfunction, including HF or SCD, with the latter often being the first manifestation of disease (Lawson, 1987; Reviewed by Marian, 2010; Spirito *et al.*, 1997).



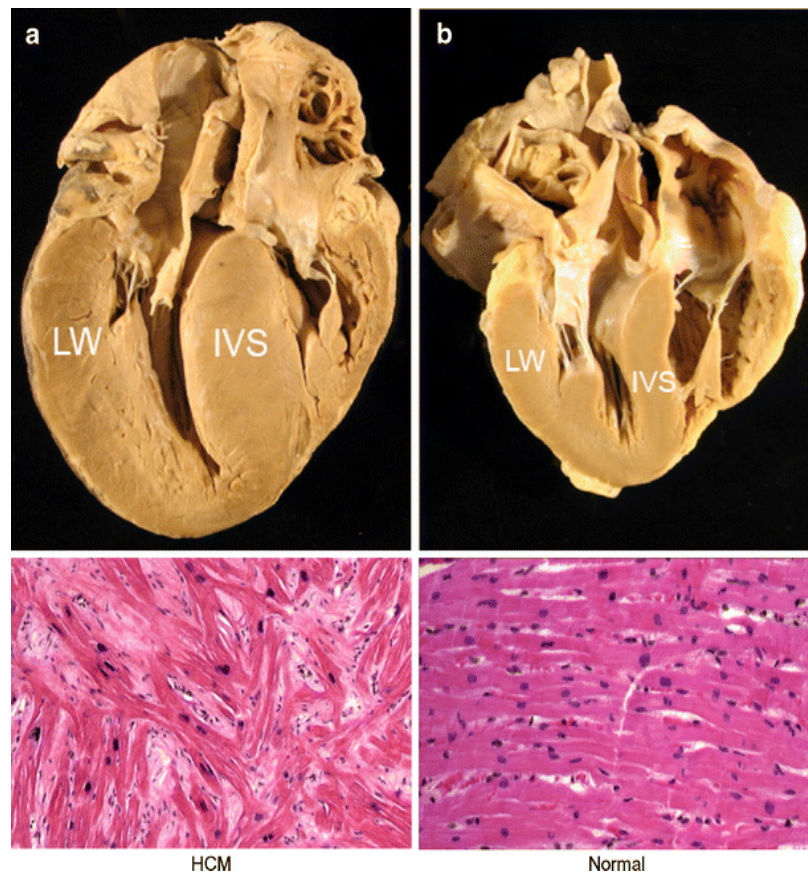


**Figure 1.1 Gross and microscopic findings of hypertrophic cardiomyopathy.** Severe concentric hypertrophy is apparent from this pathologic specimen from a patient with HCM (a), compared to a normal heart (b). With HCM, there is markedly increased wall thickness throughout the left ventricle, most prominent in the interventricular septum (IVS), but also present in the free lateral wall (LW). Histological sections, stained with hematoxylin and eosin, demonstrate the pathognomonic features of HCM, i.e. myocyte disarray and fibrosis (a). In contrast, normal myocardium demonstrates a very orderly arrangement of myocytes (b). Images are at  $\times 100$  magnification. *Images courtesy of Dr. Robert Padera, Department of Pathology, Brigham and Women's Hospital, Boston, MA (Taken from Ho, 2009)*

### 1.2.1 Molecular genetics of HCM

HCM is inherited in an autosomal dominant fashion, although both genetic and intragenic heterogeneity is present (Soor *et al.*, 2009; Reviewed by Bonne *et al.*, 1998). Classically described as a ‘disease of the sarcomere’ (Thierfelder *et al.*, 1994), with more than 1000 causative mutations (Seidman & Seidman, 2011) identified primarily in genes encoding myofilament proteins (myofilament HCM), the genetic spectrum currently extends to mutations in genes encoding sarcomeric Z-disc (Z-disc HCM) and calcium-handling (calcium-handling HCM) proteins (Willard & Ginsburg, 2009; Konno *et al.*, 2010). These HCM susceptibility genes, their relevant protein products, loci and HCM-causing mutation totals are listed in Table 1.1, according to HCM subtype.

**Table 1.1 Summary of HCM susceptibility genes grouped according to HCM subtype**

HCM subtype	Gene	Protein	Locus	HCM mutations described
<b>Myofilament HCM</b>				
Giant filament	<i>TTN</i>	Titin	2q24.3	2
Thick filament	<i>MYH7</i>	$\beta$ -Myosin heavy chain	14q11.2–q12	233
	<i>MYH6</i>	$\alpha$ -Myosin heavy chain	14q11.2–q12	2
	<i>MYL2</i>	Ventricular regulatory myosin light chain	12q23–q24.3	15
	<i>MYL3</i>	Ventricular essential myosin light chain	3p21.2–p21.3	7
Intermediate filament	<i>MYBPC3</i>	Cardiac myosin-binding protein C	11p11.2	187
Thin filament	<i>TNNT2</i>	Cardiac troponin T	1q32	39
	<i>TNNI3</i>	Cardiac troponin I	19p13.4	37
	<i>TPM1</i>	$\alpha$ -Tropomyosin	15q22.1	15
	<i>ACTC1</i>	$\alpha$ -Cardiac actin	15q14	7
	<i>TNNC1</i>	Cardiac troponin C	3p21.3–p14.3	7

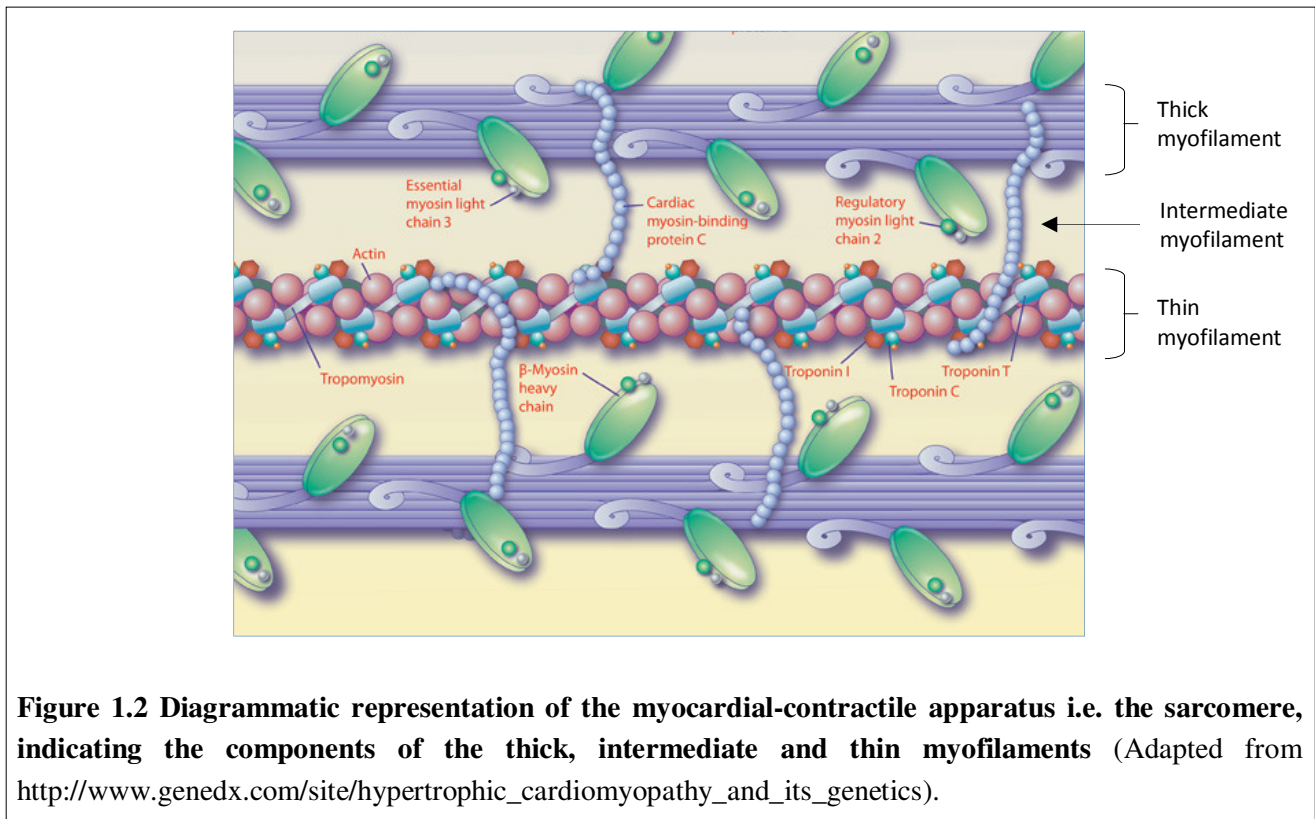
HCM subtype	Gene	Protein	Locus	HCM mutations described
<b>Z-disc HCM</b>				
	<i>ANKRD1</i>	Cardiac ankyrin repeat protein	10q23.33	3
	<i>LBD3</i>	LIM binding domain 3	10q22.2–q23.3	6
	<i>CSRP3</i>	Muscle LIM protein	11p15.1	7
	<i>TCAP</i>	Telethonin	17q12–q21.1	2
	<i>VCL</i>	Vinculin/metavinculin	10q22.1–q23	2
	<i>ACTN2</i>	$\alpha$ -actinin 2	1q42–q43	6
	<i>MYOZ2</i>	Myozenin 2	4q26–q27	2
<b>Calcium-handling HCM</b>				
	<i>JPH2</i>	Junctophilin-2	20q12	3
	<i>PLN</i>	Phospholamban	6q22.1	4

**Abbreviations:**  $\alpha$ -alpha;  $\beta$ -beta; p-short arm of chromosome; q-long arm of chromosome; HCM-Hypertrophic cardiomyopathy (Xu *et al.*, 2010;Adapted from Bos *et al.*, 2009;Alves *et al.*, 2010;Theis *et al.*, 2006;Medin *et al.*, 2007)

Myofilament HCM is the most prevalent subtype, due mainly to mutations in eight genes that encode sarcomere contractile proteins, and affects the integrity of the thin, intermediate and thick myofilaments (Willard & Ginsburg, 2009). These eight genes include the  $\beta$ -myosin heavy chain gene (*MYH7*) (Geisterfer-Lowrance *et al.*, 1990); ventricular regulatory myosin light chain (*MYL2*); ventricular essential myosin light chain (*MYL3*) (Poetter *et al.*, 1996); cardiac myosin-binding protein C (*MYBPC3*) (Watkins *et al.*, 1995a); cardiac troponin T (*TNNT2*) (Thierfelder *et al.*, 1994); cardiac troponin I (*TNNI3*) (Kimura *et al.*, 1997);  $\alpha$ -Tropomyosin (*TPM1*) (Thierfelder *et al.*, 1994);  $\alpha$ -Cardiac actin (*ACTC*) (Mogensen *et al.*, 1999) (Refer to Figure 1.2 and to Table 1.1).

Overall, the leading HCM-causing genes are *MYH7* and *MYBPC3*, collectively accounting for an estimated 50–60% of cases. Combined, the remainder of the aforementioned sarcomeric genes explain less than 20%, with the largest contributors being *TNNT2* and *TNNI3* mutations at individual gene frequencies of 3–5%. Other myofilament protein encoding genes are only rare causes of the condition (individual frequencies <1%); they include titin (*TTN*), whose contribution

to HCM is well established, and cardiac troponin C (*TNNC1*) and  $\alpha$ -Myosin heavy chain (*MYH6*), whose contributions are less concrete (Baars *et al.*, 2010; Reviewed by Marian, 2010).



Similarly, Z-disc and calcium-handling HCM occurs infrequently, with implicated genes (Refer to Table 1.1), viz. those encoding the Z-disc proteins responsible for anchoring myofibrils to the cytoskeleton and signal transduction, and calcium-handling proteins essential for excitation-contraction coupling of the cardiomyocyte, each accounting for <1% of cases. The exception to this rule is the LIM domain binding 3 (*LBD3*) gene, which accounts for 1–5% of HCM cases (Pyle & Solaro, 2004; Willard & Ginsburg, 2009).

Finally, mutations in non-myofilament genes have been implicated in HCM-mimicking disorders, so-called HCM phenocopies. These include metabolic cardiomyopathies, previously considered as metabolic-HCM, caused by mutations in AMP-activated protein kinase gamma 2 (*PRKAG2*), lysosome-associated membrane protein 2 (*LAMP2*) and  $\alpha$ -galactosidase A (*GLA*) (Nakao *et al.*, 1995; Arad *et al.*, 2005; Blair *et al.*, 2001b). Although recently revised as distinct from HCM, due to differing histopathologies, these cardiomyopathies all show LVH, thereby highlighting the contribution of metabolic genes to the development of hypertrophy that can be measured on a gross morphological scale (Bos *et al.*, 2007; Willard & Ginsburg, 2009; Konno *et al.*, 2010). The

aforementioned as well as other HCM phenocopies, including triplet repeat syndromes and mitochondrial cytopathies, are listed in Table 1.2 along with the relevant gene, locus, protein product and syndrome.

**Table 1.2 Summary of HCM Phenocopies listed according to chromosome locus**

Gene	Locus	Protein	Syndrome
<i>AGL</i>	1p21	Amylo-1,6-glucosidase	Forbes disease
<i>SOS1</i>	2p22–p21	Son of sevenless homolog 1	Noonan syndrome
<i>BRAF1</i>	3p25	V-RAF murine sarcoma viral oncogen homolog B1	CFC syndrome
<i>PRKAG2</i>	7q35–q36.36	AMP-activated protein kinase gamma 2	WPW syndrome (pre-excitation); conduction disturbances
<i>FXN</i>	9q13	Frataxin	Friedreich ataxia
<i>KRAS2</i>	12p12.1	Kirsten rat sarcoma viral oncogen homolog	Noonan syndrome, Leopard, CFC syndrome
<i>PTPN11</i>	12q24.1	Protein-tyrosine phosphatase non-receptor-type 11	Noonan syndrome, Leopard syndrome, CFC syndrome
<i>MAP2K1</i>	15q22.1–q22.33	Mitogen-activated protein kinase kinase 1	CFC syndrome
<i>GAA</i>	17q25.2–q25.3	Glucosidase alpha acid	Pompe disease
<i>DTNA</i>	18q12	$\alpha$ -dystrobrevin	Barth syndrome/LVNC
<i>MAP2K2</i>	19p13.3	Mitogen-activated protein kinase kinase 2	CFC syndrome
<i>GLA</i>	Xq22	$\alpha$ -galactosidase	Fabry disease
<i>LAMP2</i>	Xq24	Lysosome-associated membrane protein 2	Danon disease/WPW
<i>TAZ</i>	Xq28	Tarfazzin	Barth syndrome/LVNC

**Abbreviations:**  $\alpha$ -alpha;  $\beta$ -beta; **p**-short arm of chromosome; **q**-long arm of chromosome; **X**-chromosome X; **AMP**-adenosine monophosphate; **CFC**-cardiofaciocutaneous; **HCM**-Hypertrophic cardiomyopathy; **Leopard**-mnemonic for syndrome with clinical characteristics of lentiginos, electrocardiographic conduction abnormalities, ocular hypertelorism, pulmonary hypertension, abnormal genitalia, retarded growth, deafness; **LVNC**-left ventricular noncompaction; **WPW**-Wolff-Parkinson-White syndrome (Adapted from Bos *et al.*, 2009;Baars *et al.*, 2010)

### 1.2.2 Clinical variability in HCM

HCM shows marked phenotypic heterogeneity even within families, i.e. amongst individuals who carry the same causal mutation; this intrafamilial variation is comparable to the variability observed between different families, involving different mutations (Epstein *et al.*, 1992; Fananapazir & Epstein, 1994; Posen *et al.*, 1995). As previously discussed, this heterogeneity is evident in the age of onset, disease progression, risk of SCD and the severity of hypertrophy (Refer to Section 1.2).

Although the hypertrophy is most frequently asymmetric, involving the IVS, in rare instances it may present as concentric (symmetric). Further variability exists in the pattern or distribution of hypertrophy, as well as the extent of hypertrophy. Thus, hypertrophy distribution may range from diffusely distributed hypertrophy to hypertrophy localised to a single segment (e.g. apical). The extent of hypertrophy may include LV wall thicknesses (LVWT) in HCM-mutation carriers ranging from complete absence of hypertrophy, or minimal hypertrophy (with LVWT less than 13 millimetres (mm) in adults regarded as normal), to massive hypertrophy (defined as maximum LVWT of 35 mm or more in adults, and its age-adjusted value in children). For this reason, the diagnostic cut-off LVWT value used in HCM pedigrees (the extended family of HCM probands) is more stringent (11 mm), as even marginal hypertrophy may prove significant within a familial context (Reviewed by Maron, 2002; Spirito *et al.*, 1997).

This clinical heterogeneity can in part be explained by genotype/phenotype correlations pertaining to the relevant causal gene, the specific mutation therein and gene dosage, i.e. the presence of multiple sarcomeric mutations (Ho, 2010a; Reviewed by Marian, 2010). Recognised causal gene relationships include the frequent association of *MYH7* mutations with early disease onset, high disease penetrance, and severe disease, e.g. severe hypertrophy, heart failure and increased risk of SCD (Fowler *et al.*, 2009; Watkins *et al.*, 1992). In contrast, *MYBPC3* mutations have typically been characterised by a relatively late onset and a less severe clinical phenotype, as well as incomplete penetrance (Fowler *et al.*, 2009; Van Driest *et al.*, 2004). *TNNT2* mutations, on the other hand, typically present with less severe hypertrophy, but with an increased occurrence of SCD (Fowler *et al.*, 2009; Moolman *et al.*, 1997; Watkins *et al.*, 1995b).

Specific mutations within a given gene have also been thought to provide prognostic insights, with, for example, different *MYH7* mutations giving rise to varying clinical manifestations: The R403Q and R453C mutations were thought to result in the aforementioned, severe *MYH7* phenotype, whilst mutations N232S, G256E, V606M and V403Q have been associated with a more favourable outcome (Fowler *et al.*, 2009; Anan *et al.*, 1994; Marian & Roberts, 1998). Further reports include the increased risk of heart failure associated with the R719W<sub>*MYH7*</sub>, K183del<sub>*TNNI3*</sub> and IVS32del25nt<sub>*MYBPC3*</sub> mutations (Konno *et al.*, 2010).

However, genotype/phenotype correlations are clearly imperfect, with many contradictory reports of such correlations, as well as the occurrence of clinically unaffected mutation carriers (Dausse *et al.*, 1993; Carrier *et al.*, 1997). More recent description of phenotypic similarities between *MYH7*-HCM and *MYBPC3*-HCM (Van Driest *et al.*, 2004), as well as the marked clinical variability amongst homogenous carriers of the same disease-causing mutation indicate that the phenotype is not determined solely by the causal mutation. This implies the existence of additional determinants of disease expression, such as the environment, epigenetics and modifier genes.

### 1.2.3 Genetic modifiers of the hypertrophic phenotype in HCM

Modifier genes can further contribute to the genotype/phenotype disparity. These genes form part of the genetic background of a person, and are neither necessary nor sufficient to cause disease, but influence the clinical phenotype when present in addition to a disease-causing mutation (Alcalai *et al.*, 2008). The contribution of genetic background to disease expression is demonstrated in the diverse phenotypic expression of disease in families of different ethnic origin who carry the same causal mutation, as well as in monozygotic and dizygotic twin studies and transgenic animal models using different strains of animals, as described below:

Fananapazir and Epstein (1994) compared disease expression in unrelated Caucasian and Korean kindreds who carry an identical HCM-causing mutation in *MYH7*, R403Q. The phenotypic presentation varied significantly amongst the two different ethnic groups with reports of SCD and syncope or pre-syncope in the Caucasian kindred, but the complete absence thereof in the Korean family. Furthermore the majority of the Korean kindred showed LV outflow obstruction that was not observed in the Caucasian group. One possible explanation for the varying outcome is the differences in genetic make-up of the two ethnic groups.

Twin studies have shown greater intra-pair variance of LVM in dizygotic twins than in monozygotic twins, and higher concordance for cardiac size in monozygotic twins, dizygotic twins, and sibling pairs relative to non-related subjects, thereby highlighting the role of familial components, i.e. shared environment as well as shared genetic factors, in LVM (Adams *et al.*, 1985; Verhaaren *et al.*, 1991).

Numerous studies using transgenic animal models have identified genetic loci that affect LVM, independent of BP. Examples include a quantitative trait locus (QTL) on chromosome 2 and another on chromosome 3, identified via genome-wide searches, in spontaneously hypertensive rats (Innes *et al.*, 1998) and two inbred normotensive rat strains (Sebkhi *et al.*, 1999), respectively. Moreover a murine model of HCM, designated  $\alpha$ -MHC<sup>403/+</sup> as it represents the human *MYH7* R403Q causal mutation, allowed for breeding of the mutation into different mice strains, that is its introduction into different genetic backgrounds. Strain-dependent hypertrophic responses were observed in mice kept under the same conditions, thereby indicating a role for genetic modifiers that differed with the genetic background. Similar genetic loci, equivalent to the aforementioned QTLs identified in animal studies, may influence cardiac hypertrophy in humans (Semsarian *et al.*, 2001).

#### 1.2.4 Candidate genetic modifiers

Efforts aimed at identifying candidate modifier genes need to consider what is currently known regarding the pathogenesis of the cardiac phenotype in HCM. Although only partially elucidated, the latter is suggested to be multifaceted, including the primary disease-causing stimulus stemming from the diverse causal mutations and the resulting activation of signalling cascades that mediate the hypertrophic response (Kaludercic *et al.*, 2009; Alcalai *et al.*, 2008; Reviewed by Marian, 2010).

This is evident from a switch on-switch off bigenic mouse model that demonstrated induction and subsequent reversal of cardiac phenotypes of HCM as consequence of switching on and off, respectively, expression of a mutant transgene, Troponin T (TnT)-Q92, known to cause human HCM (Lutucuta *et al.*, 2004; Marian, 2009). The relevant cardiac phenotypes included interstitial fibrosis, enhanced cardiac systolic function, as well as increased expression of signalling kinases and pro-collagen genes. The same group further targeted various signalling pathways related to the cardiac hypertrophic response in animal models (Lombardi *et al.*, 2009; Marian *et al.*, 2006; Patel *et al.*, 2001; Senthil *et al.*, 2005; Tsybouleva *et al.*, 2004; Marian, 2009). These included efforts directed



at oxidative stress known to contribute to cardiac hypertrophy and fibrosis (Takimoto & Kass, 2007) and the development of HCM (Lombardi *et al.*, 2009; Marian *et al.*, 2006) via the administration of the antioxidant N-acetylcysteine (NAC) in two transgenic animal models of human HCM, namely  $\beta$ -MyHC-Q403 rabbits and cardiac troponin T (cTNT)-Q92 mice. The NAC treatment, which increases glutathione, an endogenous thiol that acts as intracellular defence against oxidative stress, reversed cardiac hypertrophy and fibrosis, whilst preventing left ventricular systolic dysfunction in these animal models.

Indeed, current opinion regarding the pathogenesis and treatment of cardiac hypertrophy in HCM suggests that the underlying molecular mechanisms are partially distinct, as the varying functional effects of the causal mutations (Refer to Section 1.2.1) give rise to diverse primary disease-causing stimuli that are suggested to be altered contractility, structure, myocardial energetics, and/or calcium ( $\text{Ca}^{2+}$ ) homeostasis. However, the eventual HCM phenotype is similar, comprising cardiac hypertrophy, thereby indicating that these different stimuli eventually activate common mechanisms pertaining to the cardiac hypertrophic response. Accordingly, the proposed targets for treatment of cardiac hypertrophy in HCM include the molecular mechanisms relevant to the initial stimulus or cardiac hypertrophic growth (Alcalai *et al.*, 2008; Ashrafian *et al.*, 2011; Reviewed by Marian, 2010). It stands to reason that as the aforementioned factors contribute to the development of cardiac hypertrophy in HCM, they can likewise be considered as candidate modifier genes, influencing the severity of the cardiac hypertrophy phenotype.

To date, it has mainly been components of pathways involved in the control of blood pressure (peptide hormones), for example, the components of the renin-angiotensin aldosterone system (RAAS), and other trophic factors such as endothelin-1 and tumor necrosis factor- $\alpha$  (TNF- $\alpha$ ) that have been investigated as hypertrophy modifiers in HCM based on their functions relating to cardiac growth and remodelling (Marian, 2002; Patel *et al.*, 2000; Alcalai *et al.*, 2008; Friedrich *et al.*, 2009; Marian, 2002; Nabel, 2003). However, replication studies in this field are few, and the few that have been reported have yielded inconsistent results (Marian, 2002; Nabel, 2003). Furthermore, it is important to note that these factors are relatively separated from the primary stimulus for cardiac hypertrophy. Arguably, the factors that closely interact with the primary stimulus have a greater capacity to modulate this stimulus, and ultimately the cardiac hypertrophic phenotype in HCM. That is to say, as the primary stimulus for hypertrophy arises from faulty sarcomeric functioning, factors that either improve or further weaken the structure or function of the sarcomere, including

sarcomere and sarcomere-associated proteins, and the enzymes that supply the sarcomere with the fuel it requires, should thus be considered as plausible candidate modifiers.

The aforementioned is supported by findings that gene dosage or the presence of multiple functional sarcomeric variants (compound and double heterozygotes), estimated to occur in 3–6% (Girolami *et al.*, 2010) of mutation positive individuals, are associated with a more severe disease expression and increased incidence of SCD (Reviewed by Keren *et al.*, 2008;Ingles *et al.*, 2005;Mohiddin *et al.*, 2003;Lekanne Deprez *et al.*, 2006;Richard *et al.*, 1999;Ho *et al.*, 2000). Similarly, more severe clinical phenotypes have been described in rare reports of triple mutations and homozygosity of causal mutations (Ho *et al.*, 2000;Girolami *et al.*, 2010;Scheffold *et al.*, 2011). The impact of additional sarcomeric variants on the hypertrophic phenotype will be discussed further in Section 1.2.4.1.

It is, therefore, important to consider the key factors that influence sarcomeric functioning together with the consequences of sarcomere gene mutations. An overview of these factors is given in the following section.

The sarcomere is the fundamental contractile unit in cardiac muscle (Refer to Figure 1.2). It is comprised of actin and myosin, the major constituents of the thin and thick filaments, respectively. They interact to produce contractile force; as a result of this, they slide over each other and ultimately give rise to muscle contraction (Reviewed by Harvey & Leinwand, 2011). This interaction, and thus contraction, is influenced by numerous factors, including adenosine-5'-triphosphate (ATP)-mediated conformational changes in myosin,  $\text{Ca}^{2+}$ -dependent changes in the spatial configuration of the trimeric troponin (Tn) complex, which indirectly determines the availability of the myosin binding site on actin, as well as additional sarcomeric proteins, which function in the assembly and integrity of the sarcomere as well as regulation of contraction (Seidman & Seidman, 2001;Flashman *et al.*, 2004;Reviewed by Chapelle, 1999).

HCM-causing mutations are mainly dominant-negative, in effect giving rise to 'poison peptides', i.e. incorporation of proteins with aberrant function into the sarcomere, affecting the function of the contractile unit. A further proposed consequence of at least some causal mutations is haploinsufficiency, which entails the reduced integration of functional protein into the sarcomere. More importantly, the causal mutations alter key biophysical properties of the contractile proteins,

including their  $\text{Ca}^{2+}$ -sensitivity, ATPase activity and maximal force production. For example, the R403Q mutant myosin isolated from HCM model mice exhibited increased actin-activated ATPase activity, actin filament sliding velocity and force production (Ho, 2010b;Palmiter *et al.*, 2000;Tyska *et al.*, 2000). Conversely, functional studies of mutant TnT indicated reduced actin-activated ATPase activity and force production (Mukherjea *et al.*, 1999). It has been suggested that these diverse defects give rise to energy deficiency and altered  $\text{Ca}^{2+}$ -handling as the primary stimulus for the development of the cardiac hypertrophy phenotype in HCM (Konno *et al.*, 2010;Ashrafian *et al.*, 2011). Collectively, the aforementioned highlight the importance of the structural integrity of the proteins of the sarcomere,  $\text{Ca}^{2+}$ -handling and myocardial energetics in normal sarcomeric functioning as well as in the development of the cardiac hypertrophy phenotype in HCM.

Thus, it can be hypothesised that amongst other possible candidate LVH-modifying genes, genes involved in sarcomere integrity and contractility or its regulation, or myocardial energetics at the sarcomere, are certainly plausible as modifiers of cardiac hypertrophy in HCM. The following sections will investigate the proof of principle for this hypothesis.

#### 1.2.4.1 Sarcomeric modifiers

To recap, HCM-causing mutations mainly compromise the integrity of sarcomeric proteins and factors in proximity, both physical and functional, to this primary defect, i.e. additional sarcomeric variants, have a greater potential to modify the outcome of the primary functional defect, owing to the complex interrelations of the sarcomeric protein components. This notion is supported by studies detailing the phenotypic consequence of multiple functional sarcomeric gene variants.

As previously mentioned, individuals homozygous, double heterozygous or compound heterozygous for sarcomeric gene variants are often more severely affected in terms of hypertrophy, and at greater risk of death, than individuals who are heterozygous for single causal mutations (Richard *et al.*, 1999;Ingles *et al.*, 2005;Keren *et al.*, 2008;Lekanne Deprez *et al.*, 2006;Mohiddin *et al.*, 2003;Tsoutsman *et al.*, 2008a;Ho *et al.*, 2000). Ho *et al.* (2000) reported on the S179F<sub>TNNT2</sub> mutation, which, when present in the heterozygous state, is associated with a benign HCM phenotype. In contrast, homozygosity for the mutation was associated with striking biventricular hypertrophy and juvenile lethality. Individuals double heterozygous for HCM-causing mutations (E483K<sub>MYH7</sub>/E1096\*<sub>MYBPC3</sub>) were first described by Richard *et al.* (1999). These authors noted

marked left ventricular hypertrophy in these patients relative to single heterozygous mutation carriers (mLVST of  $30.5 \pm 3.5$  mm vs.  $19.5 \pm 2.1$  mm;  $p < 0.05$ ). Similarly, Ingles *et al.* (2005) found that individuals compound heterozygous for causal mutations (D745G<sub>MYBPC3</sub>/P873H<sub>MYBPC3</sub>, E542Q<sub>MYBPC3</sub>/A851V<sub>MYBPC3</sub>, or R326Q<sub>MYBPC3</sub>/Q1233\*<sub>MYBPC3</sub>) showed significantly larger LVWT compared to patients heterozygous for a single mutation (LVWT of  $30.7 \pm 3.1$  mm vs.  $24.4 \pm 7.4$ ;  $p < 0.05$ ). Moreover, SCD events occurred more frequently in patients from multiple-mutation families than in affected members from single-mutation families (6/14 (43%) vs. 10/55 (18%);  $p = 0.05$ ).

Studies of transgenic animal models mirror these effects, as homozygotes and double heterozygotes proved less viable or more severely affected than heterozygotes (Fatkin *et al.*, 1999; Berul *et al.*, 2001; Tsoutsman *et al.*, 2008a). The  $\alpha$ -MHC<sup>403/403</sup> mouse model, representing homozygosity for the HCM-causing R403W<sub>MYH7</sub> mutation identified in humans, showed neonatal onset of the phenotype, characterised by decreased LVWT, reduced systolic contraction, progression to dilated cardiomyopathy (DCM), and ultimately 100% mortality by postnatal day eight (Fatkin *et al.*, 1999; Debold *et al.*, 2007). Similarly, double-mutant mice heterozygous for both the aforementioned mutation and the G203S<sub>TNNI3</sub> mutation exhibited neonatal onset of phenotype, eventual DCM, and 100% mortality albeit by age 21 days (Tsoutsman *et al.*, 2008b). However, a less severe phenotype is seen in mice heterozygous for the mutation ( $\alpha$ -MHC<sup>403/+</sup>), with a relatively later onset at 30 weeks, a normal life span and typical HCM characteristics, including left ventricular hypertrophy, myocyte disarray and fibrosis (Tsoutsman *et al.*, 2008a; Berul *et al.*, 2001).

Specific attention should be given to additional variants present in the same gene as the primary sarcomeric HCM-causing mutation (Hershberger, 2010). A *cis*-acting variant tightly linked to the latter (within the same gene) is more likely to cosegregate with the disease-allele and consistently impact on the HCM phenotype (Blair *et al.*, 2001a). As previously hypothesised, factors that closely interact with the primary stimulus have a greater capacity to influence it (Refer to Section 1.2.4). Variants in *cis* with the primary mutation are deemed closest; a striking example of their capacity to influence the primary trigger is the development of one of two distinct diseases caused by the same primary mutation (D179N) in the prion protein gene (*PRNP*). The eventual phenotype is dictated by a common polymorphism on the same allele (codon 129), with the presence of Met or Val resulting in the development of fatal familial insomnia (FFI) or Creutzfeldt-Jakob disease (CJD), respectively (Genin *et al.*, 2008; Goldfarb *et al.*, 1992). Furthermore, this study emphasizes the importance of

investigating variants present on the non-mutated allele, i.e. variants in *trans* relative to the primary mutation. The FFI disease severity varies according to the state of the codon 129 polymorphism. The homozygous Met/Met<sup>129</sup> genotype is associated with a shorter disease course and thalamic hypometabolism, whereas the heterozygous Met/Val<sup>129</sup> state is met with increased disease duration and more widespread brain hypometabolism (Taberner *et al.*, 2000; Montagna *et al.*, 2003).

Finally, *trans*-acting variants may give rise to more severe phenotypes, as these can completely abolish the normal functioning of the relevant protein (Demo *et al.*, 2009). An example is the association of a high-risk HCM phenotype with the compound genotype of R719W<sub>MYH7</sub> and M349T<sub>MYH7</sub>. Where these mutations were present in *trans*, the patient had no normal myosin, resulting in a severe phenotype characterised by cardiac arrest at age 6 and a half years. Interestingly, M349T<sub>MYH7</sub>, characterised as a recessive mutation due to its absence from 130 control individuals, was not sufficient to cause disease on its own, but exacerbated the phenotype normally associated with the R719W<sub>MYH7</sub> mutation. The latter is typically associated with a severe hypertrophy phenotype and a high incidence of SCD in young adults. These findings thus suggest that the disease phenotype may reflect effects of a *trans* allele, which would otherwise be tolerated in the presence of normal protein, but of which the effect is amplified in the absence of normal protein (Jeschke *et al.*, 1998).

A further aspect to consider is that *cis*-acting variants are believed to regulate mRNA expression, thereby contributing to inter-individual phenotypic variability, including risk of developing disease. Similarly, these *cis*-variants and the resulting variation in allelic expression may modify disease severity particularly in combination with a causal mutation (Jentarra *et al.*, 2011; Southam *et al.*, 2007; Bray *et al.*, 2003). Tuberous sclerosis complex (TSC) disorder is characterised by phenotypic heterogeneity, even amongst individuals from the same pedigree who carry an identical causal mutation (Lyczkowski *et al.*, 2007; Jentarra *et al.*, 2011), which is reminiscent of the situation in HCM. It is an autosomal dominant disease; affected individuals are therefore heterozygous mutation carriers with one mutated and one non-mutated allele (van Slegtenhorst *et al.*, 1997). Jentarra *et al.* (2011) aimed to elucidate the factors underlying the phenotypic variability and hypothesised that the expression of the two alleles relative to each other may modify the disease phenotype. For example, high expression of the mutant protein perhaps due to a *cis*-acting variant may exacerbate the severity of the disease phenotype. Conversely, high levels of expression of the non-mutated allele as a result of a variant in *trans* relative to the causal mutation, that is a variant on

the normal allele, may ameliorate the effects of the mutant protein. Considering that HCM shares many of these aspects, it could similarly be hypothesised that *cis*- or *trans*-acting variants that influence mRNA expression may modulate the HCM hypertrophy phenotype.

Moreover, the premise that a second variant may ameliorate the effects of the causal mutation is supported by investigations in *Drosophila* (Kronert *et al.*, 1999;Prado *et al.*, 1995;Naimi *et al.*, 2001). Flies exhibiting a raised wing phenotype as a consequence of the *held-up<sup>2</sup>* (*hdp<sup>2</sup>*) missense mutation in the Troponin I (*wupA*) gene were mutagenized to induce suppressor mutants. A second mutation in the Troponin I (TnI) gene rescued the structural and functional defects linked to the *hdp<sup>2</sup>* phenotype, as muscle carrying both mutations showed near normal myofibrillar structure, as compared to the *hdp<sup>2</sup>*-only muscle, which is characterised by shortened and supercontracted sarcomere and the absence of a defined M-band (Prado *et al.*, 1995). Similarly, Naimi *et al.* (2001) characterised a mutation in the Tropomyosin-2 (Tm2) gene that completely suppresses the *hdp<sup>2</sup>* phenotype. These findings evidenced a functional link between distinct sarcomeric gene mutations, where an alteration in one sarcomeric protein could suppress the effect of a mutation in another or the same sarcomeric gene, thus acting as a modifier of sarcomeric function. Intriguingly, Wei *et al.* (2010) reported that two dominant-negative mutations in the TnI and TnT genes (R111C and an abnormal splicing variant, respectively), individually implicated in the development of DCM in wild turkeys, could rescue cardiac function when present in combination in a transgenic mouse model (Biesiadecki *et al.*, 2004;Wei *et al.*, 2010;Biesiadecki & Jin, 2002).

Most importantly, the literature includes reports of sarcomeric variants that by themselves do not cause disease, but, when present in combination with an HCM-causing mutation, influence disease severity. The first example of this is the afore-described M349T<sub>MYH7</sub> mutation not found to be associated with HCM when present alone. However, compound heterozygosity of M349T<sub>MYH7</sub> and R719W<sub>MYH7</sub> is characterised by a more severe HCM phenotype than that typically associated with the R719W<sub>MYH7</sub> mutation (Jeschke *et al.*, 1998;Wang *et al.*, 2005). A further study identified the A/G<sup>1843</sup> polymorphism in the *MYBPC3* gene, and consequently revealed an association between the GG-genotype and increased LVWT (25.2 ± 5.9 mm) in HCM patients. The genotype frequencies were similar in the patient and control groups, thereby suggesting that the polymorphism is a modifier variant rather than a causal mutation (Wang *et al.*, 2005). Therefore, it seems plausible that variations in sarcomeric genes, and possibly even those that appear to be non-pathogenic in themselves, can contribute to the phenotypic expression of the causal mutation, not

only causing exacerbation of the phenotype, but, in some cases, also completely or partially suppressing the phenotype.

However, not only factors that are physically “close”, but also those that are functionally “close” to the causal mutation may plausibly be more likely to affect the phenotype. This implies that factors that relate to the pathoetiological mechanism, viz., the effect of the causal mutation, may be plausible modifiers. In HCM, this includes factors involved in sarcomeric and myocytic energetics.

#### **1.2.4.2 Energy modifiers**

Cardiac function demands a high and continuous supply of energy (Lopaschuk *et al.*, 2010). Altered cardiac energy metabolism has been linked to numerous disease states, including cardiac hypertrophy. Whether compensatory or maladaptive, it is clear that such alterations play a role in modulating disease development (Huss & Kelly, 2005;Ussher & Lopaschuk, 2006). As previously postulated, this study aimed to evaluate the contribution of sarcomere and sarcomere-associated genes as disease modifiers, as these arguably have a greater potential to influence the primary stimulus, which is disrupted sarcomere integrity (Refer to Section 1.2.4). Genes related to myocardial energetics form part of this category of candidates, as there is evidence for the binding of, for example, glycolytic enzymes to numerous regions of the sarcomere (Kraft *et al.*, 2000;Offer *et al.*, 1988;Ashby *et al.*, 1979;Freydina *et al.*, 1986). Furthermore, myosin ATPase is the main consumer of ATP in the cardiac myocyte and the disruption thereof, in keeping with the central hypothesis, would directly compromise the activity of key sarcomeric proteins and hence sarcomeric integrity (Cambronerio *et al.*, 2009). It is therefore necessary to consider the relevant energy metabolic pathways; a brief description of myocardial energetics and accompanying figures are provided in the following section:

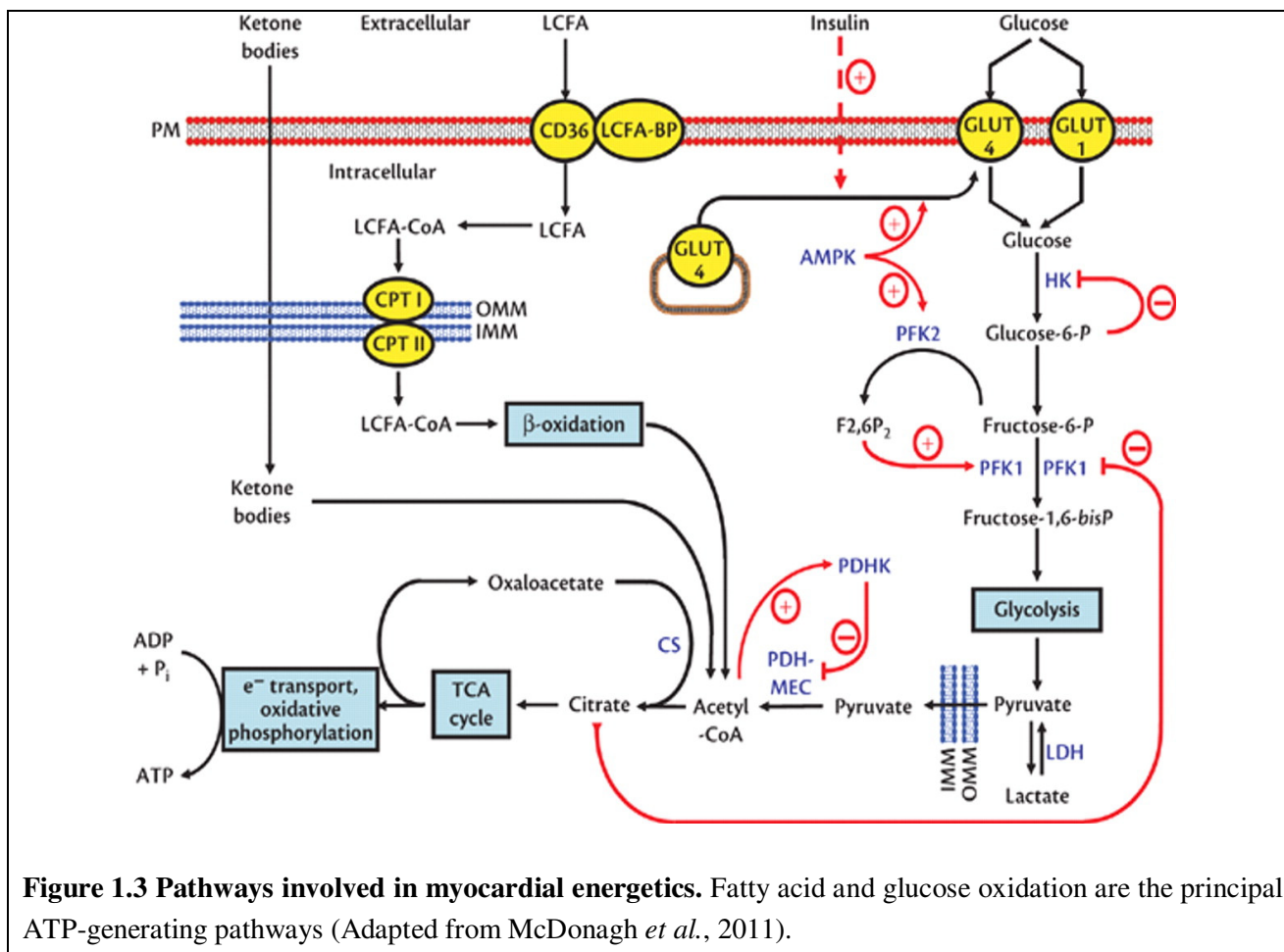
##### **1.2.4.2.1 Overview of myocardial energetics**

In the adult heart,  $\beta$ -oxidation of fatty acids is the predominant source of fuel responsible for up to 95% of ATP-production, whereas carbohydrate substrate utilisation, comprising mainly glucose breakdown via glycolysis, accounts for an estimated 5% thereof (Scolletta & Biagioli, 2010;McDonagh *et al.*, 2011) (Refer to Figure 1.3). Other substrates, including lactate, amino acids and ketone bodies, can be oxidised under specialised conditions (McDonagh *et al.*, 2011;Kodde *et*

*al.*, 2007). The initial step of lipid metabolism is the facilitated transport of long chain fatty acids (LCFAs) across the plasma membrane (PM) by means of the fatty acid translocase transmembrane protein (FAT/CD36), in combination with the plasma membrane LCFA-binding protein. Once in the cytoplasm, LCFAs are converted to their active form, LCFA-coenzyme A (LCFA-CoA), and transported across the outer and inner mitochondrial membranes (OMM and IMM) by carnitine palmitoyl transferase I and II (CPT1 and CPT2), respectively. Thereafter, LCFA-CoA undergoes stepwise degradation by the  $\beta$ -oxidation pathway to form acetyl-CoA (Luiken *et al.*, 2009;McDonagh *et al.*, 2011).

However, glucose can also be used as an energy source in heart muscle. Glucose metabolism entails firstly the transport of glucose across the plasma membrane via glucose transporter family members 1 and 4 (GLUT1 and GLUT4) (Scolletta & Biagioli, 2010;Schwenk *et al.*, 2008). Next, glucose enters the glycolytic pathway, where it is oxidized to pyruvate. The latter is transported into the mitochondria, where it undergoes further oxidation by the pyruvate dehydrogenase (PDH) complex to form acetyl-CoA (Patel & Roche, 1990;Schwenk *et al.*, 2008).





Both fatty acid- and glucose-derived acetyl-CoA condenses with oxaloacetate to form citrate, thereby entering the tricarboxylic acid (TCA) cycle (Refer to Figure 1.4). The cycle is characterised by a series of biochemical reactions that degrade the acetyl-CoA entering the cycle into its carbon, hydrogen and electron components. The first is released as carbon dioxide ( $\text{CO}_2$ ), whilst the remainder reduce the hydrogen-carrier molecules nicotinamide adenine dinucleotide ( $\text{NAD}^+$ ) and flavin adenine dinucleotide (FAD), generating NADH and  $\text{FADH}_2$ , respectively.

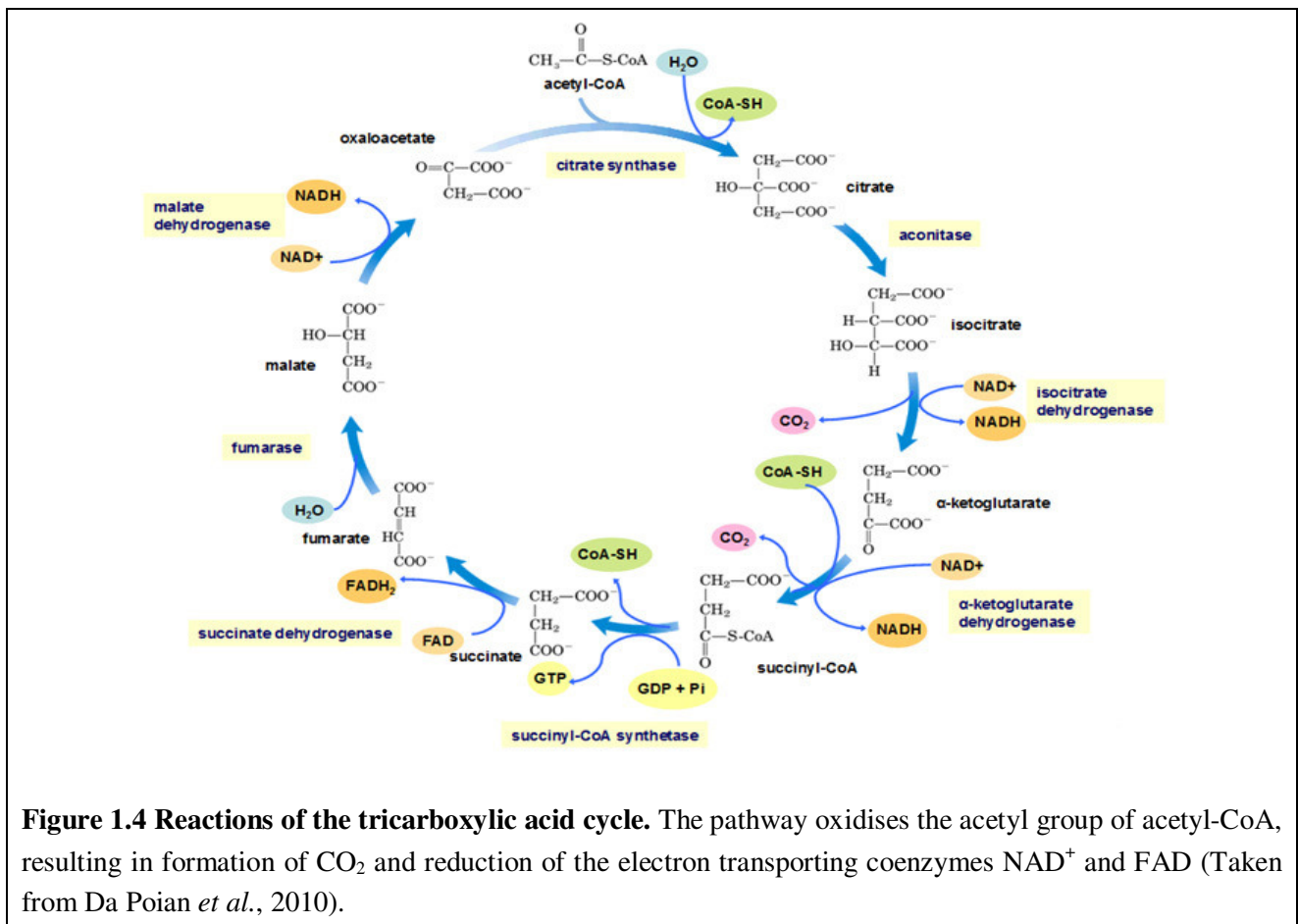


**Figure 1.4 Reactions of the tricarboxylic acid cycle.** The pathway oxidises the acetyl group of acetyl-CoA, resulting in formation of CO<sub>2</sub> and reduction of the electron transporting coenzymes NAD<sup>+</sup> and FAD (Taken from Da Poian *et al.*, 2010).

The reduced molecules subsequently enter the electron transport chain that is characterised as the primary site of ATP synthesis. More specifically, the high-energy electrons are extracted from NADH and FADH and passed down a series of electron-carrier molecules, with the energy released used to transport hydrogen ions from the mitochondrial matrix to the intermembrane space. This gives rise to both a pH gradient and a potential difference across the IMM that encourages the flow of hydrogen ions (H<sup>+</sup>) back into the matrix. The resulting movement activates the ATP synthase enzyme responsible for the formation of ATP from adenosine diphosphate (ADP) + P<sub>i</sub>. The progressive transfer of electrons concludes with oxygen (O<sub>2</sub>) as the ultimate acceptor; the process is, therefore, known as oxidative phosphorylation (Refer to Figure 1.5) (McDonagh *et al.*, 2011; Huss & Kelly, 2005; Sherwood, 2004).

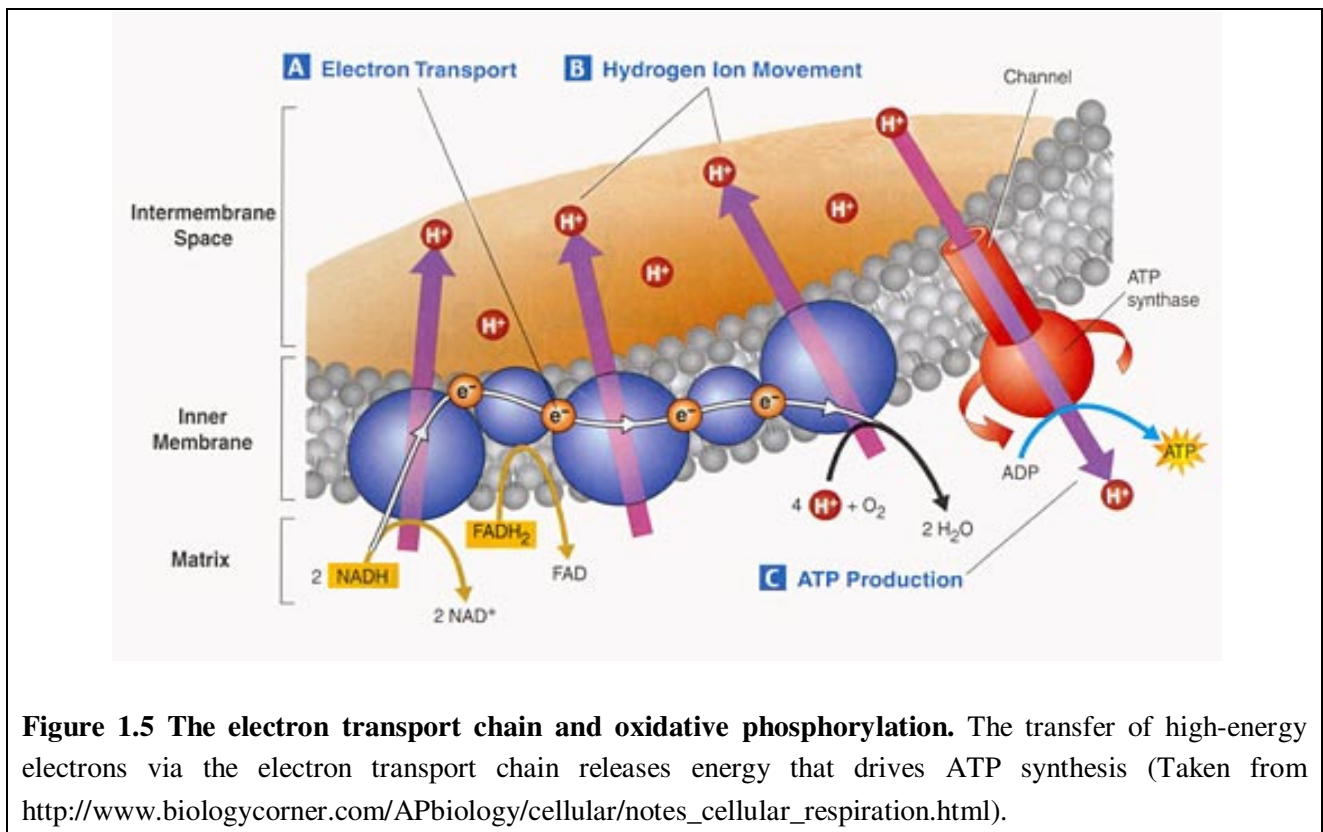
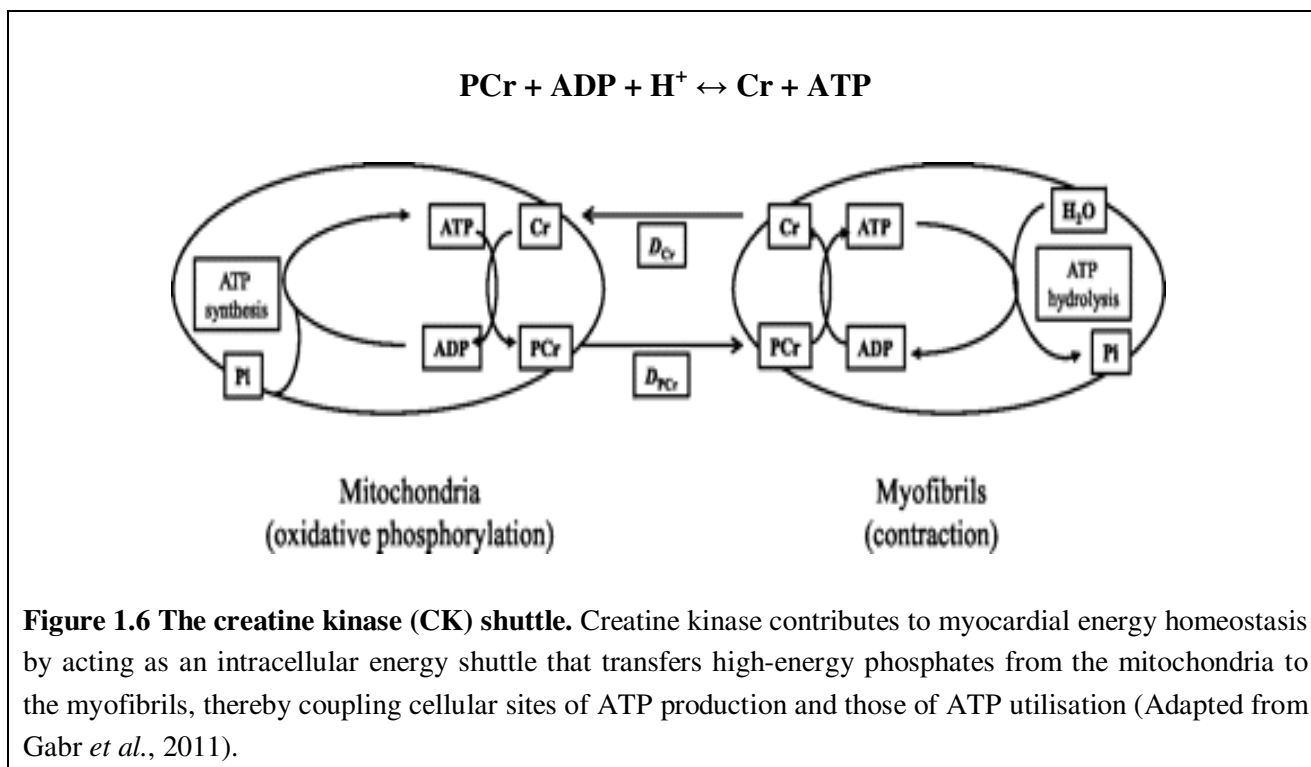


**Figure 1.5 The electron transport chain and oxidative phosphorylation.** The transfer of high-energy electrons via the electron transport chain releases energy that drives ATP synthesis (Taken from [http://www.biologycorner.com/APbiology/cellular/notes\\_cellular\\_respiration.html](http://www.biologycorner.com/APbiology/cellular/notes_cellular_respiration.html)).

ATP transfer to the site of energy consumption at the myofibrils is achieved by means of either direct channelling or via the creatine kinase (CK) energy shuttle (Refer to Figure 1.6). Firstly, the high-energy phosphate of mitochondrial ATP is transferred to creatine (Cr) to form phosphocreatine (PCr) and ADP, in a reaction catalysed by mitochondrial creatine kinase (MtCK). Next, PCr diffuses to the myofibrils, where myofibrillar/muscle-type creatine kinase (MM-CK) catalyses the reverse reaction, thereby regenerating ATP for muscle contraction. Moreover, the creatine kinase system is an essential energy buffer that maintains normal ATP levels under various conditions, including during times of rapid ATP utilisation (stressed conditions) (Scolletta & Biagioli, 2010; Bessman & Geiger, 1981; Gabr *et al.*, 2011; McDonagh *et al.*, 2011; Wilding *et al.*, 2006).



#### 1.2.4.2.2 Energy genes as candidate modifiers

Support for the hypothesised role of energy compromise in the development of hypertrophy includes the disrupted myocardial energetics observed in diseases phenotypically similar to HCM, inefficient ATP usage as consequence of sarcomeric mutations, and the decreased PCr/ATP ratio and metabolic remodelling observed in HCM patients (Ashrafian *et al.*, 2011; Jung *et al.*, 1998; Ho, 2010b; Blair *et al.*, 2001b).

For example, Friedreich ataxia is characterised by an HCM-like phenotype and is caused by the reduced expression of the mitochondrial protein frataxin due to a GAA repeat expansion in the *FRDA* gene. Results from an *in vivo* study indicated not only a consequential decrease in skeletal muscle mitochondrial ATP production but an inverse correlation thereof with the number of GAA repeats. Collectively these findings suggest that such metabolic defects may contribute to HCM development (Puccio & Koenig, 2000; Lodi *et al.*, 1999). Similarly, mutations in mitochondrial transfer RNA (tRNA) genes have shown association with syndromes phenotypically indistinguishable from HCM. Reports include a point mutation in the mitochondrial tRNA<sup>glycine</sup> gene (T-to-C transition at nucleotide 9997), where the authors noted a resulting decrease in ATP synthesis and a relationship between the degree of mutant mitochondrial DNA (mtDNA) and the

severity of symptoms. These findings propose that mitochondrial defects, and consequential disrupted energy homeostasis, could contribute to HCM, and, given the phenomenon of heteroplasmy, account for the phenotypic variability observed even amongst family members (Merante *et al.*, 1994).

The notion is supported by findings of impaired mitochondrial function and organization in HCM studies of both patients and mouse models. Observations included, amongst others, relatively fewer mitochondria in direct contact with myofibrils, as well as larger mitochondria with disorganised cristae, noted upon electron microscopic analysis of ventricular specimens taken from HCM patients. The authors speculated that the altered localisation may decrease the efficiency with which ATP produced in the mitochondria reaches the myofibrillar sites of energy consumption (Unno *et al.*, 2009; Lucas *et al.*, 2003). The equivalent was observed in an HCM animal model, as ultrastructural characterisation of TnI-203/MHC-403 mice hearts revealed altered distribution of mitochondria between myofibrils (Tsoutsman *et al.*, 2008b).

Likewise, defects in genes encoding proteins key to myocardial energetics give rise to an HCM-like phenotype (Cambroneo *et al.*, 2009). For instance, these include impaired myocardial LCFA fatty acid uptake, due to CD36-deficiency, and glycogen accumulation, due to mutations in *PRKAG2*, which encodes the gamma 2 regulatory subunit of AMP-activated protein kinase (AMPK), a sensor and regulator of energy homeostasis (Refer to section 1.2.1) (Scheffold *et al.*, 2011; Okamoto *et al.*, 1998; Hardie & Carling, 1997).

Further motivation for the proposed role of energy genes as candidate modifiers is that the numerous HCM-causing sarcomeric mutations do not exhibit unified effects on the force-generating capabilities and/or the calcium-sensitivity of the sarcomere, as they seemingly give rise to either hyper- or hypocontractility (Refer to section 1.2.4) (Luedde *et al.*, 2009; Redwood *et al.*, 1999; Reviewed by Bonne *et al.*, 1998; Blair *et al.*, 2001b). Rather, myocardial energy deficiency, resulting from inefficient or excessive ATP utilisation, has been proposed as the abnormality common to the diverse HCM-causing mutations (Ashrafian *et al.*, 2003; Ashrafian *et al.*, 2003; Crilley *et al.*, 2003; Ferrantini *et al.*, 2009; Blair *et al.*, 2001b). The contractile reserve and energy required for homeostatic function, such as  $\text{Ca}^{2+}$  re-uptake, is consequently compromised, resulting in hypertrophy (Ashrafian *et al.*, 2003; Javadpour *et al.*, 2003).

Studies of HCM mouse models bearing either the R92Q mutation in the cTnT gene or the R403Q mutation in the murine  $\alpha$ -myosin heavy chain ( $\alpha$ MyHC) gene, serve as key examples as they are believed to give rise to hypercontractility and hypocontractility, respectively, but ultimately show myocardial energy deficiency. Investigations of the first model yielded findings indicating reduced free energy of ATP hydrolysis ( $\Delta G_{-ATP}$ ), resulting from decreased [PCr], increased inorganic phosphate [Pi] and [ADP], as well as normal total creatine, and an inability to support increased contractile performance upon inotropic challenge. The authors speculated that these observations could be attributed to increased ATP consumption, either by the myofibrillar ATPase or by the sarcoplasmic reticulum  $Ca^{2+}$ -ATPase (SERCA), or to decreased ATP synthesis. Having considered additional findings from the literature, as well as their own experimental data, Javadpour *et al.* (2003) concluded that the mutation alters the TM-actin interaction, and thereby crossbridge cycling, which ultimately increases myofibrillar ATP consumption. For example, the authors noted that R92Q and non-transgenic (NTG) hearts did not differ significantly upon comparison of their SERCA mRNA levels or their ATP-generating capacity (Javadpour *et al.*, 2003; Tardiff *et al.*, 1999).

Similarly, the R403Q mouse model showed decreased [PCr] and increased [Pi], with a resulting decrease in  $\Delta G_{-ATP}$  (Javadpour *et al.*, 2003; Spindler *et al.*, 1998). Ferrantini *et al.* (2009) proposed that the decrease in the latter may prove sufficient to compromise SERCA function and  $Ca^{2+}$  reuptake into the sarcoplasmic reticulum (SR) and that, as consequence, increased  $Ca^{2+}$  concentrations within select microdomains would activate signalling pathways that mediate hypertrophy. The R403Q mutation is proposed to increase the cost of contraction, as mutant myosin heads create a drag on wild-type crossbridges, which may precipitate the aforementioned alterations in cardiac energetics (Spindler *et al.*, 1998; He *et al.*, 2007; Crilley *et al.*, 2003).

Most noteworthy is that neither of the two aforementioned mutations is located close to the myosin ATP-hydrolysis region, yet they give rise to increased ATP utilisation, which highlights the contribution of structural alterations to disrupted myocardial energetics (Javadpour *et al.*, 2003).

In addition, a muscle LIM protein (MLP)-null mouse model of HCM exhibited cytoarchitectural perturbation, which included disorganized myofibrils and looser integration of mitochondria relative to the SR and myofibrils (Wilding *et al.*, 2006). The study compared SR calcium uptake in myofibres from MLP-null mice and controls, whilst varying the method whereby ATP required for

the process was transferred from the mitochondria to the SR calcium pump, i.e. via CK-mediated transport or via mitochondrial direct ATP channelling. Calcium uptake was similar amongst mutant and wild type fibres when the energy was delivered by means of CK transport and 36% lower when provided by the mitochondria directly, despite normal mitochondrial content and oxidative capacity. Congruent with the foregoing, these findings link structural defects to altered energy transfer and compromised myocardial energetics.

Furthermore, numerous HCM-causing mutations that augment  $\text{Ca}^{2+}$ -sensitivity, also exhibit a resulting increase in energy consumption (Wu *et al.*, 2012;Ho, 2010b). More specifically, Wu *et al.* (2012) simulated the ATP consumption rates of such cardiac troponin I (cTnI) mutants (G203S, K206Q, R162W,  $\Delta$ K183, R145Q and R145G) and wild type fibres at the level of contraction, SERCA and the  $\text{Na}^+$ ,  $\text{K}^+$ -ATPase, and concluded that the higher energy consumption is specifically due to the increased demands of contraction.

The contribution of compromised myocardial energetics is further evident from  $^{31}\text{P}$  magnetic resonance spectroscopy (MRS) studies of HCM patients, as reflected by their significantly decreased PCr/ATP ratios. More importantly, clinically unaffected mutation carriers similarly exhibit decreased PCr/ATP ratios, suggesting that disrupted myocardial energetics is primary to hypertrophic growth (Luedde *et al.*, 2009;Ho, 2010b;Jung *et al.*, 1998). Parallel to these findings, Jung *et al.* (1998) observed a shift in energy substrate utilisation from fatty acid to glucose metabolism in asymptomatic HCM patients. The altered myocardial metabolism is proposed to be beneficial, as glucose metabolism produces more ATP at a lower oxygen cost relative to fatty acid utilisation (Horowitz *et al.*, 2010;Tuunanen *et al.*, 2006). In keeping with these observations, treatment of HCM patients with perhexiline, an inhibitor of the LCFA transporters CPT-1/2, corrected energy deficiency and improved exercise capacity (Ashrafian *et al.*, 2011;Abozguia *et al.*, 2010). Similarly, results from the previously mentioned Wu *et al.* (2012) simulations indicated ~40% lower fatty acid oxidation (FAO) in cTnI-mutant groups compared to wild type during high-energy-requirement conditions.

In contrast, the upregulation of metabolic genes linked to fatty acid metabolism was observed in a transgenic rat model of HCM characterised by the overexpression of a truncated cTnT (Luedde *et al.*, 2009). Upregulation was proposed to be compensatory and was identified in the absence of altered left ventricular function and morphology, again suggesting that changes in myocardial

energetics is primary in HCM development, rather than being the result of hypertrophy. The metabolic measurements of HCM patients who harbour the D175<sub>TPMI</sub> mutation showed increased myocardial FFA and oxidative metabolism (Tuunanen *et al.*, 2007). Moreover, a spontaneously hypertensive rat (SHR) model, characterised by CD36-deficiency, indicated that diet supplementation with short-chain fatty acids (SCFA), the uptake of which is CD36-independent, eliminated cardiac hypertrophy. The results linked defective fatty acid uptake, and by implication CD36, to cardiac hypertrophy, leading the authors to suggest a role for SCFA supplementation in human hypertrophic cardiomyopathy (Hajri *et al.*, 2001). Finally, acute FFA withdrawal in cardiomyopathic HF patients depressed cardiac work and efficiency. The failing heart seemingly requires both glucose and fatty acid oxidation for optimal function (Tuunanen *et al.*, 2006).

Although contradictory, these findings irrefutably implicate altered myocardial energetics in the pathogenesis of HCM and suggest that modulation of cardiac energetics should not aim to shift metabolism towards either glucose or fatty acid utilisation, but should rather focus on improving the metabolic adaptability of the heart (Kolwicz, Jr. & Tian, 2009).

In summary, the energy compromise hypothesis suggests that the HCM phenotype arises from decreased ATP synthesis (e.g. mitochondrial mutations), inefficient ATP utilisation (e.g. increased myofibrillar demand) or altered energy sensing (AMPK mutations) (Watkins *et al.*, 2011). It is probable that such energy-related factors may also act to modify the HCM phenotype, as motivated by the recent screening of a 2-year-old-boy who presented with severe HCM. Genetic analysis revealed two HCM-causing mutations in the *MYBPC3* gene (R326Q and Q1233X), and a third in the *PRKAG2* gene (P83S). The triple mutation status was further detected in his symptomatic mother, whilst only the two *MYBPC3* mutations and the *PRKAG2* mutation alone was identified in his 10-year-old unaffected brother and his 13-year-old-brother exhibiting left ventricular hypertrophy in the absence of clinical symptoms, respectively. The *PRKAG2* mutation, although not a modifier *per se*, as it is suspected to cause glycogen storage disease (GSD), augmented the severity of the HCM phenotype, whilst showing variable expression in the 2-year-old-boy and his mother (Scheffold *et al.*, 2011).



### 1.3 The present study

The present study forms part of a larger investigation aimed at identifying genetic factors that modulate the development of hypertrophy in 27 South African HCM families of either Caucasian or Mixed Ancestry descent in which one of three unique HCM-causing founder mutations, namely R92W<sub>TNNT2</sub>, R403W<sub>MYH7</sub> and A797T<sub>MYH7</sub>, segregates. Based on the preceding literature review, it is evident that factors pertaining to sarcomere integrity and contractility, as well as factors pertaining to myocardial energetics are plausible modifiers of cardiac hypertrophy in HCM. The current study thus aimed to evaluate the contributions of sarcomeric genes, encoding proteins involved most directly in the control of the crossbridge cycling, of which many have themselves been implicated as primary HCM-causing genes, as well as genes encoding enzymes and proteins involved in energy metabolism, in the modulation of LVH in this South African HCM cohort. A total of 26 candidate genes (Refer to sections 2.3.1 and 2.3.3) were selected from the literature based on their functions either as structural proteins constituting the functional part of the sarcomere, or as metabolic proteins relating to myocardial energetics. Medium-high-throughput genotyping was achieved using ABI TaqMan® SNP Validated genotyping assays. Quantitative indices of hypertrophy, including various wall thickness measurements and LVM, were then tested for association with multiple single polymorphisms within any given candidate gene, as well as genetic haplotypes, by means of family-based statistical analysis, independent of HCM-causing founder mutation and known covariates of hypertrophy.

## CHAPTER TWO

### MATERIALS AND METHODS

---

#### 2.1 Study participants

The current research project (N04/03/062) received ethical clearance by the University of Stellenbosch Health Sciences Faculty's Institutional Review Committee that adheres to the principles of the Declaration of Helsinki. All study participants gave written informed consent permitting blood sample collection, DNA extraction and molecular genetic testing.

A panel of South African HCM probands, from either Caucasian or Mixed Ancestry descent, was previously screened for HCM-causing mutations in 11 sarcomeric genes. This led to the identification of 27 probands bearing one of three mutations previously characterised by Moolman-Smook *et al.* (1999) as South African HCM-founder mutations, namely R403W in *MYH7* (*MYH7*<sub>R403W</sub>), A797T in *MYH7* (*MYH7*<sub>A797T</sub>) and R92W in *TNNT2* (*TNNT2*<sub>R92W</sub>). Pedigree tracing was performed, consenting relatives older than 18 years were entered into the modifier gene study and their carrier-status determined for each of the founder mutations.

At the time of this modifier gene study the founder-mutation familial cohort thus consisted of 388 genetically and clinically affected and unaffected individuals from 27 South African HCM families (Refer to Table 2.1) of self-reported Caucasian or Mixed Ancestry descent.

**Table 2.1 Composition of the study population of the South African HCM-families**

Pedigree number	Ethnic group	Gene	Mutation	N	
				Mutation carriers	Non-carriers
100	Mixed Ancestry	<i>TNNT2</i>	R92W	16	30
103	Mixed Ancestry	<i>TNNT2</i>	R92W	2	3
109	Mixed Ancestry	<i>TNNT2</i>	R92W	6	4
139	Mixed Ancestry	<i>TNNT2</i>	R92W	15	22
137	Mixed Ancestry	<i>TNNT2</i>	R92W	2	5
149	Mixed Ancestry	<i>TNNT2</i>	R92W	4	6
173	Mixed Ancestry	<i>TNNT2</i>	R92W	2	1
179	Mixed Ancestry	<i>TNNT2</i>	R92W	5	4
188	Mixed Ancestry	<i>TNNT2</i>	R92W	3	1
106	Mixed Ancestry	<i>MYH7</i>	R403W	29	35
134	Mixed Ancestry	<i>MYH7</i>	R403W	4	7
157	Mixed Ancestry	<i>MYH7</i>	R403W	1	3
101	Caucasian	<i>MYH7</i>	A797T	12	9
104	Mixed Ancestry	<i>MYH7</i>	A797T	7	7
123	Mixed Ancestry	<i>MYH7</i>	A797T	6	10
124	Caucasian	<i>MYH7</i>	A797T	1	4
131	Caucasian	<i>MYH7</i>	A797T	12	11
138	Caucasian	<i>MYH7</i>	A797T	13	17
145	Mixed Ancestry	<i>MYH7</i>	A797T	3	2
147	Mixed Ancestry	<i>MYH7</i>	A797T	4	5
158	Caucasian	<i>MYH7</i>	A797T	2	3
159	Mixed Ancestry	<i>MYH7</i>	A797T	5	7
163	Caucasian	<i>MYH7</i>	A797T	6	3
172	Caucasian	<i>MYH7</i>	A797T	7	10
177	Caucasian	<i>MYH7</i>	A797T	3	1
180	Caucasian	<i>MYH7</i>	A797T	4	1
190	Caucasian	<i>MYH7</i>	A797T	2	1

**Abbreviations:** A-Alanine; *MYH7*-myosin heavy chain gene 7; N-per-family number of individuals screened for variants in the present study, including mutation-carriers and non-carriers; R-Arginine; T-Threonine; *TNNT2*-troponin T gene 2, cardiac; W-Tryptophan

### 2.1.2 Clinical evaluation

Study individuals 18 years and older were clinically characterised by a single experienced cardiologist, Dr Miriam Revera (Pavia University, Italy), who performed the echocardiographic evaluations whilst being blinded to participant mutation status. The echocardiographic data included recordings in M-mode, two dimensional (2D) and Doppler blood-flow imaging acquired by a 2.5 Hertz (Hz) transducer in standard parasternal long- and short-axis orientation and apical four-chamber and two-chamber views; these were visualised with a GE Healthcare Vivid7 cardiovascular ultrasound system.

The segmental analysis of the left ventricle (LV) wall entailed acquisition of 2D-echocardiographic measurements at three levels of the heart muscle, namely, mitral valve-, papillary muscle- and supra-apex levels (see Figure 2.1). A total of 16 segments were assessed, of which six, the anterior interventricular septum (aIVS), posterior interventricular septum (pIVS), anterior wall (AW), lateral wall (LW), inferior wall (IW) and posterior wall (PW), were captured at both the mitral valve and papillary muscle levels. The remaining four measurements, viz., the IVS, AW, LW and PW segments, were acquired at supra-apex level as derived from four-chamber view (see Figure 2.2). This analysis allowed for calculation of maximal left ventricular wall thickness (mLVWT), maximal interventricular septum thickness (mIVST) and maximal posterior wall thickness (mPWT), simply defined as the largest of the relevant quantifications. All measurements were taken as per the recommendations of the American Society of Echocardiography (<http://www.asecho.org/guidelines.php>). In addition, atrium volumes were measured using the biplane area-length method (Schiller *et al.*, 1989). Table 2.2 lists the echocardiography-derived indices of the extent and distribution of the cardiac hypertrophy phenotype.

Subject demographics, including medical history and covariates of cardiac structure namely age, sex, body surface area (BSA), heart rate (HR), systolic BP (SBP), diastolic BP (DBP), were documented. Sitting blood pressure was measured twice following 5 min of rest, and the second measurement recorded. Participants were considered to be hypertensive if using anti-hypertensive medication or by documented measurement of systolic BP  $\geq 140$  mm Hg or diastolic BP  $\geq 90$  mm Hg. Resting heart rate was evaluated from standard electrocardiography performed with a MAC1200ST, recorded in the supine position, and following 5 min of rest.

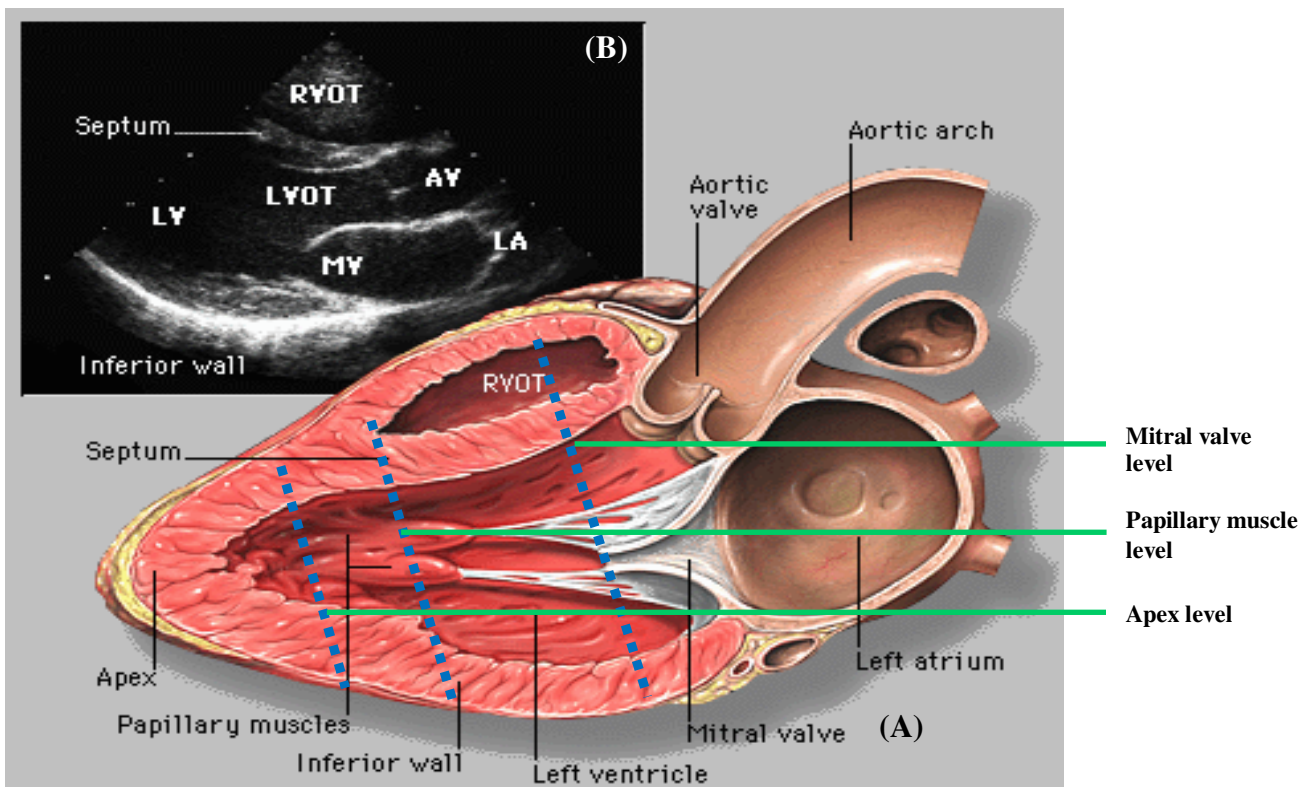


**Figure 2.1 Graphic representation of the left ventricle indicating the three levels of the heart muscle at which the wall thickness measurements were taken.** (A) Long-axis view of the left ventricle, with the three blue dotted lines indicating the three levels of the heart at which the echocardiographic parameters were measured i.e. the mitral valve-, papillary muscle- and apex level. (B) A 2D echocardiogram of the left ventricle. Abbreviations: AV- aortic valve, LA-left atrium, LV-left ventricle, LVOT-left ventricular outflow tract, MV- mitral valve, RVOT-right ventricular outflow tract. (Taken from [http://www.med.yale.edu/.../aortic\\_regurgitation.html](http://www.med.yale.edu/.../aortic_regurgitation.html) with minor modifications by JC Moolman-Smook)

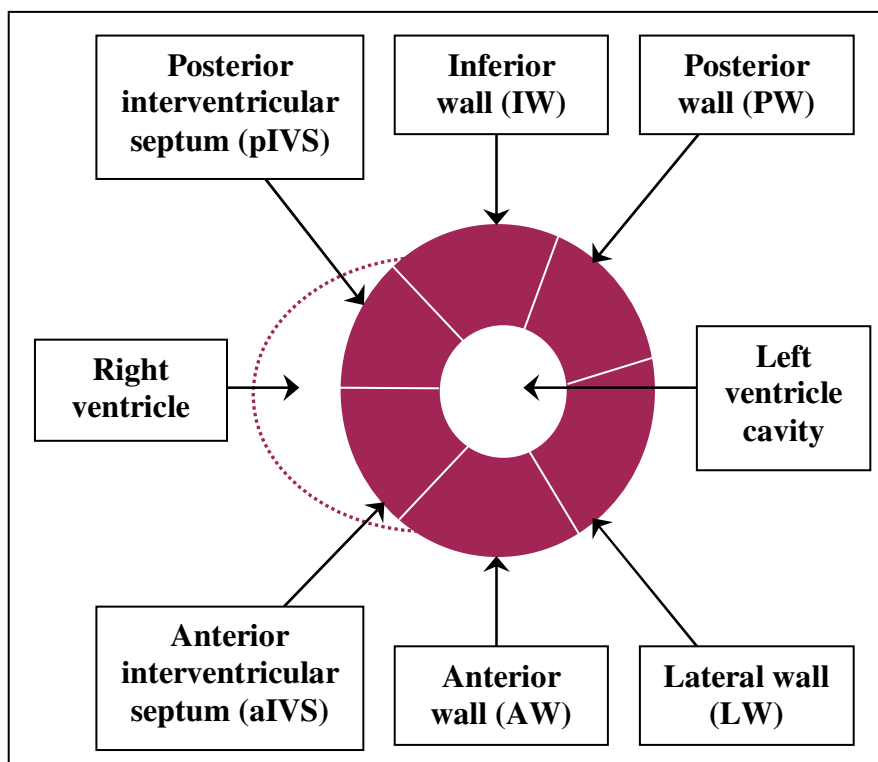


**Figure 2.2 Diagrammatic representation of the left ventricle segments assessed by echocardiography**  
Short-axis view of the six segments measured at the papillary and mitral valve levels, whilst the apex level is characterised by division into only four segments with the exclusion of the anterior- and posterior interventricular septum (Brink P, personal communication).

In addition, other hypertrophy indices were derived from the abovementioned measures, namely LVM, the cumulative wall thickness (CWT) score and the first principal component score (PC1). Calculation of LVM was done according to the American Society of Echocardiography's recommended formula for estimation of LVM from 2D-LV linear dimensions:

$$\text{LVM (g)} = 0.8 \times (1.04 \times [(\text{LVID}_d + \text{PWT}_d + \text{SWT}_d)^3 - (\text{LVID}_d)^3]) + 0.6 \text{ g}$$

g, gram; LVID<sub>d</sub>, left ventricular internal dimension at end-diastole; PWT<sub>d</sub>, posterior wall thickness at end-diastole; SWT<sub>d</sub>, intraventricular septum thickness at end-diastole

LVM index (either to height or to BSA) was not calculated as adjustments were made for BSA by incorporating it into the statistical model. The CWT score was obtained by summing the thicknesses of the 16 quantified LV wall segments. Principal component analysis (PCA) (Refer to Section 2.6.3) was used to derive PC1, a composite score or weighted sum of the 16 wall thickness measurements that best reflected the ventricle-wide hypertrophy and so the variability in LVH in the present HCM cohort as it explained 75% of the variation in the 16 wall thickness measurements.

**Table 2.2 Echocardiographically derived hypertrophy traits used to characterise the extent and distribution of the cardiac hypertrophy**

Level	Hypertrophy trait	Description
<b>Mitral valve level</b>	mLVWTmit	maximal left ventricular wall thickness at the mitral valve
	mIVSTmit	maximal interventricular septum thickness at the mitral valve
	pIVSmit	posterior interventricular septum thickness at the mitral valve
	aIVSmit	anterior interventricular septum thickness at the mitral valve
	AWmit	anterior wall thickness at the mitral valve
	LWmit	lateral wall thickness at the mitral valve
	IWmit	inferior wall thickness at the mitral valve
	PWmit	posterior wall thickness at the mitral valve
<b>Papillary level</b>	mLVWTpap	maximal left ventricular wall thickness at the papillary level
	mIVSTpap	maximal interventricular septum thickness at the papillary level
	pIVSpap	posterior interventricular septum thickness at the papillary level
	aIVSpap	anterior interventricular septum thickness at the papillary level
	AWpap	anterior wall thickness at the papillary level
	LWpap	lateral wall thickness at the papillary level
	IWpap	inferior wall thickness at the papillary level
	PWpap	posterior wall thickness at the papillary level
<b>Apex level</b>	mLVWTapx	maximal left ventricular wall thickness at the supra-apex level
	IVSapx	interventricular septum thickness at the supra-apex level
	AWapx	anterior wall thickness at the supra-apex level
	LWapx	lateral wall thickness at the supra-apex level
	PWapx	posterior wall thickness at the supra-apex level
<b>Overall</b>	LVM	left ventricular mass
	mIVST	maximal interventricular septum thickness
	mLVWT	maximal left ventricular wall thickness
	mPWT	maximal posterior wall thickness
<b>Composite scores</b>	CWTscore	cumulative wall thickness score
	PC1	principal component score 1

## 2.2 Blood sample collection and DNA extraction

A total of three blood samples were obtained from each participant, which included collection in 2× 5 ml ethylene-diamine-tetra-acetic acid (EDTA) tubes (Vacutainer, RSA) to allow for DNA extraction and a single 10 ml heparin tube (Vacutainer, RSA) for establishment of permanent lymphoblastoid cell lines. Blood samples obtained from patients at other centres in South Africa were couriered to the research laboratory within 24 hours post collection.

DNA extraction from nucleated cells was achieved by applying minor modifications to the method previously described by Corfield *et al.* (1993) whilst immortalised cell line establishment relied on the method detailed by Neitzel (1986) (Corfield *et al.*, 1993; Neitzel, 1986). The aforementioned techniques and the subsequent cell maintenance was performed by Mrs I le Roux (Refer to Appendix I for DNA extraction solutions).

## 2.3 Bioinformatics

### 2.3.1 Candidate gene selection

The role of genes linked to sarcomere integrity and contractility as well as myocardial energetics as plausible modifiers of hypertrophy in HCM has been hypothesised in Chapter 1. A comprehensive literature search utilising the Pubmed database (<http://www.pubmed.gov>) thus focused on genes encoding cardiac proteins relating to sarcomere structure and function as well as energy metabolism. The search terms utilised included ‘hypertrophic cardiomyopathy’, ‘sarcomere’, ‘energy’, ‘metabolism’, ‘structure’ and ‘genes’. Table 2.3 lists the 26 candidate modifier genes selected from the literature and their relevant details (Refer to Section 2.3.3 for detailed gene/protein descriptions).



**Table 2.3 Candidate modifier genes selected for investigation**

Gene symbol	Gene	Exon total	Size (kb)	Protein function
<b>Sarcomeric candidate modifier genes</b>				
<b>Thin filament components</b>				
<i>ACTC1</i>	Actin, alpha, cardiac muscle 1	7	7.63	Essential constituent of the cytoskeleton thin filament; Crossbridge formation with myosin to generate force
<i>TNNT2</i>	Troponin T type 2, cardiac	16	18.66	Structural constituent of the cytoskeleton thin filament; Tropomyosin-binding subunit of the Tn complex thereby contributing to Ca <sup>2+</sup> -sensitive regulation of contraction
<i>TNNI3</i>	Troponin I type 3, cardiac	8	5.91	Structural constituent of the cytoskeleton thin filament; inhibits actomyosin ATPase via the binding of actin; component of the Tn complex thereby contributing to Ca <sup>2+</sup> -sensitive regulation of contraction
<i>TPMI</i>	Tropomyosin 1, alpha	10	23.45	Structural constituent of cytoskeleton thin filament; Actin-binding subunit of the Tn complex thereby contributing to Ca <sup>2+</sup> -sensitive regulation of contraction and both stabilisation and stiffening of thin filament
<i>ACTN3</i>	Actinin, alpha 3	21	16.40	Structural constituent of the cytoskeleton thin filament; Anchors myofibrillar actin filaments; linking of sarcomere to muscle fibre membrane; binding of metabolic enzymes
<b>Thick filament components</b>				
<i>MYL3</i>	Myosin light chain 3, alkali, ventricular, skeletal, slow	7	5.62	Structural constituent of cytoskeleton thin filament; Stabilises $\alpha$ -helical myosin neck region; regulation of contraction
<i>MYH7</i>	Myosin heavy chain 7, cardiac muscle, beta	40	22.92	Principal component of the cytoskeleton thick filament; Essential for muscle contraction via its roles in actin and ATP binding and ATP hydrolysis

Gene symbol	Gene	Exon total	Size (kb)	Protein function
<i>MYL2</i>	Myosin light chain 2, regulatory cardiac, slow	7	9.73	Structural constituent of the cytoskeleton thick filament; Stabilises $\alpha$ -helical myosin neck region; Modulatory role in tuning the kinetics of the actin-myosin interaction
<b>Intermediate filament component</b>				
<i>MYBPC3</i>	Myosin binding protein C, cardiac	33	21.27	Structural constituent of the cytoskeleton intermediate filament that functions in sarcomere stability and phosphorylation-dependent modulation of contractility
<b>Energy metabolism candidate modifier genes</b>				
<b>Fatty acid metabolism components</b>				
<i>CD36</i>	CD36 antigen (FAT)	15	38.40	Membrane responsible for uptake of LCFAs across sarcolemma membrane
<i>CPT1B</i>	Carnitine palmitoyltransferase 1B, muscle	19	9.60	Essential for the transport of LCFA across the outer membrane of mitochondria for $\beta$ -oxidation of FAs
<i>PPARA</i>	Peroxisome proliferator-activated receptor alpha	10	72.42	Receptor that regulates genes involved in lipid metabolism
<i>PPARG</i>	Peroxisome proliferator-activated receptor gamma	7	82.85	Receptor that regulates genes involved in lipid metabolism
<i>PGCIA</i>	Peroxisome proliferator-activated receptor gamma, coactivator 1 alpha	13	98.10	A transcriptional coactivator for PPARs involved in fatty acid metabolism; central in mitochondrial biogenesis
<b>Glucose metabolism components</b>				
<i>ALDOA</i>	Aldolase A, fructose-bisphosphate	14	17.24	Functions as enzyme in the glycolytic pathway
<i>PFKM</i>	Phosphofructokinase, muscle	22	23.34	Enzyme that catalysing the rate-limiting step in glycolysis

Gene symbol	Gene	Exon total	Size (kb)	Protein function
<i>PDK4</i>	Pyruvate dehydrogenase kinase, isozyme 4	11	13.11	The PDH complex links glycolysis and FA metabolism by converting pyruvate to acetyl-CoA. The enzyme encoded by <i>PDK4</i> regulates the PDH complex thereby influencing choice of substrate used under various physiological conditions
<b>Creatine kinase energy shuttle components</b>				
<i>CKM</i>	Creatine kinase, muscle	8	16.46	Structural constituent of the cytoskeleton (m-bridges); Contributes to myocardial energetics by catalysing the reversible transfer of high-energy phosphates between creatine and ATP, ultimately coupling sites of ATP production and utilisation
<i>CKB</i>	Creatine kinase, brain	8	3.17	Contributes to myocardial energetics by catalysing the reversible transfer of high-energy phosphates between creatine and ATP, ultimately coupling sites of ATP production and utilisation
<b>Cellular energy homeostasis</b>				
<i>PRKAA1</i>	Protein kinase, AMP-activated, alpha 1 catalytic subunit	10	38.82	Catalytic subunit of the AMPK energy-sensing enzyme that monitors cellular energy status
<i>PRKAA2</i>	Protein kinase, AMP-activated, alpha 2 catalytic subunit	9	63.10	Catalytic subunit of the AMPK energy-sensing enzyme that monitors cellular energy status
<i>PRKAB1</i>	Protein kinase, AMP-activated, beta 1 non-catalytic subunit	7	13.67	Regulatory subunit of the AMPK energy-sensing enzyme that monitors cellular energy status
<i>PRKAB2</i>	Protein kinase, AMP-activated, beta 2 non-catalytic subunit	8	17.44	Regulatory subunit of the AMPK energy-sensing enzyme that monitors cellular energy status
<i>PRKAG1</i>	Protein kinase, AMP-activated, gamma 1 non-catalytic subunit	12	16.54	Regulatory subunit of the AMPK energy-sensing enzyme that monitors cellular energy status
<i>PRKAG2</i>	Protein kinase, AMP-activated gamma 2 non-catalytic subunit	16	321.1	Regulatory subunit of the AMPK energy-sensing enzyme that monitors cellular energy status
<i>PRKAG3</i>	Protein kinase, AMP-activated, gamma 3 non-catalytic subunit	14	9.41	Regulatory subunit of the AMPK energy-sensing enzyme that monitors cellular energy status

**Abbreviations:**  $\alpha$ -alpha;  $\beta$ -beta; AMP-Adenosine monophosphate; AMPK-AMP-activated protein kinase; ATP-Adenosine-5'-triphosphate;  $\text{Ca}^{2+}$ -calcium; FA-fatty acid; kb-kilobases; LCFAs-long chain fatty acids; PPARs-peroxisome proliferator-activated receptors; Tn-troponin complex

### 2.3.2 SNP Selection

SNPs spanning each of the identified candidate genes were selected by means of the SNPbrowser™ Software v 4.0.1 (De La Vega *et al.*, 2006) to allow for association testing. The software visually depicts SNP location and density throughout the relevant genes by utilising the embedded database containing genotype data from four Haplotype Map (HapMap) project populations to construct physical or linkage disequilibrium (LD) maps based on kb or LD Unit (LDU) distances, respectively. The HapMap populations consist of 30 trios of YRI (Yoruba in Ibadan, Nigeria), 45 unrelated samples of JPT (Japanese in Tokyo, Japan), 45 unrelated samples of CHB (Han Chinese in Beijing, China) and 30 CEPH (Centre d'Etude du Polymorphisme Humain) collected CEU trios (Utah residents with ancestry from northern and western Europe).

An LDU is an additive metric measurement representative of the genetic map distance between SNPs based on the extent of allelic association between them (Maniatis *et al.*, 2002), e.g., SNPs in complete LD have zero map distance between them, compared to SNPs with no significant correlation that are separated by over three map LDUs (De La Vega *et al.*, 2006). SNPbrowser™ employs the LD MAP program to construct metric LD (LDU) maps (Kuo *et al.*, 2007), analogous to the genetic map expressed in centi-Morgans (cM), which positions SNPs on a coordinate system as resource for population-based association study design (Collins *et al.*, 2004).

The criteria for SNP selection in the present study were 0.5 LDU even spacing in the HapMap CEU and YRI populations and ABI TaqMan® SNP Validated genotyping assay availability; SNPs meeting these criteria were identified using the default parameters of the software (De La Vega, 2007). Previous association studies from our own laboratory show that the LD structure of the CEU and YRI populations best represent the, as yet undefined, LD structure of the South African population and thereby the current study cohort (Swanepoel, 2010, PhD; Uys, 2010, PhD; Carstens, 2009, MSc). Genome-wide genotyping data has indicated that South African individuals with mixed ancestry also contain admixture from Asian populations (including CHB and JPT), although to a minor extent (de Wit *et al.*, 2010). Table 2.4 details the SNPs selected for this study whilst Figures 2.3 through 2.29 (except Figure 2.12) graphically depict their physical locations within the candidate genes.

Table 2.4 Details of the SNPs selected for genotyping

Candidate gene	Chromosome locus	SNP ID	Chromosome position (bp)	Nucleotide change	ABI Taqman assay ID
<b>Sarcomeric candidate modifier genes</b>					
<b>Thin filament components</b>					
<i>ACTC1</i>	15q11-q14	rs1370154	35082225	C/T	C__2088343_10
		rs2070664	35085201	C/T	C__15867651_10
<i>TNNT2</i>	1q32	rs2365652	201331664	A/C	C__473120_10
		rs1892028	201336641	A/G	C__469074_10
		rs947485	201345352	A/G	C__11621865_10
<i>TNNI3</i>	19q13.4	rs3729841	55665410	C/T	C__27509020_10
		rs3729838	55668310	C/G	C__27472594_10
		rs11667847	55668819	A/G	C__2829707_10
<i>TPM1</i>	15q22	rs11071720	63341996	C/T	C__493909_10
		rs4238370	63347363	G/T	C__102224_10
		rs1071646	63351840	A/C	C__9644173_10
		rs707602	63363737	C/T	C__1455653_10
<i>ACTN3</i>	11q13-q14	rs1791690	66317823	G/A	C__3109120_10
		rs2275998	66326581	C/T	C__15880288_10
		rs1815739	66328095	T/C	C__590093_1_
<b>Thick filament components</b>					
<i>MYL3</i>	3p21.3-p21.2	rs1531136	46901654	C/T	C__9698374_10
		rs3792558	46903094	C/T	C__27517244_10
<i>MYH7</i>	14q12	rs765019	23883848	C/T	C__3083715_10
		rs2277475	23888665	A/T	C__1843584_1_
		rs1951154	23897466	A/G	C__11436423_10
		rs2754163	23897507	C/T	C__1839847_10
		rs2239578	23903380	A/G	C__1839842_1_
<i>MYL2</i>	12q23-q24.3	rs933296	111352848	A/C	C__11489722_10
		rs4766517	111359712	C/G	C__27944102_10
<b>Intermediate filament component</b>					
<i>MYBPC3</i>	11p11.2	rs4752825	47352409	A/G	C__1301098_10
		rs1052373	47354787	C/T	C__8890616_10
		rs10838696	47363285	A/G	C__1301015_10
		rs11570058	47369443	A/G	C__25654298_10
<b>Energy metabolism candidate modifier genes</b>					
<b>Fatty acid metabolism components</b>					
<i>CD36</i>	7q11.2	rs10268417	80239837	A/C	C__29938396_10
		rs3211892	80290369	A/G	C__25644352_10
		rs3173804	80299850	A/T	C__1803772_10

Candidate gene	Chromosome locus	SNP ID	Chromosome position (bp)	Nucleotide change	ABI Taqman assay ID
<i>CPT1B</i>	22q13.33	rs470117	51009953	T/C	C__2531739_1_
		rs1557502	51013998	T/C	C__2531734_1_
<i>PPARA</i>	22q13.31	rs881740	46567388	A/G	C__26334975_20
		rs4823613	46598307	A/G	C__2985275_10
		rs4253776	46629479	A/G	C__2985253_1_
<i>PPARG</i>	3p25	rs12631028	12341406	C/T	C__9384466_10
		rs12490265	12384542	A/G	C__1129874_10
		rs2938392	12434608	A/G	C__11908952_10
		rs1175540	12465243	A/C	C__8756549_10
<i>PGCIA</i>	4p15.1	rs768695	23798818	A/G	C__1643185_10
		rs4619879	23834876	A/C	C__1643198_10
		rs11724368	23862933	A/T	C__1643210_10
		rs13131226	23874981	C/T	C__1643226_20
<b>Glucose metabolism components</b>					
<i>ALDOA</i>	16q22–q24	rs9928448	30072530	T/C	C__26725629_10
		rs11860935	30080780	T/C	C__3234225_10
<i>PFKM</i>	12q13.3	rs1859445	48518591	A/C	C__11477997_10
		rs10875749	48531917	A/T	C__2626552_10
<i>PDK4</i>	7q21.3	rs2073978	95215272	C/T	C__2535297_1_
		rs2301630	95221269	C/T	C__15756512_10
<b>Creatine kinase energy shuttle components</b>					
<i>CKM</i>	19q13.2q13.3	rs8111989	45809208	C/T	C__3145002_10
		rs7260463	45814860	G/T	C__3145006_10
		rs1133190	45818835	A/G	C__15757328_10
		rs344816	45825626	A/T	C__958453_10
<i>CKB</i>	14q32	rs1803283	103986255	C/T	C__1292617_20
		rs2071407	103987140	C/T	C__15868868_10
		rs1136165	103988180	G/T	C__8901441_10
<b>Cellular energy homeostasis</b>					
<i>PRKAA1</i>	5p12	rs12517210	40764440	C/T	C__30750962_10
		rs11747210	40774673	G/T	C__26082115_10
		rs466108	40796746	A/C	C__3280925_10
<i>PRKAA2</i>	1p31	rs1124900	57112222	G/T	C__26467839_10
		rs2796495	57142979	C/T	C__16120204_10
		rs932447	57170229	C/T	C__9583690_1_
<i>PRKAB1</i>	12q24.1	rs6490267	120106376	G/T	C__348015_10
		rs278143	120109014	A/G	C__339921_10
		rs10849690	120114205	C/G	C__11751875_10
		rs278149	120114507	G/T	C__2258897_10
		rs4213	120119183	G/T	C__3259867_10

Candidate gene	Chromosome locus	SNP ID	Chromosome position (bp)	Nucleotide change	ABI Taqman assay ID
<i>PRKAB2</i>	1q21.1	rs6937	146626922	T/C	C__1745071_20
		rs1348316	146643555	G/A	C__8719009_30
<i>PRKAG1</i>	12q12–q14	rs10875910	49402393	C/G	C__9260196_10
		rs2117029	49408440	A/T	C__2023779_10
<i>PRKAG2</i>	7q36.1	rs8961	151254175	C/T	C__2667965_1_
		rs2727537	151373046	A/G	C__16284061_10
		rs6464170	151476860	C/G	C__29193665_10
		rs13240743	151566914	C/G	C__31459975_10
<i>PRKAG3</i>	2q35	rs1000935	219691495	G/T	C__8841107_10
		rs16859382	219693856	C/T	C__32733031_10

**Abbreviations:** A-adenine; ABI-Applied Biosystems Incorporated; *ACTC1*-Actin, alpha, cardiac muscle 1; *ACTN3*-Actinin, alpha 3; *ALDOA*-Aldolase A, fructose-bisphosphate; bp-base pairs; C-cytosine; *CD36*-CD36 antigen, thrombospondin receptor; *CKB*-Creatine kinase, brain; *CKM*-Creatine kinase, muscle; *CTP1B*- Carnitine palmitoyltransferase 1B, muscle; G-guanine; *MYBPC3*-Myosin binding protein C, cardiac; *MYH7*-Myosin heavy chain 7, cardiac muscle, beta; *MYL2*-Myosin light chain 2, regulatory cardiac, slow; *MYL3*-Myosin light chain 3, alkali, ventricular, skeletal slow; p-short arm of chromosome; *PDK4*-Pyruvate dehydrogenase kinase, isozyme 4; *PFKM*-Phosphofructokinase, muscle; SNP-single nucleotide polymorphism; T-thymine; *TNNI3*-Troponin I type 3, cardiac; *TNNT2*-Troponin T type 2, cardiac; *TPMI*-Tropomyosin 1; *PPARA*-Peroxisome proliferator-activated receptor alpha; *PPARG*-Peroxisome proliferator-activated receptor gamma; *PGCIA*-Peroxisome proliferator-activated receptor gamma, coactivator 1 alpha; *PRKAA1*-Protein kinase, AMP-activated, alpha 1 catalytic subunit; *PRKAA2*-Protein kinase, AMP-activated, alpha 2 catalytic subunit; *PRKAB1*-Protein kinase, AMP-activated, beta 1 non-catalytic subunit; *PRKAB2*-Protein kinase, AMP-activated, beta 2 non-catalytic subunit; *PRKAG1*-Protein kinase, AMP-activated, gamma 1 non-catalytic subunit; *PRKAG2*-Protein kinase, AMP-activated gamma 2 non-catalytic subunit; *PRKAG3*-Protein kinase, AMP-activated, gamma 3 non-catalytic subunit; q-long arm of chromosome

### 2.3.3 Detailed candidate gene descriptions and graphic SNP positioning

#### 2.3.3.1 Sarcomeric candidate modifier genes

##### i) $\alpha$ -Actin

Cardiac  $\alpha$ -actin, encoded by *ACTC1*, is the predominant actin isoform in the adult heart where it functions in cytoskeletal integrity and muscle contraction. Through polymerisation, the monomeric protein (globular actin or G-actin) gives rise to fibres with a double-helical structure, F-actin, which is the principal component of the thin filament. The monomer is further divided into subdomains, of which the first allows for the binding and subsequent activation of the myosin head and motor function. This myosin-actin interaction is a key step in the crossbridge cycle that allows for the sliding of thin filaments past the thick filaments, and thus, ultimately, for muscle contraction (Bertola *et al.*, 2008; dos Remedios *et al.*, 2003; Laing & Nowak, 2005).

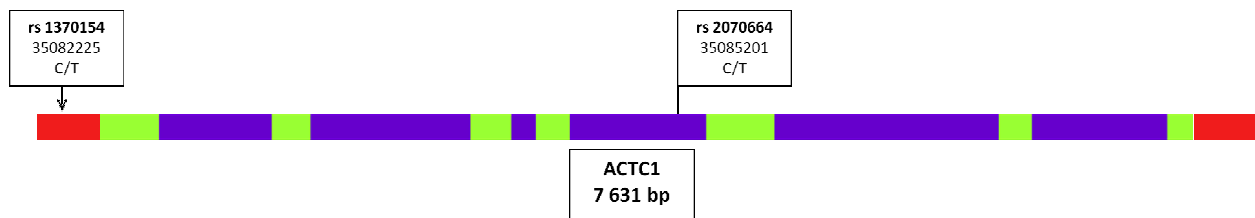


**Figure 2.3** The genomic structure of *ACTC1* and the physical locations of SNPs selected throughout this gene. Exons and introns are denoted by green and blue boxes, respectively. The upstream and downstream regions of the gene are indicated in red.

## ii) Myosin

Myosin is the principal component of the thick filament and its functions, viz., actin-binding and ATP-binding and -hydrolysis, are essential for muscle contraction. The known cardiac isoforms,  $\alpha$ -MHC and  $\beta$ -MHC, encoded by *MYH6* and *MYH7* respectively, show tissue-specific expression, i.e.  $\alpha$ -MHC is expressed predominantly in the human atrium and  $\beta$ -MHC in the human ventricle (Daloz *et al.*, 2001).

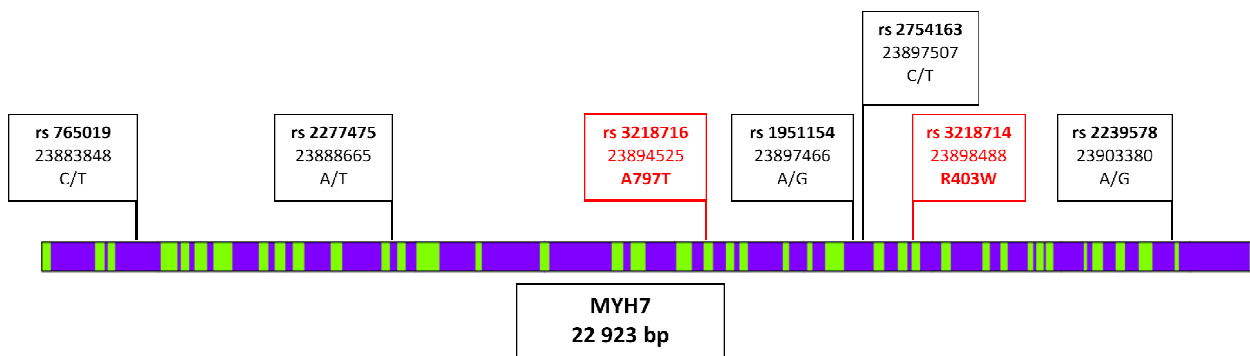


**Figure 2.4** The genomic structure of *MYH7* and the physical locations of SNPs selected throughout this gene. Exons and introns are denoted by green and blue boxes, respectively. The two HCM-causing *MYH7* mutations which segregate in the current cohort as founder mutations are indicated in red.

## iii) The Troponin (Tn) complex

The Troponin complex, consisting of three protein subunits, namely TnT, Troponin C (TnC) and TnI, is responsible for the  $\text{Ca}^{2+}$ -dependent regulation of contraction (force and velocity), which is achieved by modulating the functional interaction between actin and myosin. The complex undergoes a spatial change in configuration in response to  $\text{Ca}^{2+}$ -binding, pulling the tropomyosin



away from the myosin binding site on the actin filament. This allows the myosin heads to interact with actin for crossbridge formation and subsequent muscle contraction (Reviewed by Chappelle, 1999).

### a) Troponin T

Troponin T is the tropomyosin-binding subunit of the Tn complex; however its functions extend to actin-binding and regulation of actomyosin ATPase activity (Reviewed by Filatov *et al.*, 1999). A total of 4 cardiac isoforms, created via alternative splicing of the *TNNT2* gene, have been reported in the mammalian heart, designated cTNT1-cTNT4 (Daloz *et al.*, 2001; Anderson *et al.*, 1995; Zot & Potter, 1987).

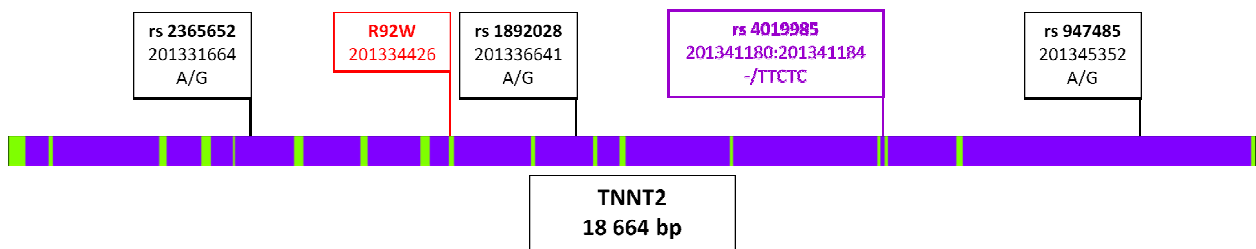


**Figure 2.5** The genomic structure of *TNNT2* and the physical locations of SNPs selected throughout this gene. Exons and introns are denoted by green and blue boxes, respectively. The HCM-causing *TNNT2* mutation which segregates in the current cohort as a founder mutation is indicated in red. The physical location of the insertion/deletion polymorphism for which the cohort was previously screened is shown in purple.

### b) Troponin I

The chief function of Troponin I is the inhibition of actomyosin ATPase activity via the binding of actin. It also interacts with the other Tn complex components; the location of their binding sites allows for the transfer of a conformational signal, induced by  $\text{Ca}^{2+}$ -binding to TNC, through TNI, to TNT and tropomyosin. In addition, these various interactions are modulated by phosphorylation of TNI by protein kinases, i.e. protein kinase A (PKA), protein kinase G (PKG) and protein kinase C (PKC). The cardiac TNI isoform is encoded by the *TNNI3* gene (Daloz *et al.*, 2001; Reviewed by Filatov *et al.*, 1999).

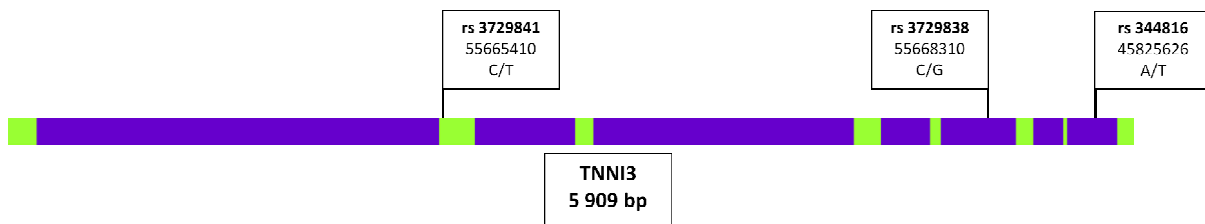


**Figure 2.6** The genomic structure of *TNNI3* and the physical locations of SNPs selected throughout this gene. Exons and introns are denoted by green and blue boxes, respectively.

#### iv) $\alpha$ -Tropomyosin

Striated muscle  $\alpha$ -TM, generated from the alternative splicing of *TPM1*, is the main isoform in cardiac muscle. It is an actin-binding protein of dual function, as it stabilises and stiffens the thin filament, in addition to regulating muscle contraction via its association with the Tn complex (Weigt *et al.*, 1990; Dalloz *et al.*, 2001). Moreover,  $\text{Ca}^{2+}$ -binding to the Tn complex results in the repositioning of TM on actin, thereby exposing the myosin crossbridge-binding sites on actin and allowing for muscle contraction (Jagatheesan *et al.*, 2009; Gunning *et al.*, 2008).

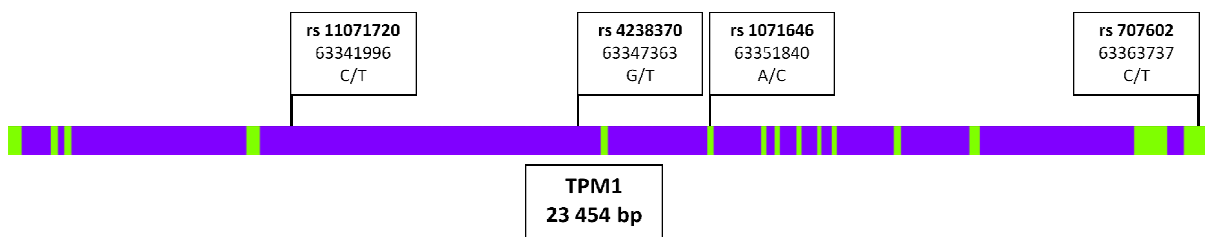


**Figure 2.7** The genomic structure of *TPM1* and the physical locations of SNPs selected throughout this gene. Exons and introns are denoted by green and blue boxes, respectively.

#### v) The myosin light chains

The essential (ELC) and regulatory (RLC) myosin light chains bind to the regulatory region of the myosin head where they stabilise and affect the rigidity of the long alpha-helical neck of the myosin. The RLC also undergoes phosphorylation, thought to regulate contractility (Dalloz *et al.*, 2001; Poetter *et al.*, 1996). Moreover, the RLC modulates the position of crossbridges relative to the actin filament, in a myosin light chain kinase (MLCK) phosphorylation-mediated manner, affecting the likelihood of crossbridge-binding and thus contraction. ELC interactions with the thin filament

have been reported, which may limit crossbridge cycling and shortening velocity, adding another layer of regulation of contractility. Cardiac ELC and RLC are encoded by *MYL3* and *MYL2*, respectively (Colson *et al.*, 2010; Harris *et al.*, 2011; Taylor *et al.*, 2004; Schaub *et al.*, 1998).

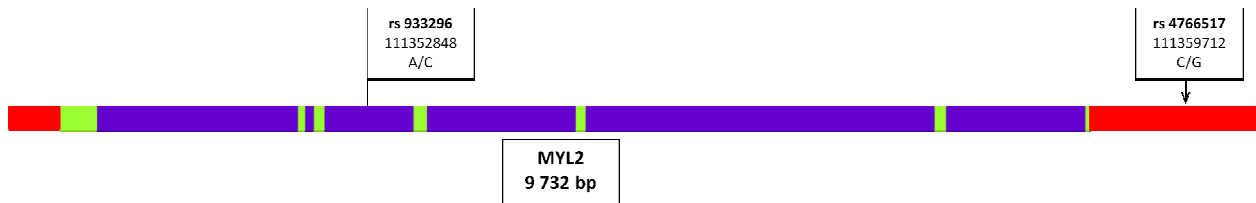


**Figure 2.8** The genomic structure of *MYL2* and the physical locations of SNPs selected throughout this gene. Exons and introns are denoted by green and blue boxes, respectively. The upstream and downstream regions of the gene are indicated in red.

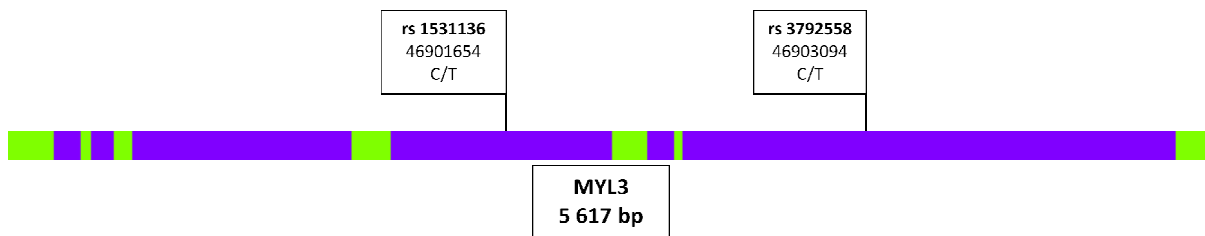


**Figure 2.9** The genomic structure of *MYL3* and the physical locations of SNPs selected throughout this gene. Exons and introns are denoted by green and blue boxes, respectively.

## vi) Myosin binding protein C

*MYBPC3* encodes cardiac myosin-binding protein-C (c-MyBP-C), which functions in sarcomere stability and modulation of contraction (Carrier *et al.*, 1997). The protein has been suggested to stabilise the thick filament structure via its interactions with the thick filament backbone and/or titin. In addition, c-MyBP-C phosphorylation via PKA increases the proximity of crossbridges to actin, thereby influencing both the speed and strength of contraction. In addition, it can reversibly bind to actin, suggesting a further means of modulating contraction (Colson *et al.*, 2010; Furst *et al.*, 1992; Labeit *et al.*, 1992; Moss *et al.*, 1983; Zoghbi *et al.*, 2008; Harris *et al.*, 2011).

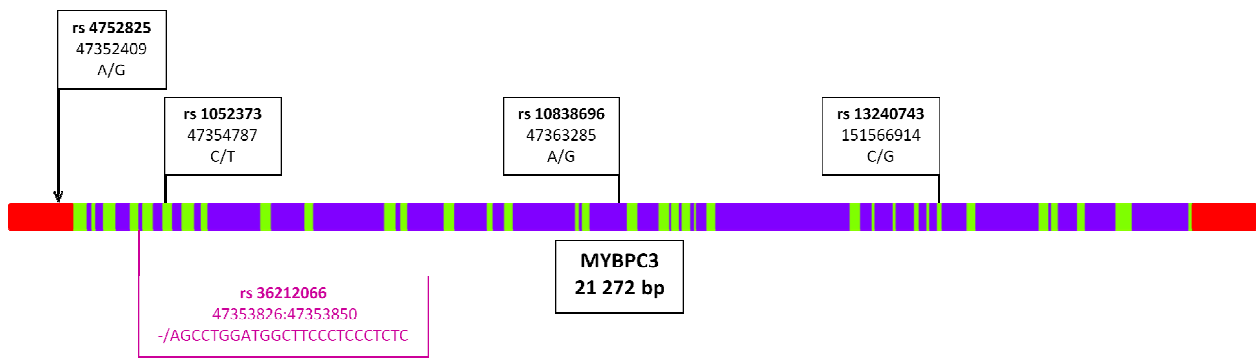


**Figure 2.10** The genomic structure of *MYBPC3* and the physical locations of SNPs selected throughout this gene. Exons and introns are denoted by green and blue boxes, respectively. The upstream and downstream regions of the gene are indicated in red. The physical location of the 25 bp deletion for which the cohort was screened is shown in purple.

### vii) $\alpha$ -Actinin-3

The *ACTN3* gene encodes  $\alpha$ -actinin-3, the expression of which, according to the bulk of the literature, is limited to skeletal muscle (North & Beggs, 1996). This is however contradicted by the presence of validated *ACTN3* transcripts in heart muscle (<http://www.genecards.org/cgi-bin/carddisp.pl?gene=ACTN3&search=actn3>). The functions of  $\alpha$ -actinins in skeletal muscle, as main components of the Z-line, relate to structure, metabolism and signalling, and may provide insight into the relevance of  $\alpha$ -actinin-3 in cardiac muscle. The  $\alpha$ -actinins interact with numerous structural proteins to ensure cytoskeletal integrity, e.g., anchoring and stabilising actin filaments from adjacent sarcomeres, as well as linking of sarcomeres to the muscle fibre membrane via dystrophin (Squire, 1997; Hance *et al.*, 1999). They also bind metabolic enzymes, including aldolase and fructose-1,6-biphosphatase, at the Z-line, possibly ensuring local energy availability (Macarthur & North, 2004; Rakus *et al.*, 2003).

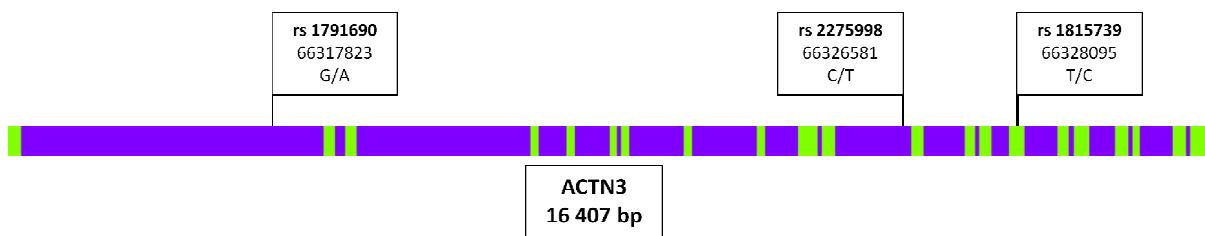


**Figure 2.11** The genomic structure of *ACTN3* and the physical locations of SNPs selected throughout this gene. Exons and introns are denoted by green and blue boxes, respectively.

### 2.3.3.2 Energy metabolism candidate modifier genes

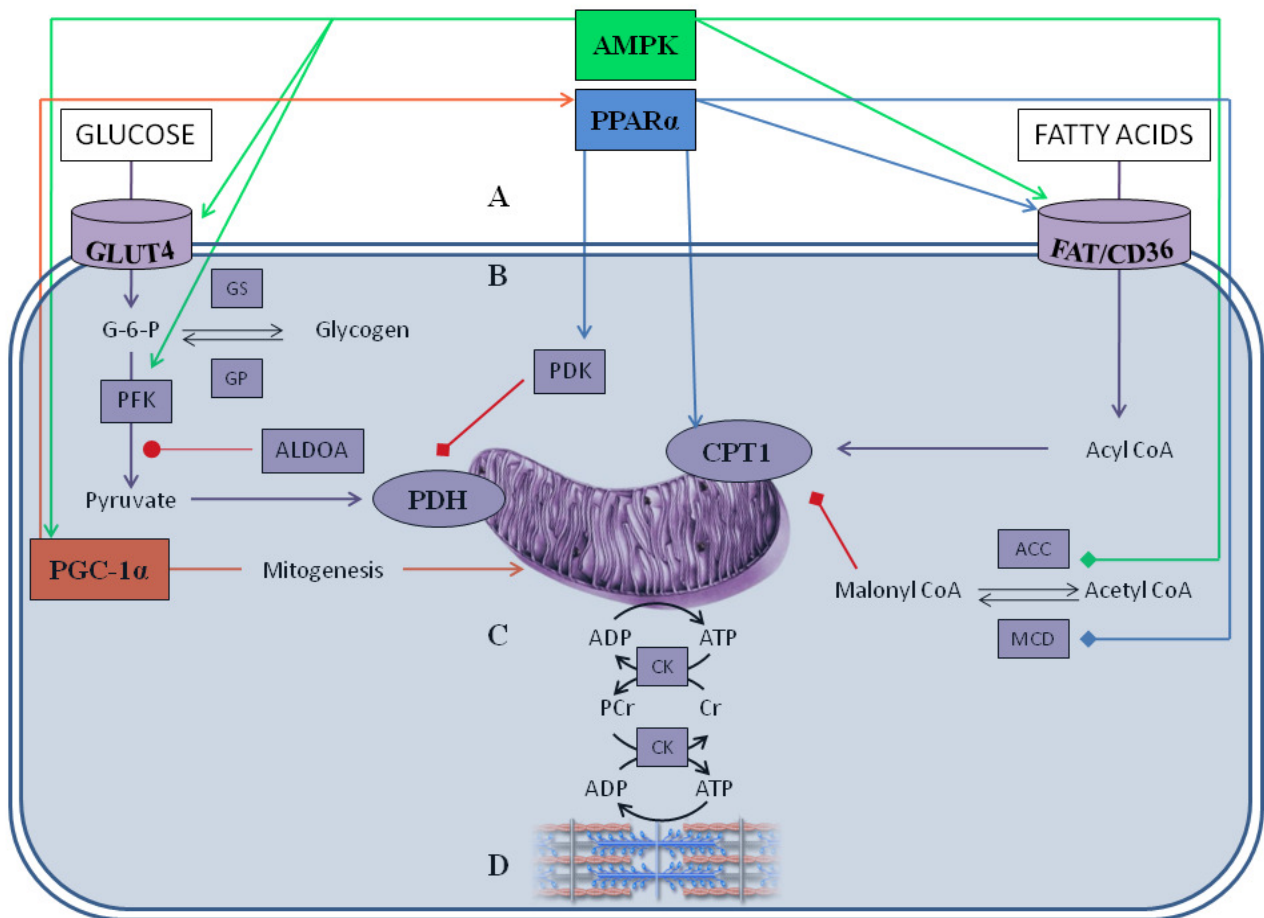


**Figure 2.12 Diagram of the candidate genes relating to myocardial energetics.** The illustration has been compiled from and summarises the succeeding overview of those candidate genes that function in myocardial energetics.

#### i) Fatty acid translocase

The *FAT/CD36* gene encodes an ubiquitously expressed, ditopic glycosylated membrane protein responsible for the uptake of LCFAs across the sarcolemmal membrane (Aras & Dilsizian, 2007; Harmon & Abumrad, 1993; Luiken *et al.*, 2003). Research has established a link between the reduced expression of CD36 and the development of an HCM-like phenotype (Cambronero *et al.*, 2009; Luedde *et al.*, 2009; Okamoto *et al.*, 1998; Soor *et al.*, 2009).

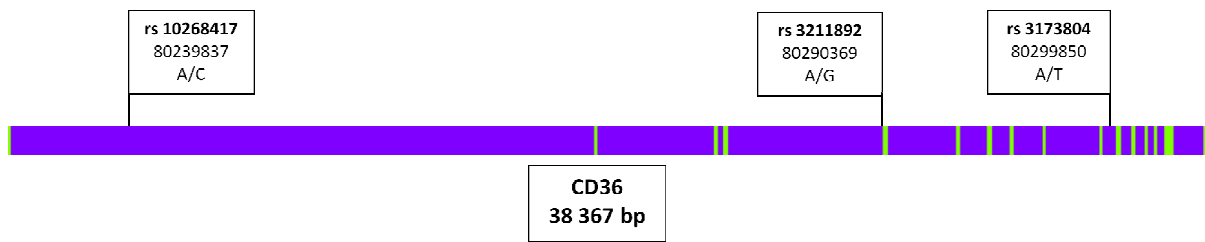


**Figure 2.13** The genomic structure of *CD36* and the physical locations of SNPs selected throughout this gene. Exons and introns are denoted by green and blue boxes, respectively.

## ii) Carnitine palmitoyltransferase I

Carnitine palmitoyltransferase is essential for the transport of LCFAs across the outer membrane of mitochondria for  $\beta$ -oxidation; this translocation is the rate-limiting step in this energy-generating process. The muscle isoform, CPT-1b, encoded by *CPT1B*, is predominantly expressed in the heart (Yamazaki *et al.*, 1996; Yamazaki *et al.*, 1996; McGarry & Brown, 1997).

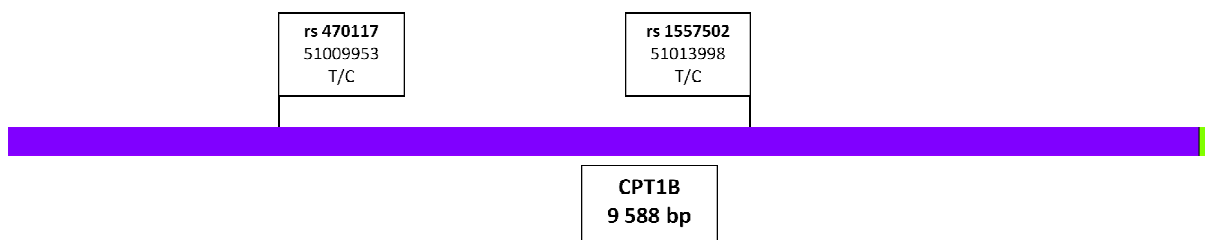


**Figure 2.14** The genomic structure of *CPT1B* and the physical locations of SNPs selected throughout this gene. Exons and introns are denoted by green and blue boxes, respectively.

## iii) Pyruvate dehydrogenase kinase

The PDH complex converts pyruvate to acetyl-CoA for subsequent ATP generation via the mitochondrial Krebs cycle, linking glycolysis and fatty acid metabolism, and thus influencing the choice of substrate used under various physiological conditions (Houten *et al.*, 2009; Randle, 1986; Patel & Roche, 1990; Patel & Roche, 1990). Its activity is regulated by pyruvate dehydrogenase kinase (PDK) enzymes, of which isoenzyme 4, encoded by *PDK4*, is predominantly expressed in skeletal and cardiac muscle (Roche *et al.*, 2001; Bowker-Kinley *et al.*, 1998).

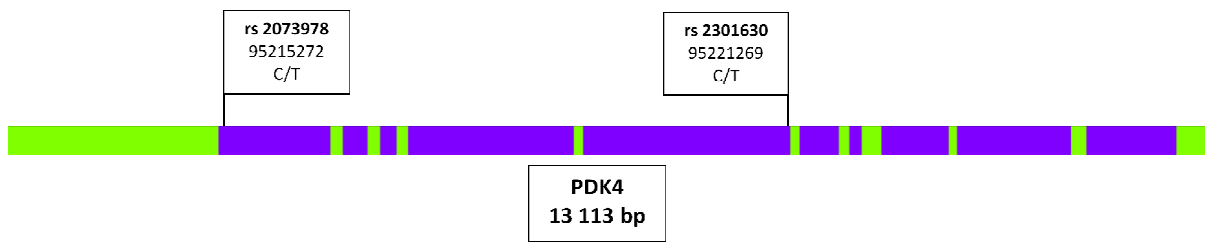


**Figure 2.15** The genomic structure of *PDK4* and the physical locations of SNPs selected throughout this gene. Exons and introns are denoted by green and blue boxes, respectively.

#### iv) Creatine kinase

Creatine kinase contributes to myocardial energy homeostasis by catalysing the reversible transfer of high-energy phosphates between creatine and ATP, ultimately coupling cellular sites of ATP production and ATP utilisation. The *CKM* and *CKB* genes encode the M-CK and B-CK subunits, respectively, which in turn combine to form the three cytosolic isoforms: brain-type (BB-CK), sarcomeric muscle type (MM-CK) and the combined isoform (MB-CK); all of these are expressed in the heart, although MB-CK is the predominant cardiac isoform (Au, 2004; Nahrendorf *et al.*, 2005; Hornemann *et al.*, 2000). A small fraction (~5–10%) of the muscle-specific isoform is known to bind to the sarcomeric M-line, suggesting not only an extension from its cytosolic enzyme function to that of an intramyofibrillar ATP regenerator at the site of high-energy demand, but also that it plays a structural role within the sarcomere, at the M-line (m-bridges) (Clark *et al.*, 2002; Hornemann *et al.*, 2000).

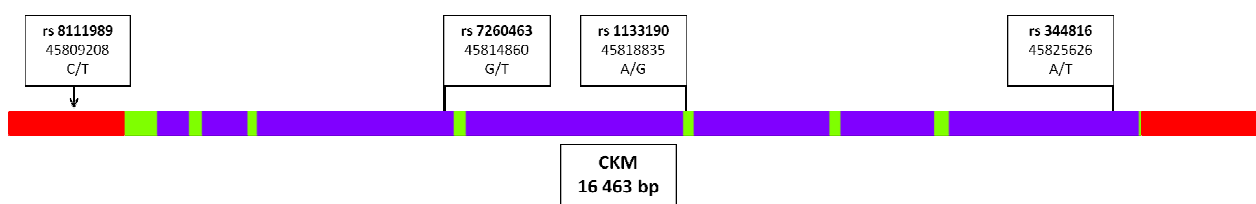


**Figure 2.16** The genomic structure of *CKM* and the physical locations of SNPs selected throughout this gene. Exons and introns are denoted by green and blue boxes, respectively. The upstream and downstream regions of the gene are indicated in red.

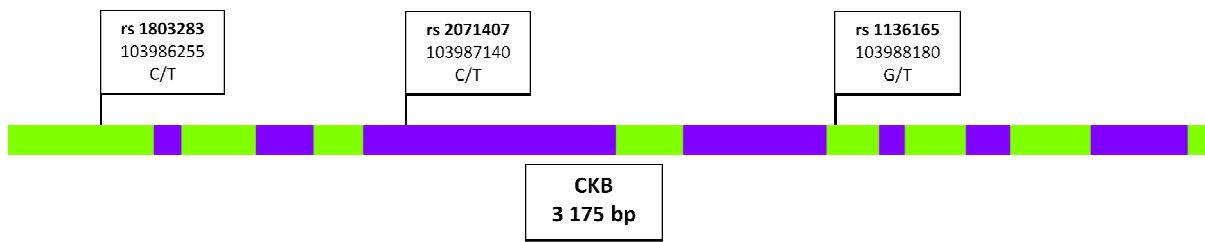


**Figure 2.17** The genomic structure of *CKB* and the physical locations of SNPs selected throughout this gene. Exons and introns are denoted by green and blue boxes, respectively.

#### v) Aldolase A

Aldolases function in the glycolytic pathway by catalysing the reversible cleavage of fructose 1,6-bisphosphate to dihydroxyacetone phosphate (DHAP) and glyceraldehyde 3-phosphate (G3P). Aldolase A, encoded by the *ALDOA* gene, is the predominant isoform in the heart, colocalising with fructose 1,6-bisphosphatase (FBPase) in the cytoplasm, including in the Z-line and the intercalated discs, and in the nucleus of cardiomyocytes (Mamczur *et al.*, 2007; Asaka *et al.*, 1983; Koeck *et al.*, 2004; Medin *et al.*, 2007; Rutter, 1964).

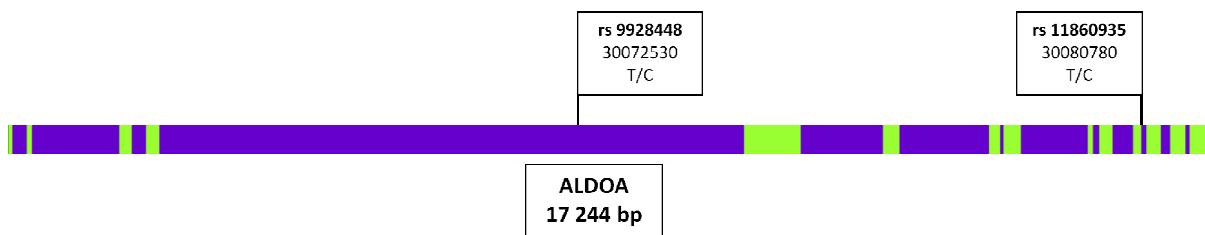


**Figure 2.18** The genomic structure of *ALDOA* and the physical locations of SNPs selected throughout this gene. Exons and introns are denoted by green and blue boxes, respectively.

#### vi) Phosphofructo-1-kinase

Phosphofructo-1-kinase catalyses the rate-limiting step in glycolysis, converting fructose-6-phosphate to fructose-1,6-bisphosphate (Swoboda *et al.*, 1997). The muscle type is the predominant isoenzyme in the heart, and mutations in its encoding gene, *PFKM*, have been associated with type VII GSD (GSDVII) (Dunaway *et al.*, 1988a; Tarui *et al.*, 1965).



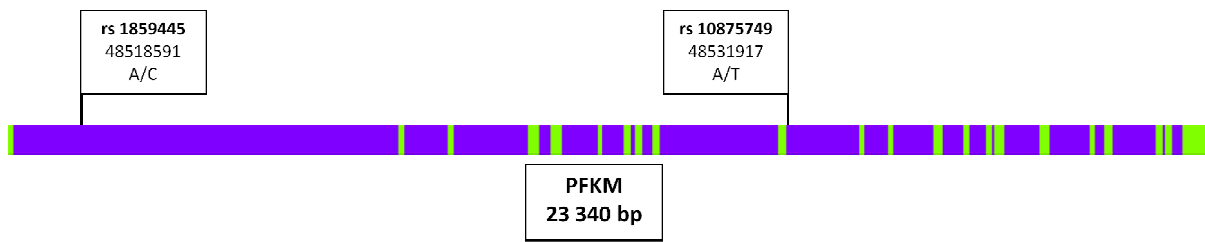


**Figure 2.19** The genomic structure of *PFKM* and the physical locations of SNPs selected throughout this gene. Exons and introns are denoted by green and blue boxes, respectively.

## vii) Peroxisome proliferator-activated receptors (PPARs)

PPARs are nuclear lipid-activated receptors that regulate numerous genes essential for lipid metabolism (Feige *et al.*, 2006; Reviewed by Desvergne & Wahli, 1999).

### a) Peroxisome proliferator-activated receptor alpha

PPAR $\alpha$  is highly expressed in the heart where it regulates the transcriptional expression of various components of lipid and glucose metabolic pathways, including FA transport protein 1 (FATP1), FAT/CD36, CPT1b, PDK4, long chain acyl-CoA synthetase (LACS) and malonyl-CoA decarboxylase (MCD) (Reviewed by Rowe *et al.*, 2010; Reviewed by Yang & Li, 2007).

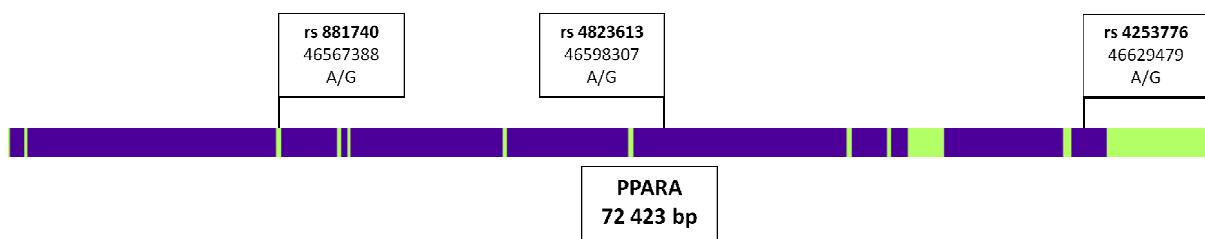


**Figure 2.20** The genomic structure of *PPARA* and the physical locations of SNPs selected throughout this gene. Exons and introns are denoted by green and blue boxes, respectively.

### b) Peroxisome proliferator-activated receptor gamma

Expression of the PPAR $\gamma$  isoform extends to cardiac tissue where it has been detected in the aorta, coronary arteries and left ventricles of healthy heart donors (Mehrabi *et al.*, 2002). A recent study by Luo *et al.* 2010 aimed to characterise the function of PPAR $\gamma$  in the heart. The researchers

commented that the ligand binding profiles of the PPARs partially overlap which suggests that PPAR $\gamma$  may have cardiac functions similar to those of PPAR $\alpha$ . Moreover, using a cardiomyocyte-restricted PPAR $\gamma$  knockout mouse model, they established that it plays an essential role in fatty acid metabolism in the adult heart and so myocardial energetics and cardiac function. The PPAR $\gamma$  deficient hearts showed decreased levels of proteins essential for fatty acid uptake and oxidation which included CD36 and CPT-1. In addition, the PPAR $\gamma$  deficient hearts exhibited decreased fatty acid utilization and cardiac contraction. Most importantly, the deficient hearts showed a modest degree of cardiac hypertrophy relative to control hearts (Luo *et al.*, 2010).

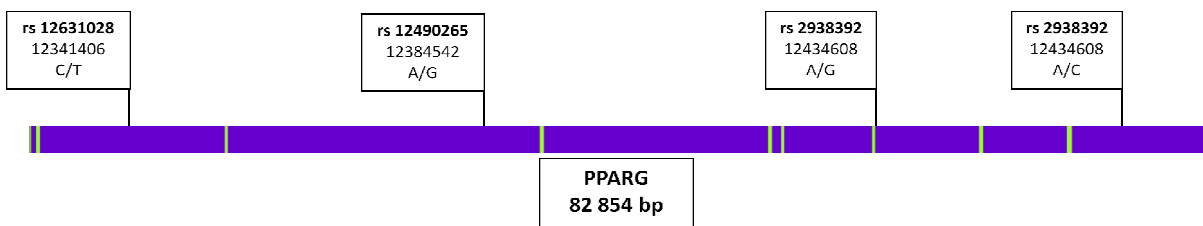


**Figure 2.21** The genomic structure of *PPARG* and the physical locations of SNPs selected throughout this gene. Exons and introns are denoted by green and blue boxes, respectively.

#### viii) Peroxisome proliferator-activated receptor gamma coactivator-1 $\alpha$

PCG-1 $\alpha$  is abundantly expressed in the heart where it acts as coactivator for PPAR $\alpha$ , allowing for initiation of target gene transcription (Finck, 2007). It similarly coactivates PPAR $\gamma$  in brown adipose tissue and may do the same in cardiomyocytes (Rowe *et al.*, 2010; Puigserver *et al.*, 1998; Young *et al.*, 2001). Moreover, PCG-1 $\alpha$  is central to mitochondrial biogenesis in the heart, indirectly regulating mitochondrial transcription factor A (MTF-A).

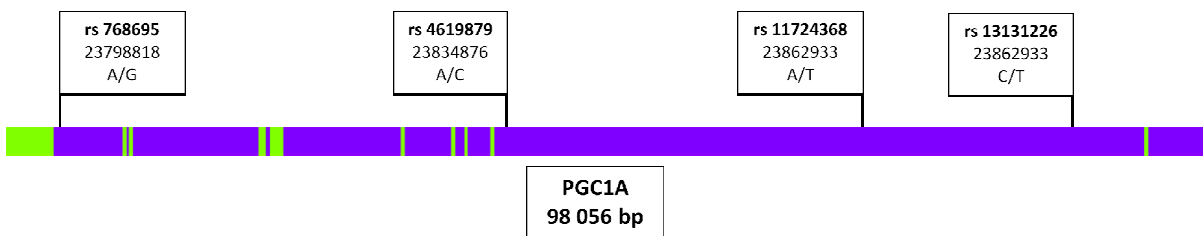


**Figure 2.22** The genomic structure of *PGC1A* and the physical locations of SNPs selected throughout this gene. Exons and introns are denoted by green and blue boxes, respectively.

### ix) AMP-activated protein kinase

The mammalian AMPK complex is a heterotrimer (Davies *et al.*, 1994) consisting of an  $\alpha$ -catalytic subunit and 2 regulatory,  $\beta$ - and  $\gamma$ - subunits (Dolinsky & Dyck, 2006). A total of 7 subunit-encoding genes exist, namely *PRKAA1*, *PRKAA2*, *PRKAB1*, *PRKAB2*, *PRKAG1*, *PRKAG2* and *PRKAG3* encoding 2  $\alpha$ -subunits ( $\alpha1$  and  $\alpha2$ ), 2  $\beta$ -subunits ( $\beta1$  and  $\beta2$ ) and 3  $\gamma$ -subunits ( $\gamma1$ ,  $\gamma2$ ,  $\gamma3$ ), respectively (Refer to Table 2.3 for full gene names) (Hardie *et al.*, 1998;Zhang *et al.*, 2009). All isoforms show cardiac expression (Watkins H, personal communication). AMPK functions as a regulator of cellular energy homeostasis via its ability to sense the AMP:ATP ratio (Hardie & Carling, 1997). An increase in the latter, attributable to metabolic stresses that elevate ATP consumption, e.g. muscle contraction, or inhibit ATP synthesis, such as glucose deprivation, results in AMPK activation (Oliveira *et al.*, 2003;Hardie *et al.*, 2003). The kinase acts to restore the balance by promoting catabolic, ATP-generating processes including glucose uptake (Russell, III *et al.*, 1999), glycolysis (Marsin *et al.*, 2000), fatty acid uptake and oxidation (Kudo *et al.*, 1995) and mitochondrial biogenesis (Zong *et al.*, 2002). In addition, it inhibits anabolic, energy-consuming pathways, such as synthesis of fatty acids (Hardie & Pan, 2002), cholesterol (Zhou *et al.*, 2001) and proteins (Horman *et al.*, 2002), preventing further ATP depletion.

In the heart, the kinase contributes to increased myocardial glucose uptake by promoting translocation of the transmembrane protein, GLUT4 (Russell, III *et al.*, 1999), to the sarcolemma. Similarly, AMPK increases glycolysis via the activation of cardiac phosphofructokinase 2 (PFK2) (Marsin *et al.*, 2000). The latter synthesises fructose 2,6-bisphosphate that in turn stimulates phosphofructokinase-1 (PFK1), the rate-limiting enzyme of glycolysis (Refer to Section 1.4.7) (Hue & Rider, 1987). AMPK and fatty acids synergistically induce PDK4 expression, subsequently reducing glucose oxidation in primary cardiomyocytes (Houten *et al.*, 2009). It, furthermore, promotes fatty acid metabolism by improving myocardial uptake and usage of fatty acids. Lipoprotein lipase (LPL) present at the coronary lumen endothelium, facilitates uptake of fatty acids from circulation, whilst FAT/CD36 and CPT-1 allows for fatty acid transport across the sarcolemmal membrane and the outer mitochondrial membrane, respectively (Refer to Sections 1.3.2.1 and 1.3.2.2) (Dyck & Lopaschuk, 2006;Harmon & Abumrad, 1993;McGarry & Brown, 1997). CPT-1 function is inhibited by malonyl-CoA, converted from acetyl CoA by the acetyl-CoA carboxylase (ACC) enzyme. AMPK activation increases LPL activity (An *et al.*, 2005), mediates FAT/CD36 translocation to the sarcolemma (Luiken *et al.*, 2003) and inactivates ACC, relieving

CPT-1 inhibition (Kudo *et al.*, 1996;Kudo *et al.*, 1995). AMPK inhibits protein synthesis via inactivation of eukaryote elongation factor-2 (eEF2) and the target-of-rapamycin (TOR) pathway, responsible for peptide elongation and mRNA translation, respectively (Gwinn *et al.*, 2008;Inoki *et al.*, 2003;Horman *et al.*, 2002). AMPK also affects mitochondrial biogenesis by activating PCG-1 $\alpha$  (Refer to Section 1.4.6) (Ren *et al.*, 2010). Mutations in the *PRKAG2* gene have previously been linked to the development of an HCM phenocopy (Blair *et al.*, 2001b).

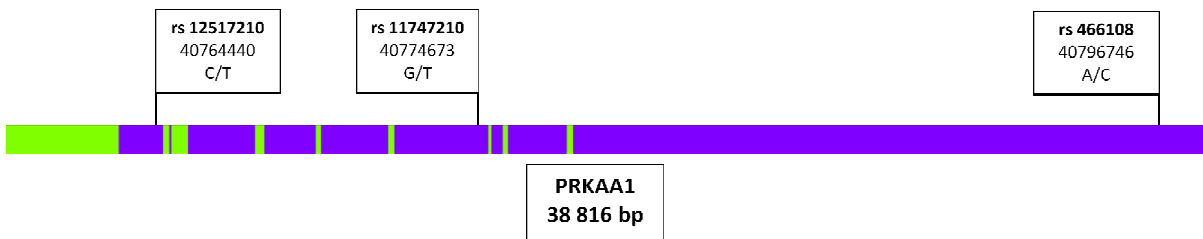


**Figure 2.23** The genomic structure of *PRKAA1* and the physical locations of SNPs selected throughout this gene. Exons and introns are denoted by green and blue boxes, respectively.

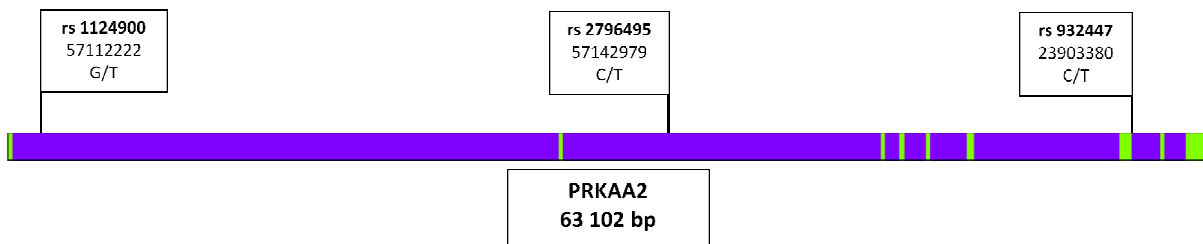


**Figure 2.24** The genomic structure of *PRKAA2* and the physical locations of SNPs selected throughout this gene. Exons and introns are denoted by green and blue boxes, respectively.

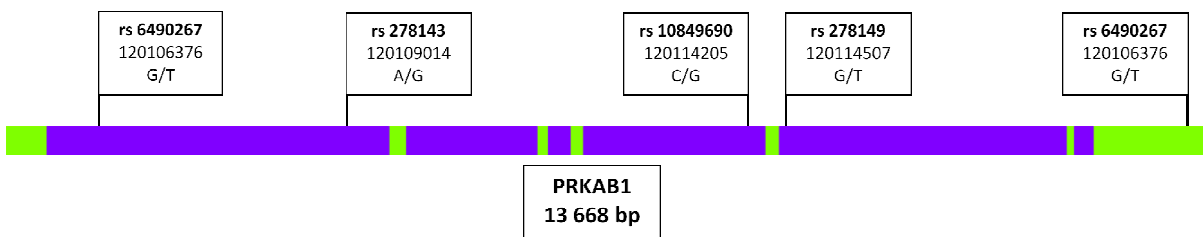


**Figure 2.25** The genomic structure of *PRKAB1* and the physical locations of SNPs selected throughout this gene. Exons and introns are denoted by green and blue boxes, respectively.

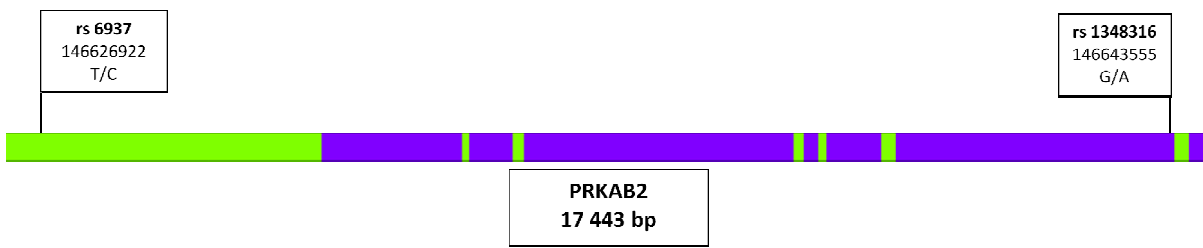


**Figure 2.26** The genomic structure of *PRKAB2* and the physical locations of SNPs selected throughout this gene. Exons and introns are denoted by green and blue boxes, respectively.

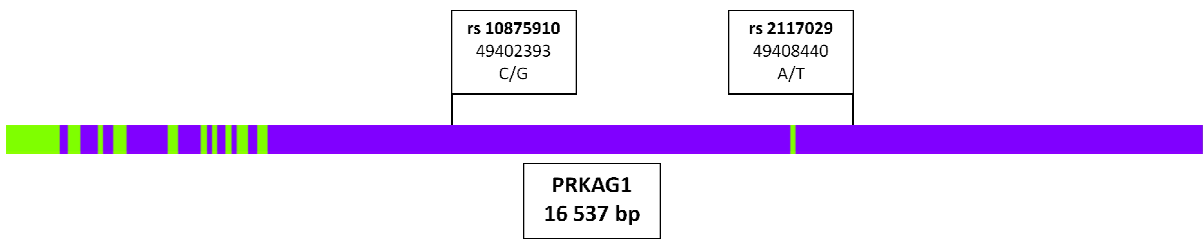


**Figure 2.27** The genomic structure of *PRKAG1* and the physical locations of SNPs selected throughout this gene. Exons and introns are denoted by green and blue boxes, respectively.

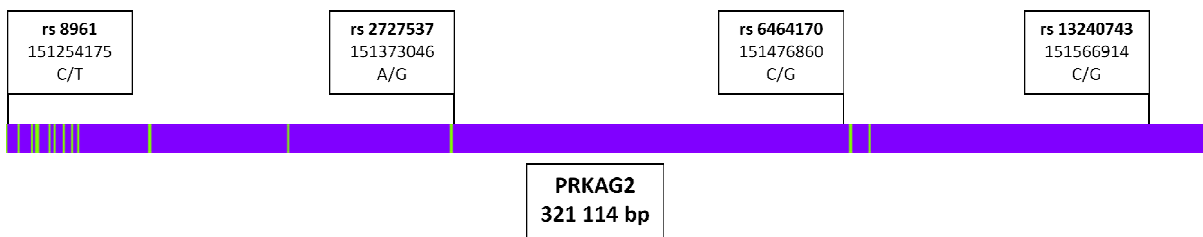


**Figure 2.28** The genomic structure of *PRKAG2* and the physical locations of SNPs selected throughout this gene. Exons and introns are denoted by green and blue boxes, respectively.

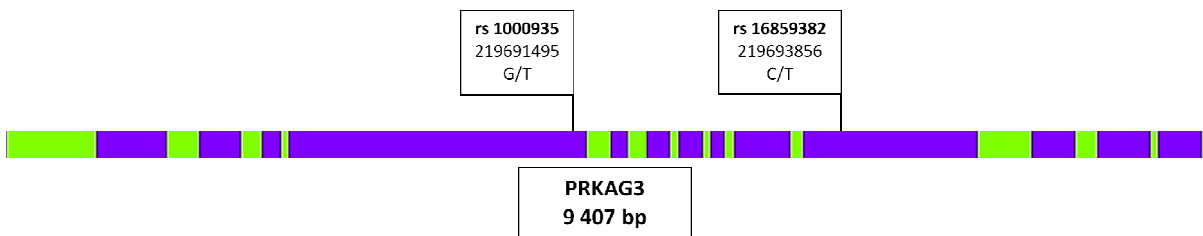


**Figure 2.29** The genomic structure of *PRKAG3* and the physical locations of SNPs selected throughout this gene. Exons and introns are denoted by green and blue boxes, respectively.

## 2.4 ABI TaqMan® SNP genotyping

The SNPs selected for investigation were genotyped within our pedigrees using ABI TaqMan® SNP Validated genotyping assays (Applied Biosystems, Foster City CA, USA). The allelic discrimination capacity of these assays relies on a PCR chemistry that combines primer/probe hybridisation and fluorophore-based detection. Each assay contains a set of primers for target sequence amplification, a pair of allele-specific probes that hybridise to the resulting amplicon, and a passive reference, ROX, for signal normalisation purposes.

Individual probes, in turn, include a minor groove binder (MGB), which increases the probe melting temperature ( $T_m$ ), and two dye attachments: a 5'-end fluorescent reporter dye that reflects allele-specific amplification (VIC for Allele 1; FAM for Allele 2) and a 3'-end non-fluorescent quencher (NFQ) that interacts with the reporter dye, quenching the fluorescent signal. The MGB incorporation increases probe-template binding stability, resulting in greater  $T_m$  differences between matched and mismatched probes, and, consequently, enhanced discriminatory power.

Signal generation occurs when the 5'-end reporter dye undergoes AmpliTaq Gold DNA polymerase 5'-exonuclease cleavage from the probe during PCR extension, thereby removing it from the inhibitory effect of the quencher, and allowing for fluorescence emission (Refer to Figure 2.30).

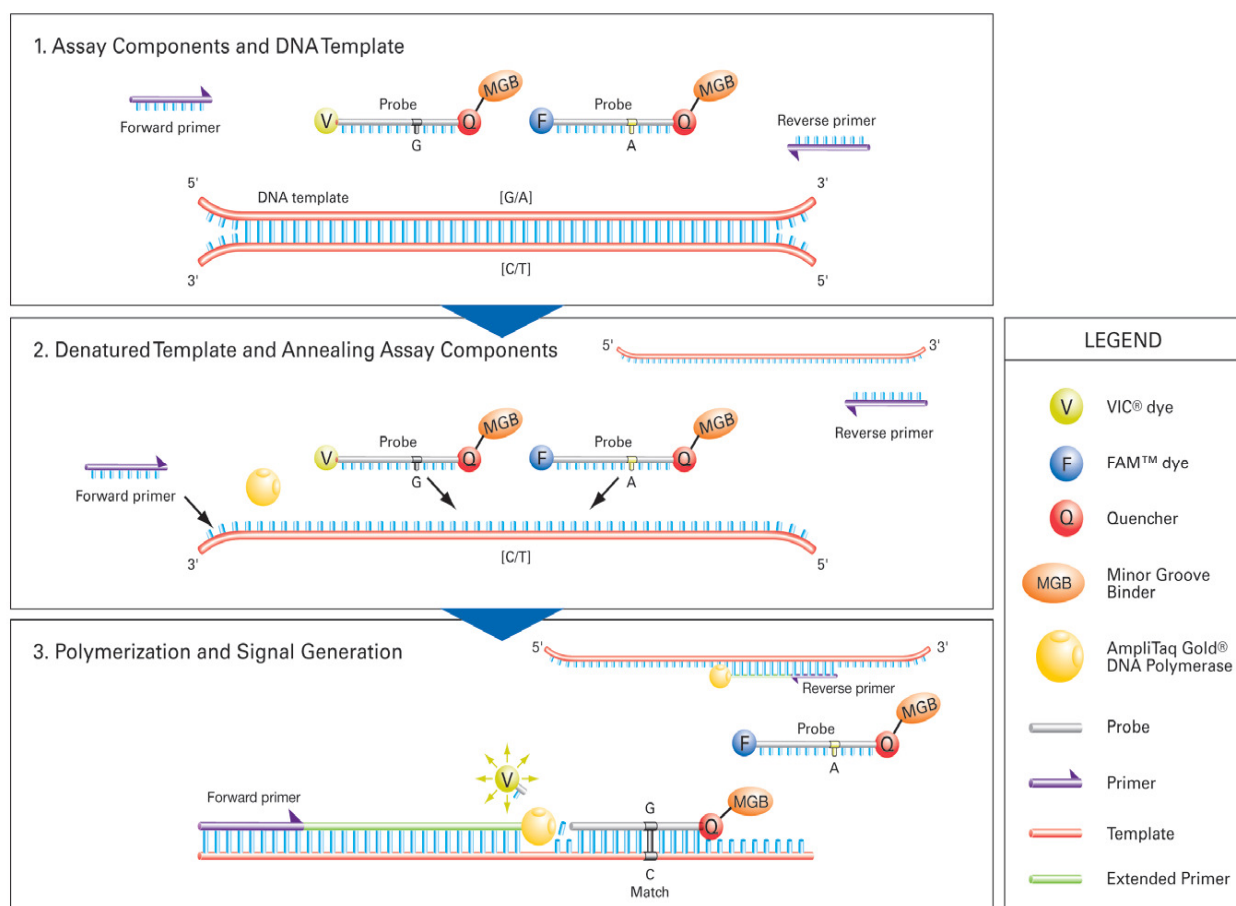


**Figure 2.30 Overview of the ABI TaqMan® SNP Validated genotyping assay hybridisation- and fluorophore-based PCR chemistry that allows for allelic discrimination.** (Taken from [www3.appliedbiosystems.com/cms/groups/mcb\\_marketing/documents/generaldocuments/cms\\_040597.pdf](http://www3.appliedbiosystems.com/cms/groups/mcb_marketing/documents/generaldocuments/cms_040597.pdf))

### 2.4.1 Real-time PCR amplification

The 5 µl PCR amplification reaction volume consisted of 2.5 µl ABI TaqMan® Universal PCR Master Mix (including passive reference ROX (Perkin-Elmer)); 0.25 µl of a 20x TaqMan® SNP genotyping assay comprised of two primer/probe sets (Refer to Section 2.4); 20 ng genomic DNA and 1.25 µl DNase-free, sterile filtered water. Reactions for 330 samples and 54 non-template controls (NTCs), were prepared within 384-well microtiter plates by means of an Eppendorf epMotion 5070 (Eppendorf, Hamburg, Germany) automated pipetting tool. Subsequent thermal cycling was performed on an ABI Prism 7900HT Sequence Detection System (Applied Biosystems Inc, Foster City CA, USA), according to the following conditions: 2 min at 50°C, 10 min at 95°C, and 40 cycles of 15 sec at 92°C and 1 min 30 sec at 60°C each.

## 2.4.2 Allelic discrimination

Allelic discrimination was achieved by means of the multicomponent algorithm within the Sequence Detection Software (SDS) v 2.3 that inferred the normalised allelic contribution per well from the end-point fluorescence measurements, as determined on an ABI Prism 7900HT Sequence Detection System (Applied Biosystems Inc, Foster City CA, USA). The SDS software automatically determines genotypes (set at 95% confidence level), and, in addition, graphs contrasting allele contributions onto allelic discrimination plots, allowing for image-based manual calling of genotypes. Furthermore, the 2-cluster calling option enabled analysis of assay results characterised by the presence of only two distinct clusters. Results were verified by visual inspection of the real-time PCR multicomponent analysis plots.

## 2.5 PCR amplification

Pedigree screening for the presence of a 25 bp deletion in the *MYBPC3* gene was performed via PCR amplification using a deletion-flanking primer set synthesised at the Synthetic DNA Laboratory, Department of Molecular and Cell Biology, University of Cape Town (UCT), Cape Town, South Africa. The primer sequences were obtained from published literature (Dhandapany *et al.*, 2009) and the relevant amplification conditions are detailed in Table 2.5.

**Table 2.5 Primer details and cycling conditions for screening of the 25 bp deletion in the *MYBPC3* gene**

Primer	Sequence	Cycling conditions
Forward	5' GTT TCC AGC CTT GGG CAT AGT C 3'	Initial denaturation at 95°C for 2 min, 35 cycles of amplification at 95°C for 30 sec, 58°C for 30 sec and 72°C for 30 sec, final elongation at 72°C for 2 min
Reverse	5' GAG GAC AAC GGA GCA AAG CCC 3'	

**Abbreviations:** A-adenine; C-cytosine; G-guanine; min-minutes; sec-seconds; T-thymine

The 50 µl reaction volume included 2× KapaTaq ReadyMix (Kapa Biosystems Inc, RSA), 7 pmol of each primer and 20 ng genomic DNA with the exclusion of the latter in the case of the NTC included as a measure for assessing contamination. Amplification was performed in a GeneAmp PCR System 2720 (Applied Biosystems Inc, Foster City CA, USA), whereafter PCR products were electrophoresed on a 2% agarose gel to verify product amplification and to allow for visual assessment of fragment size.



In addition, Dr Marshall Heradien previously performed cohort screening for a *TNNT2* insertion/deletion (I/D) polymorphism, rs4019985 (Heradien M, personal communication); these genotypes were also included in the statistical analysis performed in this study. The genotyping entailed fluorescent primer amplification and subsequent size determination on the ABI Prism 3130xl Genetic Analyser.

## 2.5.2 Agarose gel electrophoresis

PCR products were electrophoresed on a 2% (w/v) horizontal agarose gel (Appendix I) to determine successful amplification. Aliquots of 5 µl of PCR product and 3 µl bromophenol blue loading dye (Appendix I) were mixed and pipetted into each well. In addition, a BenchTop pGEM<sup>®</sup> DNA Marker (Promega Corp, Madison Wisconsin, USA) was loaded to allow for determination of fragment size. Electrophoresis was performed at 120 V for an hour in 1× SB buffer solution (Appendix I). Post-electrophoresis visualisation was achieved by ultraviolet light transillumination on the Multigenius Bio Imaging System (Syngene, Cambridge, UK).

## 2.6 Statistical analyses

The statistical evaluations required the creation of a pedigree input file. This was achieved by capturing the genotypic and phenotypic data of the study participants onto family trees using the software program Cyrillic 2.1 (Cherwell Scientific, UK), whereafter it was exported in MLINK format and combined with the relevant echocardiographic and covariate data in an Excel spreadsheet.

### 2.6.1 Descriptive Statistics

Pedstats v 6.11 (Wigginton & Abecasis, 2005) allowed for validation of input files, including genetic marker data. It was used to test Hardy-Weinberg Equilibrium (HWE) amongst unrelated individuals from the cohort and perform Mendelian inheritance checks to identifying potential genotyping inconsistencies, which were subsequently resolved via sample re-typing. In addition, Pedstats v. 6.11 was employed to graphically summarise the distribution of the quantitative traits and covariates. Certain trait values are asymmetrically distributed and the data are therefore described in terms of the median and interquartile range (Refer to Table 3.1). The interquartile

range is the pair of values (Q1 and Q3) within which the middle 50% of all the observations are located. All traits were quantile-normalised, thereby satisfying the underlying assumptions of the statistical analyses and ensuring the validity of results and conclusions (Pilia *et al.*, 2006). Quantile normalisation retains the order of magnitude of the values, while making their distribution as close as possible to symmetric and bell-shaped; it is a useful approach when traditional forms of transformation do not result in a normal distribution. Haploview v.4.2 (Barrett *et al.*, 2005) was used to calculate the minor allele frequencies (MAFs) for a set of unrelated study participants, as an estimate of SNP informativity within our HCM cohort.

### 2.6.2 Linkage disequilibrium (LD) determination

Linkage disequilibrium is defined as the occurrence of a combination of alleles in a population at a higher frequency than what is expected by random mating (Reviewed by Zondervan & Cardon, 2004). The premise that certain markers are more frequently inherited with the effect allele due to the LD between them can be exploited to evaluate the contribution of a given gene to disease development and to determine the exact effect allele i.e. indirect association mapping. Estimation of LD therefore allows us to characterise the LD structure of our own unique study cohort comprised of South African HCM families from either Caucasian or Mixed Ancestry descent and, in turn, comment on the origin of a significant association signal i.e. whether the associated allele is in LD with, or is itself, deemed the effect allele. That is, we can consider a significant association result within the context of these estimates and, accordingly, prioritize SNPs for future functional analyses and propose avenues for potential fine mapping where relevant.

There are a number of measures with which to describe the extent of LD amongst two markers, however, no one estimate is considered best. McVean (2007) noted that no single measure of LD can capture all information regarding the underlying processes. Similarly, Ardlie *et al.* (2002) explained that the various measures used to describe LD have ‘very different properties and measure different things’. A brief overview of the two most commonly used measures, the normalised disequilibrium coefficient ( $D'$ ) and the square of the correlation coefficient ( $r^2$ ), is provided in the following paragraph (Reviewed by Zondervan & Cardon, 2004; McVean, 2007; Ardlie *et al.*, 2002).

A  $D'$  measure is equal to 1 (complete LD/ no evidence of recombination) in instances where the rarer allele of a given marker is observed in combination with only one of the possible alleles of a second marker.  $D'$  is below 1 only if all four possible haplotypes from a pair of SNPs were observed. However, in instances of rare alleles, the presence of all four possible allele combinations in the larger population may not be reflected in the smaller cohort. Moreover,  $D'$  does not consider MAFs of individual markers and this may result in exaggerated estimates (McVean, 2007; Jarvik *et al.*, 2003). The  $r^2$  estimate is a more stringent measure as it will only be equal to 1 (perfect LD) when the relevant alleles are also observed at identical frequencies i.e. if only two of the four possible allele combinations are observed (Pittman *et al.*, 2005; Jarvik *et al.*, 2003).

It is important to consider that any estimates are cohort specific and they are therefore not exactly equal to the underlying population estimates. Rather, we can make predictions about the population from which our cohort stems by constructing 95% confidence intervals for both the aforementioned measures based on our cohort data. The interval is defined by a lower and upper bound between which we are 95% confident that the true estimate lies. Instead of reporting a cohort specific point estimate of  $D' = 1$ , we can say that we are 95% certain that the true  $D'$  value is greater than the lower confidence bound. Gabriel *et al.* (2002) elaborated on the use of  $D'$  confidence bounds as a means of characterizing the LD between a set of markers. Indeed, Haploview v.4.2 (Barrett *et al.*, 2005) employs the Gabriel method as its default haplotype block generating algorithm which defines SNPs to be in strong LD only in instances where the  $D'$  upper confidence bound  $> 0.98$  and the lower confidence bound  $> 0.70$  (Gabriel *et al.*, 2002).

Using Haploview v.4.2 (Barrett *et al.*, 2005), we opted to calculate pairwise LD statistics in terms of  $D'$  for all pairs of SNPs in each gene included in this study. The software selects a group of maximally informative but unrelated individuals so as to provide an accurate estimate of LD not influenced by family-relatedness. Within the extended family context, as is the case for this study, several sets of equally valid, unrelated individuals may exist. The selection of different subsets might result in varying LD values estimated from the same pedigree data. Pair-wise analyses were thus repeated successively a total of 100 times and the  $D'$  value most frequently observed, that is the mode, is reported in Chapter 3. Results were interpreted as follows:  $D'$  values of 1 indicate complete LD;  $D'$  values  $> 0.8$  indicate strong LD,  $D'$  values 0.2–0.8 classified as incomplete LD and  $D' < 0.2$  defined as negligible LD (Heward *et al.*, 2007). Haploview v.4.2 (Barrett *et al.*, 2005)

was also used to estimate pair-wise  $r^2$  values and the 95% confidence bounds for the D' estimates, however, these analyses were not repeated as done for D'.

### 2.6.3 Principal component score

As previously described the HCM hypertrophy phenotype exhibits extreme variability in terms of degree and location. The resulting inter-individual variation hampers statistical analysis as no single measure can comprehensively capture hypertrophy. Echocardiographically derived LVM is commonly used as descriptor, but may not, due to the geometric assumptions underlying the calculation, accurately account for LV shape variability. PCA identifies similarities in patterns of phenotypic variation and it was therefore applied to the 16 transformed wall thickness measurements to define the mathematical combination thereof that accounts for the largest amount of variability in the data i.e. PC1. The latter, defined as the weighted sum of the 16 wall thickness measurements, thus serves as a single cohort-specific measure fit for association testing.

To reiterate, variability defined here refers to differences in phenotype amongst study participants. The aim of the PCA analysis is to determine the extent to which individual measurements contribute to the phenotypic variability. These measurements are then combined mathematically in a way which reflects the weight of their individual contributions thereby providing a single score. A test of heritability determines if and to which extent this variability (for both individual measures and scores) can be ascribed to genetic factors (Refer to Section 2.6.5).

### 2.6.4 Confounding variables

Adjustment for confounding variables ensures that a significant association best reflects the relationship of interest i.e. between an investigated variant and phenotypic variation. The statistical models employed thus incorporated fixed effects for known covariates of hypertrophy namely age, sex, BSA, HR (as a proxy measure for tachycardia), mean arterial pressure (MAP) (as derived from systolic and diastolic BP), presence of hypertension (i.e., adjustment for anti-hypertensive therapy), ethnicity (as indication of recent population stratification) and both the individual carrier status and identity of the relevant HCM-causing founder mutation (mutation groups were treated as a factor with three categories). Inclusion of the latter served as adjustment for both the ancestral relatedness within each founder group and the potential contribution of the relevant founder mutation to the

trait variance. It is of specific relevance to the current study as the founder mutations are located within two of the candidate genes selected for investigation ( $R92W_{\text{TNN}T2}$ ,  $R403W_{\text{MYH}7}$ , and  $A797T_{\text{MYH}7}$ ). The correction thus ensures that any significant associations identified for these genes would best reflect association with variants other than the founder mutations.

### 2.6.5 Heritability

The Abecasis pedigree-based QTDT (Abecasis *et al.*, 2000) was used to estimate trait heritability, i.e. the degree to which additive genetic factors contribute to the phenotypic variation of a transformed, covariate-adjusted trait, to determine suitability for association testing. This was achieved by means of a variance components model that divides trait variance into environmental and additive genetic (polygenic) effects. The broad sense heritability is defined as the ratio of genetic variance to the total phenotypic variance.

### 2.6.6 Single nucleotide polymorphism association

Association testing was achieved by means of family-based statistical analyses, which allow for the inclusion of unaffected relatives as appropriately matched controls thereby reducing stratification. A significant association between a biallelic variant and a quantitative phenotype ( $p$ -value  $< 0.05$ ) indicates an allele dosage effect interpreted as a significant difference in mean trait value between wild type homozygotes (no minor alleles) and heterozygotes (1 minor allele) and so too, in equal measure, between heterozygotes and minor homozygotes (2 minor alleles). The measure of difference in mean phenotype due to a given allele is termed the effect size. Association testing between individual variants and hypertrophy traits was performed in R using the `lmekin` function of the kinship package (Atkinson & Therneau, 2008). It entailed specialised mixed-effect modelling as it incorporated random effects, both family- and individual-specific, as well as fixed effects to adjust for known hypertrophy covariates and allow for additive allelic association testing between a single variant and single trait (polygenic variance component). Under an additive genetic model, SNPs were coded as ordinal variables of 0, 1 or 2 reflecting the number of minor allele copies.

More specifically, modelling of family- and individual-specific random effects served as adjustments for possible intrafamilial clustering of traits and interindividual trait correlations owing to family or cryptic relatedness (Price *et al.*, 2010). The first was achieved by inclusion of a family-

membership indicator and the second was correlated according to the genetic relatedness between family members i.e. kinship coefficient. The latter, defined as the pedigree-based probability that two individuals share alleles identical by descent (IBD), was estimated with function `makekinship` in `kinship`. Given that the correlations in trait values between family members are taken into account, the models we used for inference ensure that larger families do not have disproportionately larger contributions to the estimated effects (van der Merwe L, personal communication).

To facilitate interpretation, the results obtained for the SNP association analyses are presented graphically in Chapter 3 (Refer to Figure 3.3 as an example). The figures tabulate the original p-values whilst plotting the corresponding negative logarithm base 10 ( $-\log_{10}$ ) transformed p-values ( $-\log_{10} [\text{p-value}]$ ) on bar graphs. The log transformation compresses the scale of the relevant axis whilst maintaining the ratio between values; i.e. larger values are brought closer together whilst smaller values become more separated. The p-values are therefore expressed on a  $-\log_{10}$  scale for ease of visualisation and comparison. Moreover, a red dashed horizontal line indicates the p-value significance threshold equal to 0.05. Bars which are located above this line therefore indicate significant p-values, i.e. p-values of less than 0.05. Moreover, the p-value significance increases with bar height above threshold.

It is important to note that no formal correction was made for multiple testing given the lack of an appropriate method and the explorative nature of this genetic investigation. Briefly, the existing methods are only suited to the study of family trios and not extended pedigrees as investigated in the current study. Furthermore, they are either over-conservative or require prior knowledge of the hypothesis under investigation. A more detailed discussion of these reasons is provided in Section 4.1.2.

Furthermore, comparative analyses were done to determine whether the effect of the investigated variants varied amongst the three HCM founder mutation groups. Such HCM mutation-specific effects have been reported in the literature and were thus evaluated here by statistical pair-wise comparison of the three HCM founder mutation groups with regards to variant effect on phenotype. These tests for statistical interaction between the HCM mutation groups and the investigated variant are summarised with three p-values and their corresponding effect sizes (Refer to Section 3.4.5). The interpretation of a significant interaction result is demonstrated in Section 2.6.8.

### 2.6.7 Effect sizes

As mentioned earlier, trait values were quantile-normalised to approximate normality, an important requirement for validity of the association model used. Hence, the derived effects sizes are in quantile-normalised units, which are not interpretable in terms of the original cardiac measurements. The untransformed, covariate-adjusted hypertrophy measures were therefore also analysed, as per the method detailed for modelling of the transformed data, in an attempt to estimate approximate effect sizes in the original units of measurement for all significant associations identified. An exception applies to estimation of effect sizes for PC1, as it is a composite score. Here, we estimated effect sizes based on modelling the mean of the 16 untransformed, covariate-adjusted cardiac wall thickness measurements.

### 2.6.8 Demonstrated interpretation of interaction

As described in Section 2.6.6, comparative analyses were done with the aim of determining whether the effect of the investigated variants on hypertrophy traits varied amongst the three HCM founder mutation groups i.e. mutation group and variant interaction. One of the significant results obtained by comparative analysis is discussed in the subsequent paragraphs in order to demonstrate its interpretation.

A significant interaction between HCM mutation group and the rs3729838 (*TNNI3*) variant was identified upon pair-wise comparison of the three HCM founder mutation groups, with respect to the effect of this SNP on mLVWT. The p-values for these between-group comparisons were as follows: R403W<sub>MYH7</sub> and A797T<sub>MYH7</sub> groups (p = 0.080); R92W<sub>TNNI2</sub> and A797T<sub>MYH7</sub> groups (p = 0.482); R92W<sub>TNNI2</sub> and R403W<sub>MYH7</sub> groups (p = 0.022). This indicated a significant difference in the estimated variant effect, with the addition of a G-allele resulting in a 2.45 mm higher mLVWT in the R92W<sub>TNNI2</sub> group compared to the R403W<sub>MYH7</sub> group.

Figure 2.31 illustrates the aforementioned significant interaction, in a plot of the estimated mLVWT values for 9 hypothetical ‘average’ individuals specific to the cohort, three per HCM founder mutation group, with each representing a possible rs3729838 genotype (CC, CG or GG). The demographics that define the ‘average’ individual are as follows: 41 years of age, Caucasian, male, no specific HCM mutation, treatment with anti-hypertensive medication, BSA of 1.93m<sup>2</sup>, MAP of

94 mm Hg, and HR of 69 beats per minute (bpm). The graph will adjust up or down when representing ‘real’ individuals as a reflection of the per-individual variation in hypertrophy covariate values; for instance, mutation carriers would be characterised by the addition of 4.98 units to the average values. However, the estimated difference in effect size amongst the HCM mutation groups is unvarying.

The graph illustrates that the average effect of the *TNNI3* gene variant on mLVWT, represented here as the addition of a G-allele, varies significantly relative to the specific HCM causal mutation present in a given individual. More specifically, each G-allele added will increase mLVWT in  $A797T_{MYH7}$  and  $R92W_{TNNI2}$  carriers by 1.70 mm and 1.53 mm, respectively, whilst decreasing mLVWT by 0.92 mm in  $R403W_{MYH7}$  carriers. The difference in variant effect was significant only for comparison of  $R403W_{MYH7}$  carriers to the  $R92W_{TNNI2}$  carriers. The effect of the two alleles at the locus corresponds in size, but is directionally opposite.

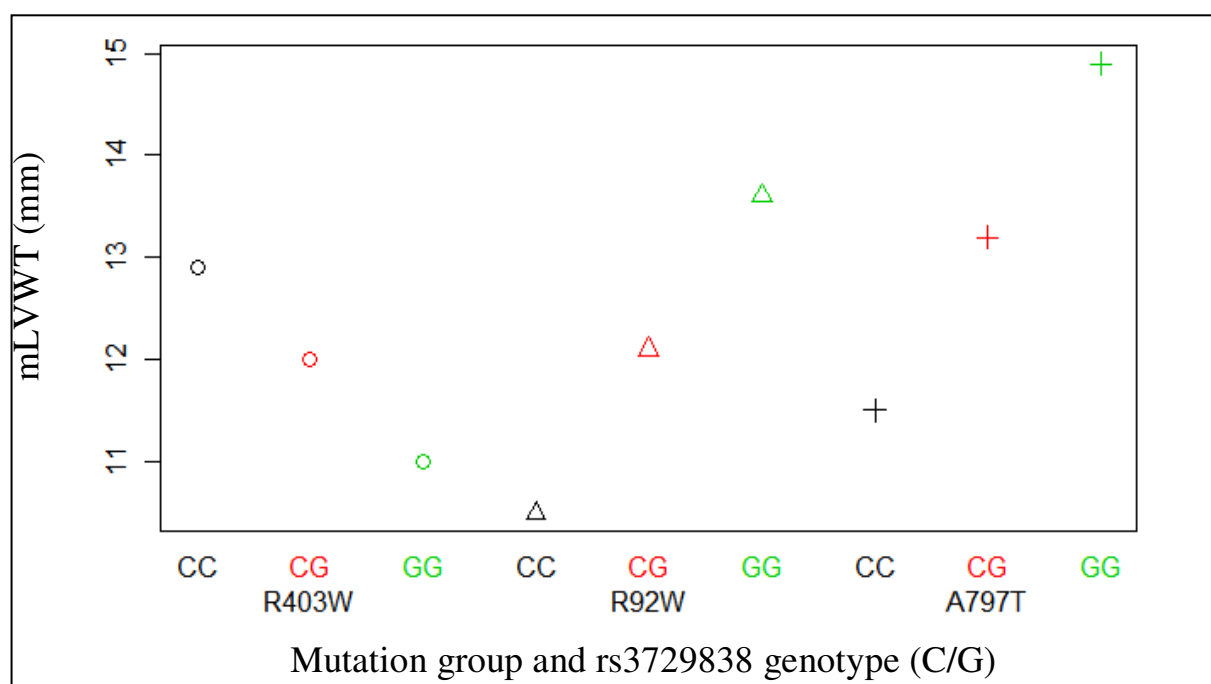


**Figure 2.31** Graph of estimated mLVWT by mutation group and rs3729838 genotype.

### 2.6.9 Haplotype assignment and association analysis

Simwalk v.2.91 (Sobel & Lange, 1996) was used to estimate the most probable, fully-typed maternal and paternal haplotype configuration for each individual in the pedigree. Each run of the software delivers a set of likely haplotypes. We arbitrarily selected 1.5% as our cut-off for



haplotype frequencies, as lower frequencies will not provide enough power to detect effects of biologically relevant sizes in our groups. Each effect size and group size provides a different power, of course. The selected frequency of 1.5% is arbitrary and conservative (van der Merwe L, personal communication).

An additive model of association was fitted using the R function `lmekin`, exactly as described for SNP evaluations (Refer to Section 2.6.6) with the coding of 0, 1 or 2 here reflecting the number of copies of an inferred haplotype. Comparative (interaction) analyses were also performed to determine whether the effect of investigated haplotypes varied amongst the three HCM founder mutation groups. The p-values obtained for the haplotype association analyses; and the tests for statistical interaction between the HCM mutation groups and investigated haplotypes are presented in Chapter 3 (Refer to Section 3.4.5). The outline and interpretation of significant results is detailed in Section 2.6.6 and 2.6.8. The use of haplotype analyses allowed us to capture the variability throughout the investigated genes and to evaluate the effect of a single variant within the context of the entire gene, as the effect seen for a single variant by itself may be altered when considering it within the context of other variants within the total gene.

### **2.6.10 Optimal selection**

We aimed to identify a subset of the variants investigated in this study that would collectively explain most of the variation in hypertrophy in the current cohort. To this end, we performed backwards stepwise-selection on the model for the PC1 trait with the goal of identifying a subset of variants that significantly affected the trait, independently of the eight hypertrophy covariates adjusted for throughout the study; and the other significant variants in the model. We focused on the composite score, PC1, as it is a weighted sum of the 16 wall thickness measurements that best reflected the ventricle-wide hypertrophy and so the variability in LVH in the present HCM cohort. Analyses were performed for the study participants with complete genotype and phenotype data.

The model first comprised the hypertrophy covariates and a total of nine variants that associated significantly with at least one hypertrophy trait in the present cohort. Thereafter, we further reduced this subset of variants, by means of backward stepwise-selection, to a set of six markers that predicted an increase in at least one of the hypertrophy indices, independent of the hypertrophy

covariates and the other significant variants, i.e. three variants that did not significantly affect the hypertrophy trait following adjustment for the other significant variants in the model were removed.

The six remaining markers were modelled on the quantile normalised traits and the untransformed trait data adjusted for the hypertrophy covariates and the other significant variants in the model, to obtain p-values and effect sizes, respectively. More specifically, as PC1 is a composite score, its estimated effect sizes are derived from the CWT score by modelling the mean of the 16 untransformed, covariate-adjusted cardiac wall thickness measurements.

All statistical analyses were designed and executed by Prof Lize van der Merwe (MRC Biostatistics Unit, South Africa), assisted by Ushma Galal and Renier van Rooyen. Also, the understanding and communication of the statistical concepts was facilitated by Prof Lize van der Merwe (van der Merwe L, personal communication).

## CHAPTER THREE

### RESULTS

---

#### 3.1 Basic cohort characteristics

The entire study cohort consisting of 388 participants underwent molecular genetic testing to determine their carrier status for each of the three HCM-causing founder mutations that segregate within the study cohort. None of the individuals were compound heterozygous for any of the founder mutations; i.e., individuals were either carriers of a single HCM-causing founder mutation, or non-carriers for all three mutations.

In addition, 256 of these study individuals consented to clinical assessment. Table 3.1 details the basic cohort characteristics with participants grouped according to mutation carrier (MC) and non-carrier (NC) status for each of the three HCM founder mutations. The data are described in terms of the median (interquartile range) as certain trait values are asymmetrically distributed.

**Table 3.1 Basic characteristics of the study cohort.** Individuals are grouped according to the relevant HCM founder mutation and mutation status as either mutation carrier (MC) or non-carrier (NC).

	<b>A797T<sub>MYH7</sub></b>			<b>R92W<sub>TNNT2</sub></b>			<b>R403W<sub>MYH7</sub></b>		
	<b>MC</b>	<b>NC</b>	<b>MC-NC†</b>	<b>MC</b>	<b>NC</b>	<b>MC-NC†</b>	<b>MC</b>	<b>NC</b>	<b>MC-NC†</b>
<b>n</b>	68	50		48	34		32	24	
<b>Age</b>	43.0 (26.8–56.8)	41.5 (29.3–53.0)		36.0 (21.0–47.0)	42.0 (25.5–49.0)		36.5 (25.0–46.8)	38.0 (31.3–50.8)	
<b>BSA (m<sup>2</sup>)</b>	1.90 (1.60–2.00)	1.90 (1.67–2.03)		1.70 (1.60–1.80)	1.80 (1.60–1.90)		1.80 (1.70–2.00)	1.95 (1.70–2.05)	
<b>SBP (mm Hg)</b>	120 (115–134)	120 (110–130)		115 (110–130)	120 (110–120)		120 (115–130)	120 (114–143)	
<b>DBP (mm Hg)</b>	80 (70–87)	80 (80–89)		73 (70–80)	80 (70–80)		80 (79–80)	80 (78–90)	
<b>HR (bpm)</b>	68 (60–75)	68 (62–76)		68 (61–76)	67 (60–73)		65 (60–76)	72 (65–84)	
<b>Anti-hypertensive therapy</b>	16	11		4	1		4	4	
<b>LVM (g)</b>	191 (135–237)	135 (109–159)	58.6, p<0.001	146 (104–185)	116 (100–144)	19.5, p=0.039	170 (134–205)	154 (115–202)	26.2, p=0.021
<b>mIVST (mm)</b>	14.5 (11.0–20.9)	10.5 (9.2–11.3)	5.7, p<0.001	14.0 (9.6–18.3)	10.0 (8.6–10.9)	3.9, p<0.001	13.6 (11.6–16.0)	11.0 (10.2–12.6)	3.7, p=0.004
<b>mLVWT (mm)</b>	14.0 (11.0–20.7)	10.5 (9.5–11.3)	5.4, p<0.001	13.4 (9.9–18.1)	10.0 (9.2–10.9)	3.5, p=0.001	13.6 (11.6–17.8)	11.2 (10.2–12.4)	3.8, p=0.003
<b>mPWT (mm)</b>	10.2 (9.1–11.8)	9.0 (8.3–10.0)	1.5, p<0.001	10.2 (8.1–11.5)	8.1 (7.5–9.1)	1.6, p<0.001	10.1 (9.1–11.5)	9.9 (8.8–10.4)	1.3, p=0.013
<b>CWT score</b>	196 (151–239)	139 (127–148)	52.3, p<0.001	159 (131–192)	131 (117–142)	31.9, p<0.001	172 (148–190)	153 (136–166)	23.0, p=0.019
<b>PC1</b>	2.12 (–0.14–4.88)	–1.31 (–2.52–0.01)	3.3, p<0.001	0.86 (–2.62–2.72)	–2.56 (–4.26–1.01)	2.0, p<0.001	1.42 (–0.34–2.42)	0.1 (–2.02–1.44)	1.4, p=0.032

\* Data summarised as median (interquartile range Q1–Q3); the interquartile range indicates the middle 50% of all the observations

† Estimated difference between mutation-carriers and non-carriers per mutation group using raw data; p-values for tests of statistical differences using quantile normalised trait values. Joint models using all individuals were employed and adjusted for age, sex, BSA, MAP, HR, use of anti-hypertensive medication and ethnicity.

**Abbreviations:** A-Alanine; bpm-beats per minute; BSA-body surface area; CWT score-cumulative wall thickness score; DBP-diastolic blood pressure; g-gram; HCM-hypertrophic cardiomyopathy; Hg-mercury; HR-heart rate; LVM-left ventricular mass; m<sup>2</sup>-per square meter; MC-HCM mutation carrier; mIVST-maximal interventricular septum thickness; mLVWT-maximal left ventricular wall thickness; mPWT-maximal posterior wall thickness; mm-millimetre; MYH7-Myosin heavy chain gene 7; NC-non-carrier; n-number of clinically evaluated participants; PC1-first principal component; Q1-first quartile; Q3-third quartile; R-Arginine; SBP-systolic blood pressure; T-Threonine; TNNT2-Troponin T gene 2, cardiac; W-Tryptophan

### 3.2 Candidate gene selection and SNP prioritisation

A comprehensive literature review allowed the identification of 26 candidate hypertrophy modifier genes selected for their contributions to sarcomere integrity and contractility and/or myocardial energetics, the disruption of which is known to contribute to the development of HCM. The SNPs investigated in the present study were selected with the aim of achieving 0.5 LDU even spacing throughout the candidate genes and were further prioritised according to ABI TaqMan® SNP Validated Genotyping Assay-availability and their MAFs. Table 3.2 lists the 26 candidate genes, the 78 SNPs selected and their MAFs for the CEU and YRI populations (Refer to Section 2.3.2).

**Table 3.2 The SNPs chosen for investigation in this study and their minor allele frequencies (MAF) in the CEU and YRI populations**

Gene symbol	Chromosome localisation	SNP ID	Nucleotide change	MAF*	
				CEU	YRI
<b>Sarcomeric candidate modifier genes</b>					
<b>Thin filament components</b>					
<i>ACTC1</i>	15q11-q14	rs1370154	T/C	0.258 (T)	0.133 (T)
		rs2070664	T/C	0.500 (T)	0.267 (C)
<i>TNNT2</i>	1q32	rs2365652	C/A	0.358 (C)	0.250 (A)
		rs1892028	G/A	0.364 (G)	0.224 (A)
		rs947485	A/G	0.356 (A)	0.242 (G)
<i>TNNI3</i>	19q13.4	rs3729841	C/T	0.117 (T)	0.000 (T)
		rs3729838	C/G	0.186 (C)	0.229 (G)
		rs11667847	A/G	-	-
<i>TPM1</i>	15q22	rs11071720	T/C	0.367 (T)	0.358 (C)
		rs4238370	G/T	0.229 (T)	0.339 (T)
		rs1071646	C/A	0.392 (C)	0.483 (C)
		rs707602	T/C	0.136 (C)	0.117 (C)
<i>ACTN3</i>	11q13-q14	rs1791690	G/A	0.433 (A)	0.280 (G)
		rs2275998	C/T	0.175 (C)	0.292 (C)
		rs1815739	C/T	0.458 (T)	0.100 (T)
<b>Thick filament components</b>					
<i>MYL3</i>	3p21.3-p21.2	rs1531136	T/C	0.175 (T)	0.067 (C)
		rs3792558	T/C	0.150 (T)	0.133 (C)
<i>MYH7</i>	14q12	rs765019	C/T	0.108 (C)	0.212 (C)
		rs2277475	T/A	0.333 (T)	0.233 (A)
		rs1951154	G/A	0.308 (A)	0.025 (A)
		rs2754163	C/T	0.300 (C)	0.308 (T)
		rs2239578	G/A	0.442 (G)	0.342 (A)
<i>MYL2</i>	12q23-q24.3	rs933296	C/A	0.354 (A)	0.071 (A)
		rs4766517	C/G	0.449 (G)	0.142 (G)

Gene symbol	Chromosome localisation	SNP ID	Nucleotide change	MAF*	
				CEU	YRI
<b>Intermediate filament components</b>					
<i>MYBPC3</i>	11p11.2	rs4752825	G/A	-	-
		rs1052373	C/T	0.254 (T)	0.500 (T)
		rs10838696	G/A	0.367 (A)	0.000 (A)
		rs11570058	G/A	0.098 (A)	0.042 (A)
<b>Energy metabolism candidate modifier genes</b>					
<b>Fatty acid metabolism components</b>					
<i>CD36</i>	7q11.2	rs10268417	C/A	0.373 (A)	0.362 (C)
		rs3211892	G/A	0.025 (A)	0.358 (A)
		rs3173804	A/T	0.492 (A)	0.083 (A)
<i>CPT1B</i>	22q13.33	rs470117	C/T	0.492 (C)	0.092 (T)
		rs1557502	C/T	0.150 (T)	0.267 (C)
<i>PPARA</i>	22q13.31	rs881740	G/A	0.092 (G)	0.317 (G)
		rs4823613	A/G	0.300 (G)	0.380 (G)
		rs4253776	G/A	0.150 (G)	0.467 (G)
<i>PPARG</i>	3p25	rs12631028	C/T	0.211 (T)	0.259 (T)
		rs12490265	G/A	0.350 (A)	0.025 (A)
		rs2938392	G/A	0.467 (A)	0.108 (A)
		rs1175540	C/A	0.342 (A)	0.225 (C)
<i>PGCIA</i>	4p15.1	rs768695	A/G	0.433 (G)	0.483 (G)
		rs4619879	C/A	0.450 (C)	0.467 (C)
		rs11724368	A/T	0.217 (T)	0.042 (T)
		rs13131226	C/T	0.316 (C)	0.481 (C)
<b>Glucose metabolism components</b>					
<i>ALDOA</i>	16q22-q24	rs9928448	C/T	0.458 (T)	0.400 (T)
		rs11860935	C/T	0.110 (T)	0.147 (T)
<i>PFKM</i>	12q13.3	rs1859445	A/C	0.300 (C)	0.150 (C)
		rs10875749	A/T	0.392 (T)	0.108 (T)
<i>PDK4</i>	7q21.3	rs2073978	C/T	0.442 (C)	0.417 (T)
		rs2301630	T/C	0.467 (T)	0.314 (C)
<b>Creatine kinase energy shuttle components</b>					
<i>CKM</i>	19q13.2-q13.3	rs8111989	T/C	0.258 (C)	0.475 (T)
		rs7260463	G/T	0.283 (T)	0.421 (G)
		rs1133190	G/A	0.350 (A)	0.225 (G)
		rs344816	T/A	0.417 (T)	0.050 (A)
<i>CKB</i>	14q32	rs1803283	C/T	0.351 (C)	0.364 (T)
		rs2071407	T/C	0.283 (T)	0.448 (T)
		rs1136165	T/G	-	-
<b>Cellular energy homeostasis</b>					
<i>PRKAA1</i>	5p12	rs12517210	T/C	0.392 (C)	0.167 (C)
		rs11747210	T/G	0.345 (G)	0.181 (G)
		rs466108	C/A	0.333 (A)	0.400 (A)
<i>PRKAA2</i>	1p31	rs1124900	G/T	0.433 (G)	0.356 (G)
		rs2796495	C/T	0.433 (T)	0.492 (T)
		rs932447	T/C	0.383 (C)	0.288 (C)

Gene symbol	Chromosome localisation	SNP ID	Nucleotide change	MAF*	
				CEU	YRI
<i>PRKAB1</i>	12q24.1	rs6490267	G/T	0.367 (T)	0.442 (T)
		rs278143	A/G	0.342 (G)	0.442(G)
		rs10849690	C/G	-	0.009 (G)
		rs278149	T/G	0.333 (T)	0.483 (T)
		rs4213	T/G	0.342 (G)	0.458 (G)
<i>PRKAB2</i>	1q21.1	rs6937	T/C	0.133 (C)	0.092 (C)
		rs1348316	G/A	0.442 (G)	0.195 (A)
<i>PRKAG1</i>	12q12-q14	rs10875910	G/C	0.283 (C)	0.075 (C)
		rs2117029	A/T	0.342 (A)	0.459 (T)
<i>PRKAG2</i>	7q36.1	rs8961	C/T	0.367 (T)	0.167 (C)
		rs2727537	G/A	0.342 (G)	0.358 (A)
		rs6464170	G/C	0.267 (G)	0.508 (C)
		rs13240743	C/G	0.373 (G)	0.425 (G)
<i>PRKAG3</i>	2q35	rs1000935	G/T	0.000 (G)	0.333 (T)
		rs16859382	C/T	0.000 (C)	0.192 (T)

\* Minor allele indicated in brackets

**Abbreviations:** A-adenine; *ACTC1*-Actin, alpha, cardiac muscle 1; *ACTN3*-Actinin, alpha 3; *ALDOA*-Aldolase A, fructose-bisphosphate; C-cytosine; *CD36*-CD36 antigen, thrombospondin receptor; CEU-Central European; *CKB*-Creatine kinase, brain; *CKM*-Creatine kinase, muscle; *CTPIB*-Carnitine palmitoyltransferase 1B, muscle; G-guanine; MAF-minor allele frequency; *MYBPC3*-Myosin binding protein C, cardiac; *MYH7*-Myosin heavy chain 7, cardiac muscle, beta; *MYL2*-Myosin light chain 2, regulatory cardiac, slow; *MYL3*-Myosin light chain 3, alkali, ventricular, skeletal slow; *PDK4*-Pyruvate dehydrogenase kinase, isozyme 4; *PFKM*-Phosphofructokinase, muscle; SNP-single nucleotide polymorphism; T-thymine; *TNNI3*-Troponin I type 3, cardiac; *TNNT2*-Troponin T type 2, cardiac; *TPMI*-Tropomyosin 1; *PPARA*-Peroxisome proliferator-activated receptor alpha; *PPARG*-Peroxisome proliferator-activated receptor gamma; *PGC1A*-Peroxisome proliferator-activated receptor gamma, coactivator 1 alpha; *PRKAA1*-Protein kinase, AMP-activated, alpha 1 catalytic subunit; *PRKAA2*-Protein kinase, AMP-activated, alpha 2 catalytic subunit; *PRKAB1*-Protein kinase, AMP-activated, beta 1 non-catalytic subunit; *PRKAB2*-Protein kinase, AMP-activated, beta 2 non-catalytic subunit; *PRKAG1*-Protein kinase, AMP-activated, gamma 1 non-catalytic subunit; *PRKAG2*-Protein kinase, AMP-activated gamma 2 non-catalytic subunit; *PRKAG3*-Protein kinase, AMP-activated, gamma 3 non-catalytic subunit; YRI-Yoruba

### 3.3 Genotyping results

#### 3.3.1 TaqMan® allelic discrimination

The ABI TaqMan® SNP validated genotyping that encompassed real-time PCR amplification and allelic discrimination, was successfully completed for all the polymorphisms selected for investigation. Poor amplification was initially achieved for a total of six of the investigated variants. The reactions were repeated a number of times and as a result insufficient assay volumes hampered successful re-typing. This is reflected by the overall genotyping success rate which ranged from 71-90% (success rate of the six assays ranged from 71-79%). The genotyping success rate, excluding

the six assays, ranged from 80-90%. Figure 3.1 represents an allelic discrimination plot for the *CD36* gene polymorphism, rs10268417, graphed by the SDS software as contrasting normalised allele contributions.

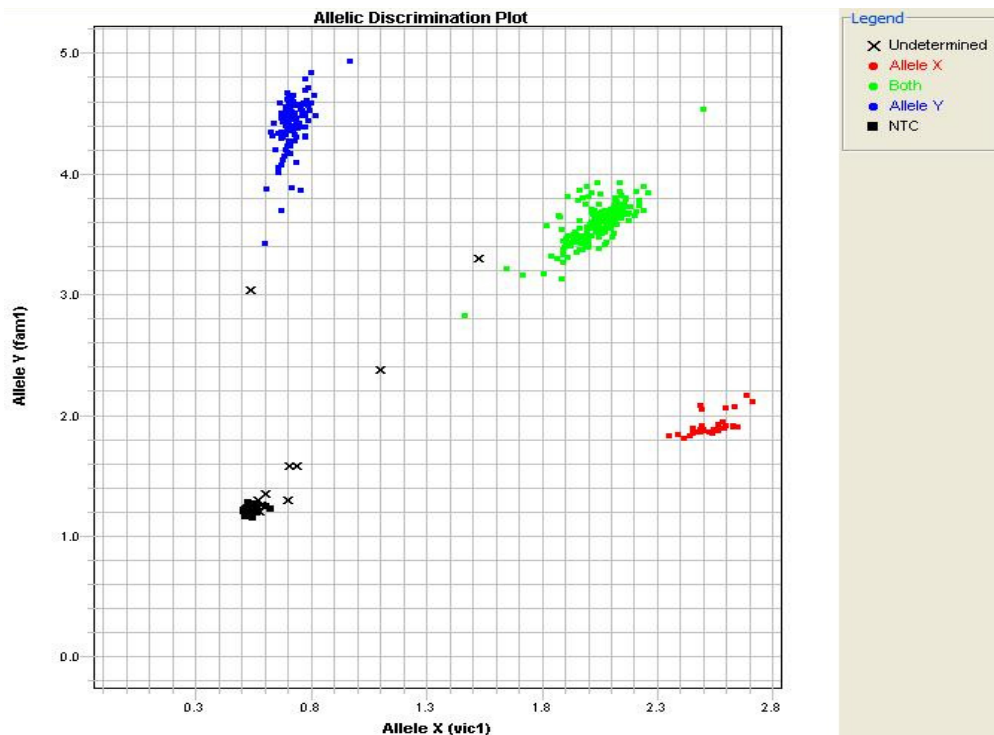


**Figure 3.1 The *CD36* rs10268417 genotypes.** Genotyping was determined by end point analyses and graphed by the SDS software as contrasting allele contributions. Blue squares indicate individuals homozygous for allele Y; red squares signify individuals homozygous for the X allele; green blocks represent heterozygous individuals; black squares denote non-template controls (NTCs); black crosses indicate undetermined samples that either did not cluster tightly or clustered with the NTC samples. Allele X: A; Allele Y: C

### 3.3.2 PCR amplification

Successful PCR amplification was achieved for the screening of the 25 bp, *MYBPC3* gene deletion. The absence of contamination was confirmed by the observed non-amplification of negative controls. Figure 3.2 is a representation of the PCR results obtained, with the entire cohort proving to be homozygous wild-type (WT) (fragment sizes: WT 403 bp; mutant 378 bp).



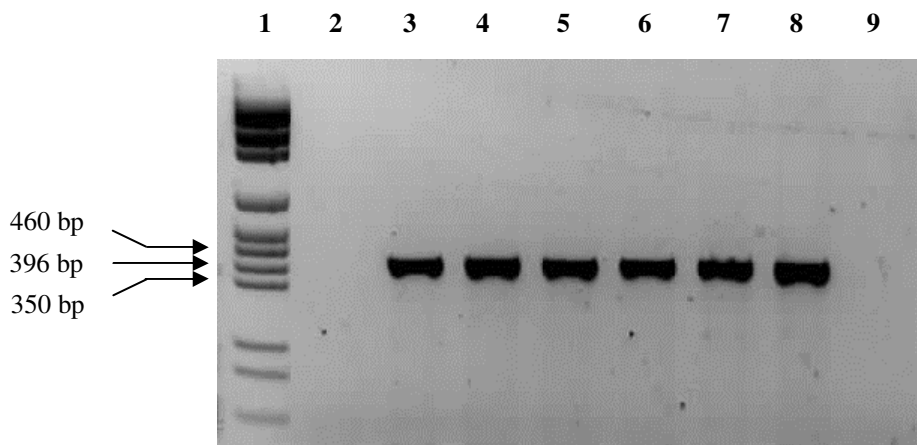


**Figure 3.2 PCR amplification of the 25bp deletion in the *MYBPC3* gene.** Representative 2% agarose gel of fragment sizes generated via PCR, indicating individual genotypes for the *MYBPC3* deletion. Lane 1: Molecular weight marker; Lanes 2–8: individual sample amplification (lane 2 denotes unsuccessful amplification resolved via subsequent re-typing); Lane 9: negative control.

All genotype results determined by end-point analyses or by visualization of PCR fragments, together with the established phenotype information, were then integrated into a database for further statistical evaluations.

### 3.4 Statistical analyses

#### 3.4.1 Descriptive statistics

The Pedstats software v 6.11 (Wigginton & Abecasis, 2005) was used to perform HWE testing amongst unrelated individuals from the cohort with the exact test p-values obtained reported in Table 3.3. Three of the investigated SNPs were excluded from further statistical analyses as the heterozygosity in one (rs3729841) was too low to be informative, whilst the genotype frequencies of the other two (rs3211892 and rs8961) departed from HWE at the p-value < 0.01 level. Moreover, the genotyping results obtained for the rs3729841 SNP indicated that the majority of individuals were homozygous for the C-allele, whilst three individuals proved to be heterozygous and a further five individuals homozygous for the T-allele.

Haploview v.4.1 was used to calculate MAFs from a set of unrelated study individuals; estimates of SNP informativity within our HCM cohort are included in Table 3.3. Also, the SNP MAFs for the CEU and YRI populations are again provided for ease of comparison. A total of 59 of the 78 SNPs

selected for investigation shared a minor allele with at least one of the HapMap reference populations of which the MAFs did not differ by  $> 0.2$  as indicated by the purple highlighting. Blue highlighting indicates instances in which the same minor allele is shared but the difference in the frequencies is  $> 0.2$ . The corresponding allele frequencies suggest that the CEU and YRI reference populations provide accurate estimates of the LD structure of our own unique study cohort. As mentioned in Chapter 2, this was also clear from previous association studies from our own laboratory. However, it should be noted that five of the SNPs investigated had different minor alleles relative to the reference populations: *ALDOA*, rs9928448; *PFKM*, rs1859445; *CKB*, rs2071407; *PRKAA1*, rs11747210; *PRKAA2*, rs2796495.

**Table 3.3 Cohort-specific descriptives: Hardy-Weinberg equilibrium test p-values and minor allele frequencies for the SNPs investigated**

Candidate gene	Chromosome locus	SNP ID	HWE p-value	MAF		
				Study cohort	CEU	YRI
<b>Sarcomeric candidate modifier genes</b>						
<b>Thin filament components</b>						
<i>ACTC1</i>	15q11-q14	rs1370154	1.000	0.302 (T)	0.258 (T)	0.133 (T)
		rs2070664	1.000	0.256 (C)	0.500 (T)	0.267 (C)
<i>TNNT2</i>	1q32	rs2365652	0.200	0.497 (A)	0.358 (C)	0.250 (A)
		rs1892028	0.220	0.490 (A)	0.364 (G)	0.224 (A)
		rs947485	0.350	0.494 (G)	0.356 (A)	0.242 (G)
<i>TNNI3</i>	19q13.4	rs3729841	-	0.009 (T)	0.117 (T)	0.000 (T)
		rs3729838	0.550	0.445 (G)	0.186 (C)	0.229 (G)
		rs11667847	0.270	0.239 (G)	-	-
<i>TPM1</i>	15q22	rs11071720	0.080	0.470 (C)	0.367 (T)	0.358 (C)
		rs4238370	0.360	0.332 (T)	0.229 (T)	0.339 (T)
		rs1071646	1.000	0.374 (C)	0.392 (C)	0.483 (C)
		rs707602	1.000	0.054 (C)	0.136 (C)	0.117 (C)
<i>ACTN3</i>	11q13-q14	rs1791690	1.000	0.422 (A)	0.433 (A)	0.280 (G)
		rs2275998	0.400	0.298 (C)	0.175 (C)	0.292 (C)
		rs1815739	0.690	0.315 (T)	0.458 (T)	0.100 (T)
<b>Thick filament components</b>						
<i>MYL3</i>	3p21.3-p21.2	rs1531136	0.100	0.489 (T)	0.175 (T)	0.067 (C)
		rs3792558	0.340	0.454 (T)	0.150 (T)	0.133 (C)
<i>MYH7</i>	14q12	rs765019	0.550	0.142 (C)	0.108 (C)	0.212 (C)
		rs2277475	0.040	0.242 (T)	0.333 (T)	0.233 (A)
		rs1951154	0.720	0.296 (A)	0.308 (A)	0.025 (A)
		rs2754163	0.060	0.299 (C)	0.300 (C)	0.308 (T)
		rs2239578	0.730	0.416 (G)	0.442 (G)	0.342 (A)
<i>MYL2</i>	12q23-q24.3	rs933296	0.170	0.201 (A)	0.354 (A)	0.071 (A)
		rs4766517	1.000	0.357 (G)	0.449 (G)	0.142 (G)

Candidate gene	Chromosome locus	SNP ID	HWE p-value	MAF		
				Study cohort	CEU	YRI
<b>Intermediate filament components</b>						
<i>MYBPC3</i>	11p11.2	rs4752825	1.000	0.472 (A)	-	-
		rs1052373	1.000	0.468 (T)	0.254 (T)	0.500 (T)
		rs10838696	0.160	0.186 (A)	0.367 (A)	0.000 (A)
		rs11570058	1.000	0.113 (A)	0.098 (A)	0.042 (A)
<b>Energy metabolism candidate modifier genes</b>						
<b>Fatty acid metabolism components</b>						
<i>CD36</i>	7q11.2	rs10268417	0.750	0.385 (A)	0.373 (A)	0.362 (C)
		rs3211892	0.002*	0.068 (A)	0.025 (A)	0.358 (A)
		rs3173804	0.520	0.453 (A)	0.492 (A)	0.083 (A)
<i>CPT1B</i>	22q13.33	rs470117	1.000	0.240 (T)	0.492 (C)	0.092 (T)
		rs1557502	0.090	0.410 (T)	0.150 (T)	0.267 (C)
<i>PPARA</i>	22q13.31	rs881740	0.020	0.194 (G)	0.092 (G)	0.317 (G)
		rs4823613	0.460	0.289 (G)	0.300 (G)	0.380 (G)
		rs4253776	1.000	0.274 (G)	0.150 (G)	0.467 (G)
<i>PPARG</i>	3p25	rs12631028	0.730	0.305 (T)	0.211 (T)	0.259 (T)
		rs12490265	0.530	0.235 (A)	0.350 (A)	0.025 (A)
		rs2938392	0.110	0.448 (A)	0.467 (A)	0.108 (A)
		rs1175540	0.740	0.430 (A)	0.342 (A)	0.225 (C)
<i>PGCIA</i>	4p15.1	rs768695	0.530	0.448 (G)	0.433 (G)	0.483 (G)
		rs4619879	1.000	0.488 (C)	0.450 (C)	0.467 (C)
		rs11724368	0.400	0.230 (T)	0.217 (T)	0.042 (T)
		rs13131226	0.320	0.427 (C)	0.316 (C)	0.481 (C)
<b>Glucose metabolism components</b>						
<i>ALDOA</i>	16q22-q24	rs9928448	0.760	0.500 (C)	0.458 (T)	0.400 (T)
		rs11860935	1.000	0.088 (T)	0.110 (T)	0.147 (T)
<i>PFKM</i>	12q13.3	rs1859445	0.340	0.456 (A)	0.300 (C)	0.150 (C)
		rs10875749	1.000	0.221 (T)	0.392 (T)	0.108 (T)
<i>PDK4</i>	7q21.3	rs2073978	1.000	0.379 (T)	0.442 (C)	0.417 (T)
		rs2301630	0.510	0.446 (C)	0.467 (T)	0.314 (C)
<b>Creatine kinase energy shuttle components</b>						
<i>CKM</i>	19q13.2-q13.3	rs8111989	1.000	0.373 (C)	0.258 (C)	0.475 (T)
		rs7260463	0.180	0.380 (T)	0.283 (T)	0.421 (G)
		rs1133190	1.000	0.477 (A)	0.350 (A)	0.225 (G)
		rs344816	0.100	0.296 (T)	0.417 (T)	0.050 (A)
<i>CKB</i>	14q32	rs1803283	0.200	0.497 (T)	0.351 (C)	0.364 (T)
		rs2071407	0.120	0.406 (C)	0.283 (T)	0.448 (T)
		rs1136165	0.110	0.424 (G)	-	-
<b>Cellular energy homeostasis</b>						
<i>PRKAA1</i>	5p12	rs12517210	0.450	0.267 (C)	0.392 (C)	0.167 (C)
		rs11747210	0.290	0.261 (T)	0.345 (G)	0.181 (G)
		rs466108	0.720	0.369 (A)	0.333 (A)	0.400 (A)

Candidate gene	Chromosome locus	SNP ID	HWE p-value	MAF		
				Study cohort	CEU	YRI
<i>PRKAA2</i>	1p31	rs1124900	0.370	0.459 (G)	0.433 (G)	0.356 (G)
		rs2796495	0.020	0.425 (C)	0.433 (T)	0.492 (T)
		rs 932447	1.000	0.356 (C)	0.383 (C)	0.288 (C)
<i>PRKAB1</i>	12q24.1	rs6490267	1.000	0.266 (T)	0.367 (T)	0.442 (T)
		rs278143	1.000	0.236 (G)	0.342 (G)	0.442(G)
		rs10849690	0.630	0.135 (G)	-	0.009 (G)
		rs278149	1.000	0.278 (T)	0.333 (T)	0.483 (T)
		rs4213	1.000	0.269 (G)	0.342 (G)	0.458 (G)
<i>PRKAB2</i>	1q21.1	rs6937	1.000	0.096 (C)	0.133 (C)	0.092 (C)
		rs1348316	0.340	0.450 (G)	0.442 (G)	0.195 (A)
<i>PRKAG1</i>	12q12-q14	rs10875910	1.000	0.343 (C)	0.283 (C)	0.075 (C)
		rs2117029	0.520	0.442 (T)	0.342 (A)	0.459 (T)
<i>PRKAG2</i>	7q36.1	rs8961	0.004*	0.480 (C)	0.367 (T)	0.167 (C)
		rs2727537	0.230	0.461 (A)	0.342 (G)	0.358 (A)
		rs6464170	0.420	0.266 (G)	0.267 (G)	0.508 (C)
		rs13240743	0.490	0.303 (G)	0.373 (G)	0.425 (G)
<i>PRKAG3</i>	2q35	rs1000935	1.000	0.261 (G)	0.000 (G)	0.333 (T)
		rs16859382	1.000	0.261 (C)	0.000 (C)	0.192 (T)

\*Genotyping frequencies departed from HWE at the p-value < 0.01 level

**Abbreviations:** *ACTC1*-Actin, alpha, cardiac muscle 1; *ALDOA*-Aldolase A, fructose-bisphosphate; *CD36*-CD36 antigen, thrombospondin receptor; *CKB*-Creatine kinase, brain; *CKM*-Creatine kinase, muscle; *CTP1B*-Carnitine palmitoyltransferase 1B, muscle; *HWE*-Hardy-Weinberg equilibrium; *MAF*-minor allele frequency; *MYBPC3*-Myosin binding protein C, cardiac; *MYH7*-Myosin heavy chain 7, cardiac muscle, beta; *MYL2*-Myosin light chain 2, regulatory cardiac, slow; *MYL3*-Myosin light chain 3, alkali, ventricular, skeletal slow; *PDK4*-Pyruvate dehydrogenase kinase, isozyme 4; *PFKM*-Phosphofructokinase, muscle; *SNP*-single nucleotide polymorphism; *TNNI3*-Troponin I type 3, cardiac; *TNNT2*-Troponin T type 2, cardiac; *TPMI*-Tropomyosin 1; *p*-short arm of chromosome; *p-value*-probability; *PPARA*-Peroxisome proliferator-activated receptor alpha; *PPARG*-Peroxisome proliferator-activated receptor gamma; *PPARGC1A*-Peroxisome proliferator-activated receptor gamma, coactivator 1 alpha; *PRKAA1*-Protein kinase, AMP-activated, alpha 1 catalytic subunit; *PRKAA2*-Protein kinase, AMP-activated, alpha 2 catalytic subunit; *PRKAB1*-Protein kinase, AMP-activated, beta 1 non-catalytic subunit; *PRKAB2*-Protein kinase, AMP-activated, beta 2 non-catalytic subunit; *PRKAG1*-Protein kinase, AMP-activated, gamma 1 non-catalytic subunit; *PRKAG2*-Protein kinase, AMP-activated gamma 2 non-catalytic subunit; *PRKAG3*-Protein kinase, AMP-activated, gamma 3 non-catalytic subunit; *q*-long arm of chromosome

### 3.4.2 LD assessment

As previously described, Haploview v.4.2 (Barrett *et al.*, 2005) was used to estimate pair-wise LD for all SNPs included in this study in terms of  $D'$  point estimates,  $r^2$  values and  $D'$  confidence bounds. The  $D'$  evaluations were repeated a total of 100 times with the mode of the observed point

estimates reported here. The  $r^2$  values and  $D'$  confidence bounds were estimated only once and these values are provided in brackets.

**Complete LD ( $D'=1$ )** was observed for all the SNPs investigated within the genes *TNNT2*; *PRKAG3* (rs1000935/rs16859382:  $r^2=1.00$ ; 0.90-1.00), *MYL3* (rs1531136/rs3792558:  $r^2=0.783$ ; 0.87-1.00), *PRKAA1*, *ACTC1* (rs1370154/rs2070664:  $r^2=0.139$ ; 0.39-1.00), *ALDOA* (rs9928448/rs11860935:  $r^2=0.094$ ; 0.14-0.99), *TNNI3* (rs3729838/rs11667847:  $r^2=0.403$ , 0.80-1.00) and *CPT1B* (rs470117/rs1557502:  $r^2=0.202$ ; 0.67-1.00). The LD structures of the genes covered by 3 or more SNPs, including the aforementioned *TNNT2* and *PRKAA1* genes, have been visually depicted in Tables 3.4 through 3.18 with the  $r^2$  and  $D'$  confidence bounds indicated in brackets and blue font. The LD structures of the remaining, 2-SNP-covered genes, ranged from **strong to negligible**: *PFKM* (rs10875749 and rs1859445:  $D'=0.00$ ;  $r^2=0.026$ ; 0.05-0.70), *MYL2* (rs4766517 and rs933296:  $D'=0.55$ ;  $r^2=0.161$ ; 0.31-0.75), *PRKAB2* (rs1348316 and rs6937:  $D'=0.65$ ;  $r^2=0.063$ ; 0.11-0.91), *PDK4* (rs2301630 and rs2073978:  $D'=0.85$ ;  $r^2=0.0020$ ; 0.00-0.31) and *PRKAG1* (rs2117029 and rs10875910:  $D'=0.95$ ;  $r^2=0.696$ ; 0.78-0.99).

LD assessment showed that the  $R92W_{TNNT2}$  founder mutation was in complete LD with all other *TNNT2* SNPs. Similarly, the  $R403W_{MYH7}$  and  $A797T_{MYH7}$  founder mutations indicated complete LD with a number of *MYH7* SNPs (Refer to Table 3.17). However, it is important to again note that the statistical evaluations corrected for the contribution of individual founder mutations to trait variance and any significant associations identified are, therefore, independent of founder mutation effect (Refer to Section 2.6.4).

**Table 3.4 Pair-wise LD structure for *PRKAA2*.** Complete LD was observed between rs932447 and both rs1124900 and rs2796495 ( $D'=1$ ), whilst strong LD was observed between rs1124900 and rs2796495 ( $D'=0.95$ ).

	rs1124900	rs2796495	rs932447
rs932447	1.00 (0.755; 0.86-1.00)	1.00 (0.505; 0.82-1.00)	
rs2796495	0.95 (0.479; 0.64-0.93)		
rs1124900			

**Table 3.5 Pair-wise LD structure for *TNNT2*.** Complete pair-wise LD ( $D'=1$ ) was observed amongst all the *TNNT2* gene variants including the R92W founder mutation and the rs4019985 insertion/deletion polymorphism.

	rs947485	rs4019985	rs1892028	R92W	rs2365652
<i>TNNT2</i>	rs2365652	1.00 (1.00; 0.93-1.00)	1.00 (0.902; 0.88-1.00)	1.00 (1.00; 0.93-1.00)	1.00 (0.036; 0.10-0.90)
	R92W	1.00 (0.056; 0.18-0.93)	1.00 (0.063; 0.20-1.00)	1.00 (0.063; 0.19-0.93)	
	rs1892028	1.00 (1.00; 0.93-1.00)	1.00 (0.897; 0.88-1.00)		
	rs4019985	1.00 (0.902; 0.88-1.00)			
	rs947485				

**Table 3.6 Pair-wise LD structure for *PPARG*.** SNPs rs2938392 and rs1175540, as well as rs12490265 and rs2938392, were in complete LD ( $D'=1$ ) whereas SNPs rs1175540 and rs12490265 were in strong LD ( $D'=0.80$ ). Evidence for incomplete LD was found between SNPs rs12631028 and rs2938392 ( $D'=0.45$ ) as well as rs12631028 and rs12490265 ( $D'=0.75$ ), whilst negligible LD was observed between rs12631028 and rs1175540 ( $D'=0.10$ ).

	rs1175540	rs2938392	rs12490265	r12631028
<i>PPARG</i>	rs12631028	0.10 (0.015; 0.01-0.48)	0.45 (0.044; 0.08-0.69)	0.75 (0.017; 0.04-0.80)
	rs12490265	0.80 (0.170; 0.39-0.88)	1.00 (0.180; 0.63-1.00)	
	rs2938392	1.00 (0.532; 0.83-1.00)		
	rs1175540			

**Table 3.7 Pair-wise LD structure for *PGCIA*.** The *PGCIA* gene polymorphisms showed little pair-wise LD with the highest  $D'$  value of 0.25, observed for SNP pair rs11724368 and rs13131226, indicating incomplete LD.

	rs13131226	rs11724368	rs4619879	rs768695
<i>PGCIA</i>	rs768695	0.02 (0.0060; 0.0-0.38)	0.20 (0.0010; 0.0-0.48)	0.10 (0.0020; 0.0-0.33)
	rs4619879	0.05 (0.012; 0.01-0.40)	0.05 (0.011; 0.02-0.57)	
	rs11724368	0.25 (0.07; 0.1-0.70)		
	rs13131226			

**Table 3.8 Pair-wise LD structure for *PRKAA1*.** Complete LD ( $D'=1$ ) was observed for all pairs of SNPs investigated in the *PRKAA1* gene.

	rs466108	rs11747210	rs12517210
<i>PRKAA1</i>	rs12517210	1.00 (0.244; 0.65-1.00)	1.00 (1.00; 0.91-1.00)
	rs11747210	1.00 (0.244; 0.65-1.00)	
	rs466108		

**Table 3.9 Pair-wise LD structure for *CD36*.** The pair-wise  $D'$  prime estimates determined for the *CD36* gene polymorphisms ranged from 0.15 to 0.22 thus indicating negligible to incomplete LD.

	rs3173804	rs3211892	rs10268417
<i>CD36</i>	rs10268417	0.22 (0.034; 0.02-0.56)	0.15 (0.00; 0.01 -0.72)
	rs3211892	0.19 (0.023; 0.02-0.56)	
	rs3173804		

**Table 3.10 Pair-wise LD structure for *PRKAG2*.** The pair-wise D' prime values observed for the *PRKAG2* gene polymorphisms ranged from 0.05 to 0.55, indicating negligible to incomplete LD.

	<b>rs13240743</b>	<b>rs6464170</b>	<b>rs2727537</b>	<b>rs8961</b>
<b><i>PRKAG2</i></b>	<b>rs8961</b>	0.55 (0.141; 0.21-0.84)	0.05 (0.076; 0.08-0.74)	0.05 (0.011; 0.00-0.35)
	<b>rs2727537</b>	0.15 (0.016; 0.02-0.47)	0.30 (0.019; 0.03-0.56)	
	<b>rs6464170</b>	0.20 (0.0010; 0.01-0.65)		
	<b>rs13240743</b>			

**Table 3.11 Pair-wise LD structure for *MYBPC3*.** Complete LD ( $D' = 1.00$ ) was observed for all pairs of polymorphisms investigated in the *MYBPC3* gene, with the exception of the rs10838696 and rs11570058 SNP pair with a D' prime value of 0.95, indicating strong LD.

	<b>rs11570058</b>	<b>rs10838696</b>	<b>rs1052373</b>	<b>rs4752825</b>
<b><i>MYBPC3</i></b>	<b>rs4752825</b>	1.00 (0.105; 0.37-1.00)	1.00 (0.145; 0.39-1.00)	1.00 (1.00; 0.93-1.00)
	<b>rs1052373</b>	1.00 (0.106; 0.38-1.00)	1.00 (0.163; 0.45-1.00)	
	<b>rs10838696</b>	0.95 (0.017; 0.09-0.99)		
	<b>rs11570058</b>			



**Table 3.12 Pair-wise LD structure for *ACTN3*.** SNPs rs1791690 and rs2275998, as well as rs2275998 and rs1815739, were in complete LD ( $D' = 1$ ), whilst evidence for strong LD was found between SNPs rs1791690 and rs1815739 ( $D' = 0.60$ ).

	rs1815739	rs2275998	rs1791690
<i>ACTN3</i>	rs1791690	0.60 (0.139; 0.21- 0.68)	1.00 (0.287; 0.71-1.00)
	rs2275998	1.00 (0.116; 0.41-1.00)	
	rs1815739		

**Table 3.13 Pair-wise LD structure for *PRKAB1*.** Overall, significant pair-wise LD, ranging from strong ( $D' = 0.90$ ) to complete ( $D' = 1.00$ ), was observed for the *PRKAB1* gene polymorphisms investigated.

	rs4213	rs278149	rs10849690	rs278143	rs6490267
<i>PRKAB1</i>	rs6490267	0.95 (0.954; 0.90-1.00)	0.93 (0.769; 0.80-0.99)	1.00 (0.508; 0.80-1.00)	0.95 (0.956; 0.91-1.00)
	rs278143	1.00 (1.00; 0.93-1.00)	0.95 (0.81; 0.81-0.99)	1.00 (0.535; 0.81-1.00)	
	rs10849690	1.00 (0.509; 0.78-1.00)	0.90 (0.46; 0.66-0.98)		
	rs278149	0.98 (0.848; 0.81-0.99)			
	rs4213				

**Table 3.14 Pair-wise LD structure for *MYH7*.** The pair-wise LD observed for the *MYH7* gene variants, including the A797T and R403W founder mutations, varied from negligible ( $D' = 0.13$ ) to complete ( $D' = 1.00$ ).

	rs2239578	R403W	rs2754163	rs1951154	A797T	rs2277475	rs765019
<i>MYH7</i>	rs765019	0.25 (0.036; 0.06-0.71)	1.00 (0.0030; 0.04-0.97)	0.76 (0.209; 0.44-0.96)	0.90 (0.049; 0.13-0.99)	1.00 (0.0020; 0.03-0.85)	0.58 (0.118; 0.16-0.76)
	rs2277475	0.20 (0.064; 0.08-0.60)	1.00 (0.0090; 0.06-0.98)	0.90 (0.575; 0.75-0.99)	0.75 (0.117; 0.48-1.00)	1.00 (0.024; 0.07-0.89)	
	A797T	0.55 (0.032; 0.06-0.81)	1.00 (0.0050; 0.04-0.97)	1.00 (0.057; 0.15-0.92)	0.83 (0.269; 0.35-0.88)		
	rs1951154	1.00 (0.221; 0.63-1.00)	1.00 (0.0070; 0.05-0.98)	1.00 (0.175; 0.63-1.00)			
	rs2754163	0.13 (0.0050; 0.00-0.32)	1.00 (0.012; 0.06-0.98)				
	R403W	1.00 (0.0010; 0.02-0.83)					
	rs2239578						

**Table 3.15 Pair-wise LD structure for *CKB*.** SNPs rs1803283 and rs1136165 ( $D' = 0.35$ ), as well as rs1803283 and rs2071407 ( $D' = 0.75$ ), showed incomplete LD. Evidence for strong LD was found between SNPs rs2071407 and rs1136165 ( $D' = 0.84$ ).

	rs1136165	rs2071407	rs1803283
<i>CKB</i>	rs1803283	0.35 (0.146; 0.18-0.58)	0.75 (0.359; 0.52-0.88)
	rs2071407	0.84 (0.618; 0.72-0.97)	
	rs1136165		

**Table 3.16 Pair-wise LD structure for *TPMI*.** The pair-wise LD observed for the *TPMI* gene variants ranged from negligible ( $D' = 0.10$ ) to complete ( $D' = 1.00$ ).

	<b>rs707602</b>	<b>rs1071646</b>	<b>rs4238370</b>	<b>rs11071720</b>
<b><i>TPMI</i></b>	<b>rs11071720</b>	0.10 (0.07; 0.09-0.99)	0.13 (0.00; 0.00-0.44)	0.30 (0.0010; 0.00-0.40)
	<b>rs4238370</b>	0.50 (0.018; 0.04-0.97)	0.65 (0.238; 0.34-0.78)	
	<b>rs1071646</b>	1.00 (0.179; 0.48-1.00)		
	<b>rs707602</b>			

**Table 3.17 Pair-wise LD structure for *CKM*.** Pair-wise LD observed for the *CKM* gene variants ranging from negligible ( $D' = 0.00$ ) to strong ( $D' = 0.88$ ).

	<b>rs344816</b>	<b>rs1133190</b>	<b>rs7260463</b>	<b>rs8111989</b>
<b><i>CKM</i></b>	<b>rs8111989</b>	0.35 (0.041; 0.05-0.42)	0.45 (0.052; 0.05-0.56)	0.88 (0.754; 0.74-0.94)
	<b>rs7260463</b>	0.35 (0.043; 0.05-0.41)	0.25 (0.03; 0.03-0.50)	
	<b>rs1133190</b>	0.00 (0.0010; 0.00-0.33)		
	<b>rs344816</b>			

**Table 3.18 Pair-wise LD structure for *PPARA*.** SNPs rs881740 and rs4253776 ( $D' = 0.30$ ), as well as rs4823613 and rs4253776 ( $D' = 0.60$ ), showed incomplete LD, whilst negligible LD was observed for SNP pair rs881740 and rs4823613 ( $D' = 0.00$ ).

	<b>rs4253776</b>	<b>rs4823613</b>	<b>rs881740</b>
<b><i>PPARA</i></b>	<b>rs881740</b>	0.30 (0.012; 0.01-0.48)	0.00 (0.021; 0.03-0.66)
	<b>rs4823613</b>	0.60 (0.221; 0.35-0.83)	
	<b>rs4253776</b>		

### 3.4.3 Principal component analysis

PCA was applied to the 16 transformed wall thickness measurements to define the mathematical combination, or weighted average, of these measurements that best captures the variability in left ventricular wall thickness measurements; that is, a single score that best reflects cohort-specific hypertrophy, as distributed throughout the left ventricle. A score, PC1, accounting for 75% of the overall variability in hypertrophy was identified, and its weighted composition is detailed in Table 3.19.

**Table 3.19 The PC1 score defined in terms of its weighted composition: the weight of each wall thickness measurement**

Wall thickness measurement	Weight contribution to PC1
pIVS at mitral valve	0.253
aIVS at mitral valve	0.261
AW at mitral valve	0.256
LW at mitral valve	0.249
IW at mitral valve	0.221
PW at mitral valve	0.221
pIVS at papillary muscle	0.262
aIVS at papillary muscle	0.269
AW at papillary muscle	0.267
LW at papillary muscle	0.254
IW at papillary muscle	0.234
PW at papillary muscle	0.238
IVS at apex	0.263
AW at apex	0.259
LW at apex	0.239
PW at apex	0.248

**Abbreviations:** **aIVS**-anterior interventricular septum thickness; **AW**-anterior wall thickness; **IVS**-interventricular septum thickness; **IW**- inferior wall thickness; **LW**-lateral wall thickness; **PC1**-first principal component; **pIVS**-posterior interventricular septum thickness; **PW**-posterior wall thickness

### 3.4.4 Heritability

The respective contributions of environmental and genetic factors (heritability) to the phenotypic variability of the traits investigated were determined as detailed in Section 2.6.5. These estimates are reported in Table 3.20 along with the p-values for each test of heritability. All six hypertrophy traits indicated a considerable genetic component after adjustment for known hypertrophy covariates described in Section 2.6.4.

**Table 3.20 The environmental and heritability estimates detailed as estimated percentage contribution to trait variance as well as the p-values for heritability**

Hypertrophy trait	Environmental (%)	Heritability (%)	p-value
<b>LVMecho</b>	41	59	< 0.0001
<b>mIVST</b>	56	44	< 0.0001
<b>mLVWT</b>	44	55	0.0001
<b>mPWT</b>	44	56	0.0002
<b>CWTscore</b>	59	41	0.0018
<b>PC1</b>	48	52	0.0009

**Abbreviations:** CWT score-cumulative wall thickness score; LVM-left ventricular mass; mIVST-maximal interventricular septum thickness; mLVWT-maximal left ventricular wall thickness; mPWT-maximal posterior wall thickness; PC1-first principal component

### 3.4.5 Association and interaction analyses

The results obtained for the association and interaction analyses are detailed per gene and in order of function, i.e. sarcomeric genes and genes relating to myocardial energetics (as per Section 2.3.3). Moreover, the original p-values for the tests of association are tabulated, whilst bar graphs plot the corresponding  $-\log_{10}$  transformed p-values against the relevant SNP- or haplotype-trait combination. A red dashed horizontal line indicates the p-value significance threshold equal to 0.05. Bars that intersect this line, therefore, indicate significant p-values (p-value < 0.05). The higher the bar, the smaller the p-value. The values reported reflect association that is independent of hypertrophy confounders, as well as independent of both carrier status and identity of the relevant HCM-causing founder mutations.

The p-values obtained for the interaction analyses, i.e. whether the effect of the investigated variants/haplotypes on individual hypertrophy traits varied amongst the three HCM founder mutation groups, are tabulated per pairwise-comparison of the three HCM founder mutation groups with respect to each SNP- or haplotype-trait evaluation. The interpretation of a significant interaction result has been demonstrated in Section 2.6.8. The graphs indicate the strength of the associations whereas characterisation of the significant results in terms of effect (protective or exacerbating) and effect size is done in the text. More specifically, in instances of significant single SNP associations the in-text descriptions are done in terms of the minor allele, which is also indicated on the graphs along with up and down arrows representing exacerbating and cardioprotective effects, respectively. Similarly, arrows are indicated on the graphs of significantly associated haplotypes to illustrate their directional effect.

### 3.4.5.1 *ACTC1*

The p-values for the *association* between the *ACTC1 SNPs* and *hypertrophy traits* are given in **Figure 3.3**; and the p-values for *pair-wise differences between mutation groups* in the association between the *ACTC1 SNPs* and *hypertrophy traits* are given in **Table 3.21**. No statistically significant single SNP effect or difference in SNP effect amongst the three HCM founder mutation groups was observed.

The p-values for the *association* between *ACTC1 haplotypes* and *hypertrophy traits* are graphically represented in **Figure 3.4**. The p-values for *pair-wise comparison between mutation groups* in the association between *ACTC1 haplotypes* and *hypertrophy traits* are given in **Table 3.22**. The effect of the CC haplotype, identified in 23% of the cohort, was an estimated decrease of 0.51 mm in LVM ( $p = 0.013$ ). The CT haplotype, present in 37% of the cohort, was associated with increases in LVM ( $p = 0.004$ ) and mIVST ( $p = 0.039$ ) of 1.55 mm and 1.05 mm, respectively. No significant difference in haplotype effect was observed amongst the mutation groups.

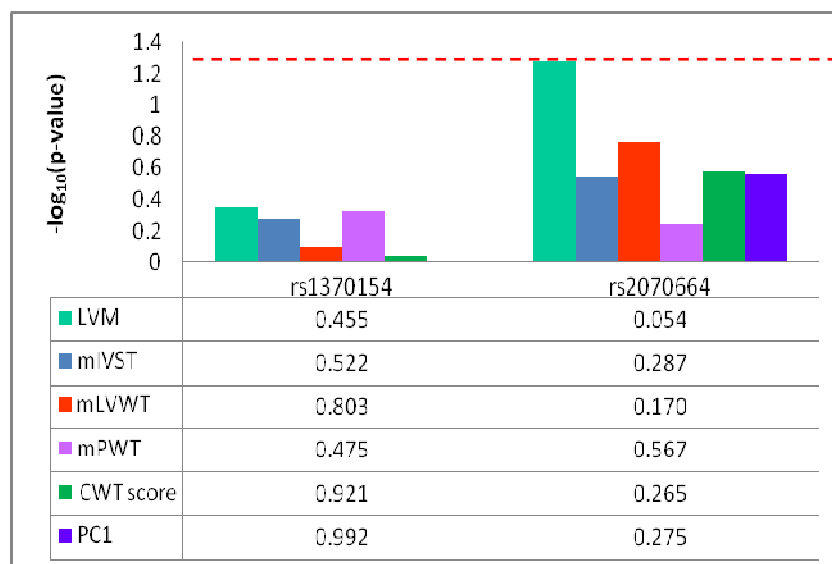


**Figure 3.3** The p-values for tests of association between single SNPs in *ACTC1* and individual hypertrophy traits. The original p-values are given in the data table, whilst the graph represents the corresponding  $-\log_{10}$  transformed values. The red dashed horizontal line indicates the p-value significance threshold equal to 0.05. Bars located above this line, therefore, indicate significant p-values (p-values<0.05). The p-value significance increases with bar height above threshold.

**Table 3.21** The p-values obtained for the analysis of interaction between mutation group and single SNPs in *ACTC1*.

SNP ID	LVM			mIVST			mLVWT			mPWT			CWT score			PC1		
	R403W vs A797T	R92W vs A797T	R92W vs R403W	R403W vs A797T	R92W vs A797T	R92W vs R403W	R403W vs A797T	R92W vs A797T	R92W vs R403W	R403W vs A797T	R92W vs A797T	R92W vs R403W	R403W vs A797T	R92W vs A797T	R92W vs R403W	R403W vs A797T	R92W vs A797T	R92W vs R403W
rs1370154	0.937	0.239	0.294	0.540	0.832	0.473	0.544	0.617	0.339	0.162	0.443	0.530	0.542	0.741	0.404	0.547	0.659	0.358
rs2070664	0.730	0.906	0.691	0.376	0.935	0.408	0.339	0.948	0.383	0.668	0.652	0.984	0.908	0.750	0.862	0.912	0.994	0.919

**Abbreviations:** A-Alanine; CWT score-cumulative wall thickness score; LVM-left ventricular mass; mIVST-maximal interventricular septum thickness; mLVWT-maximal left ventricular wall thickness; mPWT-maximal posterior wall thickness; PC1-principal component score; R-Arginine; SNP-single nucleotide polymorphism; T-Threonine; vs-versus; W-Tryptophan

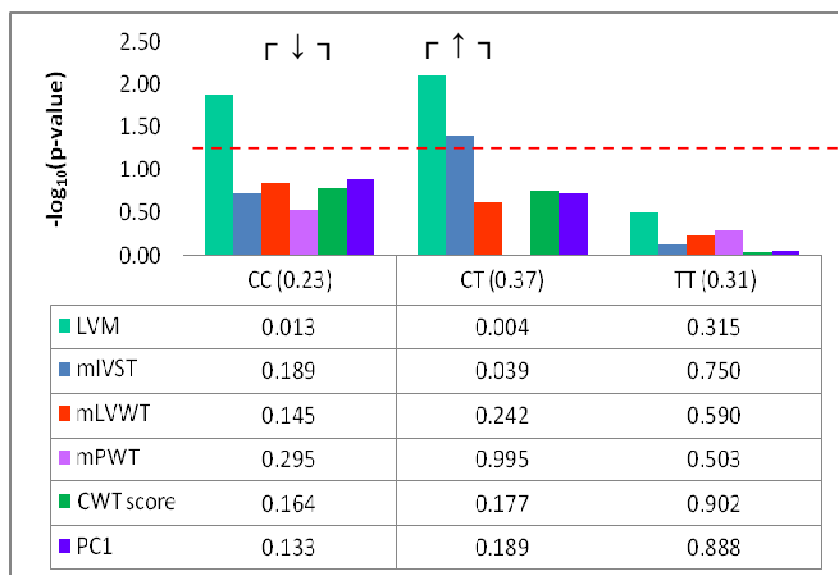


**Figure 3.4** The p-values for tests of association between *ACTC1* haplotypes and individual hypertrophy traits. The original p-values are given in the data table, whilst the graph represents the corresponding  $-\log_{10}$  transformed values. The red dashed horizontal line indicates the p-value significance threshold equal to 0.05. Bars located above this line, therefore, indicate significant p-values (p-values<0.05). The p-value significance increases with bar height above threshold. The observed haplotype frequencies are indicated in brackets.

**Table 3.22** The p-values obtained for the analysis of interaction between mutation group and *ACTC1* haplotypes.

Haplotype*		LVM			mIVST			mLVWT			mPWT			CWT score			PC1		
rs1370154	rs2070664	R403W	R92W	R92W	R403W	R92W	R92W	R403W	R92W	R92W	R403W	R92W	R92W	R403W	R92W	R92W	R403W	R92W	R92W
		vs	vs	vs	vs	vs	vs	vs	vs	vs	vs	vs	vs	vs	vs	vs	vs	vs	vs
		A797T	A797T	R403W	A797T	A797T	R403W	A797T	A797T	R403W	A797T	A797T	R403W	A797T	A797T	R403W	A797T	A797T	R403W
C	C	0.824	0.804	0.686	0.461	0.718	0.335	0.475	0.646	0.305	0.816	0.832	0.701	0.715	0.399	0.741	0.773	0.561	0.845
C	T	0.793	0.410	0.330	0.097	0.998	0.123	0.110	0.764	0.081	0.159	0.380	0.566	0.686	0.404	0.270	0.748	0.432	0.324
T	T	0.906	0.337	0.499	0.651	0.683	0.459	0.519	0.467	0.236	0.302	0.852	0.417	0.511	0.604	0.294	0.601	0.445	0.262

**Abbreviations:** A-Adenine\*; A-Alanine; CWT score-cumulative wall thickness score; C-Cytosine\*; G-Guanine\*; LVM-left ventricular mass; mIVST-maximal interventricular septum thickness; mLVWT-maximal left ventricular wall thickness; mPWT-maximal posterior wall thickness; PC1-principal component score; R-Arginine; SNP-single nucleotide polymorphism; T-Threonine; T-Thymine\*; vs-versus; W-Tryptophan



### 3.4.5.2 MYH7

**Figure 3.5** graphically represents the p-values for *association* between the *MYH7 SNPs* and *hypertrophy traits*. The rs2277475 SNP had a statistically significant effect on mLVWT ( $p = 0.016$ ), the CWT score ( $p = 0.026$ ) and PC1 ( $p = 0.045$ ). More specifically, the effect of the T-allele was an estimated decrease of 1.19 mm in mLVWT, 8.64 mm in the CWT score and 0.54 in PC1. **Table 3.23** details the p-values for *pair-wise differences between mutation groups* in the association between *MYH7 SNPs* and *hypertrophy traits*. The rs2277475 SNP also indicated a significant difference in SNP effect amongst the HCM founder mutation groups. The effect of the T-allele was higher in the R403W<sub>MYH7</sub> group compared to the A797T<sub>MYH7</sub> group with 18.2 mm on the CWT score ( $p = 0.032$ ) and 1.14 on PC1 ( $p = 0.034$ ). Its effect was lower in the R92W<sub>TNNT2</sub> group relative to the R403W<sub>MYH7</sub> group with 24.8 mm on the CWT score ( $p = 0.013$ ) and 1.55 on PC1 ( $p = 0.009$ ).

**Figure 3.6** graphically represents the p-values for *association* between *MYH7 haplotypes* and *hypertrophy traits*. No statistically significant haplotype effect was observed. **Table 3.24** details the p-values for *pair-wise comparison between mutation groups* in the association between *MYH7 haplotypes* and *hypertrophy traits*. Significant differences in haplotype effect were observed between the mutation groups for haplotypes TTGCG and TAGCA. The effect of the first, observed in 7% of the cohort, was lower in the R92W<sub>TNNT2</sub> group relative to the R403W<sub>MYH7</sub> group with 1.84 on PC1 ( $p = 0.039$ ). Conversely the effect of the second, observed in 2% of the cohort, was higher in the R92W<sub>TNNT2</sub> group relative to the R403W<sub>MYH7</sub> group: 58.4 g on LVM ( $p = 0.028$ ), 36.7 mm on the CWT score ( $p = 0.023$ ) and 2.29 on PC1 ( $p = 0.019$ ).

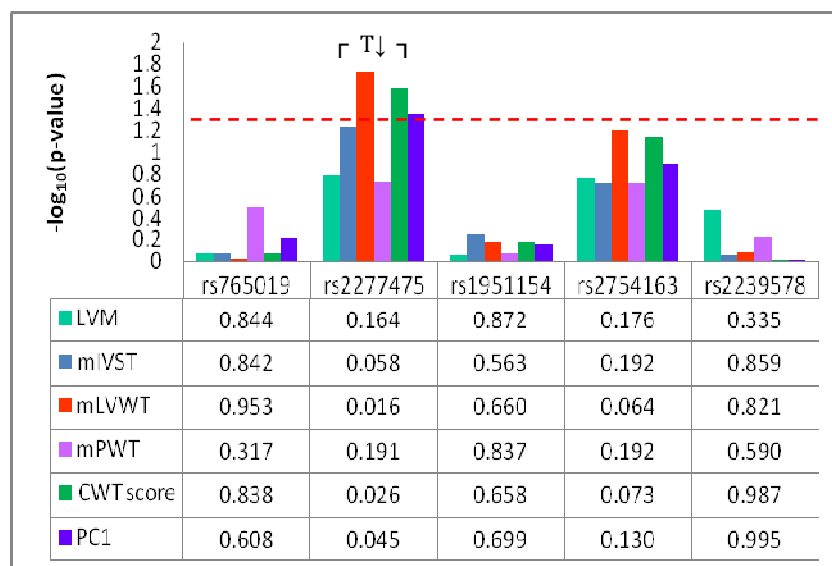


**Figure 3.5** The p-values for tests of association between single SNPs in *MYH7* and individual hypertrophy traits. The original p-values are given in the data table, whilst the graph represents the corresponding  $-\log_{10}$  transformed values. The red dashed horizontal line indicates the p-value significance threshold equal to 0.05. Bars located above this line, therefore, indicate significant p-values (p-values<0.05). The p-value significance increases with bar height above threshold.

**Table 3.23** The p-values obtained for the analysis of interaction between mutation group and single SNPs in *MYH7*. Significant results are indicated in bold red font.

SNP ID	LVM			mIVST			mLVWT			mPWT			CWT score			PC1		
	R403W vs A797T	R92W vs A797T	R92W vs R403W	R403W vs A797T	R92W vs A797T	R92W vs R403W	R403W vs A797T	R92W vs A797T	R92W vs R403W	R403W vs A797T	R92W vs A797T	R92W vs R403W	R403W vs A797T	R92W vs A797T	R92W vs R403W	R403W vs A797T	R92W vs A797T	R92W vs R403W
rs765019	0.872	0.937	0.929	0.381	0.174	0.799	0.589	0.314	0.763	0.552	0.967	0.553	0.432	0.399	0.935	0.547	0.598	0.876
rs2277475	0.900	0.648	0.628	0.117	0.468	0.347	0.305	0.679	0.190	0.607	0.251	0.160	<b>0.032</b>	0.570	<b>0.013</b>	<b>0.034</b>	0.466	<b>0.009</b>
rs1951154	0.561	0.938	0.656	0.333	0.535	0.717	0.345	0.682	0.614	0.656	0.654	0.957	0.133	0.631	0.335	0.261	0.706	0.479
rs2754163	0.666	0.649	0.986	0.441	0.358	0.948	0.672	0.927	0.624	0.726	0.933	0.676	0.364	0.938	0.417	0.322	0.948	0.366
rs2239578	0.958	0.329	0.425	0.316	0.178	0.887	0.404	0.159	0.704	0.514	0.784	0.366	0.613	0.184	0.514	0.783	0.175	0.358

**Abbreviations:** A-Alanine; **CWT score**-cumulative wall thickness score; **LVM**-left ventricular mass; **mIVST**-maximal interventricular septum thickness; **mLVWT**-maximal left ventricular wall thickness; **mPWT**-maximal posterior wall thickness; **PC1**-principal component score; **R**-Arginine; **SNP**-single nucleotide polymorphism; **T**-Threonine; **vs**-versus; **W**-Tryptophan

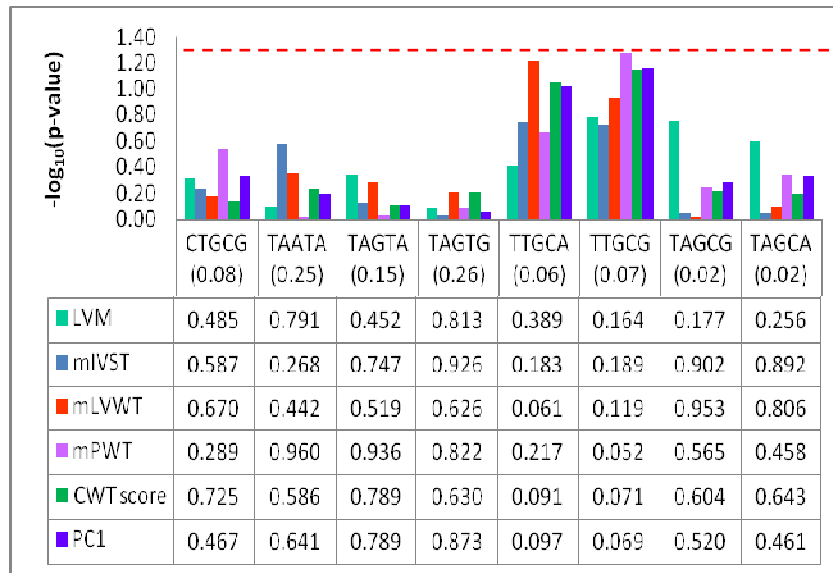


**Figure 3.6** The p-values for tests of association between *MYH7* haplotypes and individual hypertrophy traits. The original p-values are given in the data table, whilst the graph represents the corresponding  $-\log_{10}$  transformed values. The red dashed horizontal line indicates the p-value significance threshold equal to 0.05. Bars located above this line, therefore, indicate significant p-values (p-values<0.05). The p-value significance increases with bar height above threshold. The observed haplotype frequencies are indicated in brackets.

**Table 3.24** The p-values obtained for the analysis of interaction between mutation group and *MYH7* haplotypes. Significant results are indicated in bold red font.

Haplotype*		LVM			mIVST			mLVWT			mPWT			CWT score			PC1		
rs765019	rs2277475	R403W	R92W	R92W	R403W	R92W	R92W	R403W	R92W	R92W	R403W	R92W	R92W	R403W	R92W	R92W	R403W	R92W	R92W
		vs A797T	vs A797T	vs R403W	vs A797T	vs A797T	vs R403W	vs A797T	vs A797T	vs R403W	vs A797T	vs A797T	vs R403W	vs A797T	vs A797T	vs R403W	vs A797T	vs A797T	vs R403W
C	T	0.881	0.263	0.380	0.714	0.517	0.814	0.651	0.568	0.931	0.626	0.100	0.304	0.954	0.278	0.367	0.682	0.110	0.304
T	A	0.573	0.978	0.635	0.739	0.360	0.325	0.676	0.306	0.257	0.855	0.887	0.970	0.298	0.266	0.086	0.496	0.274	0.159
T	A	0.414	0.740	0.562	0.758	0.619	0.910	0.524	0.867	0.593	0.105	0.254	0.471	0.112	0.673	0.173	0.116	0.748	0.152
T	A	0.998	0.804	0.819	0.352	0.654	0.568	0.879	0.987	0.860	0.465	0.784	0.606	0.551	0.979	0.533	0.702	0.978	0.659
T	T	0.839	-	-	0.337	-	-	0.882	-	-	0.714	-	-	0.634	-	-	0.491	-	-
T	T	0.637	0.919	0.641	0.980	0.437	0.396	0.428	0.069	0.271	0.809	0.545	0.324	0.606	0.305	0.060	0.512	0.302	<b>0.039</b>
T	A	0.908	0.422	0.457	0.653	0.838	0.763	0.461	0.787	0.588	0.141	0.940	0.149	0.395	0.694	0.577	0.424	0.906	0.473
T	A	-	-	<b>0.028</b>	-	-	0.109	-	-	0.107	-	-	0.106	-	-	<b>0.023</b>	-	-	<b>0.019</b>

\*\* absence of p-values indicates unequal distribution of haplotypes in the three HCM mutation groups resulting in stratified groups of small size with insufficient statistical power for testing

**Abbreviations:** A-Adenine\*; A-Alanine; CWT score-cumulative wall thickness score; C-Cytosine\*; G-Guanine\*; LVM-left ventricular mass; mIVST-maximal interventricular septum thickness; mLVWT-maximal left ventricular wall thickness; mPWT-maximal posterior wall thickness; PC1-principal component score; R-Arginine; SNP-single nucleotide polymorphism; T-Threonine; T-Thymine\*; vs-versus; W-Tryptophan

### 3.4.5.3 *TNNT2*

The p-values for the *association* between the *TNNT2 SNPs* and *hypertrophy traits* are given in *Figure 3.7*; and the p-values for *pair-wise comparison between mutation groups* in the association of *TNNT2 SNPs* and *hypertrophy traits* are given in *Table 3.25*. No statistically significant single SNP effect was observed. The effect of the rs2365652 SNP varied significantly amongst the HCM founder mutation groups. The effect of the A-allele was estimated to be higher in the R92W<sub>*TNNT2*</sub> group relative to the A797T<sub>*MYH7*</sub> group with 2.30 mm on mIVST ( $p = 0.049$ ).

*Figure 3.8* graphically represents the p-values for *association* between *TNNT2 haplotypes* and *hypertrophy traits*. No statistically significant haplotype effect was observed. *Table 3.26* details the p-values for *pair-wise differences between mutation groups* in the association between *TNNT2 haplotypes* and *hypertrophy traits*. The AAIG and CGIA haplotypes indicated significant differences in haplotype effect amongst the three mutation groups. The effect of the first was higher on LVM (23.5 g;  $p = 0.028$ ) in the R403W<sub>*MYH7*</sub> group compared to the A797T<sub>*MYH7*</sub> group. The effect of the second was lower on mIVST (12.57 mm;  $p = 0.008$ ), mLVWT (11.34 mm;  $p = 0.034$ ) and the CWT score (89.4 mm;  $p = 0.034$ ) in the R403W<sub>*MYH7*</sub> group relative to the A797T<sub>*MYH7*</sub> group.

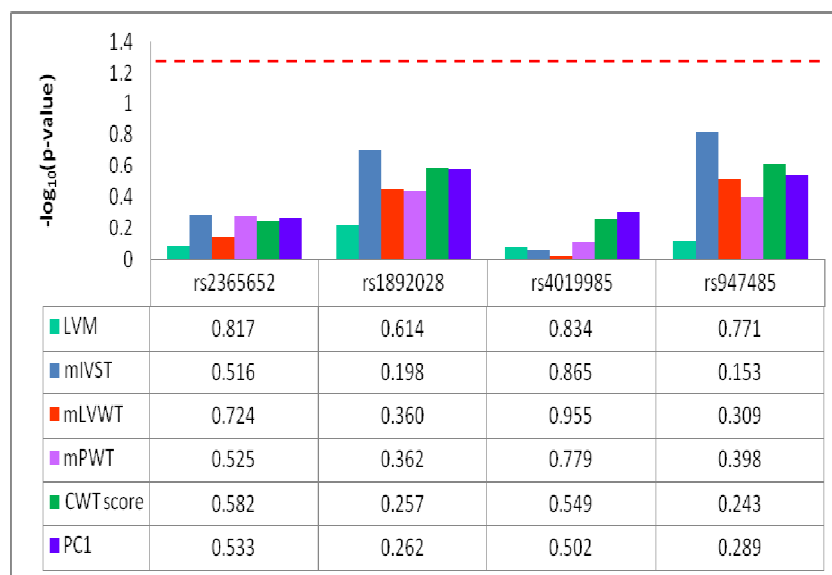


**Figure 3.7** The p-values for tests of association between single SNPs in *TNNT2* and individual hypertrophy traits. The original p-values are given in the data table, whilst the graph represents the corresponding  $-\log_{10}$  transformed values. The red dashed horizontal line indicates the p-value significance threshold equal to 0.05. Bars located above this line, therefore, indicate significant p-values (p-values<0.05). The p-value significance increases with bar height above threshold.

**Table 3.25** The p-values obtained for the analysis of interaction between mutation group and single SNPs in *TNNT2*. Significant results are indicated in bold red font.

SNP ID	LVM			mIVST			mLVWT			mPWT			CWT score			PC1		
	R403W vs A797T	R92W vs A797T	R92W vs R403W	R403W vs A797T	R92W vs A797T	R92W vs R403W	R403W vs A797T	R92W vs A797T	R92W vs R403W	R403W vs A797T	R92W vs A797T	R92W vs R403W	R403W vs A797T	R92W vs A797T	R92W vs R403W	R403W vs A797T	R92W vs A797T	R92W vs R403W
rs2365652	0.899	0.054	0.117	0.147	<b>0.049</b>	0.701	0.423	0.589	0.788	0.547	0.507	0.983	0.450	0.212	0.723	0.580	0.182	0.535
rs1892028	0.892	0.138	0.250	0.122	0.101	0.999	0.362	0.795	0.545	0.911	0.617	0.745	0.395	0.311	0.966	0.463	0.237	0.769
rs4019985	0.779	0.106	0.254	0.165	0.255	0.737	0.236	0.623	0.481	0.636	0.251	0.588	0.200	0.374	0.628	0.341	0.387	0.854
rs947485	0.879	0.083	0.178	0.090	0.094	0.908	0.294	0.727	0.508	0.899	0.587	0.729	0.314	0.220	0.941	0.425	0.175	0.703

**Abbreviations:** A-Alanine; CWT score-cumulative wall thickness score; LVM-left ventricular mass; mIVST-maximal interventricular septum thickness; mLVWT-maximal left ventricular wall thickness; mPWT-maximal posterior wall thickness; PC1-principal component score; R-Arginine; SNP-single nucleotide polymorphism; T-Threonine; vs-versus; W-Tryptophan

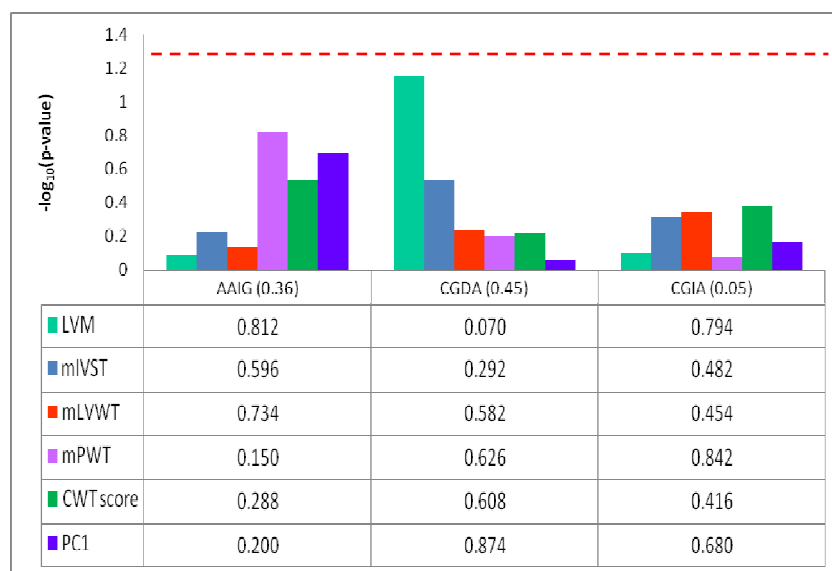


**Figure 3.8** The p-values for tests of association between *TNNT2* haplotypes and individual hypertrophy traits. The original p-values are given in the data table, whilst the graph represents the corresponding  $-\log_{10}$  transformed values. The red dashed horizontal line indicates the p-value significance threshold equal to 0.05. Bars located above this line, therefore, indicate significant p-values (p-values<0.05). The p-value significance increases with bar height above threshold. The observed haplotype frequencies are indicated in brackets.

**Table 3.26** The p-values obtained for the analysis of interaction between mutation group and *TNNT2* haplotypes. Significant results are indicated in bold red font.

Haplotype*	LVM			mIVST			mLVWT			mPWT			CWT score			PC1						
rs2365652	R403W	R92W	R92W	R403W	R92W	R92W	R403W	R92W	R92W	R403W	R92W	R92W	R403W	R92W	R92W	R403W	R92W	R92W				
rs1892028	vs	vs	vs	vs	vs	vs	vs	vs	vs	vs	vs	vs	vs	vs	vs	vs	vs	vs				
rs4019985	A797T	A797T	R403W	A797T	A797T	R403W	A797T	A797T	R403W	A797T	A797T	R403W	A797T	A797T	R403W	A797T	A797T	R403W				
rs947485	A	A	I	G	<b>0.028</b>	0.152	0.448	0.212	0.912	0.178	0.462	0.738	0.288	0.376	0.546	0.782	0.200	0.824	0.326	0.176	0.600	0.452
	C	G	D	A	0.090	0.096	0.920	0.128	0.822	0.110	0.324	0.602	0.158	0.282	0.866	0.414	0.092	0.988	0.140	0.070	0.708	0.226
	C	G	I	A	0.374	0.616	0.584	<b>0.008</b>	0.136	0.116	<b>0.034</b>	0.382	0.110	0.180	0.224	0.724	<b>0.034</b>	0.242	0.208	0.076	0.248	0.382

**Abbreviations:** A-Adenine\*; A-Alanine; **CWT score**-cumulative wall thickness score; C-Cytosine\*; D-deletion; G-Guanine\*; I-insertion; LVM-left ventricular mass; mIVST-maximal interventricular septum thickness; mLVWT-maximal left ventricular wall thickness; mPWT-maximal posterior wall thickness; PC1-principal component score; R-Arginine; SNP-single nucleotide polymorphism; T-Threonine; vs-versus; W-Tryptophan

#### 3.4.5.4 *TNNI3*

The p-values for the *association* between the *TNNI3* SNPs and *hypertrophy traits*; and the p-values for *pair-wise differences between mutation groups* in the association between *TNNI3* SNPs and *hypertrophy traits* are given in *Figure 3.9* and *Table 3.27*, respectively. No statistically significant single SNP effect was observed. However, the effects of SNPs rs3729838 and rs11667847 varied amongst the three HCM founder mutation groups. The effect of the G-allele of rs3729838 was higher on mLVWT (2.45 mm;  $p = 0.021$ ), whilst the effect of the G-allele of rs11667847 was lower on LVM (34.3 g;  $p = 0.046$ ) in the R92W<sub>TNNI2</sub> group compared to the R403W<sub>MYH7</sub> group.

The p-values for the *association* between the *TNNI3* haplotypes and *hypertrophy traits* are graphically represented in *Figure 3.10*. The p-values for *pair-wise comparison between mutation groups* in the association between *TNNI3* haplotypes and *hypertrophy traits* are given in *Table 3.28*. No statistically significant haplotype effect was observed. However, the CA and GA haplotypes, observed in 54% and 21% of the cohort, respectively, showed significant differences in haplotype effect amongst the HCM founder mutation groups. The effect of the first was lower on mLVWT (1.97 mm;  $p = 0.037$ ) in the R92W<sub>TNNI2</sub> group compared to the R403W<sub>MYH7</sub> group. The effect of the second was higher on mIVST (3.7 mm;  $p = 0.032$ ) and mLVWT (3.46 mm;  $p = 0.009$ ) in the R92W<sub>TNNI2</sub> group relative to the R403W<sub>MYH7</sub> group; and lower on mLVWT (4.47 mm;  $p = 0.045$ ) in the R403W<sub>MYH7</sub> group compared to the A797T<sub>MYH7</sub> group.

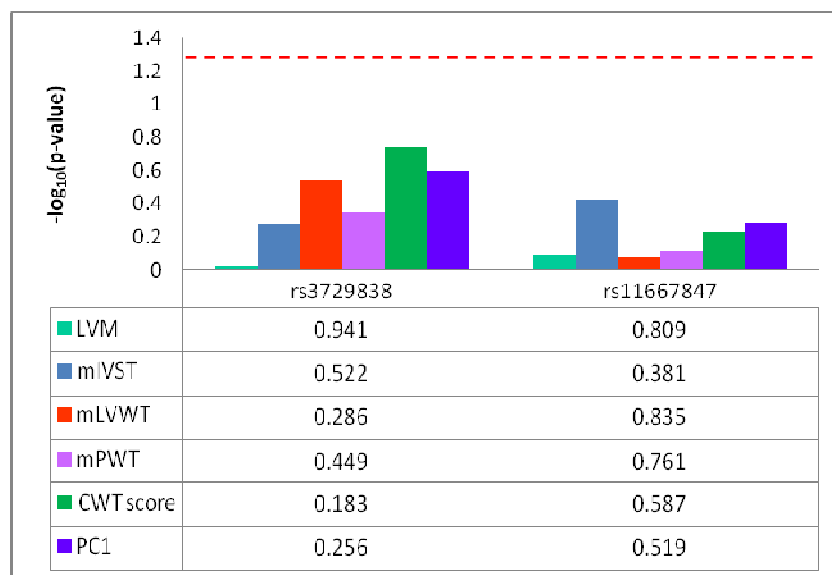


**Figure 3.9** The p-values for tests of association between single SNPs in *TNNI3* and individual hypertrophy traits. The original p-values are given in the data table, whilst the graph represents the corresponding  $-\log_{10}$  transformed values. The red dashed horizontal line indicates the p-value significance threshold equal to 0.05. Bars located above this line, therefore, indicate significant p-values (p-values<0.05). The p-value significance increases with bar height above threshold.

**Table 3.27** The p-values obtained for the analysis of interaction between mutation group and single SNPs in *TNNI3*. Significant are indicated in bold red font.

SNP ID	LVM			mIVST			mLVWT			mPWT			CWT score			PC1		
	R403W vs A797T	R92W vs A797T	R92W vs R403W	R403W vs A797T	R92W vs A797T	R92W vs R403W	R403W vs A797T	R92W vs A797T	R92W vs R403W	R403W vs A797T	R92W vs A797T	R92W vs R403W	R403W vs A797T	R92W vs A797T	R92W vs R403W	R403W vs A797T	R92W vs A797T	R92W vs R403W
rs3729838	0.783	0.284	0.456	0.274	0.743	0.182	0.080	0.482	<b>0.021</b>	0.326	0.746	0.531	0.180	0.821	0.140	0.395	0.828	0.315
rs11667847	0.552	0.219	<b>0.046</b>	0.512	0.981	0.454	0.764	0.748	0.982	0.704	0.704	0.409	0.894	0.949	0.936	0.906	0.907	0.996

**Abbreviations:** A-Alanine; **CWT score**-cumulative wall thickness score; **LVM**-left ventricular mass; **mIVST**-maximal interventricular septum thickness; **mLVWT**-maximal left ventricular wall thickness; **mPWT**-maximal posterior wall thickness; **PC1**-principal component score; **R**-Arginine; **SNP**-single nucleotide polymorphism; **T**-Threonine; **vs**-versus; **W**-Tryptophan



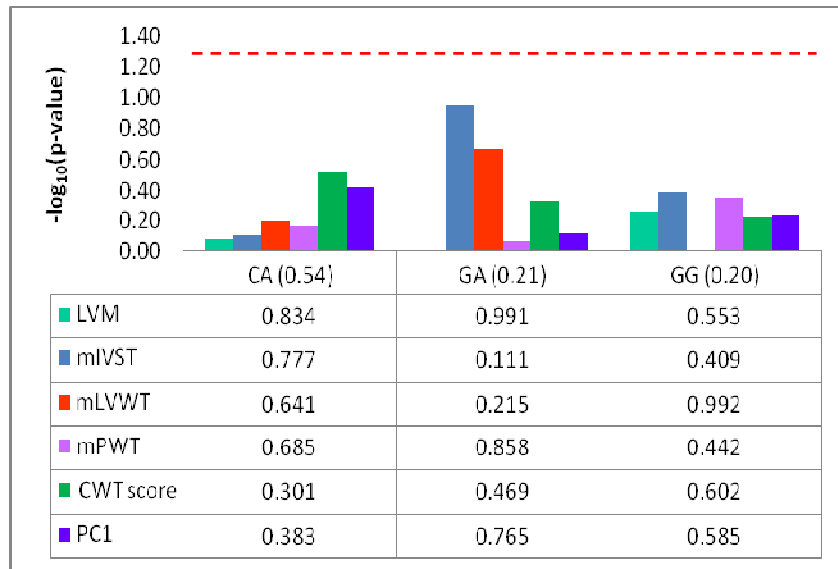


**Figure 3.10** The p-values for tests of association between *TNNT3* haplotypes and individual hypertrophy traits. The original p-values are given in the data table, whilst the graph represents the corresponding  $-\log_{10}$  transformed values. The red dashed horizontal line indicates the p-value significance threshold equal to 0.05. Bars located above this line, therefore, indicate significant p-values (p-values<0.05). The p-value significance increases with bar height above threshold. The observed haplotype frequencies are indicated in brackets.

**Table 3.28** The p-values obtained for the analysis of interaction between mutation group and *TNNT3* haplotypes. Significant results are indicated in bold red font.

Haplotype*		LVM			mIVST			mLVWT			mPWT			CWT score			PC1		
rs3729838	rs11667847	R403W	R92W	R92W	R403W	R92W	R92W	R403W	R92W	R92W	R403W	R92W	R92W	R403W	R92W	R92W	R403W	R92W	R92W
		vs	vs	vs	vs	vs	vs	vs	vs	vs	vs	vs	vs	vs	vs	vs	vs	vs	vs
C	A	0.782	0.288	0.495	0.546	0.529	0.266	0.330	0.183	<b>0.037</b>	0.493	0.916	0.463	0.407	0.732	0.273	0.687	0.673	0.450
G	A	0.484	0.870	0.404	0.110	0.495	<b>0.032</b>	<b>0.045</b>	0.464	<b>0.009</b>	0.539	0.207	0.627	0.198	0.911	0.232	0.322	0.839	0.414
G	G	0.630	0.253	0.073	0.660	0.832	0.467	0.889	0.773	0.873	0.836	0.743	0.561	0.864	0.805	0.941	0.886	0.987	0.854

**Abbreviations:** A-Adenine\*, A-Alanine; CWT score-cumulative wall thickness score; C-Cytosine\*; G-Guanine\*; LVM-left ventricular mass; mIVST-maximal interventricular septum thickness; mLVWT-maximal left ventricular wall thickness; mPWT-maximal posterior wall thickness; PC1-principal component score; R-Arginine; SNP-single nucleotide polymorphism; T-Threonine; T-Thymine\*; vs-versus; W-Tryptophan

### 3.4.5.5 *TPM1*

**Figure 3.11** graphically represents the p-values for the *association* between the *TPM1 SNPs* and *hypertrophy traits*. The effect of the C-allele of the rs11071720 variant was an estimated 0.49 mm decrease in mPWT ( $p = 0.008$ ). The C-allele of the rs1071646 variant was associated with an increase in all measures: 17.3 g in LVM ( $p = 0.006$ ), 2.02 mm in mIVST ( $p = 0.002$ ), 1.75 mm in mLVWT ( $p = 0.005$ ), 0.59 in mPWT ( $p = 0.004$ ), 17.68 mm in the CWT score ( $p < 0.001$ ) and 1.10 in PC1 ( $p < 0.001$ ). The effect of the C-allele of the rs707602 variant was an estimated increase of 1.0 mm in mLVWT ( $p = 0.031$ ) and 0.83 mm in mPWT ( $p = 0.023$ ).

**Table 3.29** details the p-values for *pair-wise differences between mutation groups* in the association between the *TPM1 SNPs* and *hypertrophy traits*. The rs11071720 SNP also indicated significant differences in SNP effect amongst the HCM founder mutation groups. The effect of the C-allele was higher in the R92W<sub>TNNT2</sub> group relative to the A797T<sub>MYH7</sub> group with 2.65 mm on mIVST ( $p = 0.024$ ). The effect of the T-allele of the rs4238370 variant was lower in the R92W<sub>TNNT2</sub> group compared to the A797T<sub>MYH7</sub> group: 48.1 g on LVM ( $p = 0.045$ ), 3.84 mm on mIVST ( $p = 0.022$ ), 4.84 mm on mLVWT ( $p = 0.016$ ), 45.6 mm on the CWT score ( $p = 0.003$ ) and 2.85 on PC1 ( $p = 0.004$ ). Also, its effect was lower in the R403W<sub>MYH7</sub> group relative to the A797T<sub>MYH7</sub> group: 3.99 mm on mIVST ( $p = 0.019$ ), 35.8 mm on the CWT score ( $p = 0.011$ ) and 2.23 on the PC1 measure ( $p = 0.019$ ).

**Figure 3.12** graphically represents the p-values for the *association* between *TPM1 haplotypes* and *hypertrophy traits* with evidence of statistically significant haplotype effects for haplotypes CGAT, CTCT and CGCT. The effect of the first, present in 27% of the cohort, was an estimated decrease of 18.1 g in LVM ( $p = 0.004$ ), 0.78 mm in mPWT ( $p = 0.001$ ), 9 mm in the CWT score ( $p = 0.042$ ) and 0.56 in PC1 ( $p = 0.006$ ). The second, observed in 6% of the cohort, was associated with an estimated increase of 3.21 mm in mIVST ( $p = 0.012$ ), 3.13 mm in mLVWT ( $p = 0.022$ ), 30.2 mm in the CWT score ( $p = 0.004$ ) and 1.89 in PC1 ( $p = 0.006$ ). The final haplotype, identified in 3% of the cohort, was associated with an increase of 47.9 g in LVM ( $p = 0.004$ ).

**Table 3.30** details the p-values for *pair-wise differences between mutation groups* in the association between *TPM1 haplotypes* and *hypertrophy traits*. The CGAT haplotype that showed a significant haplotype effect as well as the TGCT haplotype indicated significant differences in

haplotype effect amongst the HCM founder mutation groups. The effect of the CGAT haplotype was higher on mIVST (2.98 mm;  $p = 0.040$ ) and the CWT score (18.4 mm;  $p = 0.046$ ) in the R92W<sub>TNNT2</sub> group relative to the R403W<sub>MYH7</sub> group. Also, its effect was higher in the R403W<sub>MYH7</sub> group compared to the A797T<sub>MYH7</sub> group: 3.88 mm on mIVST ( $p = 0.010$ ) and 28.5 mm on the CWT score ( $p = 0.020$ ) and 1.78 on PC1 ( $p = 0.040$ ). The effect of the TGCT haplotype was lower on LVM in the R92W<sub>TNNT2</sub> group compared to the A797T<sub>MYH7</sub> group (105 g;  $p = 0.014$ ); and higher on LVM in R92W<sub>TNNT2</sub> group compared to the R403W<sub>MYH7</sub> group (105.5 g;  $p = 0.018$ ).

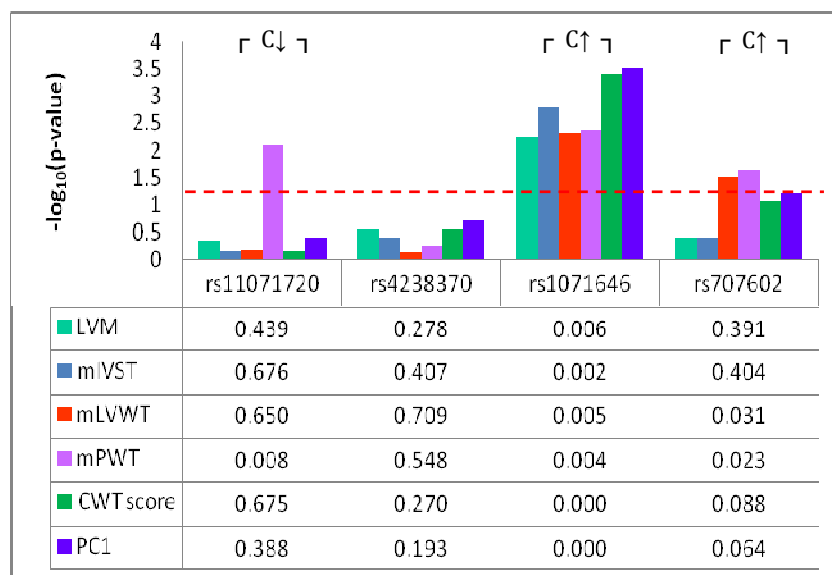


**Figure 3.11** The p-values for tests of association between single SNPs in *TPMI* and individual hypertrophy traits. The original p-values are given in the data table, whilst the graph represents the corresponding  $-\log_{10}$  transformed values. The red dashed horizontal line indicates the p-value significance threshold equal to 0.05. Bars located above this line, therefore, indicate significant p-values (p-values<0.05). The p-value significance increases with bar height above threshold.

**Table 3.29** The p-values obtained for the analysis of interaction between mutation group and single SNPs in *TPMI*. Significant results are indicated in bold red font.

SNP ID	LVM			mIVST			mLVWT			mPWT			CWT score			PC1		
	R403W vs A797T	R92W vs A797T	R92W vs R403W	R403W vs A797T	R92W vs A797T	R92W vs R403W	R403W vs A797T	R92W vs A797T	R92W vs R403W	R403W vs A797T	R92W vs A797T	R92W vs R403W	R403W vs A797T	R92W vs A797T	R92W vs R403W	R403W vs A797T	R92W vs A797T	R92W vs R403W
rs11071720	0.921	0.422	0.429	0.211	<b>0.024</b>	0.464	0.605	0.165	0.479	0.879	0.988	0.872	0.303	0.103	0.694	0.443	0.141	0.608
rs4238370	0.118	<b>0.045</b>	0.527	<b>0.019</b>	<b>0.022</b>	0.789	0.082	<b>0.016</b>	0.370	0.162	0.189	0.931	<b>0.011</b>	<b>0.003</b>	0.473	<b>0.019</b>	<b>0.004</b>	0.432
rs1071646	0.571	0.647	0.389	0.447	0.662	0.843	0.459	0.617	0.913	0.310	0.271	0.841	0.214	0.253	0.932	0.217	0.185	0.798
rs707602	0.489	0.063	0.510	0.257	0.288	0.806	0.430	0.502	0.833	0.695	0.354	0.773	0.451	0.393	0.938	0.416	0.274	0.976

**Abbreviations:** A-Alanine; **CWT score**-cumulative wall thickness score; **LVM**-left ventricular mass; **mIVST**-maximal interventricular septum thickness; **mLVWT**-maximal left ventricular wall thickness; **mPWT**-maximal posterior wall thickness; **PC1**-principal component score; **R**-Arginine; **SNP**-single nucleotide polymorphism; **T**-Threonine; **vs**-versus; **W**-Tryptophan

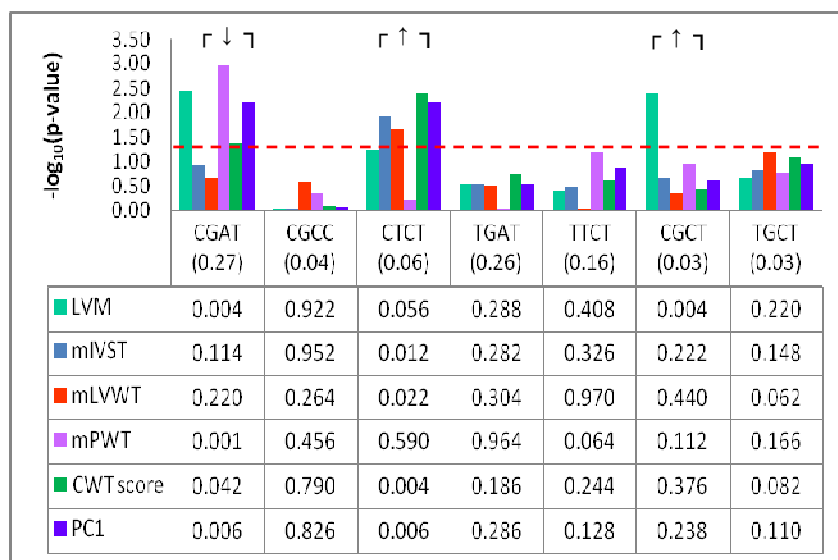


**Figure 3.12** The p-values for tests of association between *TPMI* haplotypes and individual hypertrophy traits. The original p-values are given in the data table, whilst the graph represents the corresponding  $-\log_{10}$  transformed values. The red dashed horizontal line indicates the p-value significance threshold equal to 0.05. Bars located above this line, therefore, indicate significant p-values (p-values<0.05). The p-value significance increases with bar height above threshold. The observed haplotype frequencies are indicated in brackets.

**Table 3.30** The p-values obtained for the analysis of interaction between mutation group and *TPMI* haplotypes. Significant results are indicated in bold red font.

Haplotype*	LVM			mIVST			mLVWT			mPWT			CWT score			PC1		
rs11071720	R403W	R92W	R92W	R403W	R92W	R92W	R403W	R92W	R92W	R403W	R92W	R92W	R403W	R92W	R92W	R403W	R92W	R92W
rs4238370	vs	vs	vs	vs	vs	vs	vs	vs	vs	vs	vs	vs	vs	vs	vs	vs	vs	vs
rs1071646	A797T	A797T	R403W	A797T	A797T	R403W	A797T	A797T	R403W	A797T	A797T	R403W	A797T	A797T	R403W	A797T	A797T	R403W
rs707602																		
C	0.182	0.568	0.440	<b>0.010</b>	0.576	<b>0.040</b>	0.060	0.802	0.100	0.182	0.774	0.300	<b>0.020</b>	0.786	<b>0.046</b>	<b>0.040</b>	0.760	0.088
G	-	-	-	-	-	-	-	-	-	-	-	-	-	-	-	-	-	-
A	-	-	-	-	-	-	-	-	-	-	-	-	-	-	-	-	-	-
T	0.188	0.726	0.390	0.350	0.974	0.416	0.544	0.778	0.784	0.420	0.704	0.728	0.792	0.978	0.834	0.756	0.798	0.980
T	0.846	0.936	0.880	0.186	0.750	0.210	0.138	0.526	0.254	0.468	0.770	0.568	0.094	0.274	0.346	0.142	0.210	0.594
C	-	-	-	-	-	-	-	-	-	-	-	-	-	-	-	-	-	-
T	0.908	<b>0.014</b>	<b>0.018</b>	0.538	0.094	0.252	0.984	0.280	0.288	0.724	0.178	0.296	0.590	0.078	0.160	0.732	0.114	0.176

\*\* absence of p-values indicates unequal distribution of haplotypes in the three HCM mutation groups resulting in stratified groups of small size with insufficient statistical power for testing

**Abbreviations:** A-Adenine\*; A-Alanine; CWT score-cumulative wall thickness score; C-Cytosine\*; G-Guanine\*; LVM-left ventricular mass; mIVST-maximal interventricular septum thickness; mLVWT-maximal left ventricular wall thickness; mPWT-maximal posterior wall thickness; PC1-principal component score; R-Arginine; SNP-single nucleotide polymorphism; T-Threonine; T-Thymine\*; vs-versus; W-Tryptophan

### 3.4.5.6 MYL2

**Figure 3.13** graphically represents the p-values for the *association* between the *MYL2 SNPs* and *hypertrophy traits*. A statistically significant SNP effect was observed for rs933296. The effect of the A-allele was an estimated decrease of 13.6 g in LVM ( $p = 0.018$ ), 9.57 mm in the CWT score ( $p = 0.049$ ) and 0.60 in PC1 ( $p = 0.032$ ). **Table 3.31** details the p-values for *pair-wise comparison between mutation groups* in the association between *MYL2 SNPs* and *hypertrophy traits*. No significant difference in variant effect was observed amongst the three mutation groups.

**Figure 3.14** graphically represents the p-values for the *association* between *MYL2 haplotypes* and *hypertrophy traits*. Evidence of statistically significant haplotype effects were identified for haplotypes AC and AG, present in 2% and 20% of the cohort, respectively. The effect of the AC haplotype was an estimated decrease of 25.1 g in LVM ( $p = 0.031$ ). The effect of the AG haplotype was an estimated 0.60 decrease in PC1 ( $p = 0.042$ ). **Table 3.32** details the p-values for *pair-wise differences between mutation groups* in the association between *MYL2 haplotypes* and *hypertrophy traits* with no evidence of significant differences in haplotype effect amongst the three HCM founder mutation groups.

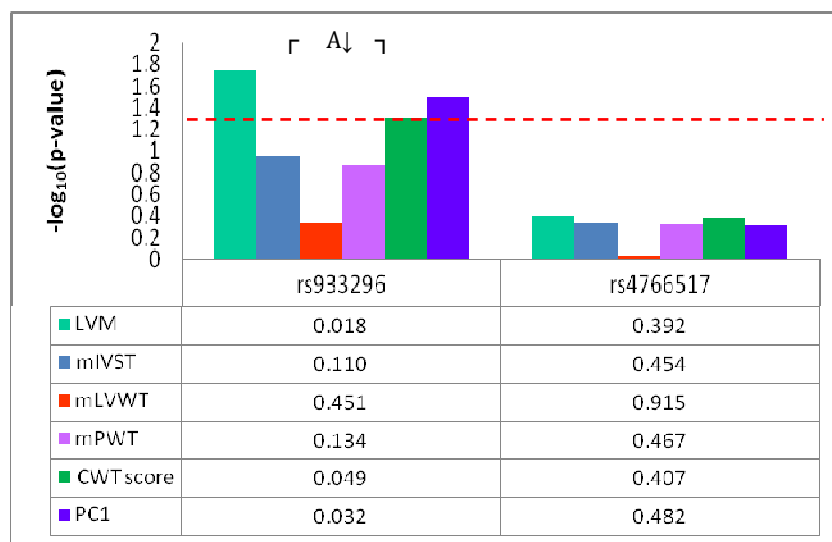


**Figure 3.13** The p-values for tests of association between single SNPs in *MYL2* and individual hypertrophy traits. The original p-values are given in the data table, whilst the graph represents the corresponding  $-\log_{10}$  transformed values. The red dashed horizontal line indicates the p-value significance threshold equal to 0.05. Bars located above this line, therefore, indicate significant p-values (p-values<0.05). The p-value significance increases with bar height above threshold.

**Table 3.31** The p-values obtained for the analysis of interaction between mutation group and single SNPs in *MYL2*.

SNP ID	LVM			mIVST			mLVWT			mPWT			CWT score			PC1		
	R403W vs A797T	R92W vs A797T	R92W vs R403W	R403W vs A797T	R92W vs A797T	R92W vs R403W	R403W vs A797T	R92W vs A797T	R92W vs R403W	R403W vs A797T	R92W vs A797T	R92W vs R403W	R403W vs A797T	R92W vs A797T	R92W vs R403W	R403W vs A797T	R92W vs A797T	R92W vs R403W
rs933296	0.644	0.537	0.966	0.717	0.381	0.274	0.530	0.548	0.258	0.221	0.489	0.077	0.341	0.337	0.085	0.314	0.257	0.056
rs4766517	0.780	0.312	0.580	0.710	0.786	0.876	0.728	0.687	0.984	0.212	0.680	0.348	0.362	0.615	0.597	0.256	0.715	0.383

**Abbreviations:** A-Alanine; CWT score-cumulative wall thickness score; LVM-left ventricular mass; mIVST-maximal interventricular septum thickness; mLVWT-maximal left ventricular wall thickness; mPWT-maximal posterior wall thickness; PC1-principal component score; R-Arginine; SNP-single nucleotide polymorphism; T-Threonine; vs-versus; W-Tryptophan

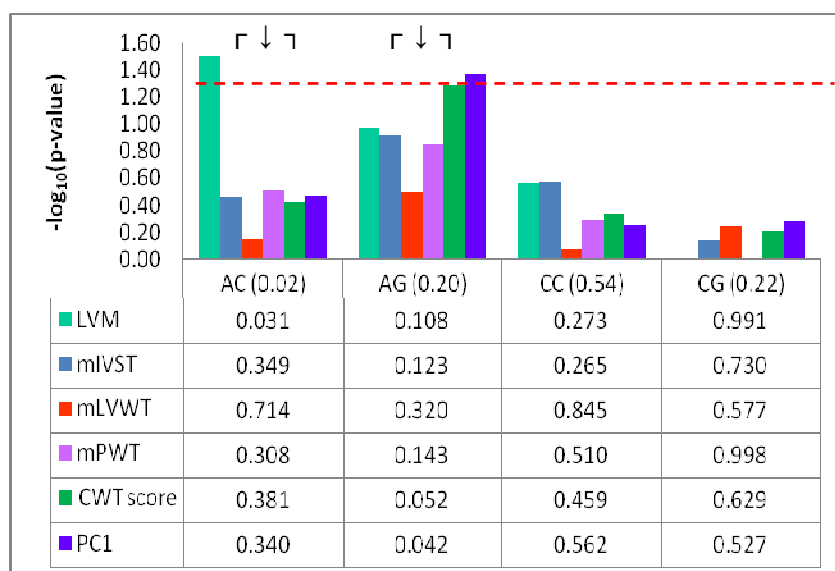


**Figure 3.14** The p-values for tests of association between *MYL2* haplotypes and individual hypertrophy traits. The original p-values are given in the data table, whilst the graph represents the corresponding  $-\log_{10}$  transformed values. The red dashed horizontal line indicates the p-value significance threshold equal to 0.05. Bars located above this line, therefore, indicate significant p-values (p-values<0.05). The p-value significance increases with bar height above threshold. The observed haplotype frequencies are indicated in brackets.

**Table 3.32** The p-values obtained for the analysis of interaction between mutation group and *MYL2* haplotypes.

Haplotype*		LVM			mIVST			mLVWT			mPWT			CWT score			PC1			
rs933296	rs4766517	R403W	R92W	R92W	R403W	R92W	R92W	R403W	R92W	R92W	R403W	R92W	R92W	R403W	R92W	R92W	R403W	R92W	R92W	
		vs	vs	vs	vs	vs	vs	vs	vs	vs	vs	vs	vs	vs	vs	vs	vs	vs	vs	
		A797T	A797T	R403W	A797T	A797T	R403W	A797T	A797T	A797T	R403W	A797T	A797T	R403W	A797T	A797T	R403W	A797T	A797T	R403W
		A	C		A	C		A	C		A	C		A	C		A	C		A
		0.826	0.564	0.728	0.804	0.403	0.362	0.513	0.677	0.389	0.791	0.851	0.721	0.676	0.780	0.564	0.627	0.918	0.628	
		0.622	0.304	0.269	0.601	0.962	0.638	0.545	0.731	0.712	0.356	0.819	0.309	0.274	0.475	0.515	0.390	0.402	0.726	
		0.546	0.864	0.693	0.571	0.579	0.331	0.682	0.898	0.634	0.114	0.757	0.250	0.830	0.750	0.941	0.877	0.879	0.990	
		0.385	0.123	0.541	0.533	0.233	0.623	0.379	0.289	0.885	0.346	0.588	0.181	0.162	0.294	0.713	0.150	0.118	0.945	

**Abbreviations:** A-Adenine\*; A-Alanine; CWT score-cumulative wall thickness score; C-Cytosine\*; G-Guanine\*; LVM-left ventricular mass; mIVST-maximal interventricular septum thickness; mLVWT-maximal left ventricular wall thickness; mPWT-maximal posterior wall thickness; PC1-principal component score; R-Arginine; SNP-single nucleotide polymorphism; T-Threonine; vs-versus; W-Tryptophan



### 3.4.5.7 MYL3

**Figure 3.15** graphically represents the p-values for the *association* between the *MYL3 SNPs* and *hypertrophy traits*. **Table 3.33** details the p-values for the *pair-wise differences between mutation groups* in the association of *MYL3 SNPs* and *hypertrophy traits*. No statistically significant single SNP effect or difference in SNP effect amongst the three HCM founder mutation groups was observed.

**Figure 3.16** graphically represents the p-values for the *association* between *MYL3 haplotypes* and *hypertrophy traits*. Significant haplotype effects were identified for haplotypes CC and TC. The effect of the first, observed in 49% of the cohort, was an estimated decrease of 8 g in LVM ( $p = 0.014$ ), 0.32 mm in mPWT ( $p = 0.026$ ), 3.7 mm in the CWT score (0.042) and 0.23 in PC1 ( $p = 0.030$ ). The effect of the second haplotype, present in 3% of the cohort, was an estimated increase of 25.6 mm in the CWT score ( $p = 0.018$ ) and 1.6 in PC1 ( $p = 0.035$ ). **Table 3.34** details the p-values for *pair-wise differences between mutation groups* in the association of *MYL3 haplotypes* and hypertrophy traits. No statistically significant difference in haplotype effect was observed amongst the three HCM founder mutation groups.



**Figure 3.15** The p-values for tests of association between single SNPs in *MYL3* and individual hypertrophy traits. The original p-values are given in the data table, whilst the graph represents the corresponding  $-\log_{10}$  transformed values. The red dashed horizontal line indicates the p-value significance threshold equal to 0.05. Bars located above this line, therefore, indicate significant p-values (p-values<0.05). The p-value significance increases with bar height above threshold.

**Table 3.33** The p-values obtained for the analysis of interaction between mutation group and single SNPs in *MYL3*.

SNP ID	LVM			mIVST			mLVWT			mPWT			CWT score			PC1		
	R403W vs A797T	R92W vs A797T	R92W vs R403W	R403W vs A797T	R92W vs A797T	R92W vs R403W	R403W vs A797T	R92W vs A797T	R92W vs R403W	R403W vs A797T	R92W vs A797T	R92W vs R403W	R403W vs A797T	R92W vs A797T	R92W vs R403W	R403W vs A797T	R92W vs A797T	R92W vs R403W
rs1531136	0.644	0.537	0.966	0.717	0.381	0.274	0.530	0.548	0.258	0.221	0.489	0.077	0.341	0.337	0.085	0.314	0.257	0.056
rs3792558	0.780	0.312	0.580	0.710	0.786	0.876	0.728	0.687	0.984	0.212	0.680	0.348	0.362	0.615	0.597	0.256	0.715	0.383

**Abbreviations:** A-Alanine; **CWT score**-cumulative wall thickness score; **LVM**-left ventricular mass; **mIVST**-maximal interventricular septum thickness; **mLVWT**-maximal left ventricular wall thickness; **mPWT**-maximal posterior wall thickness; **PC1**-principal component score; **R**-Arginine; **SNP**-single nucleotide polymorphism; **T**-Threonine; **vs**-versus; **W**-Tryptophan

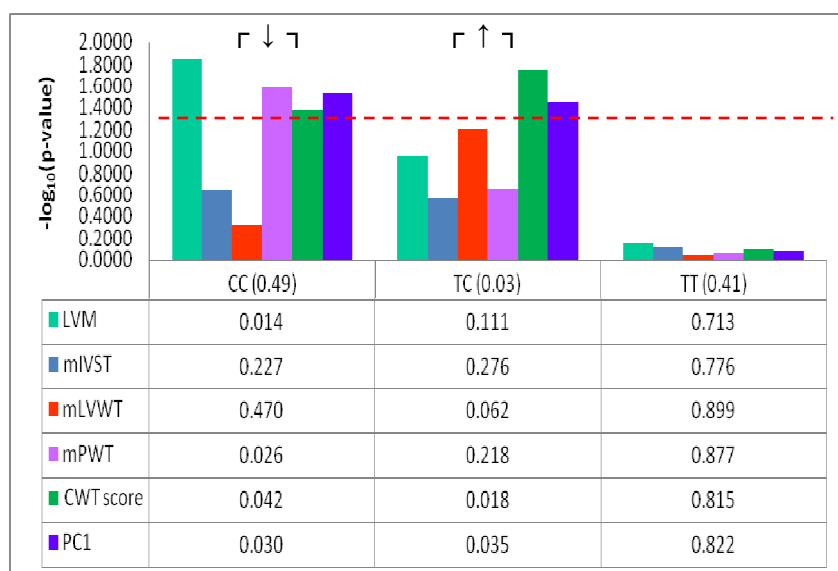


**Figure 3.16** The p-values for tests of association between *MYL3* haplotypes and individual hypertrophy traits. The original p-values are given in the data table, whilst the graph represents the corresponding  $-\log_{10}$  transformed values. The red dashed horizontal line indicates the p-value significance threshold equal to 0.05. Bars located above this line, therefore, indicate significant p-values (p-values<0.05). The p-value significance increases with bar height above threshold. The observed haplotype frequencies are indicated in brackets.

**Table 3.34** The p-values obtained for the analysis of interaction between mutation group and single haplotypes in *MYL3*.

Haplotype*		LVM			mIVST			mLVWT			mPWT			CWT score			PC1		
rs1531136	rs3792558	R403W	R92W	R92W	R403W	R92W	R92W	R403W	R92W	R92W	R403W	R92W	R92W	R403W	R92W	R92W	R403W	R92W	R92W
		vs A797T	vs A797T	vs R403W	vs A797T	vs A797T	vs R403W	vs A797T	vs A797T	vs R403W	vs A797T	vs A797T	vs R403W	vs A797T	vs A797T	vs R403W	vs A797T	vs A797T	vs R403W
C	C	0.267	0.717	0.163	0.494	0.612	0.749	0.290	0.467	0.587	0.206	0.280	0.619	0.261	0.685	0.390	0.271	0.676	0.408
T	C	0.589	0.932	0.534	0.562	0.633	0.351	0.071	0.989	0.063	0.143	0.519	0.248	0.186	0.532	0.080	0.587	0.692	0.422
T	T	0.797	0.912	0.715	0.666	0.400	0.775	0.869	0.824	0.979	0.617	0.439	0.236	0.517	0.896	0.433	0.410	0.736	0.253

**Abbreviations:** A-Alanine; CWT score-cumulative wall thickness score; C-Cytosine\*; LVM-left ventricular mass; mIVST-maximal interventricular septum thickness; mLVWT-maximal left ventricular wall thickness; mPWT-maximal posterior wall thickness; PC1-principal component score; R-Arginine; SNP-single nucleotide polymorphism; T-Threonine; T-Thymine\*; vs-versus; W-Tryptophan

### 3.4.5.8 MYBPC3

**Figure 3.17** graphically represents the p-values for the *association* between the *MYBPC3 SNPs* and *hypertrophy traits* with no evidence of statistically significant SNP effects. **Table 3.35** details the p-values for the *pair-wise comparison between mutation groups* in the association of *MYBPC3 SNPs* and *hypertrophy traits*. The effect of the A-allele of rs4752825 and the T-allele of rs1052373 was higher on LVM in the R92W<sub>TNNT2</sub> group compared to A797T<sub>MYH7</sub> group (22.6 g; p = 0.020 and 22.5 g; p = 0.019).

**Figure 3.18** graphically represents the p-values for the *association* between *MYBPC3 haplotypes* and *hypertrophy traits*. The effect of the ATGG haplotype, identified in 25% of the cohort, was an estimated decrease of 0.51 mm in mPWT (p = 0.026). **Table 3.36** details the p-values for *pair-wise comparison between mutation groups* in the association of *MYBPC3 haplotypes* and hypertrophy traits. The effect of the ATGA haplotype, observed in 10% of the cohort, was higher on LVM (65.1 g; p = 0.002), mPWT (1.66 mm; p = 0.032), the CWT score (8.6 mm; p = 0.038) and PC1 (0.54; p = 0.048) in the R403W<sub>MYH7</sub> group compared to the A797T<sub>MYH7</sub> group. Its effect was also higher on LVM (29.9 g, p = 0.046) and mPWT (1.25 mm; p = 0.046) in the R92W<sub>TNNT2</sub> group relative to the R403W<sub>MYH7</sub> group. Finally, its effect was lower on PC1 (0.05; p < 0.001) in the R92W<sub>TNNT2</sub> group compared to the A797T<sub>MYH7</sub> group. The effect of the GCGG haplotype, observed in 37% of the cohort, was lower on the LVM measure (36.8 g; p = 0.002) in the R403W<sub>MYH7</sub> group compared to the A797T<sub>MYH7</sub> group. Also, its effect was lower on LVM (30.9 g; p = 0.008), mPWT (1.13 mm; p = 0.012) and PC1 (1.10; p = 0.042) in the R92W<sub>TNNT2</sub> group relative to the R403W<sub>MYH7</sub> group.

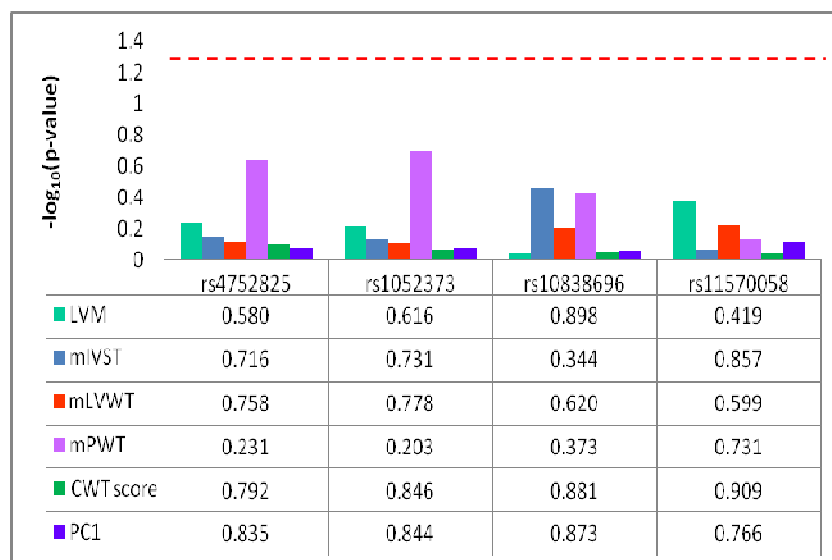


**Figure 3.17** The p-values for tests of association between single SNPs in *MYBPC3* and individual hypertrophy traits. The original p-values are given in the data table, whilst the graph represents the corresponding  $-\log_{10}$  transformed values. The red dashed horizontal line indicates the p-value significance threshold equal to 0.05. Bars located above this line, therefore, indicate significant p-values (p-values<0.05). The p-value significance increases with bar height above threshold.

**Table 3.35** The p-values obtained for the analysis of interaction between mutation group and single SNPs in *MYBPC3*. Significant results are indicated in bold red font.

SNP ID	LVM			mIVST			mLVWT			mPWT			CWT score			PC1		
	R403W vs A797T	R92W vs A797T	R92W vs R403W	R403W vs A797T	R92W vs A797T	R92W vs R403W	R403W vs A797T	R92W vs A797T	R92W vs R403W	R403W vs A797T	R92W vs A797T	R92W vs R403W	R403W vs A797T	R92W vs A797T	R92W vs R403W	R403W vs A797T	R92W vs A797T	R92W vs R403W
rs4752825	0.266	<b>0.020</b>	0.447	0.313	0.255	0.941	0.359	0.413	0.809	0.297	0.980	0.326	0.532	0.561	0.883	0.413	0.643	0.665
rs1052373	0.147	<b>0.019</b>	0.650	0.210	0.221	0.805	0.267	0.371	0.711	0.214	0.686	0.376	0.400	0.520	0.752	0.336	0.543	0.643
rs10838696	0.393	0.997	0.464	0.811	0.925	0.777	0.536	0.578	0.319	0.368	0.925	0.394	0.364	0.745	0.604	0.254	0.663	0.529
rs11570058	0.140	0.062	0.422	0.220	0.313	0.875	0.597	0.575	0.846	0.177	0.306	0.936	0.254	0.240	0.742	0.303	0.295	0.779

**Abbreviations:** A-Alanine; **CWT score**-cumulative wall thickness score; **LVM**-left ventricular mass; **mIVST**-maximal interventricular septum thickness; **mLVWT**-maximal left ventricular wall thickness; **mPWT**-maximal posterior wall thickness; **PC1**-principal component score; **R**-Arginine; **SNP**-single nucleotide polymorphism; **T**-Threonine; **vs**-versus; **W**-Tryptophan

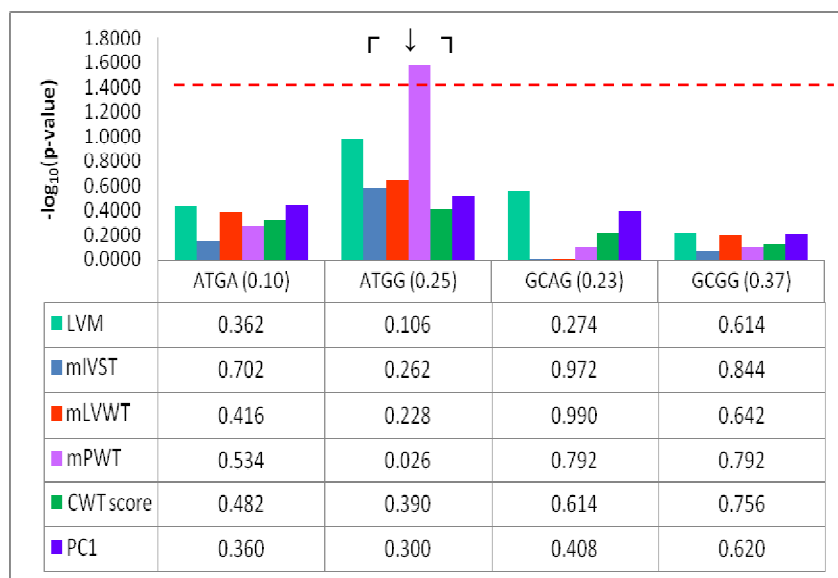


**Figure 3.18** The p-values for tests of association between *MYBPC3* haplotypes and individual hypertrophy traits. The original p-values are given in the data table, whilst the graph represents the corresponding  $-\log_{10}$  transformed values. The red dashed horizontal line indicates the p-value significance threshold equal to 0.05. Bars located above this line, therefore, indicate significant p-values (p-values<0.05). The p-value significance increases with bar height above threshold. The observed haplotype frequencies are indicated in brackets.

**Table 3.36** The p-values obtained for the analysis of interaction between mutation group and individual haplotypes in *MYBPC3*. Significant results are indicated in bold red font.

Haplotype*		LVM			mIVST			mLVWT			mPWT			CWT score			PC1				
rs4752825	rs1052373	R403W	R92W	R92W	R403W	R92W	R92W	R403W	R92W	R92W	R403W	R92W	R92W	R403W	R92W	R92W	R403W	R92W	R92W		
		vs	vs	vs	vs	vs	vs	vs	vs	vs	vs	vs	vs	vs	vs	vs	vs	vs	vs		
rs10838696	rs11570058	A797T	A797T	R403W	A797T	A797T	R403W	A797T	A797T	R403W	A797T	A797T	R403W	A797T	A797T	R403W	A797T	A797T	R403W		
A	T	G	A	<b>0.002</b>	0.800	<b>0.046</b>	0.100	0.474	0.120	0.306	0.524	0.468	<b>0.032</b>	0.382	<b>0.046</b>	<b>0.038</b>	0.262	0.158	<b>0.048</b>	<b>0.000</b>	0.158
A	T	G	G	0.192	0.794	0.926	0.782	0.994	0.838	0.706	0.986	0.764	0.314	0.622	0.776	0.738	0.710	0.532	0.760	0.262	0.582
G	C	A	G	0.988	0.736	0.160	0.936	0.760	0.840	0.806	0.640	0.474	0.860	0.488	0.400	0.294	0.978	0.306	0.268	0.344	0.182
G	C	G	G	<b>0.002</b>	0.954	<b>0.008</b>	0.130	0.794	0.094	0.206	0.526	0.064	0.260	0.140	<b>0.012</b>	0.074	0.888	0.076	0.060	0.276	<b>0.042</b>

**Abbreviations:** A-Adenine\*; A-Alanine; CWT score-cumulative wall thickness score; C-Cytosine\*; G-Guanine\*; LVM-left ventricular mass; mIVST-maximal interventricular septum thickness; mLVWT-maximal left ventricular wall thickness; mPWT-maximal posterior wall thickness; PC1-principal component score; R-Arginine; SNP-single nucleotide polymorphism; T-Threonine; T-Thymine\*; vs-versus; W-Tryptophan

### 3.4.5.9 ACTN3

The p-values for the *association* between the *ACTN3 SNPs* and *hypertrophy traits*; and the p-values for *pair-wise differences between mutation groups* in the association between the *ACTN3 SNPs* and *hypertrophy traits* are given in *Figure 3.19* and *Table 3.37*, respectively. No statistically significant single SNP effect or difference in SNP effect was observed amongst the three HCM founder mutation groups.

*Figure 3.20* graphically represents the p-values for the *association* between *ACTN3 haplotypes* and *hypertrophy traits* with no evidence of statistically significant haplotype effects. *Table 3.38* details the p-values for *pair-wise comparison between mutation groups* in the association between *ACTN3 haplotypes* and *hypertrophy traits*. The effect of the GCC haplotype, present in 23% of the cohort, was lower on the PC1 measure (1.02;  $p = 0.040$ ) in the R92W<sub>TNNT2</sub> group compared to the R403W<sub>MYH7</sub> group.

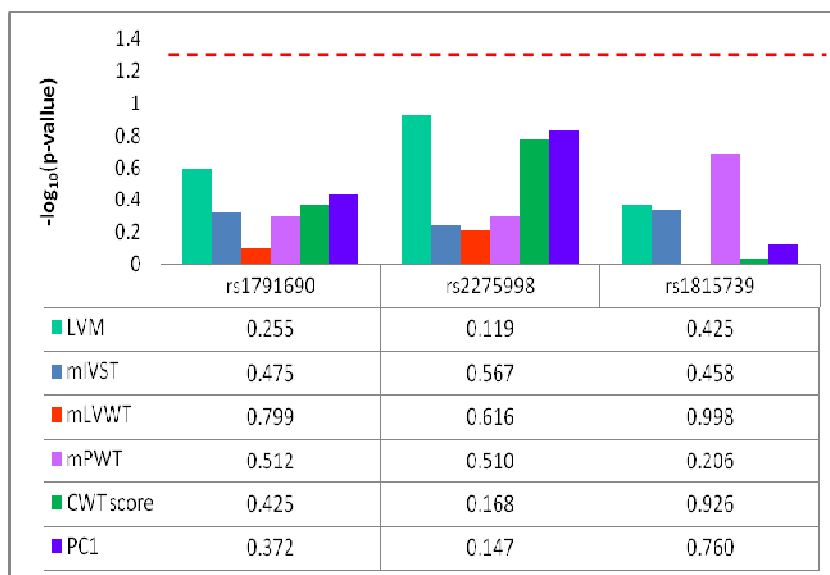


**Figure 3.19** The p-values for tests of association between single SNPs in *ACTN3* and individual hypertrophy traits. The original p-values are given in the data table, whilst the graph represents the corresponding  $-\log_{10}$  transformed values. The red dashed horizontal line indicates the p-value significance threshold equal to 0.05. Bars located above this line, therefore, indicate significant p-values (p-values<0.05). The p-value significance increases with bar height above threshold.

**Table 3.37** The p-values obtained for the analysis of interaction between mutation group and single SNPs in *ACTN3*.

SNP ID	LVM			mIVST			mLVWT			mPWT			CWT score			PC1		
	R403W vs A797T	R92W vs A797T	R92W vs R403W	R403W vs A797T	R92W vs A797T	R92W vs R403W	R403W vs A797T	R92W vs A797T	R92W vs R403W	R403W vs A797T	R92W vs A797T	R92W vs R403W	R403W vs A797T	R92W vs A797T	R92W vs R403W	R403W vs A797T	R92W vs A797T	R92W vs R403W
rs1791690	0.455	0.337	0.928	0.983	0.638	0.679	0.960	0.774	0.773	0.337	0.696	0.556	0.360	0.915	0.430	0.249	0.794	0.373
rs2275998	0.617	0.197	0.412	0.935	0.496	0.544	0.858	0.541	0.654	0.675	0.536	0.295	0.956	0.304	0.270	0.986	0.188	0.186
rs1815739	0.838	0.230	0.710	0.872	0.815	0.962	0.911	0.921	0.951	0.815	0.677	0.974	0.608	0.512	0.859	0.431	0.331	0.772

**Abbreviations:** A-Alanine; CWT score-cumulative wall thickness score; LVM-left ventricular mass; mIVST-maximal interventricular septum thickness; mLVWT-maximal left ventricular wall thickness; mPWT-maximal posterior wall thickness; PC1-principal component score; R-Arginine; SNP-single nucleotide polymorphism; T-Threonine; vs-versus; W-Tryptophan



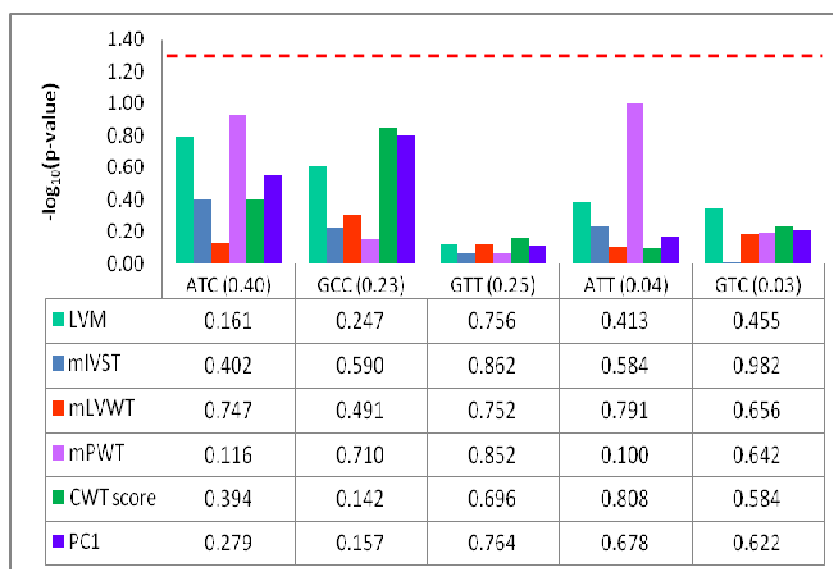


**Figure 3.20** The p-values for tests of association between *ACTN3* haplotypes and individual hypertrophy traits. The original p-values are given in the data table, whilst the graph represents the corresponding  $-\log_{10}$  transformed values. The red dashed horizontal line indicates the p-value significance threshold equal to 0.05. Bars located above this line, therefore, indicate significant p-values (p-values<0.05). The p-value significance increases with bar height above threshold. The observed haplotype frequencies are indicated in brackets.

**Table 3.38** The p-values obtained for the analysis of interaction between mutation group and *ACTN3* haplotypes. Significant results are indicated in bold red font.

Haplotype*			LVM			mIVST			mLVWT			mPWT			CWT score			PC1		
rs1791690	rs2275998	rs1815739	R403W vs A797T	R92W vs A797T	R92W vs R403W	R403W vs A797T	R92W vs A797T	R92W vs R403W	R403W vs A797T	R92W vs A797T	R92W vs R403W	R403W vs A797T	R92W vs A797T	R92W vs R403W	R403W vs A797T	R92W vs A797T	R92W vs R403W	R403W vs A797T	R92W vs A797T	R92W vs R403W
A	T	C	0.285	0.439	0.715	0.820	0.368	0.334	0.973	0.564	0.605	0.492	0.581	0.850	0.350	0.999	0.366	0.266	0.849	0.358
G	C	C	0.961	0.149	0.116	0.927	0.112	0.121	0.885	0.325	0.376	0.642	0.361	0.157	0.795	0.144	0.075	0.805	0.083	<b>0.040</b>
G	T	T	0.877	0.261	0.634	0.987	0.557	0.737	0.885	0.967	0.905	0.914	0.830	0.990	0.682	0.536	0.958	0.534	0.392	0.899
A	T	T**	0.281	0.769	0.272	0.662	0.405	0.396	0.970	0.473	0.658	-	0.436	0.585	-	0.733	-	-	0.909	-
G	T	C**	-	0.358	-	-	0.876	-	-	0.474	-	-	0.541	-	-	0.758	-	-	0.966	-

\*\* absence of p-values indicates unequal distribution of haplotypes in the three HCM mutation groups resulting in stratified groups of small size with insufficient statistical power for testing

**Abbreviations:** A-Adenine\*; A-Alanine; CWT score-cumulative wall thickness score; C-Cytosine\*; G-Guanine\*; LVM-left ventricular mass; mIVST-maximal interventricular septum thickness; mLVWT-maximal left ventricular wall thickness; mPWT-maximal posterior wall thickness; PC1-principal component score; R-Arginine; SNP-single nucleotide polymorphism; T-Threonine; T-Thymine\*; vs-versus; W-Tryptophan

### 3.4.5.10 CD36

**Figure 3.21** graphically represents the p-values for the *association* between the *CD36 SNPs* and *hypertrophy traits*. No statistically significant SNP effect was observed. **Table 3.39** details the p-values for *pair-wise comparison between mutation groups* in the association of *CD36 SNPs* and individual hypertrophy traits. The effect of the A-allele of rs10268417 was lower on mPWT (1.29 mm;  $p = 0.007$ ), the CWT score (20.7 mm;  $p = 0.041$ ) and PC1 (1.29;  $p = 0.022$ ) in the R92W<sub>TNNT2</sub> group relative to the A797T<sub>MYH7</sub> group.

**Figure 3.22** graphically represents the p-values for the *association* between *CD36 haplotypes* and *hypertrophy traits*. The effect of the CGT haplotype, present in 37% of the cohort, was an estimated decrease of 0.58 mm in mPWT ( $p = 0.020$ ), 8.6 mm in the CWT score ( $p = 0.020$ ) and 0.54 in PC1 ( $p = 0.007$ ). **Table 3.40** details the p-values for *pair-wise differences between mutation groups* in the association of *CD36 haplotypes* and *hypertrophy traits*. The effect of the AGT haplotype, present in 11% of the cohort, was lower on mPWT (1.99 mm;  $p = 0.008$ ), the CWT score (41.6 mm;  $p = 0.008$ ) and PC1 (2.6;  $p = 0.005$ ) in the R92W<sub>TNNT2</sub> group compared to the A797T<sub>MYH7</sub> group. Also, its effect was lower on the CWT score (42.5 mm;  $p = 0.047$ ) and PC1 (2.66;  $p = 0.019$ ) in the R403W<sub>MYH7</sub> group relative to the A797T<sub>MYH7</sub> group. The effect of the CGT haplotype, observed in 37% of the cohort, was higher on mIVST in the R403W<sub>MYH7</sub> group than in the A797T<sub>MYH7</sub> group (2.2 mm;  $p = 0.022$ ).

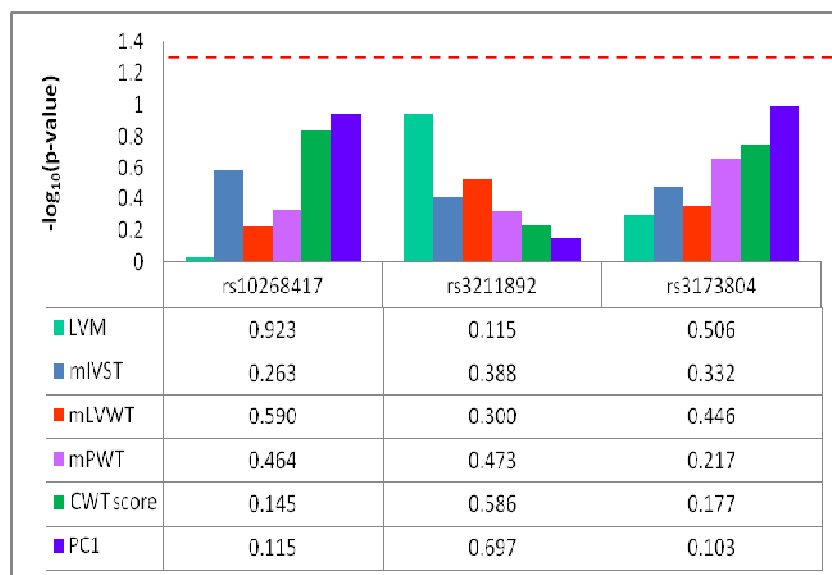


**Figure 3.21** The p-values for tests of association between single SNPs in *CD36* and individual hypertrophy traits. The original p-values are given in the data table, whilst the graph represents the corresponding  $-\log_{10}$  transformed values. The red dashed horizontal line indicates the p-value significance threshold equal to 0.05. Bars located above this line, therefore, indicate significant p-values (p-values<0.05). The p-value significance increases with bar height above threshold.

**Table 3.39** The p-values obtained for the analysis of interaction between mutation group and single SNPs in *CD36*. Significant results are indicated in bold red font.

SNP ID	LVM			mIVST			mLVWT			mPWT			CWT score			PC1		
	R403W vs A797T	R92W vs A797T	R92W vs R403W	R403W vs A797T	R92W vs A797T	R92W vs R403W	R403W vs A797T	R92W vs A797T	R92W vs R403W	R403W vs A797T	R92W vs A797T	R92W vs R403W	R403W vs A797T	R92W vs A797T	R92W vs R403W	R403W vs A797T	R92W vs A797T	R92W vs R403W
rs10268417	0.505	0.309	0.821	0.096	0.309	0.481	0.283	0.264	0.944	0.274	<b>0.007</b>	0.227	0.224	<b>0.041</b>	0.618	0.188	<b>0.022</b>	0.542
rs3211892	0.984	0.537	0.567	0.825	0.847	0.641	0.740	0.304	0.550	0.446	0.355	0.066	0.909	0.341	0.283	0.799	0.295	0.180
rs3173804	0.765	0.620	0.891	0.494	0.742	0.712	0.779	0.974	0.771	0.642	0.511	0.906	0.805	0.896	0.731	0.635	0.957	0.620

**Abbreviations:** A-Alanine; **CWT score**-cumulative wall thickness score; **LVM**-left ventricular mass; **mIVST**-maximal interventricular septum thickness; **mLVWT**-maximal left ventricular wall thickness; **mPWT**-maximal posterior wall thickness; **PC1**-principal component score; **R**-Arginine; **SNP**-single nucleotide polymorphism; **T**-Threonine; **vs**-versus; **W**-Tryptophan

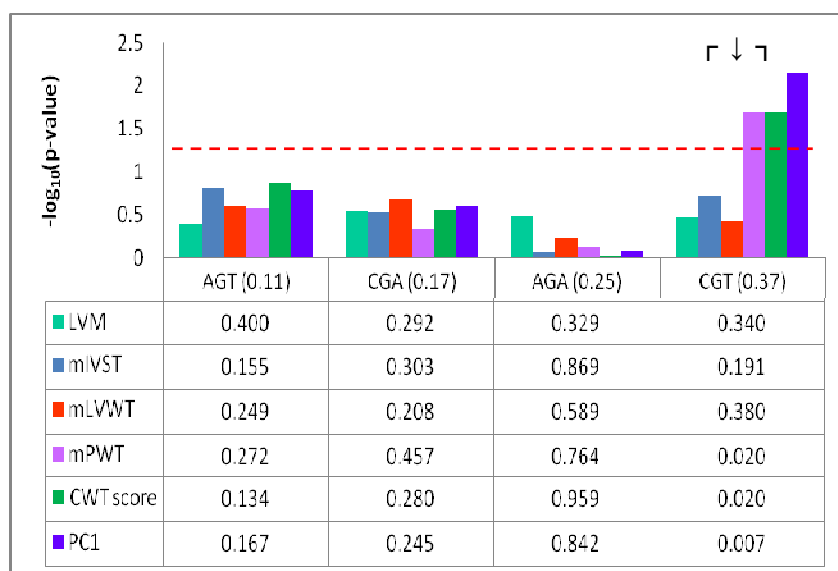


**Figure 3.22** The p-values for tests of association between *CD36* haplotypes and individual hypertrophy traits. The original p-values are given in the data table, whilst the graph represents the corresponding  $-\log_{10}$  transformed values. The red dashed horizontal line indicates the p-value significance threshold equal to 0.05. Bars located above this line, therefore, indicate significant p-values (p-values<0.05). The p-value significance increases with bar height above threshold. The observed haplotype frequencies are indicated in brackets.

**Table 3.40** The p-values obtained for the analysis of interaction between mutation group and individual haplotypes in *CD36*. Significant results are indicated in bold red font.

Haplotype*			LVM			mIVST			mLVWT			mPWT			CWT score			PC1		
rs10268417	rs3211892	rs3173804	R403W	R92W	R92W	R403W	R92W	R92W	R403W	R92W	R92W	R403W	R92W	R92W	R403W	R92W	R92W	R403W	R92W	R92W
			vs	vs	vs	vs	vs	vs	vs	vs	vs	vs	vs	vs	vs	vs	vs	vs	vs	vs
			A797T	A797T	R403W	A797T	A797T	R403W	A797T	A797T	R403W	A797T	A797T	R403W	A797T	A797T	R403W	A797T	A797T	R403W
A	G	T	0.613	0.226	0.600	0.133	0.117	0.818	0.310	0.087	0.680	0.406	<b>0.008</b>	0.147	<b>0.047</b>	<b>0.008</b>	0.956	<b>0.019</b>	<b>0.005</b>	0.841
C	G	A	0.891	0.544	0.522	0.554	0.645	0.820	0.622	0.424	0.874	0.253	0.162	0.999	0.972	0.879	0.871	0.801	0.886	0.893
A	G	A	0.899	0.421	0.542	0.384	0.548	0.882	0.557	0.622	0.987	0.456	0.105	0.392	0.986	0.252	0.326	0.866	0.190	0.214
C	G	T	0.327	0.976	0.391	<b>0.022</b>	0.410	0.174	0.138	0.337	0.606	0.520	0.586	0.298	0.092	0.231	0.597	0.097	0.329	0.488

**Abbreviations:** A-Adenine\*; A-Alanine; CWT score-cumulative wall thickness score; C-Cytosine\*; G-Guanine\*; LVM-left ventricular mass; mIVST-maximal interventricular septum thickness; mLVWT-maximal left ventricular wall thickness; mPWT-maximal posterior wall thickness; PC1-principal component score; R-Arginine; SNP-single nucleotide polymorphism; T-Threonine; T-Thymine\*; vs-versus; W-Tryptophan

### 3.4.5.11 *CPT1B*

**Figure 3.23** graphically represents the p-values for the *association* between the three *CPT1B* SNPs and *hypertrophy traits*. The effect of the T-allele of rs1557502 is an estimated increase of 0.54 mm in mPWT ( $p = 0.028$ ). **Table 3.41** details the p-values for *pair-wise differences between mutation groups* in the association of *CPT1B* SNPs and *hypertrophy traits*. No significant difference in SNP effect was observed between the HCM founder mutation groups.

**Figure 3.24** graphically represents the p-values for the *association* between *CPT1B* haplotypes and *hypertrophy traits* with no evidence of statistically significant haplotype effects. **Table 3.42** details the p-values for *pair-wise comparison between mutation groups* in the association of *CPT1B* haplotypes and *hypertrophy traits*. The effect of the CC haplotype, present in 36% of the cohort, was estimated to be lower in the R403W<sub>MYH7</sub> group compared to the A797T<sub>MYH7</sub> group: 1.8 mm on mIVST ( $p = 0.021$ ), 0.83 mm on mPWT ( $p = 0.028$ ), 18.3 mm on the CWT score ( $p = 0.034$ ) and 1.14 on the PC1 measure ( $p = 0.016$ ). Also, its effect was higher in the R92W<sub>TNNT2</sub> group relative to the R403W<sub>MYH7</sub> group: 3 mm on mIVST ( $p = 0.024$ ), 2.41 mm on mLVWT ( $p = 0.039$ ), 25.8 mm on the CWT score ( $p = 0.025$ ) and 1.61 on the PC1 measure ( $p = 0.014$ ). The effect of the CT haplotype, present in 38% of the cohort, was lower on mLVWT (3.11 mm;  $p = 0.034$ ) in the R92W<sub>TNNT2</sub> group relative to the A797T<sub>MYH7</sub> group. In addition, its effect was lower in the R92W<sub>TNNT2</sub> group compared to the R403W<sub>MYH7</sub> group: 0.95 mm on mPWT ( $p = 0.040$ ), 18.2 mm on the CWT score ( $p = 0.039$ ) and 1.14 on the PC1 measure ( $p = 0.025$ ).

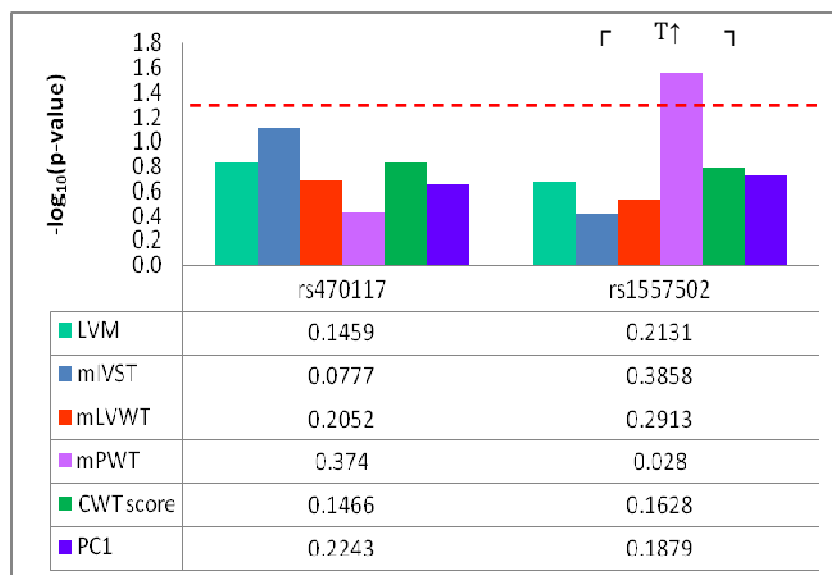


**Figure 3.23** The p-values for tests of association between single SNPs in *CPT1B* and individual hypertrophy traits. The original p-values are given in the data table, whilst the graph represents the corresponding  $-\log_{10}$  transformed values. The red dashed horizontal line indicates the p-value significance threshold equal to 0.05. Bars located above this line, therefore, indicate significant p-values (p-values<0.05). The p-value significance increases with bar height above threshold.

**Table 3.41** The p-values obtained for the analysis of interaction between mutation group and single SNPs in *CPT1B*.

SNP ID	LVM			mIVST			mLVWT			mPWT			CWT score			PC1		
	R403W vs A797T	R92W vs A797T	R92W vs R403W	R403W vs A797T	R92W vs A797T	R92W vs R403W	R403W vs A797T	R92W vs A797T	R92W vs R403W	R403W vs A797T	R92W vs A797T	R92W vs R403W	R403W vs A797T	R92W vs A797T	R92W vs R403W	R403W vs A797T	R92W vs A797T	R92W vs R403W
rs470117	0.670	0.720	0.903	0.099	0.119	0.730	0.248	0.434	0.644	0.534	0.769	0.440	0.544	0.603	0.860	0.572	0.691	0.821
rs1557502	0.951	0.920	0.982	0.736	0.627	0.449	0.733	0.172	0.421	0.652	0.660	0.413	0.428	0.598	0.223	0.272	0.787	0.186

**Abbreviations:** A-Alanine; CWT score-cumulative wall thickness score; LVM-left ventricular mass; mIVST-maximal interventricular septum thickness; mLVWT-maximal left ventricular wall thickness; mPWT-maximal posterior wall thickness; PC1-principal component score; R-Arginine; SNP-single nucleotide polymorphism; T-Threonine; vs-versus; W-Tryptophan

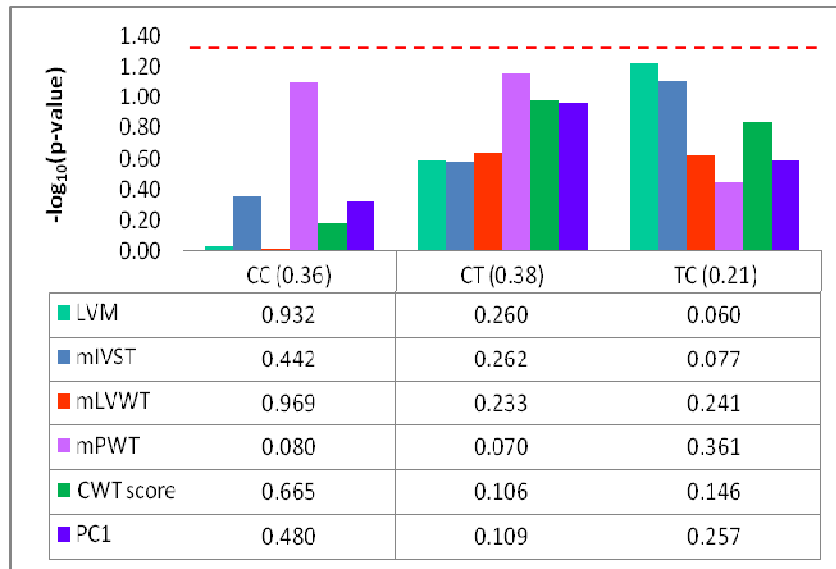


**Figure 3.24** The p-values for tests of association between *CPT1B* haplotypes and individual hypertrophy traits. The original p-values are given in the data table, whilst the graph represents the corresponding  $-\log_{10}$  transformed values. The red dashed horizontal line indicates the p-value significance threshold equal to 0.05. Bars located above this line, therefore, indicate significant p-values (p-values<0.05). The p-value significance increases with bar height above threshold. The observed haplotype frequencies are indicated in brackets.

**Table 3.42** The p-values obtained for the analysis of interaction between mutation group and *CPT1B* haplotypes. Significant results are indicated in bold red font.

Haplotype*		LVM			mIVST			mLVWT			mPWT			CWT score			PC1		
rs470117	rs1557502	R403W	R92W	R92W	R403W	R92W	R92W	R403W	R92W	R92W	R403W	R92W	R92W	R403W	R92W	R92W	R403W	R92W	R92W
		vs	vs	vs	vs	vs	vs	vs	vs	vs	vs	vs	vs	vs	vs	vs	vs	vs	vs
C	C	0.136	0.799	0.135	<b>0.021</b>	0.750	<b>0.024</b>	0.116	0.369	<b>0.039</b>	<b>0.028</b>	0.971	0.053	<b>0.034</b>	0.577	<b>0.025</b>	<b>0.016</b>	0.608	<b>0.014</b>
C	T	0.674	0.365	0.196	0.938	0.078	0.128	0.709	<b>0.034</b>	0.128	0.538	0.120	<b>0.040</b>	0.394	0.182	<b>0.039</b>	0.254	0.235	<b>0.025</b>
T	C	0.260	0.491	0.136	0.143	0.736	0.125	0.189	0.892	0.207	0.400	0.338	0.152	0.333	0.787	<b>0.289</b>	0.307	0.665	0.221

\*\* absence of p-values indicates unequal distribution of haplotypes in the three HCM mutation groups resulting in stratified groups of small size with insufficient statistical power for testing

**Abbreviations:** A-Adenine\*; A-Alanine; CWT score-cumulative wall thickness score; C-Cytosine\*; G-Guanine\*; LVM-left ventricular mass; mIVST-maximal interventricular septum thickness; mLVWT-maximal left ventricular wall thickness; mPWT-maximal posterior wall thickness; PC1-principal component score; R-Arginine; SNP-single nucleotide polymorphism; T-Threonine; T-Thymine\*; vs-versus; W-Tryptophan

### 3.4.5.12 PDK4

**Figure 3.25** graphically represents the p-values for the *association* between the *PDK4 SNPs* and *hypertrophy traits* with no evidence of statistically significant SNP effects. **Table 3.43** details the p-values for *pair-wise differences between mutation groups* in the association of *PDK4 SNPs* and *hypertrophy traits*. The effect of the T-allele of rs2073978 was higher on LVM (30.2 g;  $p = 0.034$ ), the CWT score (30.7 mm;  $p = 0.016$ ) and PC1 (1.92;  $p = 0.019$ ) in the R403W<sub>MYH7</sub> group relative to the A797T<sub>MYH7</sub> group. In addition, its effect was lower on LVM (38.4 g;  $p = 0.018$ ) in the R92W<sub>TNNT2</sub> group compared to the R403W<sub>MYH7</sub> group.

**Figure 3.26** graphically represents the p-values for the *association* between *PDK4 haplotypes* and *hypertrophy traits*. The effect of the CT haplotype, observed in 46% of the cohort, was an estimated 1.42 mm increase in mIVST ( $p = 0.037$ ). **Table 3.44** details the p-values for *pair-wise comparison between mutation groups* in the association between *PDK4 haplotypes* and *hypertrophy traits*. The CT haplotype also indicated significant differences in haplotype effect amongst the three mutation groups. Its effect was estimated to be lower on mIVST (3.2 mm;  $p = 0.028$ ), mLVWT (3.62 mm;  $p = 0.025$ ), the CWT score (31.9 mm;  $p = 0.008$ ) and PC1 (1.99;  $p = 0.011$ ) in the R403W<sub>MYH7</sub> group relative to the A797T<sub>MYH7</sub> group.



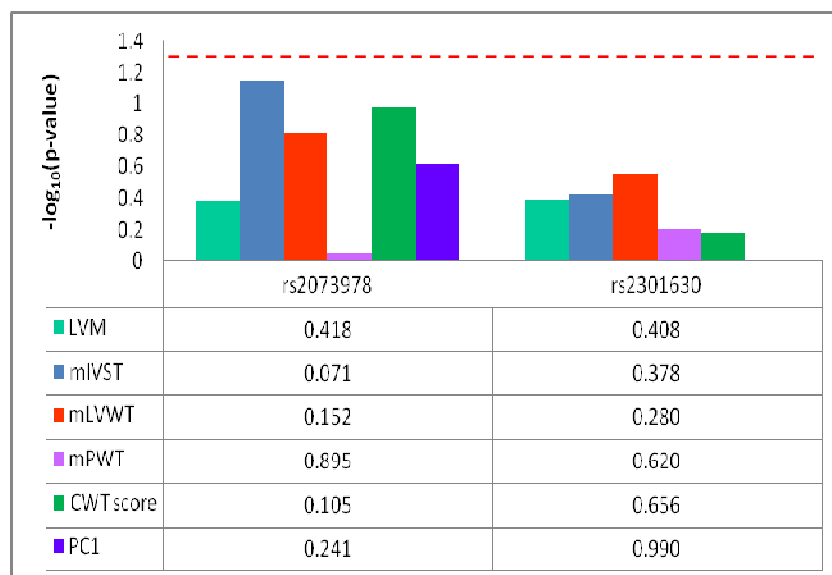


**Figure 3.25** The p-values for tests of association between single SNPs in *PDK4* and individual hypertrophy traits. The original p-values are given in the data table, whilst the graph represents the corresponding  $-\log_{10}$  transformed values. The red dashed horizontal line indicates the p-value significance threshold equal to 0.05. Bars located above this line, therefore, indicate significant p-values (p-values<0.05). The p-value significance increases with bar height above threshold.

**Table 3.43** The p-values obtained for the analysis of interaction between mutation group and single SNPs in *PDK4*. Significant results are indicated in bold red font.

SNP ID	LVM			mIVST			mLVWT			mPWT			CWT score			PC1		
	R403W vs A797T	R92W vs A797T	R92W vs R403W	R403W vs A797T	R92W vs A797T	R92W vs R403W	R403W vs A797T	R92W vs A797T	R92W vs R403W	R403W vs A797T	R92W vs A797T	R92W vs R403W	R403W vs A797T	R92W vs A797T	R92W vs R403W	R403W vs A797T	R92W vs A797T	R92W vs R403W
rs2073978	<b>0.034</b>	0.611	<b>0.018</b>	0.055	0.351	0.273	0.075	0.550	0.226	0.155	0.309	0.557	<b>0.016</b>	0.173	0.180	<b>0.019</b>	0.180	0.193
rs2301630	0.060	0.419	0.209	0.192	0.785	0.284	0.088	0.706	0.165	0.137	0.214	0.591	0.118	0.453	0.325	0.176	0.310	0.565

**Abbreviations:** A-Alanine; CWT score-cumulative wall thickness score; LVM-left ventricular mass; mIVST-maximal interventricular septum thickness; mLWT-maximal left ventricular wall thickness; mPWT-maximal posterior wall thickness; PC1-principal component score; R-Arginine; SNP-single nucleotide polymorphism; T-Threonine; vs-versus; W-Tryptophan

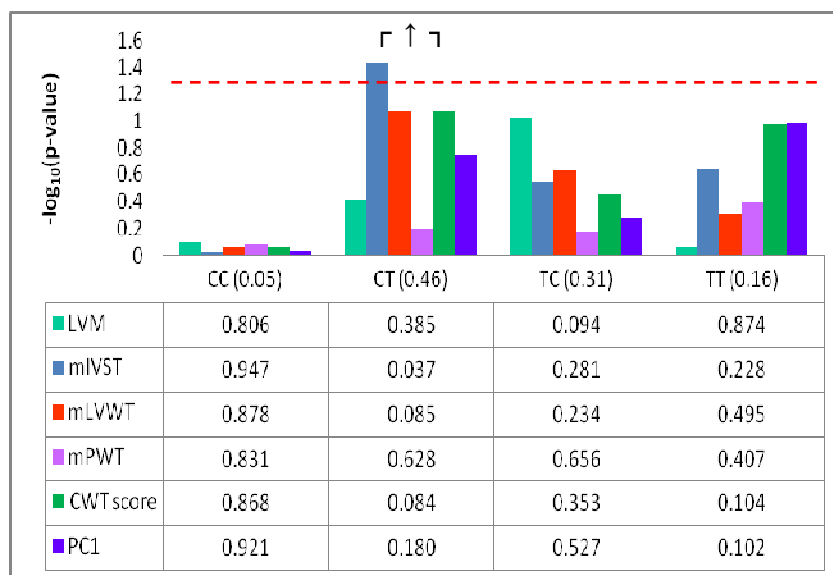


**Figure 3.26** The p-values for tests of association between *PDK4* haplotypes and individual hypertrophy traits. The original p-values are given in the data table, whilst the graph represents the corresponding  $-\log_{10}$  transformed values. The red dashed horizontal line indicates the p-value significance threshold equal to 0.05. Bars located above this line, therefore, indicate significant p-values (p-values<0.05). The p-value significance increases with bar height above threshold. The observed haplotype frequencies are indicated in brackets.

**Table 3.44** The p-values obtained for the analysis of interaction between mutation group and *PDK4* haplotypes. Significant results are indicated in bold red font.

Haplotype*		LVM			mIVST			mLVWT			mPWT			CWT score			PC1		
rs2073978	rs2301630	R403W	R92W	R92W	R403W	R92W	R92W	R403W	R92W	R92W	R403W	R92W	R92W	R403W	R92W	R92W	R403W	R92W	R92W
		vs A797T	vs A797T	vs R403W	vs A797T	vs A797T	vs R403W	vs A797T	vs A797T	vs R403W	vs A797T	vs A797T	vs R403W	vs A797T	vs A797T	vs R403W	vs A797T	vs A797T	vs R403W
C	C	0.426	0.261	0.995	0.629	0.351	0.283	0.426	0.810	0.373	0.095	0.530	0.263	0.374	0.851	0.335	0.282	0.954	0.326
C	T	0.091	0.760	0.165	<b>0.028</b>	0.240	0.247	<b>0.025</b>	0.366	0.155	0.105	0.108	0.827	<b>0.008</b>	0.064	0.250	<b>0.011</b>	0.068	0.286
T	C	0.171	0.901	0.219	0.446	0.661	0.658	0.238	0.904	0.293	0.645	0.605	0.919	0.252	0.640	0.422	0.394	0.556	0.660
T	T	0.787	0.595	0.459	0.269	0.601	0.541	0.479	0.810	0.633	0.704	0.667	0.453	0.165	0.431	0.491	0.138	0.630	0.289

**Abbreviations:** A-Alanine; **CWT score**-cumulative wall thickness score; C-Cytosine\*; G-Guanine\*; LVM-left ventricular mass; mIVST-maximal interventricular septum thickness; mLVWT-maximal left ventricular wall thickness; mPWT-maximal posterior wall thickness; PC1-principal component score; R-Arginine; SNP-single nucleotide polymorphism; T-Threonine; T-Thymine\*; vs-versus; W-Tryptophan

### 3.4.5.13 CKM

**Figure 3.27** graphically represents the p-values for the *association* between the *CKM SNPs* and *hypertrophy traits*. The effect of the T-allele of rs7260463 was an estimated 0.24 mm decrease in mPWT ( $p = 0.049$ ). **Table 3.45** details the p-values for *pair-wise differences between mutation groups* in the association of *CKM SNPs* and *hypertrophy traits*. The effect of the T-allele of rs344816 was lower on mLVWT in the R92W<sub>TNNT2</sub> group relative to both the A797T<sub>MYH7</sub> ( $p = 0.003$ , 4.21 mm) and R403W<sub>MYH7</sub> ( $p = 0.015$ , 3.42 mm) groups.

**Figure 3.28** graphically represents the p-values for the *association* between *CKM haplotypes* and *hypertrophy traits*. The effect of the CTAT haplotype, present in 4% of the cohort, was an estimated increase of 3.20 mm in mIVST ( $p = 0.018$ ), 2.72 mm in mLVWT ( $p = 0.046$ ) and 1.37 in PC1 ( $p = 0.047$ ). The TTGA haplotype, observed in 3% of the cohort, was significantly associated with a decrease of 27.4 g in LVM ( $p = 0.039$ ). The effect of the CTGT haplotype, identified in 10% of the cohort, was an estimated decrease of 17.6 g in LVM ( $p = 0.035$ ) and 7.9 mm in the CWT score ( $p = 0.039$ ). **Table 3.46** details the p-values for *pair-wise comparison between mutation groups* in the association of *CKM haplotypes* and *hypertrophy traits*. The TTGA and CTGT haplotypes also showed significant differences in haplotype effect amongst the founder mutation groups. The effect of the first was higher on LVM in the R403W<sub>MYH7</sub> group relative to both the A797T<sub>MYH7</sub> (96.4 g;  $p = 0.035$ ) and R92W<sub>TNNT2</sub> groups (120.3 g;  $p = 0.013$ ). In addition, its effect was higher on PC1 (3.97;  $p = 0.048$ ) in the R92W<sub>TNNT2</sub> group compared to the R403W<sub>MYH7</sub> group. The effect of the second was lower on mLVWT (5.1 mm;  $p = 0.002$ ) and the CWT score (32.1 mm;  $p = 0.018$ ) in the R92W<sub>TNNT2</sub> group relative to the A797T<sub>MYH7</sub> group. Also, the effect of the CTGA haplotype, identified in 9% of the cohort, was higher on mLVWT in the R92W<sub>TNNT2</sub> group relative to both the A797T<sub>MYH7</sub> ( $p = 0.048$ , 4.53 mm) and R403W<sub>MYH7</sub> ( $p = 0.042$ , 3.70 mm) groups.

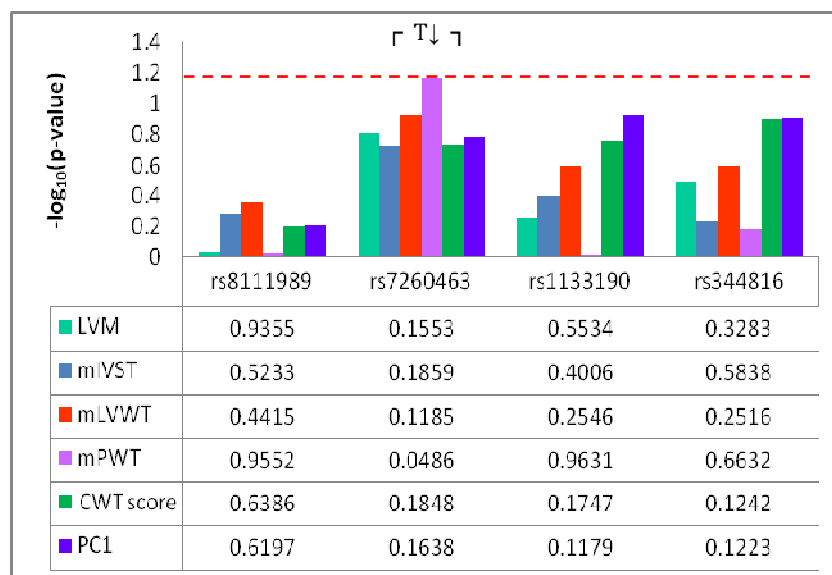


**Figure 3.27** The p-values for tests of association between single SNPs in *CKM* and individual hypertrophy traits. The original p-values are given in the data table, whilst the graph represents the corresponding  $-\log_{10}$  transformed values. The red dashed horizontal line indicates the p-value significance threshold equal to 0.05. Bars located above this line, therefore, indicate significant p-values (p-values<0.05). The p-value significance increases with bar height above threshold.

**Table 3.45** The p-values obtained for the analysis of interaction between mutation group and single SNPs in *CKM*. Significant results are indicated in bold red font.

SNP ID	LVM			mIVST			mLWWT			mPWT			CWT score			PC1		
	R403W vs A797T	R92W vs A797T	R92W vs R403W	R403W vs A797T	R92W vs A797T	R92W vs R403W	R403W vs A797T	R92W vs A797T	R92W vs R403W	R403W vs A797T	R92W vs A797T	R92W vs R403W	R403W vs A797T	R92W vs A797T	R92W vs R403W	R403W vs A797T	R92W vs A797T	R92W vs R403W
rs8111989	0.468	0.603	0.801	0.478	0.786	0.647	0.321	0.914	0.389	0.879	0.941	0.934	0.614	0.791	0.476	0.763	0.733	0.560
rs7260463	0.252	0.718	0.159	0.848	0.274	0.289	0.652	0.892	0.587	0.344	0.331	0.887	0.510	0.765	0.687	0.431	0.674	0.666
rs1133190	0.991	0.852	0.880	0.884	0.744	0.912	0.915	0.619	0.791	0.397	0.816	0.548	0.517	0.686	0.771	0.508	0.557	0.867
rs344816	0.924	0.254	0.328	0.602	0.293	0.199	0.959	<b>0.003</b>	<b>0.015</b>	0.611	0.967	0.628	0.564	0.118	0.082	0.428	0.301	0.133

**Abbreviations:** A-Alanine; **CWT score**-cumulative wall thickness score; **LVM**-left ventricular mass; **mIVST**-maximal interventricular septum thickness; **mLWWT**-maximal left ventricular wall thickness; **mPWT**-maximal posterior wall thickness; **PC1**-principal component score; **R**-Arginine; **SNP**-single nucleotide polymorphism; **T**-Threonine; **vs**-versus; **W**-Tryptophan

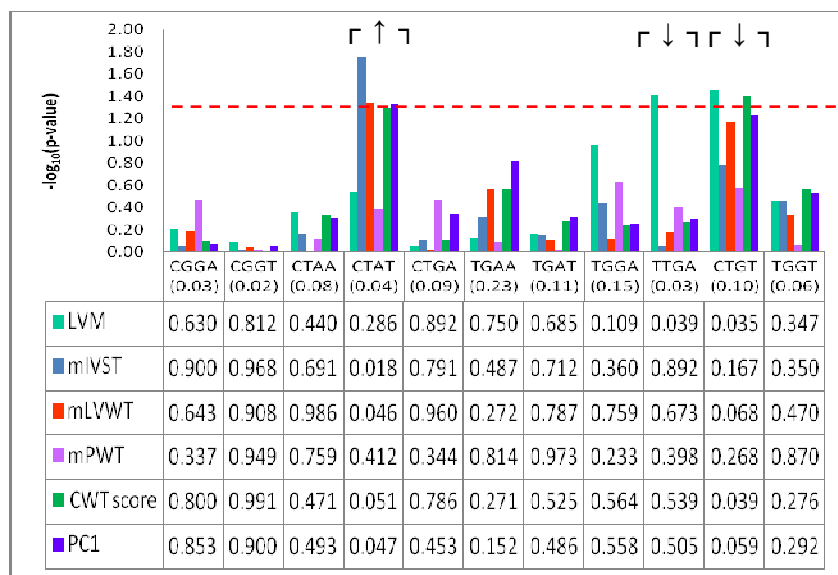


**Figure 3.28 The p-values for tests of association between *CKM* haplotypes and individual hypertrophy traits.** The original p-values are given in the data table, whilst the graph represents the corresponding  $-\log_{10}$  transformed values. The red dashed horizontal line indicates the p-value significance threshold equal to 0.05. Bars located above this line, therefore, indicate significant p-values ( $p\text{-values} < 0.05$ ). The p-value significance increases with bar height above threshold. The observed haplotype frequencies are indicated in brackets.

**Table 3.46 The p-values obtained for the analysis of interaction between mutation group and CKM haplotypes.** Significant results are indicated in bold red font.

Haplotype*				LVM			mIVST			mLVWT			mPWT			CWT score			PC1		
rs8111989	rs7260463	rs1133190	rs344816	R403W vs A797T	R92W vs A797T	R92W vs R403W	R403W vs A797T	R92W vs A797T	R92W vs R403W	R403W vs A797T	R92W vs A797T	R92W vs R403W	R403W vs A797T	R92W vs A797T	R92W vs R403W	R403W vs A797T	R92W vs A797T	R92W vs R403W	R403W vs A797T	R92W vs A797T	R92W vs R403W
C	G	G	A	0.098	0.741	0.096	0.572	0.863	0.387	0.131	0.233	0.649	0.270	0.466	0.618	0.602	0.753	0.766	0.657	0.830	0.757
C	G	G	T**	-	-	0.222	-	-	0.096	-	-	0.083	-	-	0.410	-	-	0.092	-	-	0.114
C	T	A	A	0.656	0.354	0.558	0.720	0.814	0.644	0.511	0.628	0.365	0.502	0.606	0.346	0.562	0.775	0.505	0.798	0.827	0.704
C	T	A	T	0.972	0.279	0.240	0.350	0.801	0.420	0.199	0.573	0.376	0.152	0.967	0.111	0.171	0.798	0.178	0.194	0.925	0.096
C	T	G	A	0.172	0.740	0.072	0.922	0.150	0.112	0.970	<b>0.048</b>	<b>0.042</b>	0.584	0.944	0.511	0.517	0.102	0.208	0.445	0.134	0.356
T	G	A	A	0.361	0.920	0.432	0.805	0.703	0.910	0.821	0.941	0.775	0.957	0.830	0.804	0.830	0.807	0.993	0.817	0.920	0.890
T	G	A	T	0.192	0.334	0.908	0.473	0.924	0.654	0.423	0.584	0.911	0.546	0.590	0.981	0.945	0.923	0.892	0.777	0.811	0.996
T	G	G	A	0.520	0.080	0.062	0.108	0.961	0.165	0.378	0.522	0.207	0.166	0.588	0.102	0.176	0.641	0.121	0.208	0.661	0.148
T	T	G	A	<b>0.035</b>	0.725	<b>0.013</b>	0.205	0.684	0.119	0.290	0.301	0.072	0.205	0.889	0.159	0.150	0.556	0.052	0.135	0.588	<b>0.048</b>
C	T	G	T**	-	0.143	-	-	0.080	-	-	<b>0.002</b>	-	-	0.303	-	-	<b>0.018</b>	-	-	0.053	-
T	G	G	T**	-	0.450	-	-	0.447	-	-	0.284	-	-	0.556	-	-	0.482	-	-	0.535	-

\*\* absence of p-values indicates unequal distribution of haplotypes in the three HCM mutation groups resulting in stratified groups of small size with insufficient statistical power for testing

**Abbreviations:** A-Adenine\*; A-Alanine; CWT score-cumulative wall thickness score; C-Cytosine\*; G-Guanine\*; LVM-left ventricular mass; mIVST-maximal interventricular septum thickness; mLVWT-maximal left ventricular wall thickness; mPWT-maximal posterior wall thickness; PC1-principal component score; R-Arginine; SNP-single nucleotide polymorphism; T-Threonine; T-Thymine\*; vs-versus; W-Tryptophan

### 3.4.5.14 CKB

**Figure 3.29** graphically represents the p-values for the *association* between the *CKB SNPs* and *hypertrophy traits* with no evidence of statistically significant SNP effects. **Table 3.47** details the p-values for *pair-wise differences between mutation groups* in the association between *CKB SNPs* and *hypertrophy traits*. No significant difference in SNP effect was observed amongst the three HCM founder mutation groups.

**Figure 3.30** graphically represents the p-values for the *association* between *CKB haplotypes* and *hypertrophy traits* with no evidence of statistically significant haplotype effects. **Table 3.48** details the p-values for *pair-wise comparison between mutation groups* in the association between *CKB haplotypes* and *hypertrophy traits*. The effect of the CCT haplotype, present in 3% of the cohort, was higher on LVM (86.5 g;  $p = 0.032$ ) in the R92W<sub>TNNT2</sub> group relative to the R403W<sub>MYH7</sub> group. The effect of the CTT haplotype, observed in 17% of the cohort, was lower on LVM (65.1 g;  $p = 0.032$ ) in the R92W<sub>TNNT2</sub> group relative to the R403W<sub>MYH7</sub> group. Also, its effect was higher on LVM (62.9 g;  $p = 0.032$ ) in the R403W<sub>MYH7</sub> group compared to the A797T<sub>MYH7</sub> group. The effect of the TCG haplotype, present in 6% of the cohort, was lower on the CWT score (59.4 mm;  $p = 0.032$ ) in the R403W<sub>MYH7</sub> group than the A797T<sub>MYH7</sub> group.

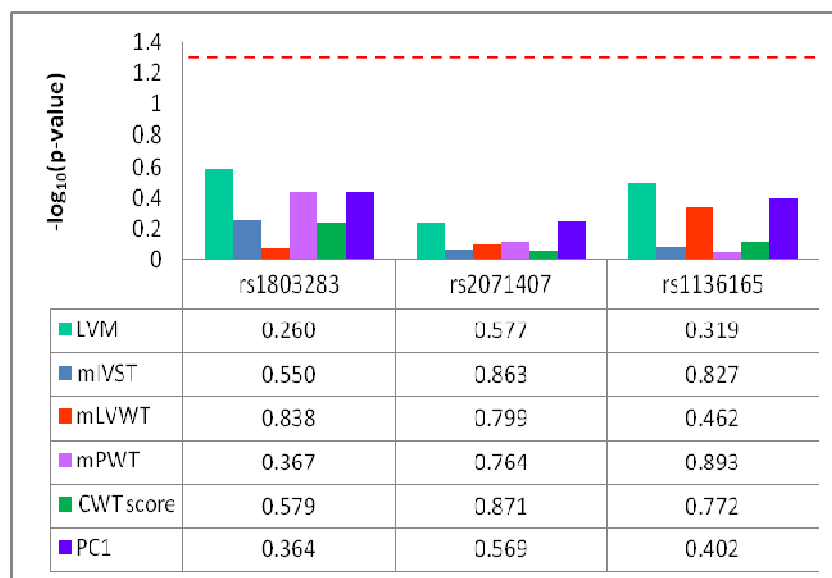


**Figure 3.29** The p-values for tests of association between single SNPs in *CKB* and individual hypertrophy traits. The original p-values are given in the data table, whilst the graph represents the corresponding  $-\log_{10}$  transformed values. The red dashed horizontal line indicates the p-value significance threshold equal to 0.05. Bars located above this line, therefore, indicate significant p-values (p-values<0.05). The p-value significance increases with bar height above threshold.

**Table 3.47** The p-values obtained for the analysis of interaction between mutation group and single SNPs in *CKB*.

SNP ID	LVM			mIVST			mLVWT			mPWT			CWT score			PC1		
	R403W vs A797T	R92W vs A797T	R92W vs R403W	R403W vs A797T	R92W vs A797T	R92W vs R403W	R403W vs A797T	R92W vs A797T	R92W vs R403W	R403W vs A797T	R92W vs A797T	R92W vs R403W	R403W vs A797T	R92W vs A797T	R92W vs R403W	R403W vs A797T	R92W vs A797T	R92W vs R403W
rs1803283	0.623	0.729	0.878	0.544	0.217	0.635	0.479	0.243	0.747	0.129	0.656	0.312	0.106	0.174	0.687	0.161	0.231	0.742
rs2071407	0.725	0.380	0.287	0.712	0.873	0.841	0.967	0.793	0.852	0.701	0.675	0.999	0.659	0.531	0.907	0.761	0.431	0.699
rs1136165	0.949	0.477	0.520	0.513	0.736	0.744	0.616	0.884	0.560	0.746	0.819	0.911	0.891	0.830	0.961	0.984	0.735	0.762

**Abbreviations:** A-Alanine; CWT score-cumulative wall thickness score; LVM-left ventricular mass; mIVST-maximal interventricular septum thickness; mLVWT-maximal left ventricular wall thickness; mPWT-maximal posterior wall thickness; PC1-principal component score; R-Arginine; SNP-single nucleotide polymorphism; T-Threonine; vs-versus; W-Tryptophan



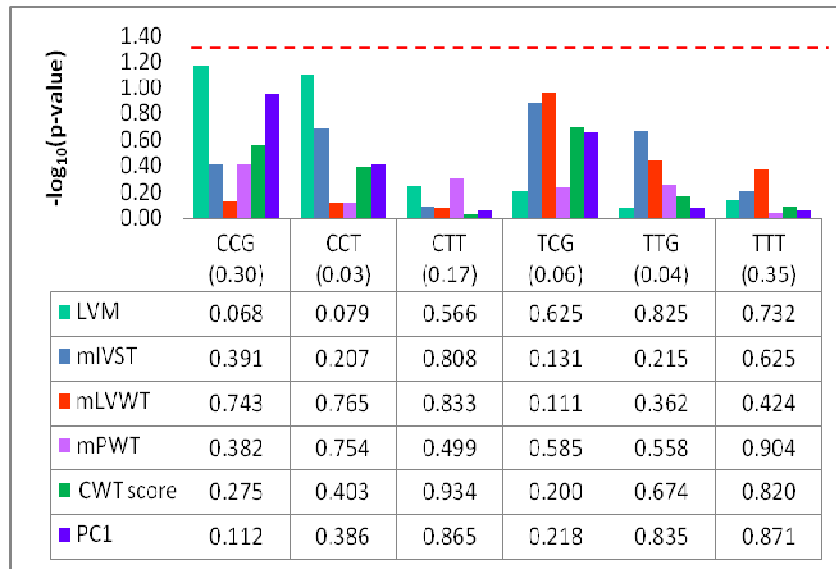


**Figure 3.30** The p-values for tests of association between *CKB* haplotypes and individual hypertrophy traits. The original p-values are given in the data table, whilst the graph represents the corresponding  $-\log_{10}$  transformed values. The red dashed horizontal line indicates the p-value significance threshold equal to 0.05. Bars located above this line, therefore, indicate significant p-values (p-values<0.05). The p-value significance increases with bar height above threshold. The observed haplotype frequencies are indicated in brackets.

**Table 3.48** The p-values obtained for the analysis of interaction between mutation group and *CKB* haplotypes. Significant results are indicated in bold red font.

Haplotype*			LVM			mIVST			mLVWT			mPWT			CWT score			PC1		
rs1803283	rs2071407	rs1136165	R403W	R92W	R92W	R403W	R92W	R92W	R403W	R92W	R92W	R403W	R92W	R92W	R403W	R92W	R92W	R403W	R92W	R92W
			vs	vs	vs	vs	vs	vs	vs	vs	vs	vs	vs	vs	vs	vs	vs	vs	vs	vs
C	C	G	0.702	0.980	0.717	0.899	0.612	0.579	0.641	0.837	0.814	0.422	0.990	0.470	0.171	0.580	0.428	0.263	0.678	0.498
C	C	T	0.119	0.495	<b>0.032</b>	0.180	0.868	0.130	0.339	0.826	0.421	0.673	0.888	0.742	0.232	0.858	0.181	0.466	0.621	0.294
C	T	T	<b>0.032</b>	0.900	<b>0.032</b>	0.220	0.231	0.575	0.415	0.504	0.663	0.342	0.775	0.285	0.183	0.529	0.319	0.145	0.661	0.224
T	C	G	0.905	0.326	0.312	0.088	0.562	0.347	0.070	0.689	0.226	0.344	0.544	0.794	<b>0.038</b>	0.811	0.099	0.055	0.983	0.081
T	T	G**	-	0.411	-	-	0.991	-	-	0.705	-	-	0.894	-	-	0.639	-	-	0.904	-
T	T	T	0.606	0.344	0.747	0.932	0.295	0.429	0.781	0.263	0.490	0.321	0.529	0.665	0.431	0.269	0.902	0.470	0.212	0.754

\*\* absence of p-values indicates unequal distribution of haplotypes in the three HCM mutation groups resulting in stratified groups of small size with insufficient statistical power for testing

**Abbreviations:** A-Alanine; CWT score-cumulative wall thickness score; C-Cytosine\*; G-Guanine\*; LVM-left ventricular mass; mIVST-maximal interventricular septum thickness; mLVWT-maximal left ventricular wall thickness; mPWT-maximal posterior wall thickness; PC1-principal component score; R-Arginine; SNP-single nucleotide polymorphism; T-Threonine; T-Thymine\*; vs-versus; W-Tryptophan

### 3.4.5.15 ALDOA

**Figure 3.31** graphically represents the p-values for the *association* between the *ALDOA SNPs* and *hypertrophy traits*. The effect of the T-allele of rs11860935 was an estimated decrease of 1.88 mm in mIVST ( $p = 0.043$ ). **Table 3.49** details the p-values for *pair-wise differences between mutation groups* in the association of *ALDOA SNPs* and *hypertrophy traits*. The effect of the C-allele of rs9928448 was lower on mIVST (2.29 mm;  $p = 0.026$ ), the CWT score (23.2 mm;  $p = 0.036$ ) and PC1 (1.45;  $p = 0.029$ ) in the R92W<sub>TNNT2</sub> group compared to the A797T<sub>MYH7</sub> group.

**Figure 3.32** graphically represents the p-values for the *association* between *ALDOA haplotypes* and *hypertrophy traits* with no evidence of statistically significant haplotype effects. **Table 3.50** details the p-values for *pair-wise differences between mutation groups* in the association of *ALDOA haplotypes* and hypertrophy traits. The effect of the CC haplotype, present in 37% of the cohort, was lower on mIVST (2.7 mm;  $p = 0.015$ ) and mLVWT (2.65 mm;  $p = 0.026$ ) in the R92W<sub>TNNT2</sub> group compared to the R403W<sub>MYH7</sub> group.

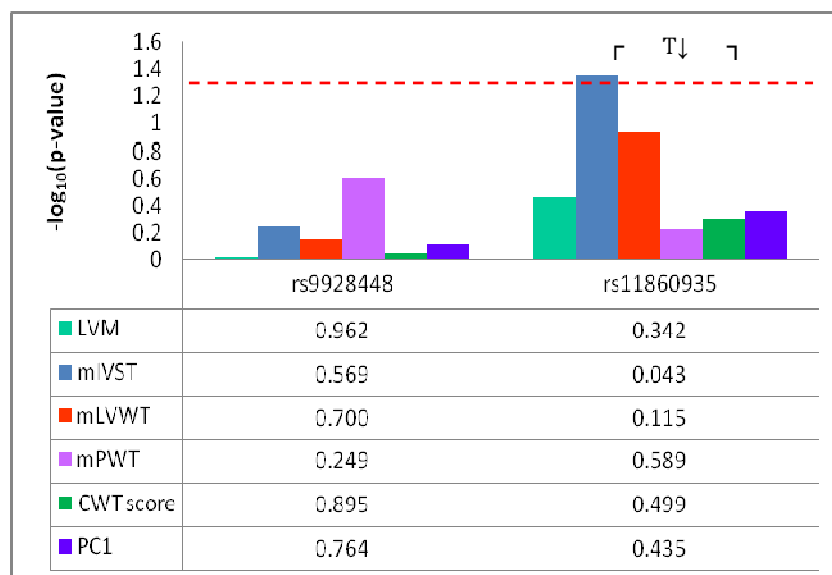


**Figure 3.31** The p-values for tests of association between single SNPs in *ALDOA* and individual hypertrophy traits. The original p-values are given in the data table, whilst the graph represents the corresponding  $-\log_{10}$  transformed values. The red dashed horizontal line indicates the p-value significance threshold equal to 0.05. Bars located above this line, therefore, indicate significant p-values (p-values<0.05). The p-value significance increases with bar height above threshold.

**Table 3.49** The p-values obtained for the analysis of interaction between mutation group and single SNPs in *ALDOA*. Significant results are indicated in bold red font.

SNP ID	LVM			mIVST			mLVWT			mPWT			CWT score			PC1		
	R403W vs A797T	R92W vs A797T	R92W vs R403W	R403W vs A797T	R92W vs A797T	R92W vs R403W	R403W vs A797T	R92W vs A797T	R92W vs R403W	R403W vs A797T	R92W vs A797T	R92W vs R403W	R403W vs A797T	R92W vs A797T	R92W vs R403W	R403W vs A797T	R92W vs A797T	R92W vs R403W
rs9928448	0.637	0.129	0.429	0.381	<b>0.026</b>	0.324	0.550	0.134	0.501	0.163	0.181	0.831	0.510	<b>0.036</b>	0.279	0.466	<b>0.029</b>	0.273
rs11860935	0.702	0.481	0.792	0.587	0.613	0.958	0.711	0.414	0.707	0.232	0.422	0.702	0.763	0.739	0.998	0.555	0.574	0.942

**Abbreviations:** A-Alanine; **CWT score**-cumulative wall thickness score; **LVM**-left ventricular mass; **mIVST**-maximal interventricular septum thickness; **mLVWT**-maximal left ventricular wall thickness; **mPWT**-maximal posterior wall thickness; **PC1**-principal component score; **R**-Arginine; **SNP**-single nucleotide polymorphism; **T**-Threonine; **vs**-versus; **W**-Tryptophan

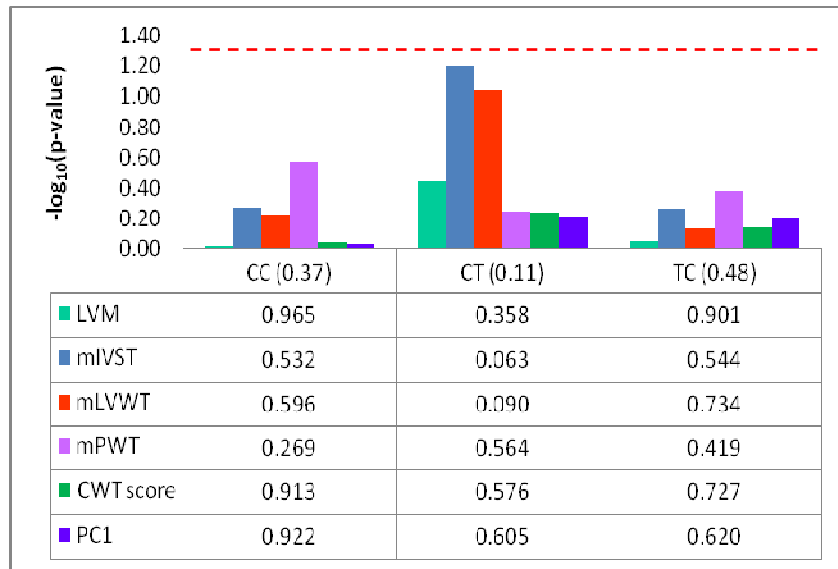


**Figure 3.32** The p-values for tests of association between *ALDOA* haplotypes and individual hypertrophy traits. The original p-values are given in the data table, whilst the graph represents the corresponding  $-\log_{10}$  transformed values. The red dashed horizontal line indicates the p-value significance threshold equal to 0.05. Bars located above this line, therefore, indicate significant p-values (p-values<0.05). The p-value significance increases with bar height above threshold. The observed haplotype frequencies are indicated in brackets.

**Table 3.50** The p-values obtained for the analysis of interaction between mutation group and *ALDOA* haplotypes. Significant results are indicated in bold red font.

Haplotype*		LVM			mIVST			mLVWT			mPWT			CWT score			PC1		
rs9928448	rs11860935	R403W	R92W	R92W	R403W	R92W	R92W	R403W	R92W	R92W	R403W	R92W	R92W	R403W	R92W	R92W	R403W	R92W	R92W
		vs	vs	vs	vs	vs	vs	vs	vs	vs	vs	vs	vs	vs	vs	vs	vs	vs	vs
		A797T	A797T	R403W	A797T	A797T	R403W	A797T	A797T	R403W	A797T	A797T	R403W	A797T	A797T	R403W	A797T	A797T	R403W
		C	C	0.985	0.486	0.531	0.326	<b>0.015</b>	0.244	0.365	<b>0.026</b>	0.269	0.649	0.253	0.580	0.451	0.086	0.429	0.567
C	T	0.541	0.490	0.919	0.789	0.864	0.944	0.995	0.730	0.754	0.284	0.228	0.862	0.668	0.480	0.801	0.455	0.286	0.768
T	C	0.496	0.406	0.969	0.288	0.182	0.939	0.341	0.316	0.940	0.330	0.889	0.420	0.303	0.199	0.949	0.298	0.183	0.925

**Abbreviations:** A-Alanine; CWT score-cumulative wall thickness score; C-Cytosine\*; G-Guanine\*; LVM-left ventricular mass; mIVST-maximal interventricular septum thickness; mLVWT-maximal left ventricular wall thickness; mPWT-maximal posterior wall thickness; PC1-principal component score; R-Arginine; SNP-single nucleotide polymorphism; T-Threonine; T-Thymine\*; vs-versus; W-Tryptophan

### 3.4.5.16 PFKM

**Figure 3.33** graphically represents the p-values for the *association* between the *PFKM SNPs* and *hypertrophy traits* with no evidence of statistically significant SNP effects. **Table 3.51** details the p-values for *pair-wise comparison between the mutation groups* in the association between *PFKM SNPs* and *hypertrophy traits*. The effect of the T-allele of rs10875749 was higher on mIVST (2.56 mm;  $p = 0.033$ ) in the R92W<sub>TNNT2</sub> group relative to A797T<sub>MYH7</sub> group. Also, its effect was higher in the R92W<sub>TNNT2</sub> group compared to the R403W<sub>MYH7</sub> group on mIVST (2.87 mm;  $p = 0.005$ ), mLVWT (2.08 mm;  $p = 0.013$ ), the CWT score (22.9 mm;  $p = 0.010$ ) and PC1 (1.43;  $p = 0.006$ ). Finally, its effect was lower on PC1 (0.92;  $p = 0.030$ ) in the R403W<sub>MYH7</sub> group compared to the A797T<sub>MYH7</sub> group.

**Figure 3.34** graphically represents the p-values for the *association* between *PFKM haplotypes* and *hypertrophy traits*. The effect of the AT haplotype, identified in 12% of the cohort, was an estimated increase of 1.03 mm in mIVST ( $p = 0.042$ ). **Table 3.52** details the p-values for *pair-wise comparison between mutation groups* in the association between *PFKM haplotypes* and *hypertrophy traits*. The effect of the AA haplotype, observed in 35% of the cohort, was higher on mPWT in the R403W<sub>MYH7</sub> group relative to the A797T<sub>MYH7</sub> group (0.88 mm;  $p = 0.048$ ). The effect of the AT haplotype, identified in 12% of the cohort, was lower in the R403W<sub>MYH7</sub> group relative to the A797T<sub>MYH7</sub> group: 3.1 mm on mIVST ( $p = 0.043$ ), 31.6 mm on the CWT score ( $p = 0.022$ ) and 1.98 on PC1 ( $p = 0.012$ ). The effect of the CA haplotype, present in 38% of the cohort, was lower in the R92W<sub>TNNT2</sub> group compared to the A797T<sub>MYH7</sub> group on mPWT (1.54 mm;  $p = 0.002$ ), the CWT score (22.1 mm;  $p = 0.030$ ) and PC1 (1.38;  $p = 0.014$ ). Also, its effect was lower in the R92W<sub>TNNT2</sub> group relative to the R403W<sub>MYH7</sub> group on PC1 (1.05;  $p = 0.046$ ). The effect of the CT haplotype, observed in 10% of the cohort, was higher in the R92W<sub>TNNT2</sub> group compared to the A797T<sub>MYH7</sub> group: 3.7 mm on mIVST ( $p = 0.004$ ), 3.03 mm on mLVWT ( $p = 0.036$ ) and 1.32 mm on mPWT ( $p = 0.045$ ).

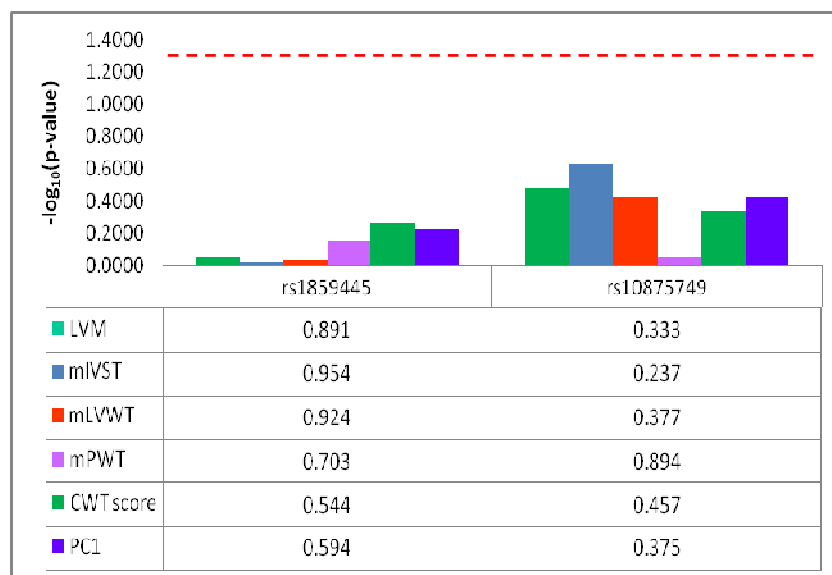


**Figure 3.33** The p-values for tests of association between single SNPs in *PFKM* and individual hypertrophy traits. The original p-values are given in the data table, whilst the graph represents the corresponding  $-\log_{10}$  transformed values. The red dashed horizontal line indicates the p-value significance threshold equal to 0.05. Bars located above this line, therefore, indicate significant p-values (p-values<0.05). The p-value significance increases with bar height above threshold.

**Table 3.51** The p-values obtained for the analysis of interaction between mutation group and single SNPs in *PFKM*. Significant results are indicated in bold red font.

SNP ID	LVM			mIVST			mLVWT			mPWT			CWT score			PC1		
	R403W vs A797T	R92W vs A797T	R92W vs R403W	R403W vs A797T	R92W vs A797T	R92W vs R403W	R403W vs A797T	R92W vs A797T	R92W vs R403W	R403W vs A797T	R92W vs A797T	R92W vs R403W	R403W vs A797T	R92W vs A797T	R92W vs R403W	R403W vs A797T	R92W vs A797T	R92W vs R403W
rs1859445	0.595	0.570	0.329	0.738	0.582	0.900	0.903	0.724	0.866	0.163	0.280	0.625	0.949	0.567	0.599	0.820	0.409	0.656
rs10875749	0.352	0.300	0.066	0.362	<b>0.033</b>	<b>0.005</b>	0.394	0.070	<b>0.013</b>	0.328	0.374	0.084	0.058	0.407	<b>0.010</b>	<b>0.030</b>	0.481	<b>0.006</b>

**Abbreviations:** A-Alanine; CWT score-cumulative wall thickness score; LVM-left ventricular mass; mIVST-maximal interventricular septum thickness; mLVWT-maximal left ventricular wall thickness; mPWT-maximal posterior wall thickness; PC1-principal component score; R-Arginine; SNP-single nucleotide polymorphism; T-Threonine; vs-versus; W-Tryptophan

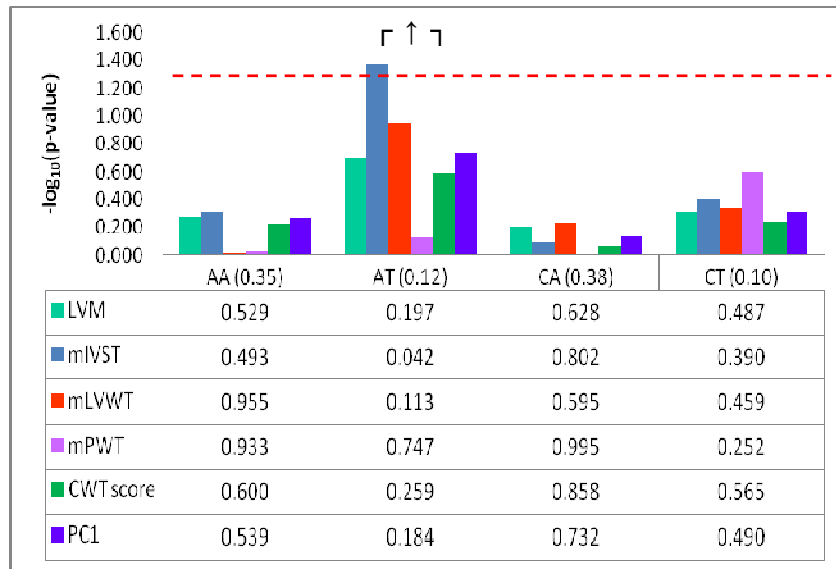


**Figure 3.34** The p-values for tests of association between *PFKM* haplotypes and individual hypertrophy traits. The original p-values are given in the data table, whilst the graph represents the corresponding  $-\log_{10}$  transformed values. The red dashed horizontal line indicates the p-value significance threshold equal to 0.05. Bars located above this line, therefore, indicate significant p-values (p-values<0.05). The p-value significance increases with bar height above threshold. The observed haplotype frequencies are indicated in brackets.

**Table 3.52** The p-values obtained for the analysis of interaction between mutation group and *PFKM* haplotypes. Significant results are indicated in bold red font.

Haplotype*		LVM			mIVST			mLVWT			mPWT			CWT score			PC1		
rs1859445	rs10875749	R403W vs A797T	R92W vs A797T	R92W vs R403W	R403W vs A797T	R92W vs A797T	R92W vs R403W	R403W vs A797T	R92W vs A797T	R92W vs R403W	R403W vs A797T	R92W vs A797T	R92W vs R403W	R403W vs A797T	R92W vs A797T	R92W vs R403W	R403W vs A797T	R92W vs A797T	R92W vs R403W
		A	A	0.736	0.325	0.586	0.576	0.759	0.439	0.530	0.931	0.518	<b>0.048</b>	0.097	0.675	0.169	0.283	0.721	0.087
A	T	0.218	0.656	0.125	<b>0.043</b>	0.829	0.106	0.095	0.898	0.167	0.088	0.097	0.991	<b>0.022</b>	0.600	0.096	<b>0.012</b>	0.414	0.106
C	A	0.705	0.061	0.056	1.000	0.062	0.123	0.838	0.068	0.187	0.215	<b>0.002</b>	0.165	0.936	<b>0.030</b>	0.065	0.998	<b>0.014</b>	<b>0.046</b>
C	T	0.484	0.241	0.866	0.500	<b>0.004</b>	0.129	0.732	<b>0.036</b>	0.219	0.771	<b>0.045</b>	0.226	0.827	0.128	0.318	0.963	0.120	0.232

**Abbreviations:** A-Adenine\*; A-Alanine; CWT score-cumulative wall thickness score; C-Cytosine\*; LVM-left ventricular mass; mIVST-maximal interventricular septum thickness; mLVWT-maximal left ventricular wall thickness; mPWT-maximal posterior wall thickness; PC1-principal component score; R-Arginine; SNP-single nucleotide polymorphism; T-Threonine; T-Thymine\*; vs-versus; W-Tryptophan

### 3.4.5.17 PPARA

**Figure 3.35** graphically represents the p-values for the *association* between the *PPARA SNPs* and *hypertrophy traits* with no evidence of statistically significant SNP effects. **Table 3.53** details the p-values for *pair-wise differences between mutation groups* in the association between the *PPARA SNPs* and *hypertrophy traits*. No significant difference in SNP effect was observed amongst the three HCM founder mutation groups.

**Figure 3.36** graphically represents the p-values for the association between *PPARA haplotypes* and *hypertrophy traits*. The effect of the GAA haplotype, present in 10% of the cohort, was an estimated increase of 30.1 g in LVM ( $p = 0.043$ ), 3.01 mm in mIVST ( $p = 0.006$ ), 3.40 mm in mLVWT ( $p = 0.001$ ), 21.0 mm in CWT score ( $p = 0.012$ ) and 1.31 in PC1 ( $p = 0.019$ ). The GGG haplotype, identified in 2% of the cohort, was associated with decreases of 49.1 g in LVM ( $p = 0.015$ ), 3.09 mm in mIVST ( $p = 0.045$ ) and 1.14 mm in mPWT ( $p = 0.046$ ). **Table 3.54** details the p-values for *pair-wise comparison between mutation groups* in the association of *PPARA haplotypes* and *hypertrophy traits*. The GGG haplotype also showed a significant difference in haplotype effect amongst the founder mutation groups. Its effect was estimated to be lower on mPWT (2.13 mm;  $p = 0.047$ ) in the R403W<sub>MYH7</sub> group relative to the A797T<sub>MYH7</sub> group. The effect of the AAA haplotype, identified in 48% of the cohort, was lower on LVM (21.9 g;  $p = 0.043$ ) in the R92W<sub>TNNT2</sub> group compared to the R403W<sub>MYH7</sub> group.



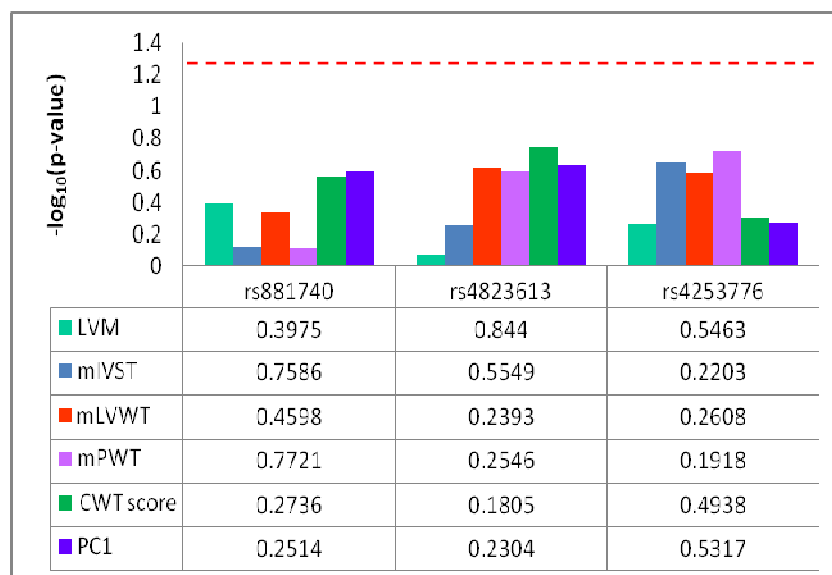


**Figure 3.35** The p-values for tests of association between single SNPs in *PPARA* and individual hypertrophy traits. The original p-values are given in the data table, whilst the graph represents the corresponding  $-\log_{10}$  transformed values. The red dashed horizontal line indicates the p-value significance threshold equal to 0.05. Bars located above this line, therefore, indicate significant p-values (p-values < 0.05). The p-value significance increases with bar height above threshold.

**Table 3.53** The p-values obtained for the analysis of interaction between mutation group and single SNPs in *PPARA*.

SNP ID	LVM			mIVST			mLVWT			mPWT			CWT score			PC1		
	R403W vs A797T	R92W vs A797T	R92W vs R403W	R403W vs A797T	R92W vs A797T	R92W vs R403W	R403W vs A797T	R92W vs A797T	R92W vs R403W	R403W vs A797T	R92W vs A797T	R92W vs R403W	R403W vs A797T	R92W vs A797T	R92W vs R403W	R403W vs A797T	R92W vs A797T	R92W vs R403W
rs881740	0.234	0.967	0.240	0.518	0.898	0.474	0.319	0.753	0.456	0.181	0.794	0.268	0.581	0.868	0.678	0.281	0.784	0.399
rs4823613	0.789	0.098	0.084	0.425	0.430	0.173	0.499	0.274	0.123	0.239	0.781	0.227	0.704	0.308	0.208	0.740	0.270	0.195
rs4253776	0.331	0.169	0.760	0.551	0.332	0.764	0.590	0.310	0.692	0.908	0.452	0.425	0.485	0.236	0.701	0.536	0.214	0.605

**Abbreviations:** A-Alanine; CWT score-cumulative wall thickness score; LVM-left ventricular mass; mIVST-maximal interventricular septum thickness; mLVWT-maximal left ventricular wall thickness; mPWT-maximal posterior wall thickness; PC1-principal component score; R-Arginine; SNP-single nucleotide polymorphism; T-Threonine; vs-versus; W-Tryptophan

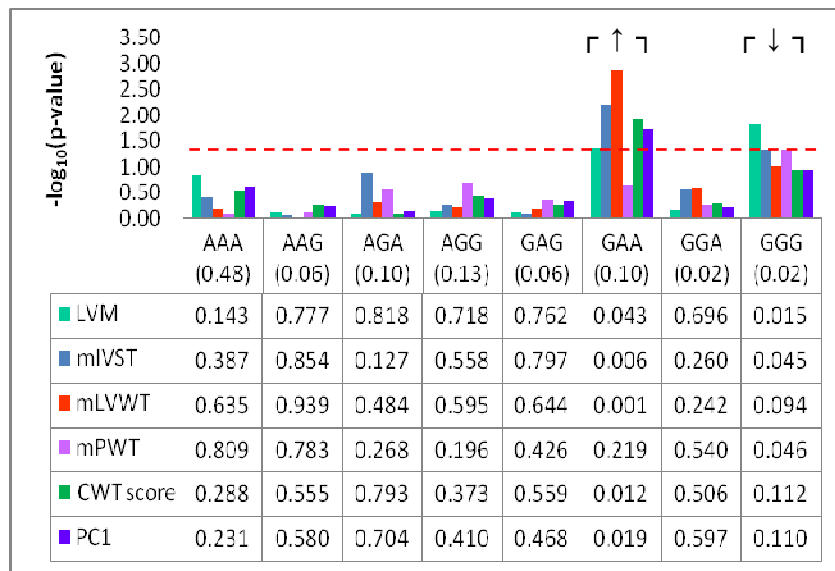


**Figure 3.36** The p-values for tests of association between *PPARA* haplotypes and individual hypertrophy traits. The original p-values are given in the data table, whilst the graph represents the corresponding  $-\log_{10}$  transformed values. The red dashed horizontal line indicates the p-value significance threshold equal to 0.05. Bars located above this line, therefore, indicate significant p-values (p-values<0.05). The p-value significance increases with bar height above threshold. The observed haplotype frequencies are indicated in brackets.

**Table 3.54** The p-values obtained for the analysis of interaction between mutation group and *PPARA* haplotypes. Significant results are indicated in bold red font.

Haplotype*			LVM			mIVST			mLVWT			mPWT			CWT score			PC1		
rs881740	rs4823613	rs4263776	R403W	R92W	R92W	R403W	R92W	R92W	R403W	R92W	R92W	R403W	R92W	R92W	R403W	R92W	R92W	R403W	R92W	R92W
			vs	vs	vs	vs	vs	vs	vs	vs	vs	vs	vs	vs	vs	vs	vs	vs	vs	vs
A	A	A	0.331	0.249	<b>0.043</b>	0.487	0.732	0.317	0.608	0.606	0.323	0.834	0.207	0.181	0.922	0.342	0.337	0.745	0.312	0.211
A	A	G	0.755	0.615	0.463	0.792	0.909	0.730	0.780	0.839	0.660	0.480	0.469	0.977	0.248	0.451	0.648	0.258	0.378	0.746
A	G	A	0.258	0.997	0.376	0.345	0.749	0.306	0.531	0.911	0.561	0.910	0.730	0.694	0.630	0.736	0.508	0.596	0.494	0.316
A	G	G	0.245	0.137	0.777	0.910	0.589	0.718	0.875	0.378	0.540	0.844	0.865	0.984	0.920	0.570	0.700	0.766	0.630	0.890
G	A	G	0.402	0.444	0.648	0.287	0.114	0.845	0.313	0.337	0.600	0.373	0.691	0.453	0.493	0.862	0.351	0.387	1.000	0.310
G	A	A	0.277	0.818	0.267	0.777	0.959	0.777	0.254	0.902	0.336	0.545	0.461	0.328	0.339	0.855	0.445	0.907	0.945	0.884
G	G	A	0.717	0.150	0.255	0.640	0.737	0.974	0.926	0.902	0.862	0.746	0.518	0.414	0.706	0.891	0.909	0.637	0.797	0.948
G	G	G	0.280	0.123	0.473	0.305	0.822	0.615	0.197	-	-	<b>0.047</b>	-	-	0.247	-	-	0.148	-	-

\*\* absence of p-values indicates unequal distribution of haplotypes in the three HCM mutation groups resulting in stratified groups of small size with insufficient statistical power for testing

**Abbreviations:** A-Adenine\*; A-Alanine; CWT score-cumulative wall thickness score; C-Cytosine\*; G-Guanine\*; LVM-left ventricular mass; mIVST-maximal interventricular septum thickness; mLVWT-maximal left ventricular wall thickness; mPWT-maximal posterior wall thickness; PC1-principal component score; R-Arginine; SNP-single nucleotide polymorphism; T-Threonine; T-Thymine\*; vs-versus; W-Tryptophan

### 3.4.5.18 PPARG

**Figure 3.37** graphically represents the p-values for the *association* between the four *PPARG SNPs* and *hypertrophy traits*. No statistically significant SNP effects were observed. **Table 3.55** details the p-values for *pair-wise comparison between mutation groups* in the association between *PPARG SNPs* and *hypertrophy traits*. The effect of the T-allele of rs12631028 was higher on mLVWT (1.71 mm;  $p = 0.040$ ) in the R92W<sub>TNNT2</sub> group compared to the A797T<sub>MYH7</sub> group.

**Figure 3.38** graphically represents the p-values for the *association* between *PPARG haplotypes* and *hypertrophy traits* with evidence of statistically significant haplotype effects for haplotypes CAGA, CGGC and CAGC. The effect of the first, present in 15% of the cohort, was an estimated decrease of 22.8 g in LVM ( $p = 0.004$ ). The second, observed in 4% of the cohort, was associated with an estimated increase of 27.1 g in LVM ( $p = 0.026$ ), 2.55 mm in mIVST ( $p = 0.034$ ), 2.73 mm in mLVWT ( $p = 0.042$ ), 23.7 mm in the CWT score ( $p = 0.022$ ) and 1.48 in PC1 ( $p = 0.042$ ). The final haplotype, present in 4% of the cohort, was associated with an estimated decrease of 0.97 mm in mPWT ( $p = 0.030$ ).

**Table 3.56** details the p-values for *pair-wise comparison between mutation groups* in the association of *PPARG haplotypes* and *hypertrophy traits*. Haplotypes CAGA and CAGC that showed significant haplotype effects as well as haplotypes TGAC and TGGA indicated significant differences in haplotype effect amongst the HCM founder mutation groups. The effect of the CAGA haplotype was lower on mIVST (4.98 mm,  $p = 0.002$ ) and mLVWT (4.83,  $p < 0.001$ ) in the R92W<sub>TNNT2</sub> group compared to the A797T<sub>MYH7</sub> group. Also, its effect was lower on mLVWT (2.85 mm,  $p = 0.026$ ) in the R403W<sub>MYH7</sub> group relative to the A797T<sub>MYH7</sub> group. The effect of the TGAC haplotype was higher on mPWT (2.52 mm,  $p = 0.012$ ) and PC1 (0.53,  $p = 0.004$ ) in the R92W<sub>TNNT2</sub> group compared to the A797T<sub>MYH7</sub> group. The effects of both the TGGA and CAGC haplotypes were lower on PC1 (0.12,  $p = 0.004$ ; 0.94,  $p = 0.044$ ) in the R92W<sub>TNNT2</sub> group compared to the A797T<sub>MYH7</sub> group.

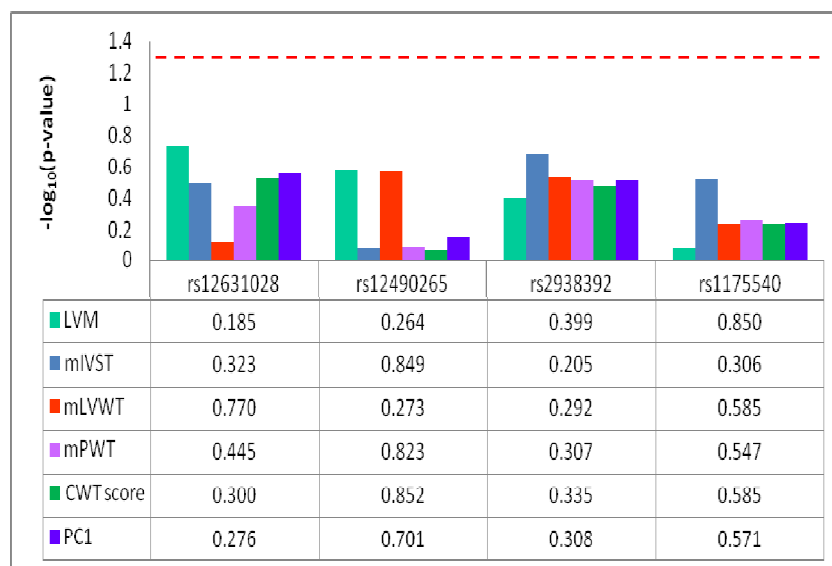


**Figure 3.37** The p-values for tests of association between single SNPs in *PPARG* and individual hypertrophy traits. The original p-values are given in the data table, whilst the graph represents the corresponding  $-\log_{10}$  transformed values. The red dashed horizontal line indicates the p-value significance threshold equal to 0.05. Bars located above this line, therefore, indicate significant p-values (p-values<0.05). The p-value significance increases with bar height above threshold.

**Table 3.55** The p-values obtained for the analysis of interaction between mutation group and single SNPs in *PPARG*. Significant results are indicated in bold red font.

SNP ID	LVM			mIVST			mLVWT			mPWT			CWT score			PC1		
	R403W vs A797T	R92W vs A797T	R92W vs R403W	R403W vs A797T	R92W vs A797T	R92W vs R403W	R403W vs A797T	R92W vs A797T	R92W vs R403W	R403W vs A797T	R92W vs A797T	R92W vs R403W	R403W vs A797T	R92W vs A797T	R92W vs R403W	R403W vs A797T	R92W vs A797T	R92W vs R403W
rs12631028	0.082	0.238	0.515	0.486	0.247	0.737	0.228	<b>0.040</b>	0.520	0.272	0.148	0.848	0.094	0.073	0.956	0.079	0.082	0.859
rs12490265	0.447	0.846	0.594	0.188	0.572	0.093	0.675	0.145	0.103	0.657	0.243	0.162	0.899	0.447	0.448	0.932	0.663	0.656
rs2938392	0.316	0.461	0.686	0.925	0.934	0.877	0.858	0.544	0.762	0.426	0.341	0.973	0.968	0.436	0.562	0.951	0.438	0.579
rs1175540	0.146	0.760	0.250	0.796	0.681	0.569	0.839	0.244	0.257	0.954	0.692	0.713	0.519	0.408	0.198	0.412	0.545	0.202

**Abbreviations:** A-Alanine; CWT score-cumulative wall thickness score; LVM-left ventricular mass; mIVST-maximal interventricular septum thickness; mLVWT-maximal left ventricular wall thickness; mPWT-maximal posterior wall thickness; PC1-principal component score; R-Arginine; SNP-single nucleotide polymorphism; T-Threonine; vs-versus; W-Tryptophan

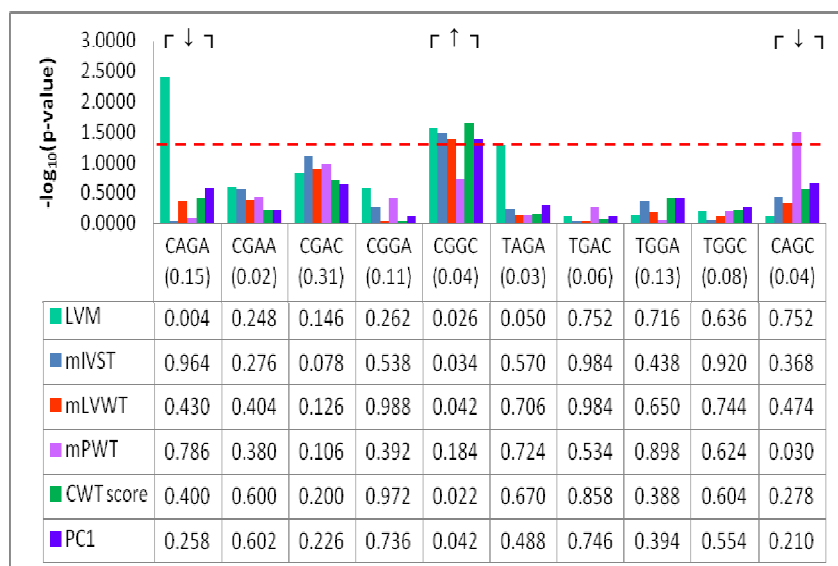


**Figure 3.38** The p-values for tests of association between *PPARG* haplotypes and individual hypertrophy traits. The original p-values are given in the data table, whilst the graph represents the corresponding  $-\log_{10}$  transformed values. The red dashed horizontal line indicates the p-value significance threshold equal to 0.05. Bars located above this line, therefore, indicate significant p-values (p-values < 0.05). The p-value significance increases with bar height above threshold. The observed haplotype frequencies are indicated in brackets.

**Table 3.56** The p-values obtained for the analysis of interaction between mutation group and single haplotypes in *PPARG*. Significant results are indicated in bold red font.

Haplotype*		LVM			mIVST			mLVWT			mPWT			CWT score			PC1			
rs12631028	rs12490265	R403W vs A797T	R92W vs A797T	R92W vs R403W	R403W vs A797T	R92W vs A797T	R92W vs R403W	R403W vs A797T	R92W vs A797T	R92W vs R403W	R403W vs A797T	R92W vs A797T	R92W vs R403W	R403W vs A797T	R92W vs A797T	R92W vs R403W	R403W vs A797T	R92W vs A797T	R92W vs R403W	
C	A	0.360	0.142	0.694	0.148	<b>0.002</b>	0.166	<b>0.026</b>	<b>0.000</b>	0.422	0.330	0.256	0.998	0.172	0.102	0.920	0.342	0.276	0.984	
C	G	A**	-	-	-	-	-	-	-	-	-	-	-	-	-	-	-	-	-	
C	G	A	0.540	0.764	0.760	0.578	0.800	0.428	0.980	0.398	0.384	0.974	0.526	0.506	0.838	0.376	0.488	0.890	0.610	0.706
C	G	A	0.244	0.662	0.588	0.890	0.566	0.492	0.384	0.844	0.586	0.772	0.320	0.216	0.260	0.680	0.616	0.202	0.698	0.516
C	G	C	0.258	0.486	0.080	0.684	0.660	0.398	0.664	0.964	0.696	0.310	0.960	0.296	0.212	0.742	0.378	0.224	0.734	0.132
T	A	A**	-	-	-	-	-	-	-	-	-	-	-	-	-	-	-	-	-	
T	G	A	0.856	0.932	0.874	0.518	0.942	0.516	0.306	0.860	0.460	0.184	<b>0.012</b>	0.222	0.440	0.598	0.864	0.402	<b>0.004</b>	0.918
T	G	A	0.718	0.764	0.194	0.760	0.548	0.364	0.240	0.414	0.604	0.900	0.494	0.422	0.728	0.790	0.500	0.904	<b>0.004</b>	0.342
T	G	C**	-	-	-	-	-	-	-	-	-	-	-	-	-	-	-	-	-	
C	A	G	0.718	0.764	0.194	0.760	0.548	0.364	0.240	0.414	0.604	0.900	0.494	0.422	0.756	0.602	0.742	0.614	<b>0.044</b>	0.846

\*\* absence of p-values indicates unequal distribution of haplotypes in the three HCM mutation groups resulting in stratified groups of small size with insufficient statistical power for testing

**Abbreviations:** A-Adenine\*; A-Alanine; CWT score-cumulative wall thickness score; C-Cytosine\*; G-Guanine\*; LVM-left ventricular mass; mIVST-maximal interventricular septum thickness; mLVWT-maximal left ventricular wall thickness; mPWT-maximal posterior wall thickness; PC1-principal component score; R-Arginine; SNP-single nucleotide polymorphism; T-Threonine; T-Thymine\*; vs-versus; W-Tryptophan

### 3.4.5.19 PGC1A

The p-values for the *association* between the *PGC1A SNPs* and *hypertrophy traits*; and the p-values for *pair-wise differences between mutation groups* in the association between *PGC1A SNPs* and *hypertrophy traits* are given in *Figure 3.39* and *Table 3.57*, respectively. No statistically significant single SNP effect or difference in SNP effect amongst the three HCM founder mutation groups was observed.

*Figure 3.40* graphically represents the p-values for the *association* between *PGC1A haplotypes* and *hypertrophy traits*. The effect of the GATT haplotype was an estimated increase of 2.92 mm in mIVST ( $p = 0.043$ ). *Table 3.58* details the p-values for *pair-wise differences between mutation groups* in the association between *PGC1A haplotypes* and *hypertrophy traits*. The effect of the GAAC haplotype, identified in 6% of the cohort, was higher on LVM (103.3 g;  $p = 0.002$ ), mIVST (7 mm;  $p = 0.019$ ), mLVWT (7.26 mm;  $p = 0.016$ ), the CWT score (65.4 mm;  $p = 0.009$ ) and PC1 (4.09;  $p = 0.030$ ) in the R92W<sub>TNNT2</sub> group compared to the A797T<sub>MYH7</sub> group. Also, its effect was higher in the R92W<sub>TNNT2</sub> group relative to the R403W<sub>MYH7</sub> group: 82 g on LVM ( $p = 0.012$ ), 5.4 mm on mIVST ( $p = 0.028$ ), 5.84 mm on mLVWT ( $p = 0.020$ ), 54.1 mm on the CWT score ( $p = 0.018$ ) and 3.38 on PC1 ( $p = 0.047$ ). The effect of the GATC haplotype, present in 5% of the cohort, was higher on the CWT score (36 mm;  $p = 0.038$ ) in the R92W<sub>TNNT2</sub> group compared to the A797T<sub>MYH7</sub> group. The effect of the GCAC haplotype, identified in 9% of the cohort, was lower in the R92W<sub>TNNT2</sub> group relative to the R403W<sub>MYH7</sub> group: 48 g on LVM ( $p = 0.018$ ), 26.9 mm on the CWT score ( $p = 0.048$ ) and 1.68 on PC1 ( $p = 0.037$ ).

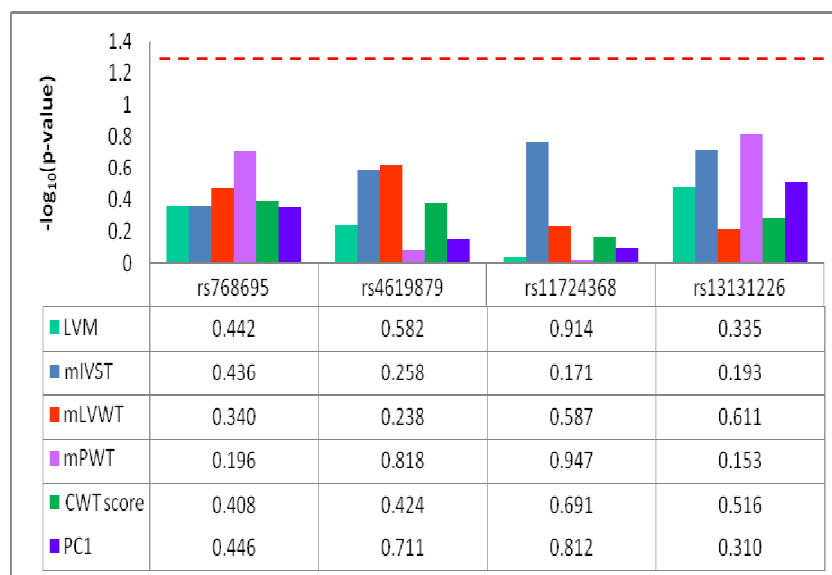


**Figure 3.39** The p-values for tests of association between single SNPs in *PGCIA* and individual hypertrophy traits. The original p-values are given in the data table, whilst the graph represents the corresponding  $-\log_{10}$  transformed values. The red dashed horizontal line indicates the p-value significance threshold equal to 0.05. Bars located above this line, therefore, indicate significant p-values (p-values<0.05). The p-value significance increases with bar height above threshold.

**Table 3.57** The p-values obtained for the analysis of interaction between mutation group and single SNPs in *PGCIA*.

SNP ID	LVM			mIVST			mLVWT			mPWT			CWT score			PC1		
	R403W vs A797T	R92W vs A797T	R92W vs R403W	R403W vs A797T	R92W vs A797T	R92W vs R403W	R403W vs A797T	R92W vs A797T	R92W vs R403W	R403W vs A797T	R92W vs A797T	R92W vs R403W	R403W vs A797T	R92W vs A797T	R92W vs R403W	R403W vs A797T	R92W vs A797T	R92W vs R403W
rs768695	0.662	0.745	0.895	0.504	0.969	0.504	0.358	0.886	0.321	0.669	0.613	0.977	0.825	0.769	0.962	0.712	0.919	0.786
rs4619879	0.352	0.547	0.705	0.557	0.315	0.782	0.587	0.468	0.918	0.528	0.417	0.940	0.855	0.225	0.427	0.804	0.300	0.286
rs11724368	0.931	0.706	0.743	0.767	0.476	0.456	0.627	0.828	0.745	0.634	0.634	0.875	0.930	0.975	0.917	0.830	0.995	0.839
rs13131226	0.375	0.185	0.746	0.461	0.163	0.611	0.908	0.272	0.300	0.764	0.491	0.764	0.709	0.196	0.473	0.604	0.220	0.597

**Abbreviations:** A-Alanine; **CWT score**-cumulative wall thickness score; **LVM**-left ventricular mass; **mIVST**-maximal interventricular septum thickness; **mLVWT**-maximal left ventricular wall thickness; **mPWT**-maximal posterior wall thickness; **PC1**-principal component score; **R**-Arginine; **SNP**-single nucleotide polymorphism; **T**-Threonine; **vs**-versus; **W**-Tryptophan



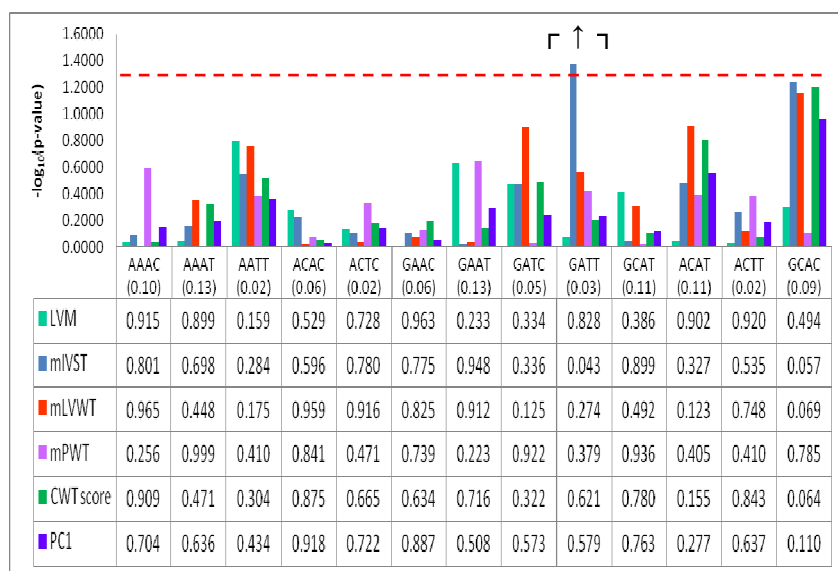


**Figure 3.40** The p-values for tests of association between *PGCIA* haplotypes and individual hypertrophy traits. The original p-values are given in the data table, whilst the graph represents the corresponding  $-\log_{10}$  transformed values. The red dashed horizontal line indicates the p-value significance threshold equal to 0.05. Bars located above this line, therefore, indicate significant p-values (p-values < 0.05). The p-value significance increases with bar height above threshold. The observed haplotype frequencies are indicated in brackets.

**Table 3.58** The p-values obtained for the analysis of interaction between mutation group and single haplotypes in *PGCIA*. Significant results are indicated in bold red font.

Haplotype*				LVM			mIVST			mLVWT			mPWT			CWT score			PC1		
rs768695	rs4619879	rs11724368	rs13131226	R403W	R92W	R92W	R403W	R92W	R92W	R403W	R92W	R92W	R403W	R92W	R92W	R403W	R92W	R92W	R403W	R92W	R92W
				vs	vs	vs	vs	vs	vs	vs	vs	vs	vs	vs	vs	vs	vs	vs	vs	vs	vs
A	A	A	C	A797T	A797T	R403W	A797T	A797T	R403W	A797T	A797T	R403W	A797T	A797T	R403W	A797T	A797T	R403W	A797T	A797T	R403W
A	A	A	C	0.116	0.116	0.913	0.619	0.408	0.733	0.328	0.236	0.859	0.853	0.933	0.898	0.552	0.344	0.719	0.527	0.373	0.807
A	A	A	T	0.732	0.541	0.798	0.714	0.932	0.801	0.473	0.867	0.417	0.542	0.141	0.412	0.969	0.568	0.547	0.849	0.402	0.310
A	A	T	T**	-	0.298	-	-	0.967	-	-	0.937	-	-	0.713	-	-	0.487	-	-	0.524	-
A	C	A	C	0.066	0.180	0.615	0.732	0.854	0.875	0.285	0.450	0.782	0.358	0.242	0.749	0.072	0.185	0.739	0.063	0.205	0.644
A	C	T	C	0.814	0.378	0.413	0.343	0.825	0.400	0.182	0.490	0.340	0.129	0.771	0.078	-	0.524	-	-	0.545	-
G	A	A	C	0.339	<b>0.002</b>	<b>0.012</b>	0.827	<b>0.019</b>	<b>0.028</b>	0.920	<b>0.016</b>	<b>0.020</b>	0.699	0.225	0.325	0.683	<b>0.009</b>	<b>0.018</b>	0.753	<b>0.030</b>	<b>0.047</b>
G	A	A	T	0.568	0.348	0.812	0.629	0.165	0.512	0.531	0.373	0.871	0.608	0.277	0.694	0.994	0.303	0.446	0.924	0.275	0.379
G	A	T	C	0.759	0.615	0.528	0.264	0.076	0.956	0.379	0.250	0.911	0.791	0.411	0.783	0.555	<b>0.038</b>	0.430	0.571	0.050	0.461
G	A	T	T	0.948	0.754	0.920	0.496	0.663	0.658	0.497	0.193	0.971	0.211	0.061	0.805	0.717	0.259	0.788	0.676	0.278	0.850
G	C	A	T	0.790	0.359	0.729	0.870	0.470	0.751	0.948	0.204	0.442	0.853	0.943	0.898	0.780	0.264	0.654	0.823	0.447	0.783
A	C	A	T	0.341	0.438	0.706	0.842	0.159	0.387	0.421	0.709	0.272	0.634	0.607	0.916	0.664	0.595	0.406	0.529	0.649	0.327
A	C	T	T	0.673	0.890	0.744	0.932	0.541	0.468	0.652	0.748	0.887	0.314	0.612	0.544	0.931	0.744	0.816	0.878	0.906	0.780
G	C	A	C	0.443	0.097	<b>0.018</b>	0.997	0.191	0.190	0.959	0.169	0.188	0.325	0.792	0.227	0.460	0.195	<b>0.048</b>	0.267	0.296	<b>0.037</b>

\*\* absence of p-values indicates unequal distribution of haplotypes in the three HCM mutation groups resulting in stratified groups of small size with insufficient statistical power for testing

**Abbreviations:** A-Adenine\*; A-Alanine; CWT score-cumulative wall thickness score; C-Cytosine\*; G-Guanine\*; LVM-left ventricular mass; mIVST-maximal interventricular septum thickness; mLVWT-maximal left ventricular wall thickness; mPWT-maximal posterior wall thickness; PC1-principal component score; R-Arginine; SNP-single nucleotide polymorphism; T-Threonine; T-Thymine\*; vs-versus; W-Tryptophan

### 3.4.5.20 PRKAA1

**Figure 3.41** graphically represents the p-values for the *association* between the *PRKAA1 SNPs* and *hypertrophy traits*. No statistically significant SNP effects were observed. **Table 3.59** details the p-values for *pair-wise comparison between mutation groups* in the association between *PRKAA1 SNPs* and *hypertrophy traits*. The effect of the C-allele of rs12517210 and the G-allele of rs11747210 (the minor allele of the rs11747210 SNP is the T allele) was higher on LVM in the R92W<sub>TNNT2</sub> group relative to the A797T<sub>MYH7</sub> group (26.9 g, p = 0.025; 26.7 g, p = 0.023). Also, their effects were higher in the R403W<sub>MYH7</sub> group compared to the A797T<sub>MYH7</sub> group on the CWT score (18.7 mm, p = 0.026; 17.9 mm, p = 0.047) and PC1 (1.17, p = 0.024; 1.12, p = 0.042). The effect of the A-allele of rs466108 was higher on mPWT (1.52 mm; p = 0.027) in the R403W<sub>MYH7</sub> group compared to the A797T<sub>MYH7</sub> group.

**Figure 3.42** graphically represents the p-values for the *association* between *PRKAA1 haplotypes* and *hypertrophy traits* with no evidence of statistically significant haplotype effects. **Table 3.60** details the p-values for *pair-wise differences between mutation groups* in the association between *PRKAA1 haplotypes* and *hypertrophy traits*. The effect of haplotype CGC, observed in 31% of the cohort, was higher on LVM in the R92W<sub>TNNT2</sub> group compared to the A797T<sub>MYH7</sub> group (21.7 g; p = 0.045). Conversely, the effect of haplotype TTC, also observed in 31% of the cohort, was lower on LVM in the R92W<sub>TNNT2</sub> group compared to the A797T<sub>MYH7</sub> group (36.4 g; p = 0.016).

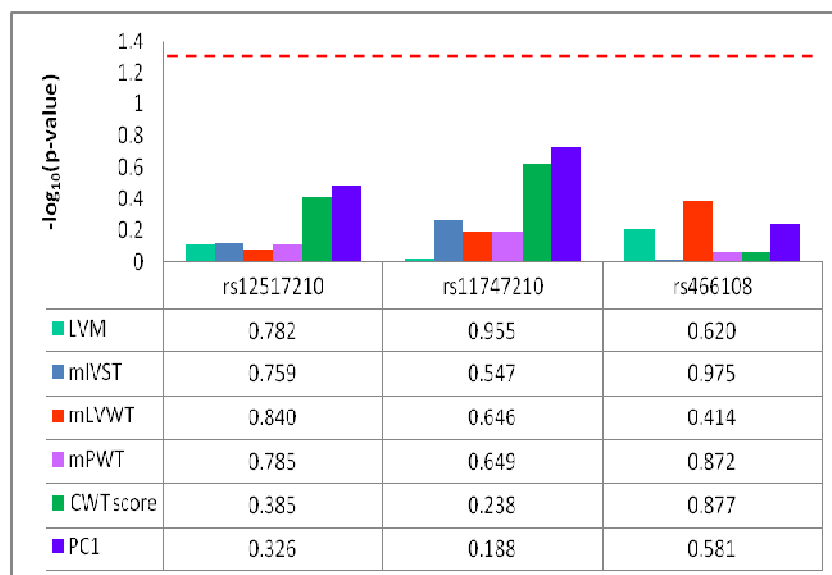


**Figure 3.41** The p-values for tests of association between single SNPs in *PRKAA1* and individual hypertrophy traits. The original p-values are given in the data table, whilst the graph represents the corresponding  $-\log_{10}$  transformed values. The red dashed horizontal line indicates the p-value significance threshold equal to 0.05. Bars located above this line, therefore, indicate significant p-values (p-values<0.05). The p-value significance increases with bar height above threshold.

**Table 3.59** The p-values obtained for the analysis of interaction between mutation group and single SNPs in *PRKAA1*. Significant results are indicated in bold red font.

SNP ID	LVM			mIVST			mLVWT			mPWT			CWT score			PC1		
	R403W vs A797T	R92W vs A797T	R92W vs R403W	R403W vs A797T	R92W vs A797T	R92W vs R403W	R403W vs A797T	R92W vs A797T	R92W vs R403W	R403W vs A797T	R92W vs A797T	R92W vs R403W	R403W vs A797T	R92W vs A797T	R92W vs R403W	R403W vs A797T	R92W vs A797T	R92W vs R403W
rs12517210	0.143	<b>0.025</b>	0.532	0.077	0.090	0.913	0.164	0.200	0.911	0.646	0.364	0.716	<b>0.026</b>	0.074	0.611	<b>0.024</b>	0.085	0.559
rs11747210	0.189	<b>0.023</b>	0.448	0.127	0.091	0.937	0.252	0.214	0.958	0.792	0.373	0.613	<b>0.047</b>	0.066	0.786	<b>0.042</b>	0.056	0.800
rs466108	0.327	0.748	0.444	0.338	0.589	0.550	0.199	0.405	0.462	<b>0.027</b>	0.693	0.053	0.474	0.281	0.947	0.302	0.197	0.800

**Abbreviations:** A-Alanine; CWT score-cumulative wall thickness score; LVM-left ventricular mass; mIVST-maximal interventricular septum thickness; mLVWT-maximal left ventricular wall thickness; mPWT-maximal posterior wall thickness; PC1-principal component score; R-Arginine; SNP-single nucleotide polymorphism; T-Threonine; vs-versus; W-Tryptophan

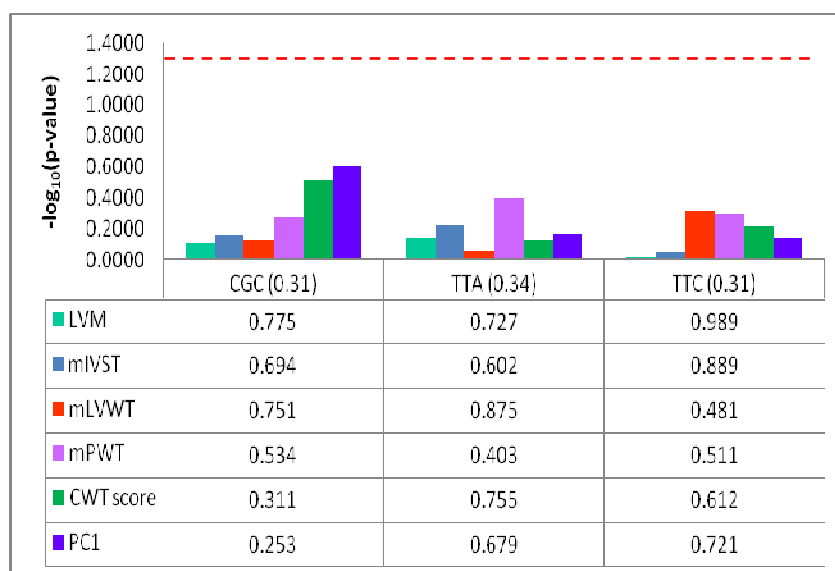


**Figure 3.42** The p-values for tests of association between *PRKAA1* haplotypes and individual hypertrophy traits. The original p-values are given in the data table, whilst the graph represents the corresponding  $-\log_{10}$  transformed values. The red dashed horizontal line indicates the p-value significance threshold equal to 0.05. Bars located above this line, therefore, indicate significant p-values (p-values<0.05). The p-value significance increases with bar height above threshold. The observed haplotype frequencies are indicated in brackets.

**Table 3.60** The p-values obtained for the analysis of interaction between mutation group and single haplotypes in *PRKAA1*. Significant results are indicated in bold red font.

Haplotype*			LVM			mIVST			mLVWT			mPWT			CWT score			PC1		
rs12517210	rs11747210	rs466108	R403W vs A797T	R92W vs A797T	R92W vs R403W	R403W vs A797T	R92W vs A797T	R92W vs R403W	R403W vs A797T	R92W vs A797T	R92W vs R403W	R403W vs A797T	R92W vs A797T	R92W vs R403W	R403W vs A797T	R403W vs A797T	R92W vs A797T	R92W vs R403W	R403W vs A797T	
C	G	C	0.140	<b>0.045</b>	0.717	0.180	0.230	0.853	0.272	0.494	0.699	0.804	0.629	0.859	0.055	0.136	0.601	0.054	0.142	0.583
T	T	A	0.540	0.701	0.389	0.348	0.891	0.400	0.194	0.538	0.366	0.054	0.557	0.121	0.393	0.560	0.599	0.257	0.442	0.483
T	T	C	0.326	<b>0.016</b>	0.202	0.376	0.067	0.422	0.750	0.385	0.625	0.299	0.298	0.050	0.301	0.170	0.874	0.490	0.242	0.743

**Abbreviations:** A-Adenine\*; A-Alanine; CWT score-cumulative wall thickness score; C-Cytosine\*; G-Guanine\*; LVM-left ventricular mass; mIVST-maximal interventricular septum thickness; mLVWT-maximal left ventricular wall thickness; mPWT-maximal posterior wall thickness; PC1-principal component score; R-Arginine; SNP-single nucleotide polymorphism; T-Threonine; T-Thymine\*; vs-versus; W-Tryptophan

### 3.4.5.21 *PRKAA2*

The p-values for the *association* between the *PRKAA2 SNPs* and *hypertrophy traits*; and the p-values for *pair-wise differences between mutation groups* in the association between *PRKAA2 SNPs* and *hypertrophy traits* are given in *Figure 3.43* and *Table 3.61*, respectively. No statistically significant single SNP effect or difference in SNP effect amongst the three HCM founder mutation groups was observed.

The p-values for the *association* between *PRKAA2 haplotypes* and *hypertrophy traits* are graphically represented in *Figure 3.44*. The p-values for *pair-wise comparison between mutation groups* in the association of *PRKAA2 haplotypes* and *hypertrophy traits* are provided in *Table 3.62*. The effect of the TTT haplotype, observed in 14% of the study cohort, was an estimated increase of 0.45 in PC1 ( $p = 0.043$ ). No statistically significant difference in haplotype effect was observed amongst the three HCM founder mutation groups.

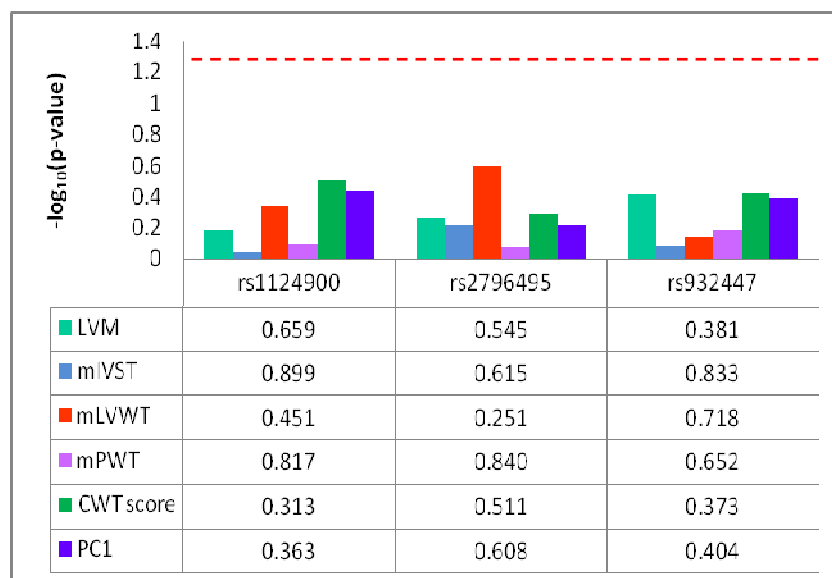


**Figure 3.43** The p-values for tests of association between single SNPs in *PRKAA2* and individual hypertrophy traits. The original p-values are given in the data table, whilst the graph represents the corresponding  $-\log_{10}$  transformed values. The red dashed horizontal line indicates the p-value significance threshold equal to 0.05. Bars located above this line, therefore, indicate significant p-values (p-values<0.05). The p-value significance increases with bar height above threshold.

**Table 3.61** The p-values obtained for the analysis of interaction between HCM founder mutation group and single SNPs in *PRKAA2*.

SNP ID	LVM			mIVST			mLVWT			mPWT			CWT score			PC1		
	R403W vs A797T	R92W vs A797T	R92W vs R403W	R403W vs A797T	R92W vs A797T	R92W vs R403W	R403W vs A797T	R92W vs A797T	R92W vs R403W	R403W vs A797T	R92W vs A797T	R92W vs R403W	R403W vs A797T	R92W vs A797T	R92W vs R403W	R403W vs A797T	R92W vs A797T	R92W vs R403W
rs1124900	0.852	0.617	0.822	0.983	0.950	0.976	0.992	0.703	0.758	0.679	0.435	0.330	0.952	0.263	0.337	0.820	0.261	0.486
rs2796495	0.783	0.629	0.884	0.618	0.296	0.685	0.927	0.907	0.853	0.503	0.742	0.717	0.567	0.781	0.749	0.675	0.531	0.893
rs932447	0.817	0.754	0.642	0.914	0.756	0.876	0.853	0.920	0.803	0.676	0.707	0.499	0.868	0.285	0.454	0.691	0.319	0.637

**Abbreviations:** A-Alanine; CWT score-cumulative wall thickness score; LVM-left ventricular mass; mIVST-maximal interventricular septum thickness; mLVWT-maximal left ventricular wall thickness; mPWT-maximal posterior wall thickness; PC1-principal component score; R-Arginine; SNP-single nucleotide polymorphism; T-Threonine; vs-versus; W-Tryptophan

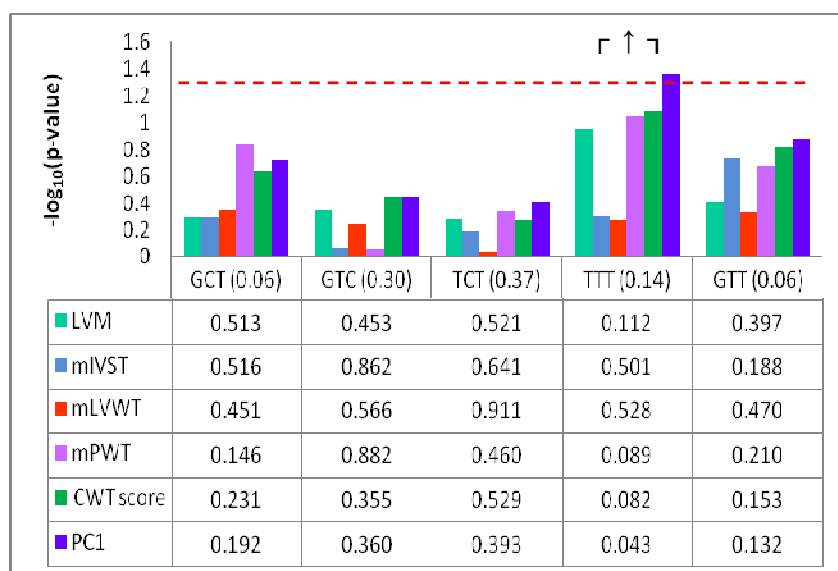


**Figure 3.44** The p-values for the tests of association between *PRKAA2* haplotypes and individual hypertrophy traits. The original p-values are given in the data table, whilst the graph represents the corresponding  $-\log_{10}$  transformed values. The red dashed horizontal line indicates the p-value significance threshold equal to 0.05. Bars located above this line, therefore, indicate significant p-values (p-values<0.05). The p-value significance increases with bar height above threshold. The observed haplotype frequencies are indicated in brackets.

**Table 3.62** The p-values obtained for the analysis of interaction between mutation group and *PRKAA2* haplotypes.

Haplotype*		LVM			mIVST			mLVWT			mPWT			CWT score			PC1			
rs1124900	rs2796495	R403W	R92W	R92W	R403W	R92W	R92W	R403W	R92W	R92W	R403W	R92W	R92W	R403W	R92W	R92W	R403W	R92W	R92W	
		vs	vs	vs	vs	vs	vs	vs	vs	vs	vs	vs	vs	vs	vs	vs	vs	vs	vs	
		A797T	A797T	R403W	A797T	A797T	R403W	A797T	A797T	R403W	A797T	A797T	R403W	A797T	A797T	R403W	A797T	A797T	R403W	
G	C	T	0.289	0.387	0.717	0.409	0.437	0.941	0.648	0.652	0.994	0.451	0.525	0.828	0.392	0.476	0.784	0.408	0.451	0.899
C	T	C	0.851	0.381	0.599	0.883	0.724	0.890	0.734	0.811	0.896	0.720	0.677	0.510	0.655	0.126	0.416	0.533	0.133	0.532
T	C	T	0.424	0.993	0.453	0.558	0.501	0.975	0.773	0.940	0.741	0.096	0.843	0.154	0.321	0.844	0.414	0.351	0.594	0.623
T	T	T	0.547	0.943	0.533	0.502	0.145	0.114	0.510	0.602	0.330	0.402	0.814	0.520	0.413	0.134	0.104	0.616	0.115	0.172
G	T	T	0.866	0.535	0.632	0.424	0.416	0.874	0.750	0.784	0.993	0.848	0.147	0.109	0.627	0.426	0.699	0.824	0.277	0.362

**Abbreviations:** A-Alanine; CWT score-cumulative wall thickness score; C-Cytosine\*; G-Guanine\*; LVM-left ventricular mass; mIVST-maximal interventricular septum thickness; mLVWT-maximal left ventricular wall thickness; mPWT-maximal posterior wall thickness; PC1-principal component score; R-Arginine; SNP-single nucleotide polymorphism; T-Threonine; T-Thymine\*; vs-versus; W-Tryptophan



### 3.4.5.22 *PRKAB1*

**Figure 3.45** graphically represents the p-values for the *association* between the *PRKAB1 SNPs* and *hypertrophy traits* with no evidence of statistically significant SNP effects. **Table 3.63** details the p-values for *pair-wise comparison between mutation groups* in the association between the *PRKAB1 SNPs* and *hypertrophy traits*. The effect of the T-allele of rs278149 was higher on the CWT score (25 mm;  $p = 0.041$ ) and PC1 (1.56;  $p = 0.025$ ) in the R92W<sub>TNNT2</sub> group compared to the A797T<sub>MYH7</sub> group.

**Figure 3.46** graphically represents the p-values for the *association* between *PRKAB1 haplotypes* and *hypertrophy traits* with evidence of statistically significant haplotype effects for the TGGTG haplotype, present in 14% of the cohort. Its effect was an estimated decrease of 18.3 g in LVM ( $p = 0.010$ ). **Table 3.64** details the p-values for *pair-wise differences between mutation groups* in the association of *PRKAB1 haplotypes* and *hypertrophy traits*. The TGGTG haplotype that showed a significant haplotype effect as well as the GACGT haplotype indicated significant differences in haplotype effect amongst the HCM founder mutation groups. The effect of the TGGTG haplotype was higher on LVM (41.6 g;  $p = 0.020$ ) in the R92W<sub>TNNT2</sub> group compared to the A797T<sub>MYH7</sub> group. The effect of the GACGT haplotype, present in 68% of the cohort, was lower on mPWT (1.21 mm;  $p = 0.004$ ) in the R403W<sub>MYH7</sub> group compared to the A797T<sub>MYH7</sub> group.

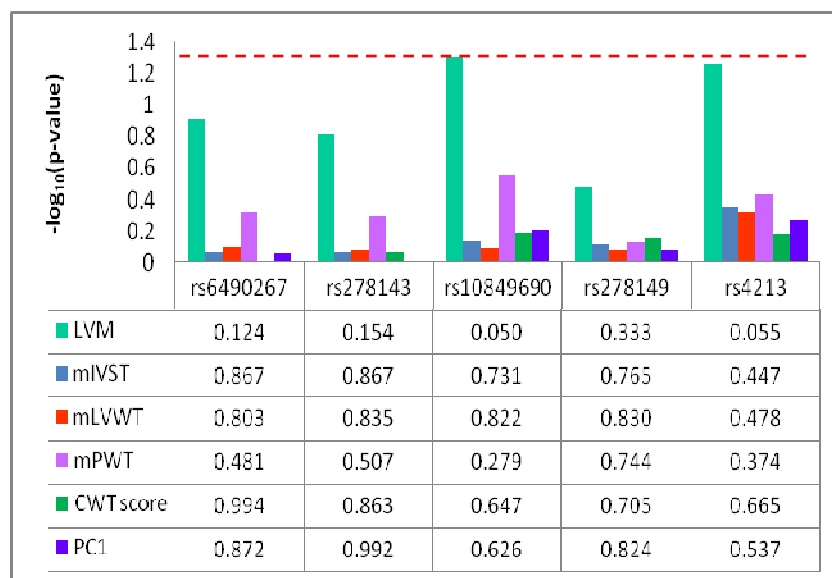


**Figure 3.45** The p-values for tests of association between single SNPs in *PRKAB1* and individual hypertrophy traits. The original p-values are given in the data table, whilst the graph represents the corresponding  $-\log_{10}$  transformed values. The red dashed horizontal line indicates the p-value significance threshold equal to 0.05. Bars located above this line, therefore, indicate significant p-values (p-values<0.05). The p-value significance increases with bar height above threshold.

**Table 3.63** The p-values obtained for the analysis of interaction between mutation group and single SNPs in *PRKAB1*. Significant results are indicated in bold red font.

SNP ID	LVM			mIVST			mLVWT			mPWT			CWT score			PC1		
	R403W vs A797T	R92W vs A797T	R92W vs R403W	R403W vs A797T	R403W vs R92W	R92W vs A797T	R92W vs R403W	R403W vs A797T	R403W vs R92W	R92W vs A797T	R403W vs A797T	R403W vs R92W	R92W vs A797T	R403W vs A797T	R403W vs R92W	R92W vs A797T	R403W vs A797T	R403W vs R92W
rs6490267	0.555	0.142	0.093	0.949	0.372	0.440	0.729	0.108	0.311	0.446	0.139	0.576	0.863	0.093	0.118	0.991	0.082	0.147
rs278143	0.587	0.112	0.080	0.951	0.273	0.348	0.747	0.078	0.245	0.461	0.123	0.528	0.803	0.078	0.089	0.953	0.070	0.115
rs10849690	0.935	0.082	0.115	0.992	0.292	0.356	0.963	0.207	0.252	0.755	0.940	0.766	0.476	0.262	0.122	0.575	0.245	0.142
rs278149	0.493	0.068	0.347	0.316	0.102	0.606	0.289	0.118	0.689	0.151	0.066	0.722	0.522	<b>0.041</b>	0.226	0.368	<b>0.025</b>	0.244
rs4213	0.516	0.284	0.151	0.939	0.625	0.643	0.741	0.169	0.400	0.495	0.104	0.459	0.824	0.150	0.156	0.959	0.129	0.182

**Abbreviations:** A-Alanine; CWT score-cumulative wall thickness score; LVM-left ventricular mass; mIVST-maximal interventricular septum thickness; mLVWT-maximal left ventricular wall thickness; mPWT-maximal posterior wall thickness; PC1-principal component score; R-Arginine; SNP-single nucleotide polymorphism; T-Threonine; vs-versus; W-Tryptophan

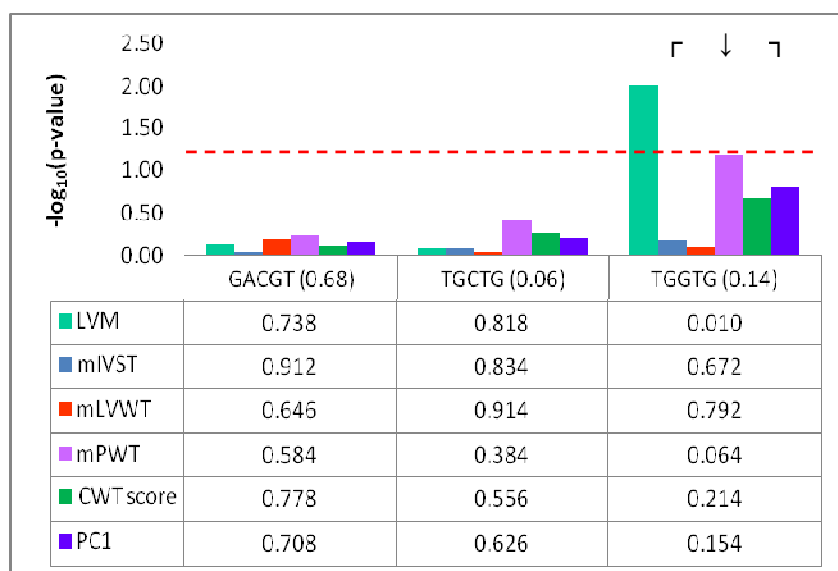


**Figure 3.46** The p-values for tests of association between *PRKABI* haplotypes and individual hypertrophy traits. The original p-values are given in the data table, whilst the graph represents the corresponding  $-\log_{10}$  transformed values. The red dashed horizontal line indicates the p-value significance threshold equal to 0.05. Bars located above this line, therefore, indicate significant p-values (p-values<0.05). The p-value significance increases with bar height above threshold. The observed haplotype frequencies are indicated in brackets.

**Table 3.64** The p-values obtained for the analysis of interaction between mutation group and *PRKABI* haplotypes. Significant results are indicated in bold red font.

Haplotype*	LVM			mIVST			mLVWT			mPWT			CWT score			PC1		
rs6490267 rs278143 rs10849690 rs278149 rs4213	R403W vs A797T	R92W vs A797T	R92W vs R403W	R403W vs A797T	R92W vs A797T	R92W vs R403W	R403W vs A797T	R92W vs A797T	R92W vs R403W	R403W vs A797T	R92W vs A797T	R92W vs R403W	R403W vs A797T	R92W vs A797T	R92W vs R403W	R403W vs A797T	R92W vs A797T	R92W vs R403W
G A C G T	0.410	0.178	0.554	0.102	0.602	0.358	0.154	0.844	0.148	<b>0.004</b>	0.086	0.520	0.164	0.354	0.786	0.090	0.260	0.736
T G C T G	0.618	0.894	0.602	0.762	0.902	0.912	0.612	0.820	0.538	0.116	0.406	0.700	0.496	0.972	0.560	0.310	0.854	0.524
T G G T G	0.058	<b>0.020</b>	0.774	0.238	0.178	0.774	0.366	0.376	0.714	0.730	0.152	0.340	0.326	0.136	0.824	0.302	0.200	0.958

**Abbreviations:** A-Adenine\*; A-Alanine; CWT score-cumulative wall thickness score; C-Cytosine\*; G-Guanine\*; LVM-left ventricular mass; mIVST-maximal interventricular septum thickness; mLVWT-maximal left ventricular wall thickness; mPWT-maximal posterior wall thickness; PC1-principal component score; R-Arginine; SNP-single nucleotide polymorphism; T-Threonine; T-Thymine\*; vs-versus; W-Tryptophan

### 3.4.5.23 *PRKAB2*

*Figure 3.47* graphically represents the p-values for the *association* between the *PRKAB2 SNPs* and *hypertrophy traits*. The effect of the G-allele of rs1348316 was an estimated increase of 0.36 mm in mPWT ( $p = 0.049$ ). *Table 3.65* details the p-values for *pair-wise differences between mutation groups* in the association between *PRKAB2 SNPs* and *hypertrophy traits*. No statistically significant difference in SNP effect was observed amongst the three HCM founder mutation groups.

The p-values for the *association* between the *PRKAB2 haplotypes* and *hypertrophy traits*; and the p-values for *pair-wise differences between mutation groups* in the association between the *PRKAB2 haplotypes* and *hypertrophy traits* are given in *Figure 3.48* and *Table 3.66*, respectively. No statistically significant haplotype effect or difference in haplotype effect amongst the three HCM founder mutation groups was observed.

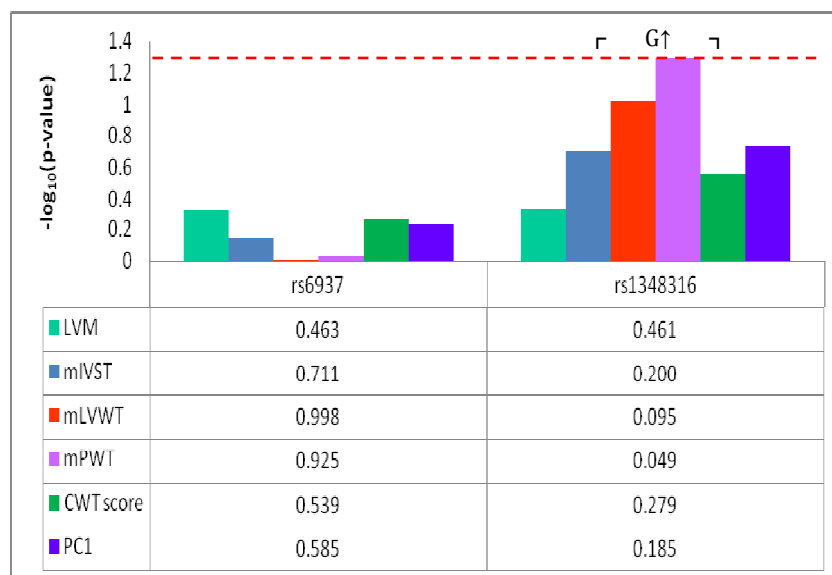


**Figure 3.47** The p-values for tests of association between single SNPs in *PRKAB2* and individual hypertrophy traits. The original p-values are given in the data table, whilst the graph represents the corresponding  $-\log_{10}$  transformed values. The red dashed horizontal line indicates the p-value significance threshold equal to 0.05. Bars located above this line, therefore, indicate significant p-values (p-values<0.05). The p-value significance increases with bar height above threshold.

**Table 3.65** The p-values obtained for the analysis of interaction between mutation group and single SNPs in *PRKAB2*.

SNP ID	LVM			mIVST			mLVWT			mPWT			CWT score			PC1		
	R403W vs A797T	R92W vs A797T	R92W vs R403W	R403W vs A797T	R92W vs A797T	R92W vs R403W	R403W vs A797T	R92W vs A797T	R92W vs R403W	R403W vs A797T	R92W vs A797T	R92W vs R403W	R403W vs A797T	R92W vs A797T	R92W vs R403W	R403W vs A797T	R92W vs A797T	R92W vs R403W
rs6937	0.576	0.393	0.883	0.446	0.647	0.585	0.393	0.652	0.523	0.877	0.853	0.805	0.646	0.578	0.851	0.554	0.326	0.914
rs1348316	0.481	0.586	0.909	0.739	0.898	0.865	0.800	0.679	0.875	0.800	0.733	0.603	0.808	0.966	0.861	0.854	0.738	0.891

**Abbreviations:** A-Alanine; CWT score-cumulative wall thickness score; LVM-left ventricular mass; mIVST-maximal interventricular septum thickness; mLVWT-maximal left ventricular wall thickness; mPWT-maximal posterior wall thickness; PC1-principal component score; R-Arginine; SNP-single nucleotide polymorphism; T-Threonine; vs-versus; W-Tryptophan

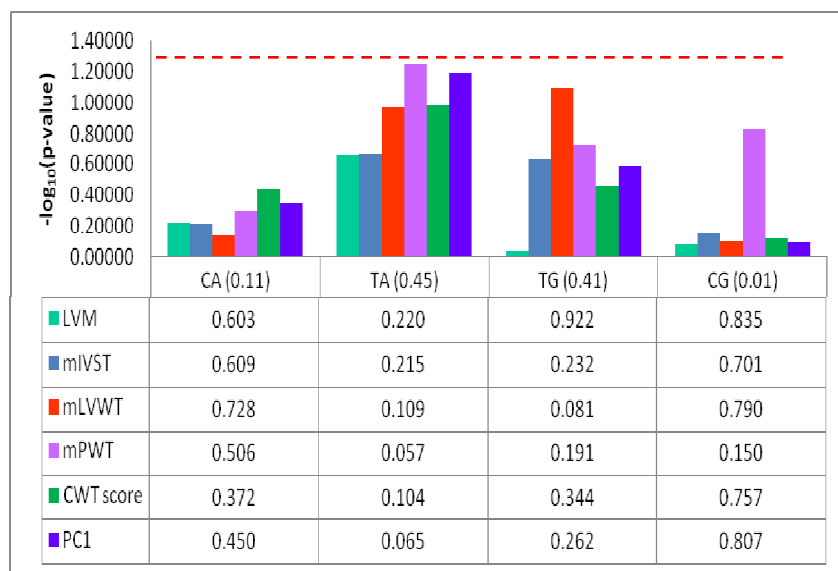


**Figure 3.48** The p-values for tests of association between *PRKAB2* haplotypes and individual hypertrophy traits. The original p-values are given in the data table, whilst the graph represents the corresponding  $-\log_{10}$  transformed values. The red dashed horizontal line indicates the p-value significance threshold equal to 0.05. Bars located above this line, therefore, indicate significant p-values (p-values<0.05). The p-value significance increases with bar height above threshold. The observed haplotype frequencies are indicated in brackets.

**Table 3.66** The p-values obtained for the analysis of interaction between mutation group and *PRKAB2* haplotypes.

Haplotype*		LVM			mIVST			mLVWT			mPWT			CWT score			PC1		
rs6937	rs1348316	R403W	R92W	R92W	R403W	R92W	R92W	R403W	R92W	R92W	R403W	R92W	R92W	R403W	R92W	R92W	R403W	R92W	R92W
		vs	vs	vs	vs	vs	vs	vs	vs	vs	vs	vs	vs	vs	vs	vs	vs	vs	vs
		A797T	A797T	R403W	A797T	A797T	R403W	A797T	A797T	R403W	A797T	A797T	R403W	A797T	A797T	R403W	A797T	A797T	R403W
		C	A	0.817	0.209	0.803	0.991	0.554	0.834	0.984	0.606	0.828	0.631	0.860	0.676	0.979	0.626	0.871	0.937
T	A	0.317	0.330	0.906	0.940	0.868	0.942	0.826	0.600	0.796	0.615	0.806	0.479	0.807	0.920	0.730	0.927	0.939	0.869
T	G	0.230	0.936	0.342	0.839	0.472	0.637	0.753	0.307	0.513	0.408	0.233	0.078	0.989	0.479	0.520	0.939	0.294	0.316
C	G	0.773	0.759	0.614	0.519	0.737	0.388	0.339	0.660	0.210	0.801	0.552	0.492	0.533	0.871	0.627	0.469	0.682	0.699

**Abbreviations:** A-Adenine\*; A-Alanine; CWT score-cumulative wall thickness score; C-Cytosine\*; G-Guanine\*; LVM-left ventricular mass; mIVST-maximal interventricular septum thickness; mLVWT-maximal left ventricular wall thickness; mPWT-maximal posterior wall thickness; PC1-principal component score; R-Arginine; SNP-single nucleotide polymorphism; T-Threonine; T-Thymine\*; vs-versus; W-Tryptophan

#### 3.4.5.24 *PRKAG1*

The p-values for the *association* between the *PRKAG1 SNPs* and *hypertrophy traits*; and the p-values for *pair-wise differences between mutation groups* in the association between *PRKAG1 SNPs* and *hypertrophy traits* are given in *Figure 3.49* and *Table 3.67*, respectively. No statistically significant single SNP effect or difference in SNP effect amongst the three HCM founder mutation groups was observed.

The p-values for the *association* between the *PRKAG1 haplotypes* and *hypertrophy traits* are given in *Figure 3.50*; and the p-values for *pair-wise comparisons between mutation groups* in the association between *PRKAG1 haplotypes* and *hypertrophy traits* are given in *Table 3.68*. No statistically significant haplotype effect or difference in haplotype effect amongst the HCM founder mutation groups was observed.

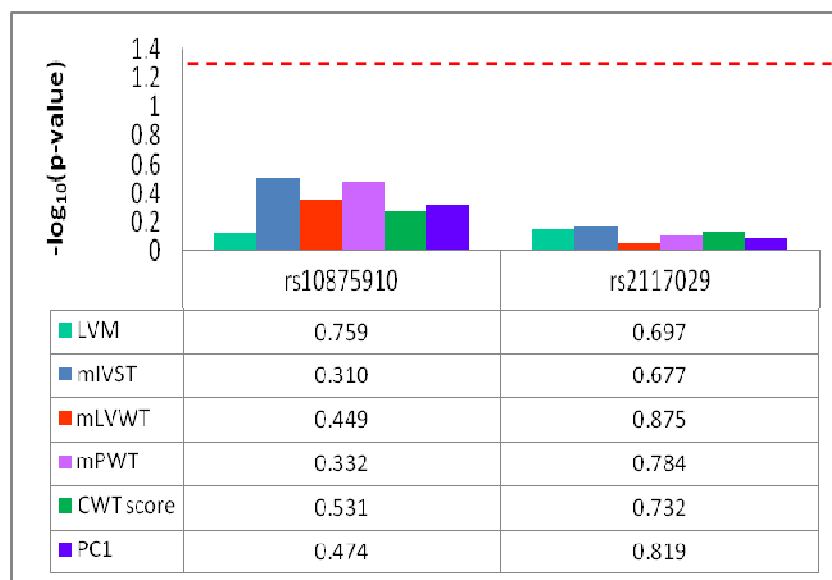


**Figure 3.49** The p-values for tests of association between single SNPs in *PRKAG1* and individual hypertrophy traits. The original p-values are given in the data table, whilst the graph represents the corresponding  $-\log_{10}$  transformed values. The red dashed horizontal line indicates the p-value significance threshold equal to 0.05. Bars located above this line, therefore, indicate significant p-values (p-values<0.05). The p-value significance increases with bar height above threshold.

**Table 3.67** The p-values obtained for the analysis of interaction between mutation group and single SNPs in *PRKAG1*.

SNP ID	LVM			mIVST			mLVWT			mPWT			CWT score			PC1		
	R403W vs A797T	R92W vs A797T	R92W vs R403W	R403W vs A797T	R92W vs A797T	R92W vs R403W	R403W vs A797T	R92W vs A797T	R92W vs R403W	R403W vs A797T	R92W vs A797T	R92W vs R403W	R403W vs A797T	R92W vs A797T	R92W vs R403W	R403W vs A797T	R92W vs A797T	R92W vs R403W
rs10875910	0.736	0.693	0.535	0.998	0.881	0.904	0.641	0.643	0.948	0.642	0.690	0.458	0.962	0.973	0.985	0.852	0.833	0.989
rs2117029	0.445	0.845	0.387	0.663	0.316	0.205	0.271	0.997	0.317	0.416	0.761	0.316	0.446	0.722	0.305	0.413	0.786	0.315

**Abbreviations:** A-Alanine; **CWT score**-cumulative wall thickness score; **LVM**-left ventricular mass; **mIVST**-maximal interventricular septum thickness; **mLVWT**-maximal left ventricular wall thickness; **mPWT**-maximal posterior wall thickness; **PC1**-principal component score; **R**-Arginine; **SNP**-single nucleotide polymorphism; **T**-Threonine; **vs**-versus; **W**-Tryptophan



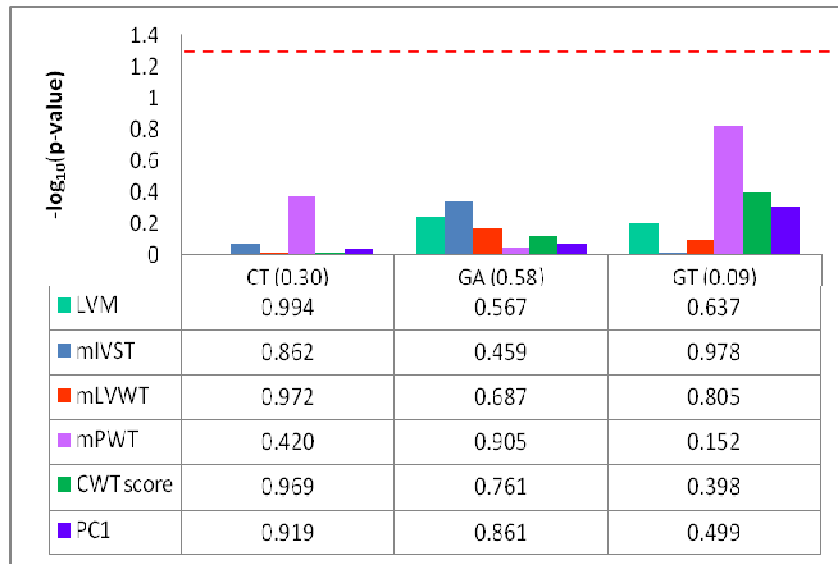


**Figure 3.50** The p-values for tests of association between *PRKAG1* haplotypes and individual hypertrophy traits. The original p-values are given in the data table, whilst the graph represents the corresponding  $-\log_{10}$  transformed values. The red dashed horizontal line indicates the p-value significance threshold equal to 0.05. Bars located above this line, therefore, indicate significant p-values (p-values<0.05). The p-value significance increases with bar height above threshold. The observed haplotype frequencies are indicated in brackets.

**Table 3.68** The p-values obtained for the analysis of interaction between mutation group and *PRKAG1* haplotypes.

Haplotype*		LVM			mIVST			mLVWT			mPWT			CWT score			PC1		
rs10875910	rs2117029	R403W	R92W	R92W	R403W	R92W	R92W	R403W	R92W	R92W	R403W	R92W	R92W	R403W	R92W	R92W	R403W	R92W	R92W
		vs	vs	vs	vs	vs	vs	vs	vs	vs	vs	vs	vs	vs	vs	vs	vs	vs	vs
		A797T	A797T	R403W	A797T	A797T	R403W	A797T	A797T	R403W	A797T	A797T	R403W	A797T	A797T	R403W	A797T	A797T	R403W
C	T	0.571	0.878	0.678	0.982	0.922	0.959	0.517	0.648	0.788	0.505	0.678	0.351	0.659	0.760	0.837	0.543	0.669	0.780
G	A	0.412	0.639	0.717	0.524	0.875	0.476	0.197	0.463	0.575	0.343	0.284	0.978	0.402	0.598	0.737	0.369	0.490	0.799
G	T	0.527	0.852	0.632	0.898	0.106	0.067	0.688	0.469	0.178	0.722	0.977	0.720	0.951	0.377	0.248	0.965	0.366	0.246

**Abbreviations:** A-Adenine\*; A-Alanine; CWT score-cumulative wall thickness score; C-Cytosine\*; G-Guanine\*; LVM-left ventricular mass; mIVST-maximal interventricular septum thickness; mLVWT-maximal left ventricular wall thickness; mPWT-maximal posterior wall thickness; PC1-principal component score; R-Arginine; SNP-single nucleotide polymorphism; T-Threonine; T-Thymine\*; vs-versus; W-Tryptophan

### 3.4.5.25 PRKAG2

**Figure 3.51** graphically represents the p-values for the *association* between the *PRKAG2 SNPs* and *hypertrophy traits* with no evidence of statistically significant SNP effects. **Table 3.69** details the p-values for *pair-wise differences between mutation groups* in the association between *PRKAG2 SNPs* and *hypertrophy traits*. The effect of the C-allele of rs8961 was higher on LVM (23.8 g;  $p = 0.047$ ) in the R92W<sub>TNNT2</sub> group relative to the A797T<sub>MYH7</sub> group. Also, its effect was higher in the R403W<sub>MYH7</sub> group compared to the A797T<sub>MYH7</sub> group: 3.25 mm on mIVST ( $p = 0.033$ ), 3.23 mm on mLVWT ( $p = 0.023$ ) and 24.0 mm on the CWT score ( $p = 0.043$ ). The effect of the G-allele of the rs6464170 variant was higher on mIVST (3.09 mm;  $p = 0.023$ ) in the R92W<sub>TNNT2</sub> group compared to the A797T<sub>MYH7</sub> group. The effect of the G-allele of the rs13240743 variant was lower in the R92W<sub>TNNT2</sub> group relative to the A797T<sub>MYH7</sub> group on LVM (15.4 g;  $p = 0.012$ ), mPWT (0.77 mm;  $p = 0.039$ ), the CWT score (13.3 mm;  $p = 0.042$ ) and PC1 (0.83;  $p = 0.023$ ). In addition, its effect was lower on LVM (44.7 g;  $p = 0.004$ ), mIVST (3.63 mm;  $p = 0.038$ ) and mLVWT (3.30 mm;  $p = 0.049$ ) in the R92W<sub>TNNT2</sub> group compared to the R403W<sub>MYH7</sub> group.

**Figure 3.52** graphically represents the p-values for the *association* between *PRKAG2 haplotypes* and *hypertrophy traits*. The effect of the CACC haplotype, observed in 10% of the cohort, was an estimated increase of 1.48 mm in mIVST ( $p = 0.044$ ). The TGGG haplotype, observed in 7% of the cohort, was associated with a decrease in mLVWT of 2.03 mm ( $p = 0.014$ ). **Table 3.70** details the p-values for *pair-wise comparison between mutation groups* in the association of *PRKAG2 haplotypes* and *hypertrophy traits*. The effect of the CGCC haplotype, observed in 11% of the cohort, was higher on LVM (42.6 g;  $p = 0.047$ ) in the R403W<sub>MYH7</sub> group relative to the A797T<sub>MYH7</sub> group. Also, its effect was higher in the R92W<sub>TNNT2</sub> group compared to the A797T<sub>MYH7</sub> group: 57.3 g on LVM ( $p = 0.001$ ), 4.4 mm on mIVST ( $p = 0.008$ ), 3.76 mm on mLVWT ( $p = 0.021$ ), 30.1 mm on the CWT score ( $p = 0.012$ ) and 1.88 on PC1 ( $p = 0.015$ ). The effect of the CGCG haplotype, observed in 5% of the cohort, was lower in the R92W<sub>TNNT2</sub> group compared to the R403W<sub>MYH7</sub> group: 90 g on LVM ( $p = 0.021$ ), 7.6 mm on mIVST ( $p = 0.033$ ), 7.6 mm on mLVWT ( $p = 0.017$ ), 92.3 mm on the CWT score ( $p = 0.018$ ) and 5.77 on PC1 ( $p = 0.020$ ). In addition, its effect was lower in the R92W<sub>TNNT2</sub> group relative to the A797T<sub>MYH7</sub> group: 1.72 mm on mPWT ( $p = 0.013$ ) and 0.68 on PC1 ( $p = 0.049$ ). The effect of the CGGC haplotype, present in 7% of the cohort, was lower on mIVST in the R92W<sub>TNNT2</sub> group than the A797T<sub>MYH7</sub> group (7.3 mm;  $p = 0.028$ ). The effect of

the TAGC haplotype, observed in 4% of the cohort, was lower in the R403W<sub>MYH7</sub> group compared to the A797T<sub>MYH7</sub> group: 7.4 mm on mIVST (p = 0.040) and 7.18 mm on mLVWT (p = 0.048).

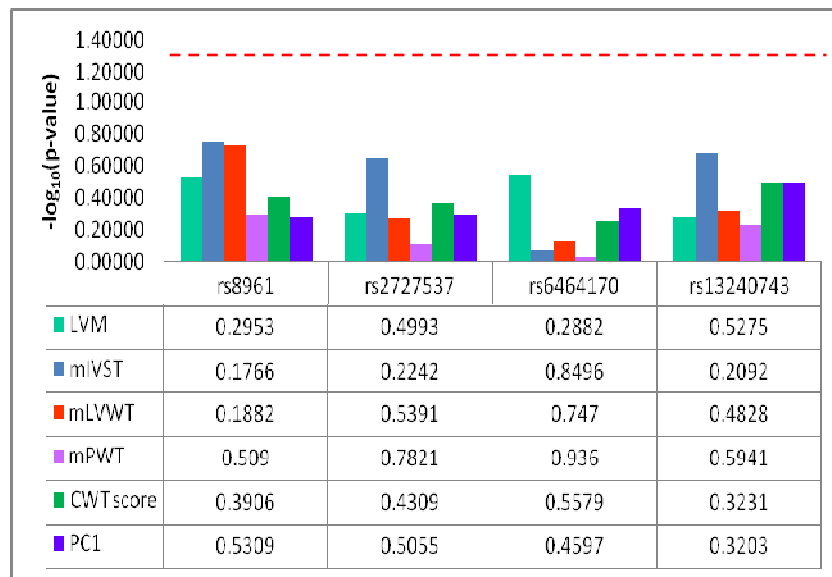


**Figure 3.51** The p-values for tests of association between single SNPs in *PRKAG2* and individual hypertrophy traits. The original p-values are given in the data table, whilst the graph represents the corresponding  $-\log_{10}$  transformed values. The red dashed horizontal line indicates the p-value significance threshold equal to 0.05. Bars located above this line, therefore, indicate significant p-values (p-values<0.05). The p-value significance increases with bar height above threshold.

**Table 3.69** The p-values obtained for the analysis of interaction between mutation group and single SNPs in *PRKAG2*. Significant results are indicated in bold red font.

SNP ID	LVM			mIVST			mLVWT			mPWT			CWT score			PC1		
	R403W vs A797T	R92W vs A797T	R92W vs R403W	R403W vs A797T	R92W vs A797T	R92W vs R403W	R403W vs A797T	R92W vs A797T	R92W vs R403W	R403W vs A797T	R92W vs A797T	R92W vs R403W	R403W vs A797T	R92W vs A797T	R92W vs R403W	R403W vs A797T	R92W vs A797T	R92W vs R403W
rs8961	0.097	<b>0.047</b>	0.908	<b>0.033</b>	0.076	0.602	<b>0.023</b>	0.062	0.627	0.200	0.546	0.482	<b>0.043</b>	0.062	0.733	0.146	0.152	0.869
rs2727537	0.109	0.350	0.472	0.245	0.861	0.240	0.574	0.579	0.352	0.936	0.654	0.794	0.951	0.673	0.708	0.784	0.773	0.638
rs6464170	0.133	0.313	0.623	0.067	<b>0.023</b>	0.643	0.091	0.190	0.703	0.059	0.109	0.773	0.100	0.077	0.878	0.162	0.071	0.665
rs13240743	0.338	<b>0.012</b>	<b>0.004</b>	0.453	0.077	<b>0.038</b>	0.320	0.180	<b>0.049</b>	0.913	<b>0.039</b>	0.131	0.630	<b>0.042</b>	0.052	0.831	<b>0.023</b>	0.061

**Abbreviations:** A-Alanine; CWT score-cumulative wall thickness score; LVM-left ventricular mass; mIVST-maximal interventricular septum thickness; mLVWT-maximal left ventricular wall thickness; mPWT-maximal posterior wall thickness; PC1-principal component score; R-Arginine; SNP-single nucleotide polymorphism; T-Threonine; vs-versus; W-Tryptophan

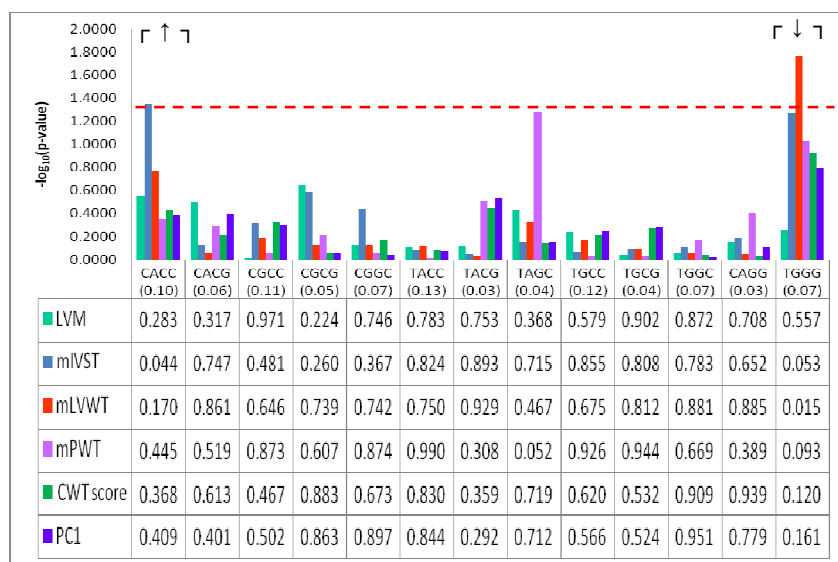


**Figure 3.52** The p-values for tests of association between *PRKAG2* haplotypes and individual hypertrophy traits. The original p-values are given in the data table, whilst the graph represents the corresponding  $-\log_{10}$  transformed values. The red dashed horizontal line indicates the p-value significance threshold equal to 0.05. Bars located above this line, therefore, indicate significant p-values (p-values < 0.05). The p-value significance increases with bar height above threshold. The observed haplotype frequencies are indicated in brackets.

**Table 3.70** The p-values obtained for the analysis of interaction between mutation group and individual haplotypes in *PRKAG2*. Significant results are indicated in bold red font.

Haplotype*		LVM			mIVST			mLVWT			mPWT			CWT score			PC1		
SNP	Haplotype	R403W	R92W	R92W	R403W	R92W	R92W	R403W	R92W	R92W	R403W	R92W	R92W	R403W	R92W	R92W	R403W	R92W	R92W
		vs	vs	vs	vs	vs	vs	vs	vs	vs	vs	vs	vs	vs	vs	vs	vs	vs	vs
rs8961	C A C C	0.616	0.225	0.707	0.908	0.227	0.353	0.949	0.894	0.971	0.817	0.388	0.704	0.977	0.385	0.571	0.962	0.270	0.478
rs2727537	C A C G	0.617	0.931	0.691	0.530	0.510	0.920	0.131	0.231	0.558	0.155	0.784	0.257	0.143	0.522	0.313	0.382	0.637	0.586
rs6464170	C G C C	<b>0.047</b>	<b>0.001</b>	0.584	0.195	<b>0.008</b>	0.496	0.501	<b>0.021</b>	0.281	0.260	0.059	0.767	0.906	<b>0.012</b>	0.128	0.970	<b>0.015</b>	0.101
rs13240743	C G C G	0.214	0.106	<b>0.021</b>	0.142	0.348	<b>0.033</b>	0.180	0.112	<b>0.017</b>	0.742	<b>0.013</b>	0.220	0.111	0.141	<b>0.018</b>	0.195	<b>0.049</b>	<b>0.020</b>
	C G G C	0.364	0.458	0.987	0.214	<b>0.028</b>	0.159	0.580	0.140	0.222	0.429	0.522	0.992	0.339	0.112	0.325	0.398	0.131	0.319
	T A C C	0.575	0.776	0.815	0.873	0.818	0.966	0.976	0.797	0.833	0.810	0.624	0.585	0.707	0.595	0.497	0.529	0.730	0.453
	T A C G**	-	0.473	-	-	0.666	-	-	0.686	-	-	0.878	-	-	0.994	-	-	0.919	-
	T A G C	0.289	0.626	0.392	<b>0.040</b>	0.126	0.401	<b>0.048</b>	0.145	0.411	0.598	0.846	0.626	0.333	0.283	0.946	0.742	0.512	0.685
	T G C C	0.726	0.749	0.507	0.812	0.566	0.444	0.697	0.907	0.788	0.943	0.941	0.890	0.969	0.467	0.459	0.834	0.521	0.406
	T G C G	0.152	0.732	0.182	0.633	0.542	0.230	0.583	0.523	0.192	0.689	0.830	0.804	0.875	0.967	0.882	0.716	0.710	0.947
	T G G C	0.341	0.205	0.444	0.468	0.279	0.383	0.686	0.350	0.199	0.307	0.202	0.536	0.413	0.185	0.230	0.380	0.173	0.254
	C A G G**	-	0.765	-	-	0.553	-	-	0.858	-	-	0.305	-	-	0.605	-	-	0.463	-
	T G G G	0.557	0.180	0.304	0.614	0.169	0.287	0.843	0.278	0.222	0.293	0.314	0.911	0.549	0.145	0.262	0.498	0.121	0.255

\*\* absence of p-values indicates unequal distribution of haplotypes in the three HCM mutation groups resulting in stratified groups of small size with insufficient statistical power for testing

**Abbreviations:** A-Adenine\*; A-Alanine; CWT score-cumulative wall thickness score; C-Cytosine\*; G-Guanine\*; LVM-left ventricular mass; mIVST-maximal interventricular septum thickness; mLVWT-maximal left ventricular wall thickness; mPWT-maximal posterior wall thickness; PC1-principal component score; R-Arginine; SNP-single nucleotide polymorphism; T-Threonine; T-Thymine\*; vs-versus; W-Tryptophan

### 3.4.5.26 *PRKAG3*

The p-values for the association between the *PRKAG3* SNPs and *hypertrophy traits*; and the p-values for *pair-wise comparison between mutation groups* in the association between *PRKAA2* SNPs and *hypertrophy traits* are given in *Figure 3.53* and *Table 3.71*, respectively. No statistically significant single SNP effect or difference in SNP effect amongst the three HCM founder mutation groups was observed.

*Figure 3.54* graphically represents the p-values for the association between *PRKAG3* haplotypes and *hypertrophy traits*. The effect of the TT haplotype, observed in 74% of the cohort, was an estimated decrease of 13.4 g in LVM ( $p = 0.031$ ). *Table 3.72* details the p-values for *pair-wise differences between mutation groups* in the association between *PRKAG3* haplotypes and *hypertrophy traits*. No statistically significant difference in haplotype effect was observed amongst the three HCM founder mutation groups.

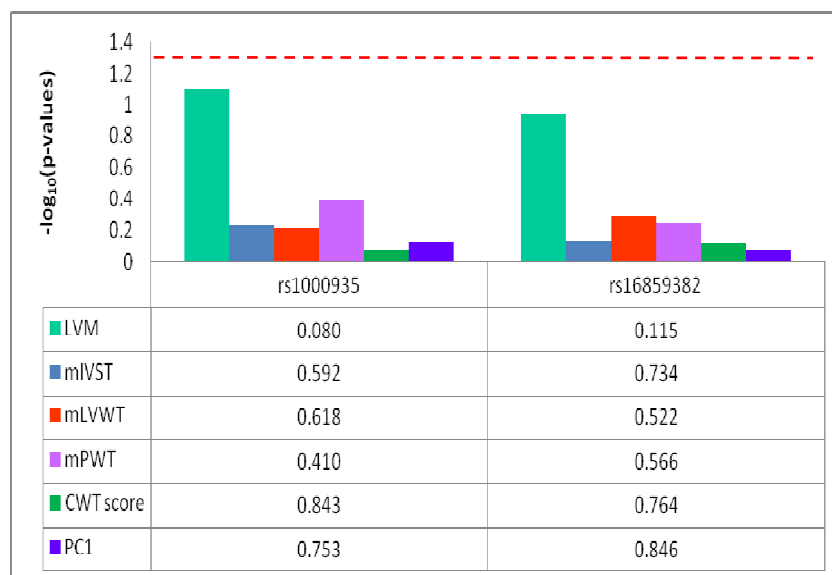


**Figure 3.53** The p-values for tests of association between single SNPs in *PRKAG3* and individual hypertrophy traits. The original p-values are given in the data table, whilst the graph represents the corresponding  $-\log_{10}$  transformed values. The red dashed horizontal line indicates the p-value significance threshold equal to 0.05. Bars located above this line, therefore, indicate significant p-values (p-values<0.05). The p-value significance increases with bar height above threshold.

**Table 3.71** The p-values obtained for the analysis of interaction between mutation group and single SNPs in *PRKAG3*.

SNP ID	LVM			mIVST			mLVWT			mPWT			CWT score			PC1		
	R403W vs A797T	R92W vs A797T	R92W vs R403W	R403W vs A797T	R92W vs A797T	R92W vs R403W	R403W vs A797T	R92W vs A797T	R92W vs R403W	R403W vs A797T	R92W vs A797T	R92W vs R403W	R403W vs A797T	R92W vs A797T	R92W vs R403W	R403W vs A797T	R92W vs A797T	R92W vs R403W
rs1000935	0.911	0.641	0.670	0.592	0.804	0.722	0.927	0.864	0.749	0.705	0.814	0.859	0.945	0.760	0.625	0.852	0.871	0.647
rs16859382	0.932	0.733	0.759	0.599	0.740	0.801	0.883	0.908	0.747	0.630	0.814	0.755	0.928	0.742	0.585	0.822	0.840	0.575

**Abbreviations:** A-Alanine; CWT score-cumulative wall thickness score; LVM-left ventricular mass; mIVST-maximal interventricular septum thickness; mLVWT-maximal left ventricular wall thickness; mPWT-maximal posterior wall thickness; PC1-principal component score; R-Arginine; SNP-single nucleotide polymorphism; T-Threonine; vs-versus; W-Tryptophan

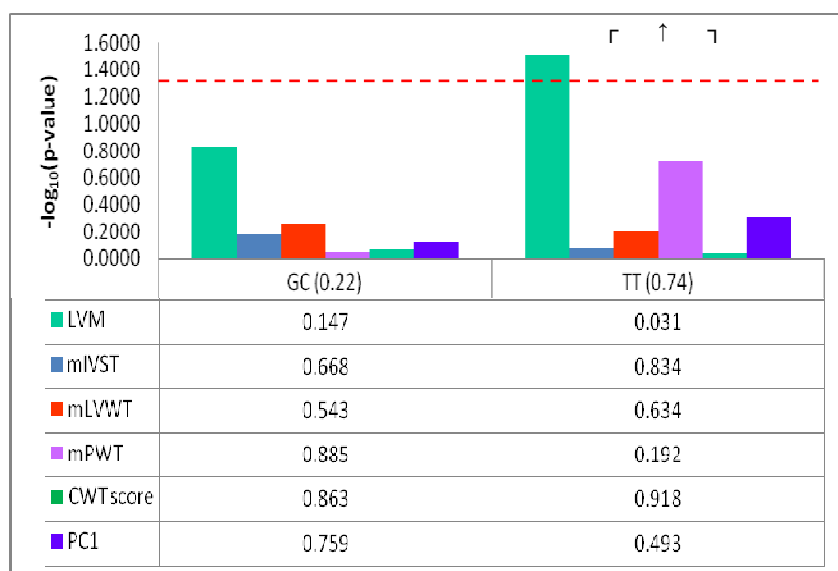


**Figure 3.54** The p-values for tests of association between *PRKAG3* haplotypes and individual hypertrophy traits. The original p-values are given in the data table, whilst the graph represents the corresponding  $-\log_{10}$  transformed values. The red dashed horizontal line indicates the p-value significance threshold equal to 0.05. Bars located above this line, therefore, indicate significant p-values (p-values<0.05). The p-value significance increases with bar height above threshold. The observed haplotype frequencies are indicated in brackets.

**Table 3.72** The p-values obtained for the analysis of interaction between mutation group and haplotypes in *PRKAG3*.

Haplotype*		LVM			mIVST			mLVWT			mPWT			CWT score			PC1		
rs1000935	rs16859382	R403W	R92W	R92W	R403W	R92W	R92W	R403W	R92W	R92W	R403W	R92W	R92W	R403W	R92W	R92W	R403W	R92W	R92W
		vs	vs	vs	vs	vs	vs	vs	vs	vs	vs	vs	vs	vs	vs	vs	vs	vs	vs
G	C	0.975	0.490	0.425	0.447	0.734	0.604	0.855	0.874	0.673	0.441	0.670	0.663	0.893	0.860	0.683	0.770	0.996	0.692
T	T	0.719	0.777	0.909	0.988	0.793	0.801	0.912	0.524	0.564	0.735	0.710	0.450	0.970	0.811	0.807	0.990	0.884	0.845

**Abbreviations:** A-Alanine; CWT score-cumulative wall thickness score; C-Cytosine\*; G-Guanine\*; LVM-left ventricular mass; mIVST-maximal interventricular septum thickness; mLVWT-maximal left ventricular wall thickness; mPWT-maximal posterior wall thickness; PC1-principal component score; R-Arginine; SNP-single nucleotide polymorphism; T-Threonine; T-Thymine\*; vs-versus; W-Tryptophan



### 3.4.6 Optimal selection

We employed stepwise-selection on the model for the PC1 trait to identify a subset of the variants investigated in this study that together explain most of the variation in hypertrophy in the current cohort. A total of six markers predicted an increase in at least one of the hypertrophy indices, independent of the hypertrophy covariates and the other significant variants contained in the model.

The effect of each of the six alleles that conferred an increased risk for hypertrophy development is provided in terms of the estimated increase in PC1 per allele per SNP in Table 3.73. The combined effect of one of each of the six alleles increased the PC1 score by 2.852 with an average effect per allele of 0.475. Table 3.74 indicates the distribution of the number of ‘pro-LVH’ alleles in MC and NC individuals.

**Table 3.73 Allelic effects of variants predicting a significant increase in hypertrophy in the current cohort**

Gene	Polymorphism	Minor Allele	‘pro-LVH’ Allele	PC1 (n = 129)
<i>MYL2</i>	rs933296	A	C	0.488
<i>MYH7</i>	rs2277475	T	A	0.425
<i>TPM1</i>	rs11071720	C	T	0.138
<i>TPM1</i>	rs1071646	C	C	1.169
<i>CKM</i>	rs7260463	T	G	0.119
<i>PRKAB2</i>	rs1348316	G	G	0.513
<b>Combined effect on hypertrophy trait</b>				2.852
<b>Average effect per allele</b>				0.475

**Abbreviations:** *CKM*-Creatine kinase, muscle; *LVH*-left ventricular hypertrophy; *MYL2*-Myosin light chain 2, regulatory cardiac, slow; *MYH7*-Myosin heavy chain 7, cardiac muscle, beta; *n*-total; *PC1*-first principal component; *PRKAB2*-Protein kinase, AMP-activated, beta 2 non-catalytic subunit; *TPM1*-Tropomyosin 1

**Table 3.74 The distribution of the number of ‘pro-LVH’ alleles in MC and NC individuals**

Number of ‘pro-LVH’ alleles carried	2	3	4	5	6	7	8	9	10	11
MC	0	0	4	12	9	19	14	13	5	0
NC	1	3	2	8	11	11	9	5	2	1

**Abbreviations:** MC-mutation carrier, NC-non-mutation carrier

## CHAPTER FOUR

### DISCUSSION

---

The importance of efficient patient risk stratification and treatment in HCM becomes apparent when considering that it is the most common inherited cardiac disorder and the leading cause of SCD in young adults; and that its main clinical feature, LVH, is an independent predictor of morbidity and mortality (Fokstuen *et al.*, 2011; Dahlof *et al.*, 2002).

However, considerable genotype/phenotype disparity exists for the numerous HCM-causing mutations and treatment aiming to correct the direct consequences thereof remains challenging, e.g. achieving adequate intracellular oligonucleotide levels to ensure chronic suppression of individual HCM missense mutations (Ashrafian *et al.*, 2011; Carrier *et al.*, 1997; Dausse *et al.*, 1993). The phenotypic diversity observed for a given causal mutation is seen even in homogenous individuals from the same family, thereby highlighting the contribution of factors other than the primary genetic defect. This certainly includes the influence of modifier genes, as is evident from the literature review presented in Chapter 1.

A previous genome-wide analysis that identified human HCM modifier loci showed greater effect sizes for modifier alleles present in the homozygous state relative to the causal mutation, which typically presents as heterozygous in autosomal dominant disorders (Marian, 2010). Moreover, modifier loci can ameliorate the effects of a causal mutation and in some instances even completely suppress the phenotype (Wei *et al.*, 2010). Identification of modifiers will thus improve the current understanding of disease development and potentially highlight new targets for patient risk screening and treatment (Daw *et al.*, 2008).

To date, efforts aimed at identifying modifiers of hypertrophy in HCM have focused mainly on genes encoding proteins that function in cardiac growth and hypertrophy (Friedrich *et al.*, 2009). However, the few replication studies reported in the literature have delivered inconsistent results (Marian, 2002; Nabel, 2003). It is reasonable to suggest that the genetic factors that cause HCM also have the potential to modify its development and a review of the primary defects and their direct consequences highlight genes relating to sarcomeric structure, function and myocardial energetics as candidate modifier genes. This study, therefore, set out to evaluate the hypertrophy-modifying capacity of these factors by means of SNP-based association testing within South African HCM families.

The study identified a modifying role in the development of hypertrophy in HCM for each of the candidate genes investigated, in many instances for the first time, with the exception of the metabolic protein-encoding gene, *PRKAG1*. Single SNPs within the genes *MYH7*, *TPM1* and *MYL2* which encode structural proteins of the sarcomere as well as the genes *CPT1B*, *CKM*, *ALDOA* and *PRKAB2* which encode metabolic proteins, indicated significant association results and hence hypertrophy modifying effects. Similarly, haplotypes comprising variants within the genes *ACTC*, *TPM1*, *MYL2*, *MYL3* and *MYBPC3* which encode structural proteins of the sarcomere as well as the genes *CD36*, *PDK4*, *CKM*, *PFKM*, *PPARA*, *PPARG*, *PGC1A*, *PRKAA2*, *PRKAG2* and *PRKAG3* which encode metabolic proteins, showed significant association results indicative of combined-variant hypertrophy modifying effects. Also, a number of variants and haplotypes showed statistically significant differences in effect amongst the three HCM founder mutation groups.

#### **4.1 Caveats in association studies**

A statistically significant association between a marker and a phenotypic trait can reflect the functional significance of the marker itself or a marker with which it is in LD; or can be ascribed to chance or artefact. It is, therefore, necessary to consider and, if needed, appropriately correct for a number of factors, which may negatively impact on the reproducibility of association studies for complex genetic traits (Cardon & Palmer, 2003). The following sections will discuss these factors within the context of the present study.

##### **4.1.1 Population stratification**

The association analyses essentially aimed to correlate differences in allele frequencies for a given SNP with differences in trait levels using cases and unaffected relatives (Cardon & Palmer, 2003). In instances where the study sample comprises several population groups, as was the case for the present cohort, the allele frequencies and disease risks may vary amongst them and so give rise to spurious association between an allele and disease trait (Colhoun *et al.*, 2003). The current study population comprises South African HCM families from either Caucasian or Mixed Ancestry descent. The latter is considered an ethnic admixture group, which originated from the intermingling of a number of populations, including Khoi, San, Dutch and black African individuals (Loubser *et al.*, 1999). More specifically, South African individuals with mixed ancestry contain admixture from mainly Khoi San Africans (32-43%), non-Khoi San Africans (20-36%), Europeans (21-28%)

and, to a lesser extent, Asian populations (9-11%) (de Wit *et al.*, 2010). Also, we incorporated both within- and between-family components of association in an effort to maximise the power of the study.

As consequence, this study employed specialised mixed-effects models that are able to incorporate both fixed and random effects. Self-reported ethnicity was included as a fixed effect to partially control for population substructure whilst family- and individual-specific random effects were modelled as adjustment for intrafamilial clustering of traits and interindividual trait correlations i.e. confounding due to family or cryptic relatedness (Price *et al.*, 2010).

Although not employed in the current study, it is important to note the alternative methods of correcting for ancestry other than self-reported ethnicity. If genome-wide data is available for the study group, principal components or ancestry proportions (estimated by solving a multinomial model given the genome-wide data) can be used as covariates in a regression model to adjust for population stratification. The covariance structure between individuals, estimated from the genome-wide data, or genomic control, that applies a correction factor to association test statistics, can also be used (Wu *et al.*, 2011; Alexander *et al.*, 2009). Alternatively, if genome-wide data is not available but ancestry informative markers (AIMs) have been genotyped for the individuals in the study, principal component or ancestry proportion covariates can be used to adjust for stratification (Daya M, personal communication; Paschou *et al.*, 2008; Tsai *et al.*, 2005).

#### **4.1.2 Multiple testing**

Statistical evaluation of a number of tests within a single study is believed to increase the probability of identifying a significant association by chance (type I error). It is, therefore often considered important to statistically compensate in instances of multiple testing, such as the current study where numerous markers were tested against various heritable hypertrophy traits. However, the literature is not in agreement regarding the necessity of such a correction (Rothman, 1990).

The first option would be to perform multiple testing correction using the Bonferroni adjustment, which entails multiplying the p-value obtained for each of the independent tests by the total number of evaluations performed. However, this correction is not suitable, as it is considered to be over-conservative. Moreover, the tests used in this study are not mutually independent, as the traits

investigated are all derived from the 16 wall thickness measurements; and certain SNPs are in LD, albeit incomplete. The alternative approach to multiple testing correction, i.e., Bayesian methods, utilise prior information regarding the hypothesis, i.e. the relationship between the genetic factor and trait investigated, to adjust the statistical significance level in an informed manner. This approach too is unsuitable to the current study, as the functional significance and thus the prior probabilities, have not been characterised for all genetic variants (Campbell & Rudan, 2002). Also, this study was undertaken as a hypothesis-generating rather than a hypothesis-testing investigation. Therefore, as mentioned in Section 2.6.6, no formal correction was made given the lack of an appropriate method of adjustment and the explorative nature of the genetic study. Moreover, existing methods of adjustment are applicable only to family trios and would have to be further modified for use with extended pedigrees such as those used here; however, this type of computational modification was beyond the scope of the present study. A further means of addressing the issue of multiple testing would be to consider the statistical results generated at a reduced threshold for significance e.g.  $p < 0.01$ .

#### 4.1.3 Confounding variables

When evaluating the potential contribution of a given factor to the development of hypertrophy it is necessary to ensure that the groups/individuals under investigation are similar in structure with respect to the distribution of all factors known to confer risk of hypertrophy development, i.e. covariates, so as to avoid confounding defined as the distortion of the effect measure as either inflated or masked. To ensure that a significant association most accurately reflects the relationship between the investigated variant and trait rather than the influence of these confounding variables, the statistical models employed here made adjustments for known covariates of hypertrophy, namely age (Fleg & Strait, 2012; Lasky-Su *et al.*, 2008), sex (Maass *et al.*, 2004; Okin *et al.*, 2000), BSA, HR (as a proxy measure for tachycardia i.e. elevated resting HR) (Saba *et al.*, 2001), mean arterial pressure (MAP; as derived from systolic and diastolic BP) (Roman *et al.*, 2010), presence of hypertension (i.e., adjustment for anti-hypertensive therapy) (Kraja *et al.*, 2011; Levy *et al.*, 1990b; Puntmann *et al.*, 2010; Sipola *et al.*, 2011), ethnicity (as indication of recent population stratification) (Okin *et al.*, 2000), and HCM-causing founder mutation (Moolman *et al.*, 1997).

#### 4.1.4 Statistical power

The statistical power of an association study is defined as the likelihood that it will correctly detect a specific true association (Cardon & Bell, 2001). The purpose of a power analysis is to determine the minimum study group size that would enable us to detect a specific effect size. For such a calculation to be informative, we would have to select a minimum specific effect size and be able to increase our study population accordingly were it not sufficiently large. The power of the current study was not formally estimated for a number of reasons. Firstly, although HCM hypertrophy modifier investigations typically report small effect sizes (Lechin *et al.*, 1995; Mayosi *et al.*, 2003), the candidate modifiers presented here were tested in an HCM cohort in this study for the first time, and we were unsure of what type of effect sizes to anticipate. Secondly, as this study is considered to be an explorative investigation, i.e. hypothesis-generating, we wanted to report all effects and not merely those above a given cut-off. Furthermore, the maximum possible sample size was already utilised, as all consenting members of the HCM cohort were included in the evaluations, and there were no means of increasing the cohort size at present. Finally, no power calculation has been derived for family-based association studies comprising extended pedigrees.

Rather, the study aimed to optimise the factors, other than genetic effect size, that are known to influence power; these included disease allele frequency (marker informativeness) and the accuracy of both the phenotype definition and genotyping results (Cardon & Bell, 2001; Gordon & Finch, 2005).

#### 4.1.5 SNP selection

The informativeness of a given marker is characterised by a number of factors, including its MAF and its ability to represent the variability throughout a given gene in a specific population. Strong statistical power is required to draw meaningful conclusions about rare alleles. Functional variants typically have low heterozygosity values that may compromise the power of an association study and SNP prioritisation according to potential functional significance is therefore less suitable (Shastry, 2007). Markers with relatively high MAFs are therefore considered more appropriate, i.e. informative, for modifier studies in complex diseases where the effect sizes are typically small, such as HCM. This is also true in instances where the study population is relatively small; and our own study cohort is modest in size given the estimated prevalence of HCM of 1 in 500 in young adults.

The potential exists, given the occurrence of LD amongst markers, to capture the total variation throughout a gene of interest by genotyping only a subset of all the variants therein. The LDU method of selection can minimise the number of SNPs required to accurately capture the variability throughout a candidate gene, owing to the observation that the human genome comprises sizeable regions of high-LD interspersed with short segments of very low LD (Goldstein, 2001;Daly *et al.*, 2001). The literature suggests that a small number of tag-SNPs can sufficiently represent the haplotype structure of these high LD regions and that the LDU method can, therefore, reduce cost and genotyping effort without a significant loss of power (Patil *et al.*, 2001;Johnson *et al.*, 2001;Zhang *et al.*, 2002). Moreover, Maniatis *et al.* (2005) described greater power for association mapping when utilising LDU compared to a kb map (Maniatis *et al.*, 2005).

In order to take into account the afore-described factors upon marker selection we would require the relevant SNP detail specific to our study population. However, a comprehensive study of LD in all the populations in South Africa is still needed. To circumvent this limitation, one could refer to a suitable reference population. De Bakker *et al.* (2006) demonstrated that tag-SNPs validated in HapMap population samples could efficiently capture the common genetic variation in samples from multiple populations, i.e. tag-SNP transferability (de Bakker *et al.*, 2006).

A further means to amplify the informativeness of selected markers is to perform haplotype analyses. Moreover, the literature suggests that the power and robustness of association tests are increased when using haplotypes relative to single SNPs (Akey *et al.*, 2001). Haplotype analyses may provide valuable information relevant to fine mapping and/or the effect of the specific allele combination on the trait i.e. effect of a single variant within the context of the relevant gene (Schaid *et al.*, 2002;Marian, 2002). The latter specifically refers to epistatic interactions where the phenotype is significantly influenced not by individual SNP effects, but rather by the interactions between multiple SNPs. Alternatively, individual SNPs may influence the phenotype, but may do so to a lesser degree than the corresponding SNP-derived haplotypes; e.g. individual variants may show weak effects, but their cumulative effects observed upon haplotype analysis will provide a more significant association (Winkelmann *et al.*, 2003;Newton-Cheh & Hirschhorn, 2005). This is of specific relevance given that candidate modifier genes investigated in HCM to date have yielded small effect sizes (and thus there existed a potential for small effect sizes for the candidates in this study), the complex nature of HCM, and the definition of a modifier as dependent on the context of a given disease-causing mutation.

In this study, the selection of SNPs throughout the relevant candidate genes was achieved by means of the SNPbrowser<sup>TM</sup> v.4.0.1, a free resource that efficiently integrates and displays the information required for SNP-based association study design, thereby affording an easy interface (De La Vega *et al.*, 2006). For example, the software visually depicts SNP positions and density based on either kb (physical map) or LDU distances (metric LD map).

In an effort to select informative markers congruent with the afore-described considerations, the present study aimed to achieve an even SNP spacing of 0.5 LDU; and prioritized SNPs with a minimum MAF of 0.05. Moreover, SNPs were selected using the metric LD maps for the HapMap CEU and YRI populations. As mentioned in Chapter 2 (Refer to Section 2.3.2), previous association studies from our own laboratory showed that the LD structure of the CEU and YRI populations, at least in certain gene regions, best represent the as-yet undefined LD structure of the South African population and, thereby the current study cohort. Indeed, this was the case in the current study, as seen upon comparison of most of the MAFs from the current study cohort to those of the CEU and YRI reference populations (Refer to Section 3.4.1). Finally, we included haplotype analyses as a means of capturing the variability throughout the genes investigated; and detecting within-gene epistatic effects. However, no formal statistical test for epistasis was performed in the present study.

#### **4.1.6 Phenotypic heterogeneity**

As described for population stratification, comprehensive and accurate phenotype definition and ascertainment is imperative in optimizing the power and reproducibility of an association study so as to avoid spurious or null association (Rao & Gu, 2008). In HCM, this proves challenging owing to the marked phenotypic heterogeneity of this complex disease, especially with respect to the extent and distribution of cardiac hypertrophy. As a consequence, no single measure can adequately capture the degree of hypertrophy throughout the entire cohort. Composite scores that integrate a number of hypertrophy measurements to circumvent this problem, but the issue of which score best reflects the hypertrophy phenotype remains unresolved.

In the present study, segmental analysis of the LV wall, i.e. 16 wall thickness measurements at three levels of the heart (Refer to Section 2.1.2), was achieved by means of echocardiography. Although not as sensitive and reproducible as evaluation via cardiac magnetic resonance imaging (cMRI), the



method is less costly and more readily available (Reviewed by Bauml & Underwood, 2010). To minimise measurement error, evaluations were performed according to a standardised protocol by a single experienced echocardiographer who was kept blinded to participant mutation status. Echocardiographically derived LVM was determined as it is a descriptor often used in the literature, thus allowing for comparison to similar studies. However, its accuracy as an estimate of hypertrophy is limited by the underlying assumption of ellipsoid geometry. PCA was, therefore applied to the wall thickness measurements to define a single cohort-specific measure, PC1, which comprehensively captures ventricle-wide hypertrophy and so the variability in LVH. In addition, we used single measurements of maximum hypertrophy as estimates of the extent of hypertrophy. To ensure accurate statistical analysis, trait values were transformed to approximate normality, thereby accommodating a key assumption of the association test employed.

#### **4.1.7 Genotyping approach**

The ABI Validated TaqMan® genotyping platform proved to be more efficient than the PCR-based methods previously utilised to genotype the current cohort as it offers a number of advantages pertaining to assay design, reaction setup and data analysis.

Taqman® assays are pre-designed and validated, thereby eliminating the need for costly and time-consuming design, optimization and verification (e.g. additional sequencing). In the present study, 5 µl reactions were set up within 384-well plates by means of an automated pipetting tool, thus ensuring high-throughput, reproducibility and accuracy, whilst minimising cost and human error. In addition, the technique is DNA-sparing, as assays require a starting template in the range of only 5-20 ng. Sample amplification, end-point data collection and automatic allele calling via the SDS software, as derived from sample fluorescence signals, are all achieved on the ABI Prism 7900HT Sequence Detection System (Applied Biosystems Inc, Foster City CA, USA), thus avoiding post-PCR processing. To ensure stringent genotype assignment the quality value of the SDS autocaller was kept at the default  $\geq 95.0$  with samples below this cut-off marked as undetermined. Genotyping results were exported to text file format for direct import into the existing database further minimising human error, i.e. typographical errors. Collectively, the use of pre-designed assays and the afore-described largely automated protocol provides accurate and reproducible results.

It should be mentioned that conventional PCR-based genotyping methods remain less expensive than the ABI Validated TaqMan® genotyping system on a sample by sample basis, and that not all SNPs are available in the collection of predesigned assays. A TaqMan® custom assay service is available, but requires optimization and verification of accuracy.

## 4.2 Association analyses results

The research efforts of our laboratory are directed toward identifying genes that modify the development of hypertrophy in South African HCM families. The seemingly monogenic disease was investigated at the outset as a simpler genetic model of hypertrophy, as the LVH occurs in the absence of precipitating clinical factors. However, the observation of extreme phenotypic heterogeneity in HCM, even amongst members of the same family, highlighted the contribution of gene modifiers. Our research aims were expanded accordingly, with the current study focused on investigating sarcomeric genes and genes related to myocardial energetics as candidate modifiers of hypertrophy. The results of the investigations of this study will be discussed in the following sections. All significant associations reflect p-values calculated following adjustment for all relevant hypertrophy covariates and family relatedness. These adjustments are detailed in the foregoing section (Refer to Sections 4.1.1 and 4.1.3).

### 4.2.1 Sarcomeric genes

The sarcomeric genes included in this study have all, with the exception of *ACTN3*, previously been implicated in the development of HCM as causal mutations (Refer to Section 1.2.1). They were, therefore revisited with the aim of here evaluating their capacity to modify, as opposed to directly causing, the development of hypertrophy in HCM within the current cohort.

#### i) $\alpha$ -Actin

Muscle contraction essentially entails sliding of the thin filaments past the thick filaments. Actin is the major constituent of the thin filament and, therefore contributes to sarcomere structure and enables contraction. The main isoform in the heart, cardiac  $\alpha$ -actin, is encoded by the *ACTC1* gene (Bertola *et al.*, 2008; dos Remedios *et al.*, 2003; Laing & Nowak, 2005).

The *ACTC1* SNPs, rs1370154 and rs2070664, revealed significant haplotype effects. The effect of the CC haplotype was an estimated decrease of 0.51 mm in mIVST and it is, therefore considered to be cardioprotective. Conversely, the effect of the CT haplotype was an estimated increase of 1.55 mm in mIVST and 1.05 mm in mLVWT. The third haplotype, TT, did not have a significant effect on any of the traits. These effects were found in the absence of significant single SNP effects or significant differences in SNP/haplotype effect amongst the mutation groups. The two SNPs were found to be in complete LD based on the point estimate of  $D' = 1$ . Collectively, the results suggest that the observed effects may be ascribed to the combined effects of the two SNPs, or markers with which they are in LD.

Both SNPs are at present functionally uncharacterised, and are located in the 3' untranslated region (3' UTR) and an intron, respectively (<http://www.ncbi.nlm.nih.gov/SNP>). This prompted *in silico* evaluation by means of the splice site prediction program Netgene2 (Brunak *et al.*, 1991; Hebsgaard *et al.*, 1996). *In silico* evaluations refer to computer-based computational algorithms, i.e. bioinformatic tools, used to predict, in this instance, splice motifs in the human. Briefly, the predictive algorithm is accessed online with the variant and its flanking sequences serving as input. The alternative alleles of a given variant are analysed individually and the respective outputs comprising the various predicted splice motifs are then compared to identify any difference in sequence recognition. *In silico* analyses did not reveal significant functional consequences for either of the two variants as no splice site alterations were observed. The SNPbrowser<sup>TM</sup> v.4.0.1 LD maps for both the CEU and YRI populations indicated that the numerous variants found to be in LD with the investigated SNPs are all positioned intronically (<http://www.ncbi.nlm.nih.gov/SNP>, SNPbrowser<sup>TM</sup> v.4.0.1). Although not assessed *in silico*, any functional effect of these intronic SNPs in LD with the two associated SNPs is not immediately obvious.

## ii) Myosin

Myosin is the main component of the thick filament and its (biological) interaction with actin as well as its role in ATP binding and hydrolysis is central in muscle contraction. The ventricular isoform,  $\beta$ -MHC, is encoded by *MYH7* with mutations therein previously characterised as HCM-causing, two of which, R403W<sub>MYH7</sub> and A797T<sub>MYH7</sub>, segregate in the current cohort as founder mutations (Daloz *et al.*, 2001) (Refer to Sections 1.2.1 and 2.3.3.1).

The T-allele of rs2277475 presented as cardioprotective as its effect was an estimated decrease of 1.19 mm in mLVT, 8.64 mm in the CWT score and 0.54 in PC1. The A-allele, under the additive allelic model, would thus result in a corresponding increase in these measures. Significant associations with the CWT score require further interpretation, as the trait reflects the sum of the 16 independent wall thickness measurements. Therefore, an 8.64 mm decrease in CWT, as seen for the T-allele of rs2277475, represents an average decrease of ~0.54 mm (8.64/16) in each of the 16 measurements. LD evaluation revealed that the SNP is in complete LD with the two founder mutations, based on the point estimates of  $D' = 1$  (Refer to Table 3.14). However, statistical adjustments for founder mutation carrier status were incorporated and the observed effects can thus be ascribed to the variant itself or variants, other than the founder mutations, with which it is in LD.

The SNP is intronic and *in silico* evaluations were performed as described for *ACTC1* (<http://www.ncbi.nlm.nih.gov/SNP>). The comparisons revealed no splicing motif alterations and the SNP is, therefore unlikely to be of functional consequence (Brunak *et al.*, 1991; Hebsgaard *et al.*, 1996). Next, non-synonymous coding variants in LD with the associated SNP were considered, as they may be more likely to be functionally significant. Identification of such SNPs was achieved using the LD structures of the HapMap CEU and YRI populations, as amongst the HapMap data, these populations best represent the current study cohort (Refer to Sections 2.3.2 and 4.1.5, SNPbrowser<sup>TM</sup> v.4.0.1). A single variant, rs3729823, was in LD with rs2277475, and has been characterized as a missense mutation that entails the substitution of the neutral polar Serine (Ser) with the neutral, slightly polar Cysteine (Cys) (TCC → TGC; S1491C) (<http://www.ncbi.nlm.nih.gov/SNP>). The effects of the amino acid substitution on protein function was predicted using the SIFT algorithm, which showed it to be tolerated (Kumar *et al.*, 2009). HCM studies have reported the presence of the variant at low frequencies in both HCM patients and controls (Blair *et al.*, 2002; Hougs *et al.*, 2005). This led Hougs *et al.* (2005) to describe it as a relatively rare polymorphism in the control population and to suggest that it may act as disease modifier. Furthermore, variants rs2277475 and rs3729823 were detected upon mutation screening of patients harbouring functionally identical Dutch truncating *MYBPC3* founder mutations namely c.2373dupG, p.Arg943X or c.28644\_2865delCT. The study did not report the exact combinations detected but discussed that the complex sarcomeric genetic status observed in their investigation did not significantly modify the severity of the HCM phenotype (Michels, 2011).

Moreover, the LD blocks of both the YRI and CEU populations extend to the neighbouring *MYH6* gene, and function-altering, non-synonymous coding variants therein may thus also play a modifying role. A single variant, rs442275, was in LD with rs2277475 in both CEU and YRI HapMap populations. Defined as a missense mutation, it leads to the substitution of Glutamic acid (Glu) by Glutamine (Gln) (CAG → GAG; E88Q), which, according to the SIFT analysis (Kumar *et al.*, 2009), is predicted to be damaging to function (<http://www.ncbi.nlm.nih.gov/SNP>). Replacement of the acidic polar Glu with the neutral polar Gln may affect protein tertiary structure, and, thereby, protein interactions/function. Although the mutation itself has not been linked to HCM, the possibility cannot be excluded, as defects in *MYH6* have proven to be HCM-causing (Refer to Section 1.2.1). Thus, the significant single SNP association of rs2277475 may reflect the as yet unknown consequence of the SNP itself, or the effect of an exonic (rs3729823 in *MYH7* or rs442275 *MYH6*) or intronic variant(s), in either *MYH6* or *MYH7*, with which it is in LD. The most significant variants are believed to be located within exons and they should, therefore be prioritised for further evaluation within a different and larger cohort and on a functional level.

The rs2277475 SNP also demonstrated significant differences in effect amongst the HCM founder mutation groups. The effect of the T-allele was higher in the R403W<sub>MYH7</sub> group relative to both the A797T<sub>MYH7</sub> (18.2 mm for the CWT score and 1.14 for PC1) and R92W<sub>TNNT2</sub> groups (24.8 mm for the CWT score and 1.55 for PC1). Therefore, the degree of variation in the CWT score and PC1 measures as a result of rs2277475 (or a variant with which it is in LD) is significantly dependent on the causal mutation with which it occurs, i.e. there is SNP and founder mutation group interaction.

This observation is somewhat surprising, considering that the statistical analyses corrected for the effect of individual founder mutations, which would lead one to expect that the effect size of the associated SNP would be equal across the founder mutation groups. One possible explanation for this is that the result reflects the influence of secondary mechanisms flowing from the effects of the founder mutations. More specifically, the effect of the modifier allele is context dependent, with the latter dictated by the direct consequences of the individual founder mutations and/or the resulting activation of signalling cascades and trophic factors (Marian *et al.*, 2001) (Refer to Section 1.2.4). The exact secondary consequences and the time of activation thereof may vary amongst the primary causal mutations. That is, the numerous HCM-causing mutations may place varying degrees of stress on the sarcomere, giving rise to different secondary pathway profiles, including those involved in calcium handling and energy metabolism. Indeed, the molecular pathways implicated in

the development of HCM have been described as diverse and partially independent, and it is here where the difference in modifier effect may manifest (Marian, 2010). Considered on a biological level, the modifier protein may directly interact with the mutated protein encoded by a HCM causal mutation and/or perhaps with a protein in a secondary signalling pathway. A specific modifier allele may therefore be more or less relevant within different secondary pathways and at various stages of disease development.

In contrast, the effect rs2277475 on mLVWT did not vary amongst the founder mutation groups. The SNP had a significant effect on this measure when the entire cohort was considered, but no significant difference in its effect on mLVWT was detected upon pair-wise comparison between mutation groups. Similar results were observed for a number of genes and this clarification is thus applicable to the relevant SNPs/haplotypes that are yet to be discussed.

Significant differences in haplotype effects were observed for two haplotypes that differ with respect to the rs2277475 and rs2239578 variants (relevant alleles are underlined). The effect of the TTGCG haplotype was lower on PC1 (1.84) in the R92W<sub>TNNT2</sub> group relative to the R403W<sub>MYH7</sub> group. The effect of the TAGCA haplotype was higher in the R92W<sub>TNNT2</sub> group relative to the R403W<sub>MYH7</sub> group: 58.4 g on LVM, 36.7 mm on the CWT score and 2.29 on PC1. These results reflect combined SNP effects (combined effects of loci contained in the haplotype or variants with which they are in LD) as they do not mirror the single SNP effect of rs2277475; and these haplotype effects are significantly influenced by the founder mutation context in which they occur. Certain comparisons could not be made owing to the unequal distribution of haplotypes in the three HCM mutation groups, e.g. haplotype TTGCA (Refer to Table 3.24). However, the lack of significant differences in effect for the TAGCG haplotype suggests that the haplotype effect may involve rs2239578 or a marker with which it is in LD.

The rs2239578 SNP is intronically positioned and relevant *in silico* evaluations were performed. Netgene2 evaluations revealed no difference in splice site signals (Brunak *et al.*, 1991; Hebsgaard *et al.*, 1996). A single exonic variant, rs2069540, was found to be in LD with rs2239578, but it is characterised as a synonymous coding SNP. It should be noted that the haplotype effects may reflect the combined effects of other variants within the haplotype. It is, however, clear that the TTGCG and TAGCA haplotypes modify the development of hypertrophy in the current cohort and the extent of their effects is significantly influenced by the founder mutation context.

It is necessary to re-emphasize the results of rs2277475. Alone, it had a significant effect on the CWT score, PC1 and mLVT. However, within the context of a haplotype, i.e. when considering its effect collectively with the effects of other variants in the gene (that is within gene context) its effects varied significantly: (rs2277475 is underlined) TAGCG influenced LVM, the CWT score and PC1, whilst TAGCA did not influence any of the traits. Similar ‘within gene context’ effects were observed for several of the genes yet to be discussed and this clarification should thus be considered where applicable in the remainder of the discussion.

### iii) The Troponin (Tn) complex

The Tn complex, consisting of TnT, TnI and TnC, regulates muscle contraction via its association with tropomyosin, the molecule that overlays the myosin binding site on actin. More specifically, the complex undergoes a conformational change in response to Ca<sup>2+</sup>-binding, which facilitates the movement of tropomyosin from its inhibitory position, allowing for crossbridge formation and muscle contraction (Reviewed by Chapelle, 1999).

#### a) Troponin T

TnT links the Tn complex to tropomyosin, whilst also binding actin and regulating actomyosin ATPase activity. The four known cardiac isoforms are all encoded by *TNNT2* and variants therein have previously been implicated in HCM development (Dalloz *et al.*, 2001; Anderson *et al.*, 1995; Zot & Potter, 1987). One of the HCM-causing mutations therein, R92W<sub>TNNT2</sub>, segregates in the current cohort as a founder mutation (Refer to Sections 1.2.1 and 2.3.3.1).

LD evaluation showed that all the investigated variants are in complete LD with one another as well as with the founder mutation (point estimates of D' = 1). Statistical adjustments for founder mutation carrier status were incorporated into the evaluations and the lack of statistically significant single SNP association confirms the adequacy thereof.

The effect of the A-allele of rs2365652 was higher on mIVST (2.30 mm) in the R92W<sub>TNNT2</sub> group relative to the A797T<sub>MYH7</sub> group. The rs2365652 variant is positioned intronically and *in silico* evaluation was performed (<http://www.ncbi.nlm.nih.gov/SNP>). The Netgene2 evaluations did not show any splice signal alterations and the observed result is either due to the as yet unknown effects

of rs2365652, or more likely as a result of a variant(s) with which it is in LD (Brunak *et al.*, 1991; Hebsgaard *et al.*, 1996). The variant is in LD with two coding, non-synonymous variants, namely rs4523540 (AAC → TAC; N276Y) and rs2996496 (AGA → AAA; R139K) (<http://www.ncbi.nlm.nih.gov/SNP>, SNPbrowser<sup>TM</sup> v.4.0.1). SIFT predictions indicated that the first comprises a potentially functionally damaging amino acid substitution (Kumar *et al.*, 2009). The change is characterised as a change from the neutral polar Aspartic acid (Asp) to the also neutral polar Tyrosine (Tyr); however, the latter is considered to be more polar owing to its hydrocarbon benzene ring (<http://www.elmhurst.edu/~chm/vchembook/561aminostructure.html>). The SNPs themselves have, to date, not been functionally characterised or linked to disease development. The effect of rs2365652 (or a variant with which it is in LD) on the hypertrophy phenotype is significantly influenced by the founder mutation with which it occurs, i.e. there is variant and mutation group interaction. To clarify, rs2365652 may have an effect in one founder mutation group and the opposite, or no effect in the other(s), and as a result no significant effect was observed when the combined cohort was considered. This explanation also applies to similar results, i.e. significant differences in SNP/haplotype effect amongst the mutation groups in the absence of significant SNP/haplotype effects in the total cohort, observed for a number of genes still to be discussed.

The AAIG and CGIA haplotypes indicated significant differences in haplotype effect amongst the three mutation groups. The effect of the first was higher on LVM (23.5 g;  $p = 0.028$ ) in the R403W<sub>MYH7</sub> group compared to the A797T<sub>MYH7</sub> group. The effect of the second was lower on mIVST (12.57 mm;  $p = 0.008$ ), mLVWT (11.34 mm;  $p = 0.034$ ) and the CWT score (89.4 mm;  $p = 0.034$ ) in the R403W<sub>MYH7</sub> group relative to the A797T<sub>MYH7</sub> group. These results do not reflect the afore-described significant SNP effects; therefore these haplotype effects suggest that the trait variance can be ascribed to the combined effects of variants contained within the respective haplotypes. Certainly, the extent to which the SNPs/haplotypes modify the hypertrophy in HCM is significantly influenced by the specific founder mutation with which it presents.

## **b) Troponin I**

TnI is responsible for the binding of actin and, thereby the inhibition of actomyosin ATPase activity. Moreover, it conveys the conformational signal from TnC to TnT and tropomyosin. The cardiac isoform of TnI is encoded by *TNNI3* and a total of three SNPs therein was selected for



statistical evaluations (Daloz *et al.*, 2001; Reviewed by Filatov *et al.*, 1999). However, genotyping of the rs3729841 variant showed an uninformative number of heterozygous individuals and it was, therefore, excluded from further analyses. The variant is characterized as a synonymous change in the coding region.

LD evaluation indicated that the remaining two SNPs are in complete LD ( $D' = 1$ ). The effects of these SNPs varied significantly amongst the mutation groups: the effect of the G-allele of rs3729838 was higher on mLVWT (2.45mm); and the effect of the G-allele of the rs11667847 variant was higher on LVM (34.3 g) in the R92W<sub>TNNT2</sub> group compared to the R403W<sub>MYH7</sub> group. The effect of these SNPs (or variants with which they are in LD) on the hypertrophy phenotype is thus significantly influenced by the founder mutation with which it occurs, i.e. variant and mutation group interaction was present. To reiterate, they may have an effect in one founder mutation group and the opposite, or no effect in the other(s), and as a result no significant effect was observed upon consideration of the combined cohort. The SNPs are located intronically and *in silico* predictions were thus performed to determine their potential effects on mRNA splicing (<http://www.ncbi.nlm.nih.gov/SNP>). The Netgene2 evaluations did not indicate any splice signal alterations (Brunak *et al.*, 1991; Hebsgaard *et al.*, 1996). All the exonic variants shown to be in LD with the investigated SNPs are defined as synonymous changes (<http://www.ncbi.nlm.nih.gov/SNP>, SNPbrowser<sup>TM</sup> v.4.0.1).

Significant differences in haplotype effects were observed for haplotypes CA and GA. The effect of the first was lower on mLVWT (1.97 mm) in the R92W<sub>TNNT2</sub> group relative to the R403W<sub>MYH7</sub> group. The effect of the second was higher on mIVST (3.7 mm) and mLVWT (3.46 mm) in the R92W<sub>TNNT2</sub> group relative to the R403W<sub>MYH7</sub> group. Also, its effect was higher on mLVWT (4.47 mm) in the A797T<sub>MYH7</sub> group compared to the R403W<sub>MYH7</sub> group. These results do not reflect the afore-described significant SNP effects; therefore these haplotype effects suggest that the trait variance can be ascribed to the combined effects of variants contained within the respective haplotypes. Moreover, the extent to which the SNPs/haplotypes modify the hypertrophy in HCM is significantly influenced by the specific founder mutation with which it presents.

#### iv) $\alpha$ -Tropomyosin

The  $\alpha$ -TM protein, encoded by *TPM1*, binds actin, thereby stabilising and stiffening the thin filament. In addition, it regulates muscle contraction as is clear from the preceding sections (Daloz *et al.*, 2001; Weigt *et al.*, 1990).

The C-allele of rs1071646 associated with increases in all hypertrophy traits: 17.3 g in LVM, 2.02 mm in mIVST, 1.75 mm in mLVWT, 0.59 in mPWT, 17.68 mm in the CWT score and 1.10 in PC1. Cardioprotective effects were observed for the C-allele of the rs11071720 variant associated with a decrease of 0.49 mm in mPWT whilst the C-allele of the rs707602 variant associated with increases of 1.0 mm in mLVWT and 0.83 mm in mPWT. LD estimates showed only the rs1071646 and rs707602 variants to be in complete LD ( $D' = 1$ ).

Significant differences in SNP effect amongst the founder mutation groups were also observed. The effect of the C-allele of the rs11071720 variant was higher on mIVST (2.65 mm) in the R92W<sub>TNNT2</sub> group relative to the A797T<sub>MYH7</sub> group. The effect of the T-allele of the rs4238370 variant was lower in the R92W<sub>TNNT2</sub> group compared to the A797T<sub>MYH7</sub> group: 48.1 g for LVM, 3.84 mm for mIVST, 4.84 mm for mLVWT, 45.6 for the CWT score and 2.85 for PC1. Also, its effect was lower in the R403W<sub>MYH7</sub> group relative to the A797T<sub>MYH7</sub> group: 3.99 mm on mIVST, 35.8 on the CWT score and 2.23 on the PC1 measure. Collectively, these findings suggest that the extent to which the SNPs effect hypertrophy development is significantly influenced by the founder mutation context. As explained in previous paragraphs the effect of a SNP may vary greatly amongst the founder mutations i.e. its effect in one founder mutation group(s) may be masked by its opposite or no effect in the other(s) and as a result no significant association signal is observed upon consideration of the entire cohort. This may be the case for rs4238370, as it showed significant difference in effect amongst the mutation groups, but no significant single SNP effect in the total cohort.

The rs11071720 and rs4238370 SNPs are both intronic (<http://www.ncbi.nlm.nih.gov/SNP>). The rs707602 SNP is positioned within the 3'-UTR and the rs1071646 SNP is characterised as a synonymous coding variant. The relevant *in silico* evaluations were performed to predict their potential functional significance. However, no significant differences in recognition of splice site motifs were identified (Brunak *et al.*, 1991; Hebsgaard *et al.*, 1996). The literature recently identified an association between the rs11071720 polymorphism and mean platelet volume (MPV)

stating that myosin-actin interaction is key in platelet formation (Soranzo *et al.*, 2009). However, the variant is yet to be implicated in hypertrophy development and functionally characterised. Similarly, the remainder of the SNPs have not been linked to disease or evaluated on a functional level. According to the LD structures of the HapMap CEU and YRI populations, all the variants are in LD with one another and a single coding, non-synonymous SNP namely rs1131003. The missense mutation is characterised a change from the acidic polar Glu to the neutral polar Gln (GAA → CAA; E196Q) and predictions with SIFT suggested that the change is tolerated (Kumar *et al.*, 2009). This mutation too is yet to be functionally characterised or and evaluated within the context of disease development.

Statistically significant haplotype effects were identified for CGAT, CTCT and CGCT. The effect of the first was an estimated decrease of 18.1 g in LVM, 0.78 mm in mPWT, 9 mm in the CWT score and 0.56 in PC1. Conversely, the effect of the second was an estimated increase of 3.21 mm in mIVST, 3.13 mm in mLVWT, 30.2 mm in the CWT score and 1.89 in PC1. The effect of CGCT was an estimated increase of 47.9 g in LVM. The results do not mirror the observed significant SNP effects. More strikingly, CGAT and CGCT differ only with respect to rs4238370 (underlined), but show very different trait profiles. Collectively the results suggest that the trait variance can be ascribed to the combined effects of variants contained within the respective haplotypes.

The CGAT haplotype that showed significant haplotype effects, as well as a further haplotype, TGCT, indicated significant differences in haplotype effects amongst the HCM founder mutation groups. The effect of the CGAT haplotype was higher on mIVST (2.98 mm) and the CWT score (18.4 mm) in the R92W<sub>TNNT2</sub> group relative to the R403W<sub>MYH7</sub> group. Also, its effect was higher in the R403W<sub>MYH7</sub> group compared to the A797T<sub>MYH7</sub> group: 3.88 mm on mIVST, 28.5 mm on the CWT score and 1.78 on PC1. The effect of the TGCT haplotype was lower on LVM (105 g) in the R92W<sub>TNNT2</sub> group relative to the A797T<sub>MYH7</sub> group whilst its effect was higher on LVM (105.5 g) in the R92W<sub>TNNT2</sub> group compared to the R403W<sub>MYH7</sub> group. The effects of haplotypes CGAT and TGCT on the hypertrophy phenotype are thus significantly influenced by the founder mutation context.

## v) The myosin light chains

The functions of the myosin light chains, ELC and RLC, are twofold as they contribute to sarcomere structure and regulation of contractility (Poetter *et al.*, 1996). The cardiac RLC and ELC are encoded by *MYL2* and *MYL3*, respectively, and mutations in both have been implicated in the development of HCM (Colson *et al.*, 2010; Harris *et al.*, 2011; Taylor *et al.*, 2004; Schaub *et al.*, 1998).

### a) *MYL2*

The A-allele of rs933296 appeared to be cardioprotective as its effect was an estimated decrease of 13.6 g in LVM, 9.57 mm in the CWT score and 0.60 in PC1. The significant haplotype effects observed for the AC and AG haplotypes were also seemingly cardioprotective. The effect of the first was an estimated 25.1 g decrease in LVM, whilst the effect of the second was an estimated decrease of 0.60 in PC1. The significantly associated haplotypes, interestingly, share the A-allele of the significantly associated rs933296 variant, whilst varying with respect to the alleles of the non-significantly associated rs4766517 variant. Moreover, the two significant haplotype associations are with different traits. Collectively, the results suggest the presence of combined effects of the associated SNP and the second investigated SNP (or a SNP with which it is in LD). This again motivates the importance of investigating the effect of SNPs within the context of the entire gene.

The rs933296 and rs4766517 variants are positioned intronically and in the 5' near gene region, respectively. *In silico* evaluations were performed to determine their potential effects on mRNA splicing (<http://www.ncbi.nlm.nih.gov/SNP>, SNPbrowser<sup>TM</sup> v.4.0.1). Netgene2 evaluation of the significantly associated rs933296 indicated that the C-allele thereof was characterised by the recognition of an additional donor splice site relative to the A-allele.

Briefly considered, intronic variants may affect splicing in a number of ways. In instances where variants give rise to additional intronic sequences homologous to donor and acceptor sites, the possibility exists that it would be recognised and a part of the intron then retained in the mRNA. This, in turn, may disrupt the splicing of the succeeding exon and in case of a frameshift, the coding of all of the remaining exons. If a variant leads to the loss of such a donor or acceptor site, splicing of a given exon may be skipped. Although such changes may only affect a section of the mRNA it

could ultimately disrupt functional domains and/or the 3D structure of the entire protein and significantly influence the disease phenotype.

We could hypothesize that the C-allele gives rise to aberrant mRNA splicing given its association with increased measures of LVM, the CWT score and PC1. The variant is positioned in intron 3 and it may therefore significantly influence splicing of exon 4 (and the eventual DNA reading frame) (Andersen *et al.*, 2001; <http://www.ncbi.nlm.nih.gov/SNP>). RLC mutations are typically associated with mild or benign phenotypes. However, exceptions include the R58Q<sub>MYL2</sub> mutation located in exon 4, which gives rise to a malignant phenotype characterised by increased LVWT, early onset and SCD (Harris *et al.*, 2011;Mettikolla *et al.*, 2011;Mettikolla *et al.*, 2011;Kabaeva *et al.*, 2002;Flavigny *et al.*, 1998).

Greenberg *et al.* (2010) described that the RLC surrounds and thereby supports the  $\alpha$ -helical myosin neck region (lever arm); and that this localization modulates force and movement by allowing energy transmission from the site of ATP hydrolysis (catalytic site) down the neck domain. They further described that the RLC may influence the mechanical properties of the lever arm which, in turn, determines the degree of force transmission from the myosin lever arm to the catalytic site i.e. strain-sensing. The latter is essential as the myosin cycle kinetics is strain-dependent. In support thereof, they describe that mutations that reduce the stiffness of the lever-arm give rise to mutant myosins that exhibit a reduction in force. The R58Q<sub>MYL2</sub> mutation abolishes the Ca<sup>2+</sup> binding capacity and, as result, the structure of the RLC. Such changes may affect the ability of the RLC to stabilize the  $\alpha$ -helical myosin neck region and so the transmission of strain. Moreover, R58Q<sub>MYL2</sub> mutant transgenic mouse myosins exhibit reduced force and power output (Greenberg *et al.*, 2010;Harris *et al.*, 2011). Considered within the context of these findings, the rs933296 variant may, similarly, influence the stiffness and strain-sensing ability of the  $\alpha$ -helical myosin neck ultimately leading to a compensatory hypertrophy phenotype as reflected in its significant association with LVM, the CWT score and PC1.

Allelic comparison of the rs476617 variant did not indicate differences pertaining to the recognition of splicing acceptor or donor sites suggesting that it may have an as yet undetermined functional consequence (Brunak *et al.*, 1991;Hebsgaard *et al.*, 1996). Alternatively, the observed results may be attributed to the effects a functional variant(s) in LD with rs933296 and/or rs476617. However, all of the coding variants shown to be in LD with the two investigated SNPs are characterised as

synonymous changes (SNPbrowser<sup>TM</sup> v.4.0.1 software). The SNPs themselves have, to date, not been functionally characterised or implicated in disease.

## b) *MYL3*

SNPs rs1531136 and rs3792558 revealed significant haplotype effects in the absence of significant SNP effects. This suggests that the trait variance can be explained by the combined effects of variants contained within the haplotype which are not significantly influenced by the founder mutation context. The CC haplotype was seemingly cardioprotective as its effect was an estimated decrease of 8 g in LVM, 0.32 mm in mPWT, 3.7 mm in the CWT score and 0.23 in PC1. The effect of the TC haplotype was an estimated increase of 25.6 mm in the CWT score and 1.6 in PC1. LD estimates indicated complete LD between the two SNPs ( $D' = 1.00$ ). It is important to note that a third haplotype, TT, was observed, but was not significantly associated. The result clearly points to complex haplotype interactions, either amongst the investigated SNPs or between variants with which they are in LD. According to the SNPbrowser<sup>TM</sup> v.4.0.1 software, all of the coding variants shown to be in LD with the two investigated SNPs are characterised as synonymous changes. To date, neither of the SNPs have been linked to disease or characterised functionally.

The two investigated variants are both positioned within introns; therefore, *in silico* evaluations were performed to determine their potential effects on mRNA splicing (<http://www.ncbi.nlm.nih.gov/SNP>, SNPbrowser<sup>TM</sup> v.4.0.1). The rs1531136 variant did not indicate any differences in splice site motifs upon Netgene2 investigation (Brunak *et al.*, 1991; Hebsgaard *et al.*, 1996). Significantly, Netgene2 evaluation of the rs3792558 showed differences in recognition of splice sites with the identification of an additional donor motif upon analysis of the T-allele (complementary strand) relative to the C-allele. The variant may thus give rise to aberrant mRNA splicing that, given its position in intron 1, could significantly affect the splicing of exon 2 (and potentially the reading frame of all succeeding exons). According to our knowledge, all *MYL3* HCM-causing mutations identified to date are located within either exon 3 or 4 (Andersen *et al.*, 2012; Harris *et al.*, 2011). Interestingly, the predicted domain structure as determined by Hernandez *et al.* (2007) suggests that parts of exons 2 and 3 code for the EF-hand  $Ca^{2+}$ -binding motif (EF1 domain). We can therefore look to the known mutations within the relevant section of exon 3 as predictive of the effects of our significantly associated variant, namely E56G<sub>MYL3</sub>, A57G<sub>MYL3</sub>, V79L<sub>MYL3</sub> and R81H<sub>MYL3</sub>. The ELC interacts with the myosin IQ1 motif, thereby stabilising the

lever arm of the myosin head and ensuring normal force production (Hernandez *et al.*, 2007; Andersen *et al.*, 2012). The E56G<sub>MYL3</sub> and A57G<sub>MYL3</sub> mutations are located in the  $\alpha$ -helix of the EF-hand. Significantly, the E56G<sub>MYL3</sub> mutation reduces binding to the myosin lever arm (30-fold reduced binding) (Lossie *et al.*, 2012). Moreover, the V79L<sub>MYL3</sub> and R81H<sub>MYL3</sub> mutations are located close to the IQ1 motif and they may thus disrupt the stabilising interaction and give rise to disease. Indeed, *MYH7* mutations within the IQ1 motif have been characterised as HCM-causing (Andersen *et al.*, 2012).

The rs3792558 variant may, in part, explain the significant haplotype effects via aberrant mRNA splicing. More specifically, it may decrease or completely disrupt ELC interaction with myosin, negatively impacting on the stability of the myosin lever arm and ultimately force production.

#### vi) Myosin binding protein C

*MYBPC3* encodes the cardiac myosin binding protein-C, which functions in modulating contraction and stabilising the thick filament (Carrier *et al.*, 1997).

Significant differences in SNP effects were observed amongst the HCM founder mutation groups: the effect of the A-allele of rs4752825 and the T-allele of rs1052373 was higher, 22.6 g and 22.5 g, respectively, on LVM in the R92W<sub>TNNI2</sub> group compared to the A797T<sub>MYH7</sub> group. These results suggest that the extent to which these SNPs modify the hypertrophy phenotype is significantly influenced by the founder mutation context. Also, it is possible that the observed effects actually reflect one another as the effects sizes are nearly identical and the LD between the two SNPs is estimated to be complete ( $D' = 1$ ).

The rs4752825 and rs1052373 variants are positioned within the 5' near gene region and in an exon, respectively (<http://www.ncbi.nlm.nih.gov/SNP>). *In silico* evaluations of the first SNP did not identify any differences in recognition of splice sites (Brunak *et al.*, 1991; Hebsgaard *et al.*, 1996). The second is characterised as a coding synonymous change (GAG  $\rightarrow$  GAA; E1096E) (<http://www.ncbi.nlm.nih.gov/SNP>) (Erdmann *et al.*, 2003). The significant differences in effect are potentially due to the as yet unknown effects of these two SNPs, as neither have been characterized functionally or implicated in disease development. The effects are more likely due to variants in LD

with rs4752825 and/or rs1052373. The LD structures of the HapMap CEU and YRI populations show that these variants are in LD with only coding, synonymous SNPs (SNPbrowser<sup>TM</sup> v.4.0.1).

A significant haplotype effect and statistically significant differences in haplotype effect amongst HCM founder mutation groups was observed; and it did not reflect the significant SNP effects suggesting that the trait variance is due to the combined effects of variants contained within the haplotype. The ATGG haplotype appeared to be cardioprotective as its effect was an estimated decrease of 0.51 mm in mPWT. The effect of ATGA was higher on LVM (65.1 g), mPWT (1.66 mm), the CWT score (8.6 mm) and PC1 (0.54) in the R403W<sub>MYH7</sub> group compared to the A797T<sub>MYH7</sub> group. Also, its effect was higher on LVM (29.9 g) and mPWT (1.25 mm) in the R92W<sub>TNNT2</sub> group compared to the R403W<sub>MYH7</sub> group. Finally, its effect was lower on PC1 (0.05) in the R92W<sub>TNNT2</sub> group compared to A797T<sub>MYH7</sub> group. The effect of GCGG was lower on the LVM measure (36.8 g) in the R403W<sub>MYH7</sub> group compared to the A797T<sub>MYH7</sub> group; and lower on LVM (30.9 g), mPWT (1.13 mm) and PC1 (1.10) in the R92W<sub>TNNT2</sub> group relative to the R403W<sub>MYH7</sub> group. The ATGA and GCGG haplotypes modify the development of hypertrophy with the extent of their effects differing significantly depending on founder mutation context.

#### vii) $\alpha$ -actinin-3

The  $\alpha$ -actinin-3 protein is encoded by *ACTN3* and its function in cardiac muscle is poorly characterised. Based on the functions of  $\alpha$ -actinins in skeletal muscle, this protein is speculated to contribute to cytoskeletal integrity and myocardial energetics at the sarcomere level (Macarthur & North, 2004; Rakus *et al.*, 2003; Hance *et al.*, 1999; Rakus *et al.*, 2003; Squire, 1997). It interacts with signalling proteins, including members of the calsarcin family, which, in turn, bind to the Ca<sup>2+</sup>- and calmodulin-dependent protein phosphatase, calcineurin. The latter has been implicated in the development of skeletal and cardiac muscle hypertrophy (Olson & Williams, 2000; Molkenin *et al.*, 1998). Furthermore, investigation of *ACTN3*-knockout mice, which are homozygous for a premature stop codon (R577X, rs1815739), showed reduced mass in muscles known to express  $\alpha$ -actinin-3. The *ACTN3*-knockout mice and wild-type hearts did not vary in size and the expression of *ACTN3* is believed to be restricted to skeletal muscle (Berman & North, 2010). However, validated *ACTN3* transcripts have been identified in heart muscle and the lack of variation in heart size may be attributable to unknown factors (<http://www.genecards.org/cgi-bin/carddisp.pl?gene=ACTN3&search=actn3>). The functional variant was, therefore included in the



current study. Finally, the protein product of *ACTN2*, an HCM-causing gene (Refer to Section 1.2.1), shares high sequence homology with  $\alpha$ -actinin-3 (Macarthur & North, 2004).

A significant difference in the haplotype effect amongst the mutation groups was observed for the GCC haplotype. Its effect was lower on the PC1 measure (1.02) in the R92W<sub>TNNT2</sub> group compared to that in the R403W<sub>MYH7</sub> group. The absence of any significant single SNP effects suggests that the haplotype effect is due to the combined effects of variants contained within the haplotype. Furthermore, the extent of the haplotype effect on trait variance is significantly influenced by the founder mutation context.

#### 4.5.2 Energy genes

##### i) Fatty acid translocase

The FAT/CD36 gene encodes a protein that facilitates uptake of LCFAs across the sarcolemmal membrane (Harmon & Abumrad, 1993; Aras & Dilsizian, 2007; Luiken *et al.*, 2003). Expression QTL studies in a SHR model indicated that renal CD36 determines both BP and risk of hypertension (Pravenec *et al.*, 2008). Similarly, a human study of Japanese individuals showed that those deficient in CD36 had higher BP relative to controls (Miyaoka *et al.*, 2001). More recently, Hall and colleagues (2011) identified an association between LVM, determined by either echocardiography or electrocardiography, and a CD36 variant in a cohort comprising families recruited by means of a hypertensive proband (in the top 5% of blood pressure distribution) (Hall *et al.*, 2011). Further SHR investigations, characterised by CD36 deficiency, indicated that diet supplementation with SCFA, the uptake of which is CD36-independent, eliminated cardiac hypertrophy. The results linked defective fatty acid uptake, and by implication CD36, to cardiac hypertrophy, leading the authors to suggest a role for SCFA supplementation in human hypertrophic cardiomyopathy (Hajri *et al.*, 2001). Finally, abnormal myocardial fatty acid uptake and reduced CD36 expression has been linked to an HCM-like phenotype i.e. the development of a clinical phenotype indistinguishable from HCM (Cambronero *et al.*, 2009; Luedde *et al.*, 2009; Okamoto *et al.*, 1998; Soor *et al.*, 2009; Ashrafian *et al.*, 2003).

In this study, the rs10268417 SNP showed a significant difference in effect amongst the founder mutation groups, indicating that the extent of its effect on trait variance is significantly influenced

by the founder mutation context. The effect of the A-allele was lower in the R92W<sub>TNNT2</sub> group compared to A797T<sub>MYH7</sub> group: 1.29 mm on mPWT, 20.7 mm on CWT score and 1.29 on PC1.

The SNP is positioned intronically and *in silico* evaluations were performed accordingly (<http://www.ncbi.nlm.nih.gov/SNP>). However, allelic comparison did not indicate any significant differences in recognition of splice site motifs (Brunak *et al.*, 1991; Hebsgaard *et al.*, 1996). The difference in SNP effect is, therefore due to the as yet unknown effect of the SNP itself or a variant with which it is in LD. The LD structures of the HapMap CEU and YRI populations show that the variant is in LD with a coding, non-synonymous SNP in only the CEU population namely rs13306227 (SNPbrowser<sup>TM</sup> v.4.0.1). The latter is a missense mutation characterised as a change from the basic polar Arginine (Arg) to neutral non-polar Leucine (Leu) (CGG → CTG; R5L) (<http://www.ncbi.nlm.nih.gov/SNP>) with SIFT predictions characterising it as damaging (Kumar *et al.*, 2009). This change may affect the tertiary structure of the relevant protein and perhaps give rise to altered protein function/interactions. The two SNPs have to date not been investigated on a functional level or implicated in the development of disease.

The CGT haplotype appeared to be cardioprotective as its effect was an estimated decrease of 0.58 mm in mPWT, 8.6 mm in the CWT score and 0.54 in PC1. This result did not mirror the single SNP effect, suggesting that the phenotype arises from the combined effects of variants contained in the haplotype. Significant differences in haplotype effect were observed amongst the founder mutation groups for the AGT and CGT haplotypes. The effect of the first was lower in the R92W<sub>TNNT2</sub> group relative to A797T<sub>MYH7</sub> group: 1.99 mm for mPWT, 41.6 mm for the CWT score and 2.6 for PC1. The effect of the second was higher in the R403W<sub>MYH7</sub> group compared to the A797T<sub>MYH7</sub> group: 2.2 mm on mIVST. Again, the significant haplotype effects may be due to combined effects of variants contained within the respective haplotypes; and the extent to which these haplotypes modify the development of hypertrophy is also significantly influenced by founder mutation context.

## ii) Carnitine palmitoyltransferase I

Carnitine palmitoyltransferase is responsible for the transport of LCFA across the outer membrane of mitochondria. The predominant cardiac isoform, CPT-1b, is encoded by *CPT1b* (Yamazaki *et al.*, 1996; McGarry & Brown, 1997).

The T-allele of rs1557502 was associated with an estimated increase of 0.54 mm in mPWT. The variant is located intronically and its potential functional significance was evaluated *in silico* (<http://www.ncbi.nlm.nih.gov/SNP>). Netgene2 comparison revealed differences in recognition of acceptor splice sites, suggesting that the variant alters mRNA splicing (Brunak *et al.*, 1991; Hebsgaard *et al.*, 1996). More specifically, the T-allele was characterised by the recognition of three additional acceptor sites (1 in the direct strand; 2 in the complement strand) relative to the C-allele.

Differential expression of CPT-1b has been observed under various physiological conditions e.g. decreased content in HF and upregulation thereof, hypothesized to be compensatory, in a transgenic rat model of HCM characterised by the overexpression of a truncated cardiac troponin T (Luedde *et al.*, 2009). Its cardiac effects are diverse, as CPT-I inhibitors reverse the progression to heart failure in the pressure-overloaded heart, whilst, in contrast, chronic inhibition thereof can lead to moderate cardiac hypertrophy and increased  $\alpha$ -MHC expression (Turcani & Rupp, 1997; Mengi & Dhalla, 2004). Given the contradictory observations, it is difficult to speculate as to the exact consequences of the significantly associated SNP. However, energy compromise is hypothesised to play a key role in the development of HCM. We thus propose that the T-allele of the rs1557502 variant may, via aberrant mRNA splicing, contribute to the burden of disrupted myocardial energetics and ultimately increase the compensatory hypertrophy phenotype, as is evident from its association with an increased mPWT measure. The variant, according to our knowledge, does not affect the transmembrane domains or mitochondrial targeting sequence of the protein directly, but the proposed aberrant splicing could change the reading frame and ultimately the final protein product/function (van der Leij *et al.*, 2002).

Alternatively, the observed effect may be the result of a functional variant in LD with rs1557502. The SNP was found to be in LD with a number of coding, non-synonymous changes as determined from the CEU and YRI LD maps generated by the SNPbrowser<sup>TM</sup> v.4.0.1 software: rs1804702 (TCC  $\rightarrow$  TAC; S630Y), rs470117 (GAG  $\rightarrow$  AAG; E497K), rs8142477 (TCC  $\rightarrow$  TGC; S393C), rs2269383 (GGC  $\rightarrow$  GAC; G286D) and rs3213445 (ATC  $\rightarrow$  GTC; I66V). SIFT predictions suggested that two of these missense mutations, S630Y and G286D, may be damaging (Kumar *et al.*, 2009). The first shows a change from the neutral polar Ser to the neutral polar Tyr. The Tyr amino acid comprises a hydrocarbon benzene ring and it is, therefore considered less polar than Ser (<http://www.elmhurst.edu/~chm/vchembook/561aminostructure.html>). The second variant is

characterised by the substitution of the neutral non-polar Gly by an acidic polar Aspartic acid (Asp). These substitutions may alter the tertiary structure of the respective proteins and, thereby potentially alter the protein function. However, the two SNPs have as yet not been evaluated on a functional level or linked to disease development.

The effect of the CC haplotype was lower on mIVST (1.8 mm), mPWT (0.83 mm), the CWT score (18.3 mm) and the PC1 measure (1.14) in the R403W<sub>MYH7</sub> group compared to the A797T<sub>MYH7</sub> group. Also, its effect was higher on mIVST (3 mm), mLVWT (2.41 mm), the CWT score (25.8) and the PC1 measure (1.61) in the R92W<sub>TNNT2</sub> group relative to the R403W<sub>MYH7</sub> group. The effect of the CT haplotype was lower in the R92W<sub>TNNT2</sub> group relative to the A797T<sub>MYH7</sub> group: 3.11 mm on mLVWT. Moreover, its effect was lower in the R92W<sub>TNNT2</sub> group compared to the R403W<sub>MYH7</sub> group: 0.95 mm for mPWT, 18.2 mm for the CWT score and 1.14 for the PC1 measure. These observations do not mirror the significant SNP effect of rs1557502, suggesting that the trait variance may be explained by the combined effect of variants contained within the respective haplotypes; and these haplotype effects are significantly influenced by the founder mutation context. The haplotypes comprise two alleles and the potential functional significance of the second SNP, rs470117, was, therefore considered. It was described in the foregoing section as a tolerated missense mutation in LD with the significantly associated single SNP.

### iii) Pyruvate dehydrogenase kinase

The PDH complex is responsible for the conversion of pyruvate to acetyl-CoA which is utilised to generate ATP via the mitochondrial Krebs cycle. This step thus links glycolysis and fatty acid metabolism and can, therefore, regulate the choice of substrate used under various physiological conditions (Houten *et al.*, 2009; Randle, 1986; Patel & Roche, 1990). PDH activity in the heart is mainly regulated by *PDK4* as it is the predominantly expressed cardiac isoform (Roche *et al.*, 2001; Bowker-Kinley *et al.*, 1998). Findings from the literature showed that *PDK4* gene expression is decreased in neonatal rat cardiomyocytes in a phenylephrine-induced model of cardiac hypertrophy (Planavila *et al.*, 2005). Conversely, cardiac-specific overexpression of the enzyme exacerbated calcineurin-induced cardiomyopathy in mice (Zhao *et al.*, 2008).

The effect of the C-allele of rs2073978 was lower in the R403W<sub>MYH7</sub> group relative to the A797T<sub>MYH7</sub> group: 30.2 g on LVM, 30.7 mm on the CWT score and 1.92 on PC1. The extent to

which the SNP contributes to trait variance is, therefore significantly influenced by the founder mutation context. The SNP is located intronically and its potential functional consequence was predicted *in silico* (<http://www.ncbi.nlm.nih.gov/SNP>). The allelic comparisons did not reveal any differences with respect to the recognition of splicing acceptor or donor motifs, suggesting that the SNP may have an as yet unknown functional consequence (Brunak *et al.*, 1991; Hebsgaard *et al.*, 1996). These differences in effect may also be explained by a variant in LD with rs2073978. However, the SNP was not found to be in LD with any coding, non-synonymous changes as determined from the CEU and YRI LD maps generated by the SNPbrowser<sup>TM</sup> v.4.0.1 software. To date, the SNP has not been functionally characterised or implicated in disease.

The effect of the CT was an estimated 1.42 mm increase in mIVST. In addition, its effect was lower in the R403W<sub>MYH7</sub> group relative to the A797T<sub>MYH7</sub> group: 3.2 mm for mIVST, 3.62 for the mLVWT, 31.9 mm for the CWT score and 1.99 for PC1. The results do not reflect the observed single SNP effect and, therefore, suggest that the trait variance can be ascribed to the combined effects of variants contained within the haplotype, and that the extent to which the haplotype modifies the hypertrophy phenotype is significantly influenced by the founder mutation context. The potential functional implication of the second variant, rs2301630, was, therefore also predicted *in silico*. The allelic comparison did not indicate differences with respect to the recognition of splicing motifs (Brunak *et al.*, 1991; Hebsgaard *et al.*, 1996). As previously mentioned, the variant may be in LD with an effect allele. However, the SNPbrowser<sup>TM</sup> v.4.0.1 software LD maps of both the CEU and YRI populations did not indicate any coding, non-synonymous variants. The rs2301630 variant has been investigated within the context of type 2 diabetes and metabolic syndrome, however, no significant correlations were identified (Moon *et al.*, 2012). The afore-described SNPs have as yet not been characterised functionally or implicated in the development of disease.

#### iv) Creatine kinase

Creatine kinase catalyses the reversible transfer of high-energy phosphates between creatine and ATP and, therefore, plays an important role in the coupling of energy supply and demand. All three CK isoforms i.e. MM-CK, BB-CK and MB-CK, which are encoded by the *CKM* and *CKB* genes (Refer to Section 2.3.3.2), show cardiac expression (Hornemann *et al.* 2000; Au 2004; Nahrendorf

*et al.* 2005). In addition, the muscle-specific isoform binds to the sarcomeric M-line where it is believed to fulfil a structural role (Clark *et al.*, 2002;Hornemann *et al.*, 2000).

An *in situ* study in skeletal muscle showed binding of MM-CK to the I-band via aldolase and PFK. This CK association with glycolytic enzymes may function to supply PFK with, but prevent its inhibition by ATP i.e. maintaining a proper ATP/ADP ratio nearby (Kraft *et al.*, 2000). More recently, mutations in the *TRIM63* gene encoding MuRF1 have been associated with human hypertrophic cardiomyopathy. One of these mutations is located within the CK-M binding domain and the result was mislocalisation to the sarcomere M-line. This indirectly suggests that disrupted CK-M integrity may, by means of this interaction, contribute to the development of HCM (Chen *et al.*, 2010). A canine model of pressure overload hypertrophy showed decreased myocardial PCr, creatine, PCr/ATP, and ATP. Decreased CK-MM and increased CK-MB levels with normal total CK activity was also reported. However, the authors remarked on the lack of CK-MB compartmentalisation within the cell, as is the case for CK-MM (Jameel & Zhang, 2009). Finally studies of CK-M<sup>-/-</sup>-knockout mice showed impaired K<sub>ATP</sub> channel function, with deficiency of the latter implicated in the development of left ventricular hypertrophy (Abraham *et al.*, 2002).

#### a) *CKM*

The effect of the T-allele of rs7260463 appeared to be cardioprotective as an estimated decrease of 0.24 mm in mPWT. The effect of the T-allele of rs344816 was lower on mLVWT in the R92W<sub>TNNT2</sub> group relative to both the A797T<sub>MYH7</sub> (4.21 mm) and R403W<sub>MYH7</sub> groups (3.42 mm) suggesting that its effect on trait variance is significantly influenced by the founder mutation context.

These two variants are both located intronically and *in silico* evaluations were performed to predict their potential functional effects (<http://www.ncbi.nlm.nih.gov/SNP>). The variants did not show variation in the recognition of splicing motifs (Brunak *et al.*, 1991;Hebsgaard *et al.*, 1996). The significant association/effects may be due to a variant(s) in LD with the investigated SNPs. According to the LD maps for the CEU and YRI populations generated by the SNPbrowser<sup>TM</sup> v.4.0.1 software, only the rs7260463 SNP is in LD with a coding, non-synonymous variant (and only in the CEU population) namely rs17875653. However, SIFT predictions characterised the change from the neutral, non-polar Leucine (Leu) to the similarly neutral, non-polar Valine (Val) as tolerated (CTC → GTC; L127V) (Kumar *et al.*, 2009). The rs7260463 and rs344816 variants have

previously been investigated within the context of elite endurance performance, but no significant correlations were identified (Doring *et al.*, 2011).

Significant haplotype effects and differences in haplotype effect amongst the founder mutation groups were observed for this gene. The effect of the CTAT haplotype was an estimated increase of 3.20 mm in mIVST, 2.72 mm in mLVWT and 1.37 in PC1. The effect of the TTGA haplotype was an estimated decrease of 27.4 g in LVM. Its effect was higher on LVM (96.4 g) in the R403W<sub>MYH7</sub> group relative to the A797T<sub>MYH7</sub> group and lower on LVM (120.3 g) in R92W<sub>TNNT2</sub> group compared to the R403W<sub>MYH7</sub> group. Also, its effect was higher on PC (13.97) in the R92W<sub>TNNT2</sub> group compared to the R403W<sub>MYH7</sub> group. The effect of the CTGT haplotype was an estimated decrease of 17.6 g in LVM and 7.9 mm in the CWT score. Its effect was lower on mLVWT (5.1 mm) and the CWT score (32.1 mm) in the R92W<sub>TNNT2</sub> group relative to the A797T<sub>MYH7</sub> group. The effect of the CTGA was higher on mLVWT in the R92W<sub>TNNT2</sub> group relative to both the A797T<sub>MYH7</sub> (4.53 mm) and R403W<sub>MYH7</sub> groups (3.70 mm). The results do not mirror the significant SNP effects identified for rs7260463. Rather, the extent to which the haplotypes influence the hypertrophy phenotype may be ascribed to combined effect of variants contained within the respective haplotypes; and these haplotype effects are significantly influenced by the founder mutation context.

#### **b) CKB**

Significant differences in haplotype effects were identified for CCT, CTT and TCG. The effect of the first was higher on LVM (86.5 g) in the R92W<sub>TNNT2</sub> group relative to the R403W<sub>MYH7</sub> group. The effect of the second was lower on LVM (65.1 g) in the R92W<sub>TNNT2</sub> group relative to the R403W<sub>MYH7</sub> group. Also, its effect was higher on LVM (62.9 g) in the R403W<sub>MYH7</sub> group compared to the A797T<sub>MYH7</sub> group. The effect of the third was lower on the CWT score (59.4 mm) in the R403W<sub>MYH7</sub> group relative to the A797T<sub>MYH7</sub> group. The results suggest that the modifying effects of the relevant haplotypes can be attributed to the combined effects of variants contained within the respective haplotypes which are further significantly influenced by the founder mutation context.

The haplotypes comprise SNPs rs1803283, rs1136165 and rs2071407 of which the first two are considered synonymous coding variants. The rs2071407 SNP is located intronically and relevant *in silico* evaluations were performed. Allelic comparison indicated differences pertaining to the recognition of acceptor splice sites with, interestingly, both alleles indicating the identification of an

additional acceptor site relative to the other (T-allele: direct strand; C-allele: complementary strand) (Brunak *et al.*, 1991; Brunak *et al.*, 1991; Hebsgaard *et al.*, 1996). The Netgene2 results suggest that the SNP alters mRNA splicing, however it is challenging to speculate about which of the two rs2071407 alleles confer risk as we are considering significant haplotype associations which in all probability reflect complex combined (biological) effects of the variants contained within the respective haplotypes.

However, creatine kinase is essential in myocardial energy homeostasis. CK-MB is the predominant cardiac isoform showing increased levels in a canine model of pressure overload whilst CK-MM decreased and normal total CK activity was maintained (Jameel & Zhang, 2009). It is, therefore, reasonable to suggest that aberrant mRNA splicing of variants in the *CKB* gene will significantly impact on MB-CK function and, as a result, myocardial energy homeostasis. We thus propose that the rs2071407 variant may, via aberrant mRNA splicing, contribute to the burden of disrupted myocardial energetics and ultimately increase the compensatory hypertrophy phenotype as is evident from the haplotype associations with numerous hypertrophy traits. We aimed to further predict the functional consequences of rs2071407 based on current literature. However, investigations pertaining to *CKB* mutations and *CKB* functional domains, specifically with respect to cardiac disease, are, according to our knowledge, limited.

#### v) Aldolase A

Aldolases are enzymes of the glycolytic pathway responsible for catalysing the reversible cleavage of fructose 1,6-bisphosphate to DHAP and G3P. The *ALDOA* gene encodes the predominant cardiac isoform, Aldolase A (Mamczur *et al.*, 2007; Asaka *et al.*, 1983; Koeck *et al.*, 2004; Medin *et al.*, 2007; Rutter, 1964). Hypertrophied left ventricles of SHR rats showed a reduction in the expression of Aldolase A (Zamorano-Leon *et al.*, 2010). Moreover, a study of Dahl-salt sensitive rats allowed for two-phase gene expression measurements in heart muscle, i.e. during disease progression to cardiac hypertrophy and HF. Aldolase A expression was increased during the progression stage, but subsequently reduced during HF (Ueno *et al.*, 2003).

The T-allele of rs11860935 appeared to be cardioprotective as its effect was an estimated decrease of 1.88 mm in mIVST. The SNP is intronic and the relevant *in silico* predictions were performed (<http://www.ncbi.nlm.nih.gov/SNP>). Netgene2 evaluation of the significantly associated



rs11860935 indicated that the T-allele thereof was characterised by the recognition of an additional donor splice site relative to the C-allele (Brunak *et al.*, 1991; Hebsgaard *et al.*, 1996). Considering the association of the C-allele with increased mIVST, it is possible that the absence of the donor site may in fact lead to aberrant mRNA splicing. The *ALDOA* gene functions in glycolysis, making it a valuable contributor to myocardial energetics. We could, therefore, speculate that the proposed aberrant mRNA splicing may disrupt myocardial energy homeostasis and increase the burden on the sarcomere; ultimately giving rise to compensatory hypertrophy as is reflected by the significant association with mIVST. An alternative hypothesis is that rs11860935 may show an association with the hypertrophy phenotype due to  $\text{Ca}^{2+}$  dysregulation and, as consequence, altered contractility. This notion is supported by the finding that rabbit skeletal Aldolase A biologically interacts with and modulates the activity of  $\text{Ca}^{2+}$  release channels (ryanodine receptors) *in vitro*; and it may also do so in cardiac muscle (Kramerova *et al.*, 2008).

It is also possible that the significant effects may be attributable to a coding, non-synonymous variant(s) in LD with rs11860935. The SNPbrowser<sup>TM</sup> v.4.0.1 software indicated that a total of six missense mutations were found to be in LD with the variant within both the CEU and YRI populations: rs3098416 (GCG → TCG; A280S), rs3112557 (GAC → GCC; D196A), rs11553121 (AGT → ACT; S176T), rs11553113 (CGC → TGC; R134C), rs11553115 (GCC → TCC; A41S) and rs11553114 (GGC → GAC; G27D). Interestingly, SIFT predictions indicated that all of these missense mutations are considered to be damaging (Kumar *et al.*, 2009). However, according to the literature to date, none of these mutations or rs11860935 have been characterised functionally or implicated in disease. The effect of the C-allele of rs9928448 was lower in the R92W<sub>TNNI2</sub> group compared to the A797T<sub>MYH7</sub> group: 2.29 mm on mIVST, 23.2 mm on the CWT score and 1.45 on PC1. The extent to which it contributes to trait variance is thus significantly influenced by the founder mutation context.

A significant difference in haplotype effect amongst the founder mutation groups, which does not mirror the significant rs11860935 effect, was observed, suggesting that the trait variance may be due to the combined effects of variants contained within the haplotype; and the degree to which the haplotype effect contributes to the hypertrophy phenotype is significantly influenced by the founder mutation context. The effect of the CC haplotype was lower on mIVST (2.7 mm) and mLVWT (2.65 mm) in the R92W<sub>TNNI2</sub> group compared to the R403W<sub>MYH7</sub> group. The rs9928448 SNP is the second variant of the CC haplotype and was, therefore evaluated *in silico*. Allelic comparison

revealed no differences pertaining to recognition of splicing donor or acceptor sites (Brunak *et al.*, 1991; Hebsgaard *et al.*, 1996). Moreover, the effects may be attributed to a functional variant(s) in LD with rs9928448. The relevant coding, non-synonymous missense mutations are the same as described for the rs11860935 variant.

#### vi) Phosphofructo-1-kinase

Phosphofructo-1-kinase catalyses the conversion of fructose-6-phosphate to fructose-1,6-bisphosphate which is considered to be the rate-limiting step in glycolysis (Swoboda *et al.*, 1997). The predominant cardiac isoenzyme, the muscle type, is encoded by *PFKM* (Dunaway *et al.*, 1988a; Dunaway *et al.*, 1988b). A study of PFKM deficient (*Pfkm*<sup>-/-</sup>) mice showed marked metabolic changes in the heart which resulted in cardiac hypertrophy (Garcia *et al.*, 2009).

The effect of the T-allele of rs10875749 was higher on mIVST (2.56 mm) in the R92W<sub>TNNI2</sub> group relative to A797T<sub>MYH7</sub> group. Also, its effect was higher in the R92W<sub>TNNI2</sub> group compared to the R403W<sub>MYH7</sub> group: 2.87mm for mIVST, 2.08 mm for mLVWT, 22.9 for the CWT score and 1.43 for PC1. Furthermore, its effects was lower on PC1 (0.92) in the R403W<sub>MYH7</sub> group compared to the A797T<sub>MYH7</sub> group. The effect of rs10875749 (or a variant with which it is in LD) on the hypertrophy phenotype is thus significantly influenced by the founder mutation context.

The rs10875749 variant is positioned intronically and *in silico* evaluations was performed accordingly (<http://www.ncbi.nlm.nih.gov/SNP>). Allelic comparison indicated no differences with respect to recognition of acceptor and donor motifs (Brunak *et al.*, 1991; Hebsgaard *et al.*, 1996). The SNPbrowser<sup>TM</sup> v.4.0.1 LD maps for both the CEU and YRI populations indicate that the variant is in LD with two coding, non-synonymous changes, rs2228500 (CGA → CAA; R100Q) and rs11552506 (GAC → TAC; D368Y). SIFT predictions characterised the first SNP as tolerated, whilst the second was considered damaging (Kumar *et al.*, 2009). The rs11552506 missense mutation is characterised by a change from the acidic polar Aspartic acid (Asp) to a neutral polar Tyr, which could affect the tertiary protein structure and, thereby, protein function. The R100Q mutation, although predicted to be tolerated, has been implicated in the development of GSDVII (Musumeci *et al.*, 2011). As previously described, certain HCM phenocopies are characterised by GSD and the mutation may thus play a role in the development of hypertrophy (Refer to Section

1.2.4.2.2). The remainder of the SNPs have not been implicated in the development of disease or characterised functionally.

A significant haplotype effect, which did not reflect the significant rs10875749 effect, was observed, suggesting that the trait variance may be ascribed to the combined effects of variants contained within the haplotype. The effect of the AT haplotype was an estimated increase of 1.03 mm in mIVST. Significant differences in haplotype effect amongst the founder mutation groups were also observed for haplotypes AA, AT, CA and CT suggesting that the extent to which they influence the hypertrophy phenotype is significantly influenced by the founder mutation context. The effect of the AA haplotype was higher on mPWT (0.88 mm) in the R403W<sub>MYH7</sub> group relative to the A797T<sub>MYH7</sub> group. The effect of the AT haplotype was lower in the R403W<sub>MYH7</sub> group relative to the A797T<sub>MYH7</sub> group: 3.1 mm for mIVST, 31.6 mm for the CWT score and 1.98 for PC1. The effect of the CA haplotype was lower in the R92W<sub>TNNI2</sub> group compared to the A797T<sub>MYH7</sub> group: 1.54 mm for mPWT, 22.1 mm for the CWT score and 1.38 for PC1. Also, its effect was lower in the R92W<sub>TNNI2</sub> group relative to the R403W<sub>MYH7</sub> group: 1.05 for PC1. The effect of CT was higher in the R92W<sub>TNNI2</sub> group compared to the A797T<sub>MYH7</sub> group: 3.7 mm for mIVST, 3.03 mm for mLVWT and 1.32 mm for mPWT.

The rs1859445 SNP, the second variant in the two-allele haplotypes, is intronic and it was, therefore, evaluated *in silico*. Allelic comparison indicated the recognition of an additional acceptor splice site upon evaluation of the A-allele relative to the C-allele, suggesting that the variant alters mRNA splicing (Brunak *et al.*, 1991; Hebsgaard *et al.*, 1996). To recap, all four possible haplotypes were observed, but only AT (rs1859445 underlined) showed a significant association; and it did not reflect the significant rs10875749 association. These observations make it difficult to speculate as to the exact contribution of rs1859445 to the haplotype effect. More generally, PFKM is a key component of myocardial glycolysis; and PFKM-deficient mice develop cardiac hypertrophy (Garcia *et al.*, 2009; Swoboda *et al.*, 1997). Incorrect splicing of the *PFKM* gene may thus disrupt myocardial energetics and give rise to a compensatory hypertrophy phenotype. Indeed, the rs1859445 variant may contribute to the haplotype effect via aberrant mRNA splicing of the *PFKM* gene, as is evident from its correlation with numerous hypertrophy traits.

Alternatively, the effects may be ascribed to the coding, non-synonymous mutations in LD with rs1859445 and they are the same variants described to be in LD with rs10875749. The rs1859445 variant has to date not been evaluated functionally or linked to disease development.

## **vii) Peroxisome proliferator-activated receptors (PPARs)**

PPARs contribute to myocardial energetics by regulating numerous genes essential for lipid metabolism (Reviewed by Desvergne & Wahli, 1999; Feige *et al.*, 2006)

### **a) Peroxisome proliferator-activated receptor alpha**

PPAR $\alpha$  is encoded by the *PPARA* gene and shows high cardiac expression. It plays a key role in myocardial energy homeostasis, as it induces the expression of various components of lipid and glucose metabolism (Reviewed by Rowe *et al.*, 2010; Reviewed by Yang & Li, 2007). Decreased transcriptional activity of PPAR $\alpha$  has been observed in hypertrophied left ventricles due to aortic banding and cardiomyocytes following phenylephrine (PE)-induced hypertrophy (Sack *et al.*, 1997; Barger *et al.*, 2000). Conversely, cardiac-specific overexpression of PPAR- $\alpha$  in transgenic mice led to the development of ventricular hypertrophy and dysfunction (Finck *et al.*, 2002). Reactivation of PPAR $\alpha$  in the hypertrophied heart setting was met with enhanced fatty acid oxidation (FAO), but impairment of cardiac function. These findings support the suggested adaptive role of decreased FAO in cardiac hypertrophy (Young *et al.*, 2001).

Significant haplotype effects were identified in the absence of significant SNP effects suggesting that the hypertrophy phenotype is modified as a result of the combined effects of variants contained within the respective haplotypes. The effect of the GAA haplotype was an estimated increase of 30.1 g in LVM, 3.01 mm in mIVST, 3.40 mm in mLVT, 21.0 in the CWT score and 1.31 in PC1. The effect of the GGG haplotype was an estimated decrease of 49.1 g in LVM, 3.09 mm in mIVST and 1.14 mm in mPWT. The haplotype comprises three SNPs, which are all located intronically and *in silico* evaluations were performed to determine their potential effects on mRNA splicing (<http://www.ncbi.nlm.nih.gov/SNP>, SNPbrowser<sup>TM</sup> v.4.0.1). However, allelic comparisons did not reveal any significant differences in recognition of acceptor or donor sites (Brunak *et al.*, 1991; Hebsgaard *et al.*, 1996). The SNPbrowser<sup>TM</sup> v.4.0.1 LD structures of the HapMap CEU and YRI populations showed that these SNPs are in LD with a number of coding, non-synonymous

variants: rs1800234 (V227A), rs1800206 (L162V), rs1800204 (R127Q), rs1800243 (R409T), rs1800242 (D304N) and rs1042311 (A268V). Reinhard et al. (2008) investigated the potential association of variants rs881740, rs4823613, rs4253776 and L162V with MI; however, no significant association was identified. The rs4253776 variant has been associated with the development of type 2 diabetes (Cresci, 2007; Reinhard *et al.*, 2008). V227A has been implicated in non-alcoholic fatty liver disease, whilst L162V has been linked to aspects of metabolic syndrome and reduced adiposity (Robitaille *et al.*, 2004; Bosse *et al.*, 2002; Chen *et al.*, 2007). Such metabolic changes may contribute to the hypertrophy phenotype in keeping with the notion that altered myocardial energetics is primary in the development of HCM, as described in Chapter 1 (Refer to Section 1.2.4.2.2).

Significant differences in haplotype effects amongst the founder mutation groups were observed for both haplotypes AAA and GGG. These results reflect the combined effects of variants contained within the respective haplotypes which are further significantly influenced by the founder mutation context. The effect of the AAA haplotype was lower on LVM (21.9 g) in the R92W<sub>TNNI2</sub> group compared to the R403W<sub>MYH7</sub> group. The effect of the GGG haplotype, found to be significantly associated upon evaluation of the entire cohort, was lower on mPWT (2.13 mm) in the R403W<sub>MYH7</sub> group relative to the A797T<sub>MYH7</sub> group.

#### **b) Peroxisome proliferator-activated receptor gamma**

The PPAR $\gamma$  protein, encoded by *PPARG*, is expressed in the heart where it is believed to contribute to fatty acid metabolism (Luo *et al.*, 2010; Luo *et al.*, 2010; Mehrabi *et al.*, 2002). The PPAR $\gamma$  isoform has been implicated in the control of human BP evident from an association between deleterious dominant-negative mutations in the gene and early-onset hypertension (Barroso *et al.*, 1999). Moreover, previous studies have shown that PPAR $\gamma$  activation suppresses TNF- $\alpha$  (Takano *et al.*, 2000) and interleukin-1 $\beta$  (IL-1 $\beta$ ) (Jiang *et al.*, 1998) expression, factors considered as potential stimuli for myocyte hypertrophy (Hefti *et al.*, 1997). Considering the high expression of PPAR $\gamma$  in human heart ventricles and its effects on hypertrophy signals, Mehrabi *et al.* (2002) suggested a role for the receptor in the treatment of hypertrophic cardiomyopathy. Further cardiac-protective effects include the development of cardiac hypertrophy in a cardiomyocyte-specific PPAR $\gamma$  knockout mouse model (Duan *et al.*, 2005), the inhibition of aortic constriction-induced cardiac hypertrophy by PPAR $\gamma$  activators in rats (Sakai *et al.*, 2002) and the more prominent pressure-induced cardiac

hypertrophy observed in heterozygous PPAR $\gamma$  deficient mice relative to wild-type controls (Asakawa *et al.*, 2002).

The effect of the T-allele of rs12631028 was is higher on mLVWT (1.71 mm) in the R92W<sub>TNNT2</sub> group compared to the A797T<sub>MYH7</sub> group. The effect of the SNP on the trait is thus significantly influenced by the founder mutation with which it presents. To date, the SNP has not been explored functionally and its contribution to disease development, if any, remains to be established.

The effects of the CAGA and CAGC haplotypes appeared to be cardioprotective with estimated decreases of 22.8 g in LVM and 0.97 mm in mPWT, respectively. The effect of the CGGC haplotype was an estimated increase of 27.1 g in LVM, 2.55 mm in mIVST, 2.73 mm in mLVWT, 23.7 mm in the CWT score and 1.48 in PC1. Haplotypes CAGA and CAGC that showed significant haplotype effects as well as haplotypes TGAC and TGGA indicated significant differences in haplotype effect amongst the HCM founder mutation groups. The effect of the CAGA haplotype was lower on mIVST (4.98 mm) and mLVWT (4.83 mm) in the R92W<sub>TNNT2</sub> group compared to the A797T<sub>MYH7</sub> group. Also, its effect was lower on mLVWT (2.85 mm) in the R403W<sub>MYH7</sub> group relative to the A797T<sub>MYH7</sub> group. The effect of the TGAC haplotype was higher on mPWT (2.52 mm) and PC1 (0.53) in the R92W<sub>TNNT2</sub> group compared to the A797T<sub>MYH7</sub> group. The effects of both the TGGA and CAGC haplotypes were lower on PC1 (0.12; 0.94) in the R92W<sub>TNNT2</sub> group compared to the A797T<sub>MYH7</sub> group.

The significant haplotype effects did not mirror the significant single SNP result, suggesting that the phenotype arises from the combined effects of variants contained in the respective haplotypes; and the extent to which the CAGA and CAGC haplotypes modify the development of hypertrophy is also significantly influenced by founder mutation context.

#### **viii) Peroxisome proliferator-activated receptor gamma coactivator-1 $\alpha$**

PGC-1 $\alpha$  is encoded by the *PGC1* gene and shows high cardiac expression where it functions as coactivator for PPAR $\alpha$  (Finck, 2007). It similarly coactivates PPAR $\gamma$  in brown adipose tissue and it may also do so in the heart (Puigserver *et al.*, 1998; Rowe *et al.*, 2010; Young *et al.*, 2001). PGC-1 $\alpha$  further functions in cardiac mitochondrial biogenesis by indirectly regulating mitochondrial transcription factor A (MTF-A). Knockout or deficiency of PGC-1 $\alpha$  results in significant alterations

in cardiac function (Ren *et al.*, 2010; Handschin & Spiegelman, 2008). Moreover, mice deficient in PGC-1 $\alpha$  showed accelerated cardiac dysfunction and HF in response to transverse aortic constriction (TAC). Similar findings, resulting from PGC-1 $\alpha$  repression in cultured cardiac cells, could be reversed upon introduction of ectopic PGC-1 $\alpha$ , suggesting a cardioprotective function (Arany *et al.*, 2006). The coordinated reduction of PPAR $\alpha$ , PGC-1 $\alpha$  and FAO enzymes was observed in hypertrophied left ventricles of mice subjected to TAC (Lehman & Kelly, 2002).

Significant haplotype effects were observed in the absence of significant SNP effects suggesting that the hypertrophy phenotype is modified as a result of the combined effects of variants contained within the respective haplotypes. The effect of the GATT haplotype was an estimated increase of 2.92 mm in mIVST.

Also, significant differences in haplotype effect were observed amongst the mutation groups indicating that the trait variance may be explained not only by the combined effects of variants contained within the respective haplotypes, but the founder mutation context in which the haplotypes present. The effect of the GAAC haplotype was higher on LVM (103.3 g), mIVST (7 mm), mLVWT (7.26 mm), the CWT score (65.4 mm) and PC1 (4.09) in the R92W<sub>TNNT2</sub> group compared to the A797T<sub>MYH7</sub> group. Also, its effect was higher in the R92W<sub>TNNT2</sub> group relative to the R403W<sub>MYH7</sub> group: 82 g for LVM, 5.4 mm for mIVST, 5.84 mm for mLVWT, 54.1 mm for the CWT score and 3.38 for PC1. The effect of the GATC haplotype was higher on the CWT score (36 mm) in the R92W<sub>TNNT2</sub> group compared to the A797T<sub>MYH7</sub> group. The effect of the GCAC haplotype was lower in the R92W<sub>TNNT2</sub> group relative to the R403W<sub>MYH7</sub> group: 48 g for LVM, 26.9 mm for the CWT score and 1.68 for PC1.

#### **ix) AMP-activated protein kinase**

As described, AMPK monitors the cellular energy homeostasis via its ability to sense the AMP:ATP ratio (Refer to Section 2.3.3.2) (Hardie & Carling, 1997). The mammalian AMPK complex is a heterotrimer comprising an  $\alpha$ -catalytic subunit and 2 regulatory,  $\beta$ - and  $\gamma$ - subunits (Dolinsky & Dyck, 2006). The genes that encode the respective subunits were evaluated and the results are subsequently described.

### a) *PRKAA1*

The *PRKAA1* gene encodes the  $\alpha 1$  catalytic subunit of AMPK. It is structurally characterised by a conserved N-terminal containing a Ser/Thr kinase domain activated upon phosphorylation of the Threonine 172 in the activation loop, an autoinhibitory sequence (AIS) inhibiting activity of the kinase domain and a C-terminal domain that allows binding to the  $\beta$ -subunit (Crute *et al.*, 1998; Hawley *et al.*, 1996; Pang *et al.*, 2007).

Significant differences in SNP effects amongst the mutation groups were observed, suggesting that the extent to which these SNPs influence the trait variance is significantly influenced by the founder mutation with which it presents. The effect of the C-allele of rs12517210 variant and the G-allele of rs11747210 (the minor allele of the rs11747210 SNP is the T allele) was higher on LVM in the R92W<sub>TNNT2</sub> group relative to the A797T<sub>MYH7</sub> group (26.9 g; 26.7 g). Also, their effects were higher in the R403W<sub>MYH7</sub> group compared to the A797T<sub>MYH7</sub> group on the CWT score (18.7 mm; 17.9 mm) and PC1 (1.17; 1.12). Both SNPs are intronic and the relevant *in silico* predictions were performed (<http://www.ncbi.nlm.nih.gov/SNP>). Neither of the two variants indicated differences in recognition of splicing acceptor or donor motifs (Brunak *et al.*, 1991; Hebsgaard *et al.*, 1996). The effects may be attributed to functional variants in LD with rs12517210 and rs11747210. However, according to the SNPbrowser<sup>TM</sup> v.4.0.1 software, all coding variants in LD with the investigated SNPs are characterised as synonymous changes. The two SNPs have as yet not been linked to disease or evaluated functionally.

Statistically significant differences in haplotype effects were seen for the CGC and TTC haplotypes. These results do not mirror the significant SNP effects for rs12517210 and rs11747210 suggesting that the trait variance may be due to the combined effects of variants contained within the respective haplotypes. Also, these haplotype effects are significantly influenced by the founder mutation context. The effect of the first was higher on LVM (21.7 g) in the R92W<sub>TNNT2</sub> compared to the A797T<sub>MYH7</sub> group. Conversely, the effect of the second was lower on LVM (36.4 g) in the R92W<sub>TNNT2</sub> group relative to the A797T<sub>MYH7</sub> group.



**b) *PRKAA2***

The human *PRKAA2* gene encodes the  $\alpha 2$  catalytic subunit of AMPK and its structure is as described for *PRKAA1*.

The effect of the TTT haplotype was an estimated 0.45 increase in PC1. No significant single SNP effects were observed and the results may thus be ascribed to the combined effects of variants contained within the haplotype. The haplotype comprises three SNPs which are all located intronically and *in silico* evaluations were performed to determine their potential effects on mRNA splicing (<http://www.ncbi.nlm.nih.gov/SNP>, SNPbrowser<sup>TM</sup> v.4.0.1). The rs1124900 variant did not indicate any differences in splice site signals upon investigation with Netgene2 (Brunak *et al.*, 1991; Hebsgaard *et al.*, 1996). However, the literature notes that an interaction between this variant and a SNP in the RAC-alpha serine/threonine-protein kinase gene (*AKT1*) was significantly associated with the percent change in mass-adjusted strength of the arm, i.e. skeletal muscle hypertrophy, after resistance exercise training. A similar result was seen for the interaction of the rs1124900 variant and a second *PRKAA2* variant, rs2796516 positioned intronically (Newman & University of Pittsburgh, 2008). However, no significant differences in splice signal motifs were identified upon *in silico* evaluations strongly suggesting that rs2796516 is perhaps in LD with the effect allele. The remaining two SNPs, rs2796495 and rs932447, have been investigated within the context of risk of type 2 diabetes. However, they have as yet not been characterised functionally and *in silico* evaluations were, therefore, performed. The Netgene2 results showed no differences in splice site signals (Brunak *et al.*, 1991; Hebsgaard *et al.*, 1996). Collectively, the results propose that the variants themselves (in combination) modify hypertrophy development via currently unknown mechanisms or that they are in LD with functional variants. According to the SNPbrowser<sup>TM</sup> v.4.0.1 software, all coding variants in LD with the investigated SNPs are characterised as synonymous changes.

**c) *PRKAB1***

The *PRKAB1* gene encodes the  $\beta 1$  regulatory subunit of the AMPK complex. The  $\beta$  subunits vary with respect to their N-terminals, whilst the remainder is conserved including a carbohydrate-binding molecule (CBM), which allows the AMPK complex to associate with glycogen, and a C-

terminal domain that acts as scaffold for  $\alpha$ - and  $\gamma$ -subunit binding (Iseli *et al.*, 2005; Polekhina *et al.*, 2003; Steinberg & Kemp, 2009).

The effect of the T-allele of rs278149 was higher on the CWT score (25 mm) and PC1 (1.56) in the R92W<sub>TNNT2</sub> group compared to the A797T<sub>MYH7</sub> group. The extent to which the SNP (or a variant with it is in LD) influences the development of hypertrophy is significantly influenced by the founder mutation context. The SNP is intronic and the relevant *in silico* predictions were performed (<http://www.ncbi.nlm.nih.gov/SNP>). Allelic comparison revealed no differences in recognition of splicing donor or acceptor motifs (Brunak *et al.*, 1991; Hebsgaard *et al.*, 1996). As mentioned, the effect may be owing to a functional variant in LD with rs278149. The SNPbrowser<sup>TM</sup> v.4.0.1 LD structures of the HapMap CEU and YRI populations showed that the variant is in LD with two coding, non-synonymous SNPs namely rs11546695 and rs1043354. SIFT predictions suggest that both these missense mutations result in amino acid changes which are tolerated (Kumar *et al.*, 2009). To date, none of these variants have been linked to disease or evaluated on a functional level.

The TGGTG haplotype appeared to be cardioprotective as its effect was an estimated decrease of 18.3 g in LVM. Also, it showed significant differences in haplotype effect amongst the founder mutation groups along with the GACGT haplotype. The effect of the first was higher on LVM (41.6 g;  $p = 0.020$ ) in the R92W<sub>TNNT2</sub> group relative to A797T<sub>MYH7</sub> group. The effect of the second was lower on mPWT (1.21 mm;  $p = 0.004$ ) in the R403W<sub>MYH7</sub> group compared to the A797T<sub>MYH7</sub> group. The significant haplotype effects did not mirror the significant single SNP result, suggesting that the phenotype arises from the combined effects of variants contained in the respective haplotypes; and the extent to which the TGGTG and GACGT haplotypes modify the development of hypertrophy is also significantly influenced by founder mutation context.

#### d) *PRKAB2*

The *PRKAB2* gene encodes the  $\beta 2$  regulatory subunit of the AMPK complex and its structure is as described for *PRKAB1*.

The effect of the G-allele of rs1348316 was an estimated increase of 0.36 mm in mPWT. The effects may be due to the SNP itself or variants with which it is in LD. The SNP is intronic and the relevant *in silico* predictions were performed (<http://www.ncbi.nlm.nih.gov/SNP>). The allelic

comparison with Netgene2 did not indicate any differences in splice site motifs (Brunak *et al.*, 1991; Hebsgaard *et al.*, 1996). According to the SNPbrowser<sup>TM</sup> v.4.0.1 LD structures of the HapMap CEU and YRI populations, the SNP is in LD with two coding, non-synonymous SNPs namely rs1048051 and rs3413734. SIFT predictions suggest that the first is damaging, whilst the second is tolerated (Kumar *et al.*, 2009). The rs1048051 missense mutation is characterised by the change from the basic polar Histidine to the neutral polar Tyrosine (CAT → TAT; H211Y), which could affect the tertiary protein structure and, thereby protein function. These afore-described SNPs have not yet been investigated functionally or implicated in disease development.

#### e) *PRKAG1*

The  $\gamma$ -subunit isoforms are, with the exception of their varying N-terminals, similar in domain structure sharing a conserved  $\beta$ -subunit binding region and four conserved cystathionine  $\beta$ -synthase motifs (CBS). The CBS motifs interact pairwise creating two Bateman domains responsible for binding two ATP or two AMP molecules, antagonistically (Scott *et al.*, 2004; Viana *et al.*, 2007).

The human *PRKAG1* gene encodes the  $\gamma$ 1 non-catalytic, regulatory subunit of AMPK. More specifically, the Asp-90 residue binds AMP ribose, which in turn activates AMPK activity (Steinberg & Kemp, 2009). No statistically significant results were identified for the *PRKAG1* gene and it is, therefore, not considered a modifier of hypertrophy in HCM within the current cohort.

#### f) *PRKAG2*

The *PRKAG2* gene encodes the  $\gamma$ 2 non-catalytic, regulatory subunit of AMPK and mutations therein have previously been implicated in the development of an HCM phenocopy (Blair *et al.*, 2001b). Its structure and functions are as described for *PRKAG1*.

The effect of the C-allele of rs8961 was higher on LVM (23.8 g) in the R92W<sub>TNNI2</sub> group relative to the A797T<sub>MYH7</sub> group. Also, its effect was higher in the R403W<sub>MYH7</sub> group compared to the A797T<sub>MYH7</sub> group: 3.25 mm for mIVST, 3.23 mm for mLVWT and 24 mm for the CWT score. The effect of the G-allele of rs6464170 was higher on mIVST (3.09 mm) in the R92W<sub>TNNI2</sub> group compared to the A797T<sub>MYH7</sub> group. The effect of the G-allele of rs13240743 was lower in the R92W<sub>TNNI2</sub> group relative to the A797T<sub>MYH7</sub> group: 15.4 g for LVM, 0.77 mm for mPWT, 13.3 for

the CWT score and 0.83 for PC1. In addition, its effect was lower in the R92W<sub>TNNT2</sub> group compared to the R403W<sub>MYH7</sub> group: 44.7 g for LVM, 3.63 mm for mIVST and 3.30 mm for mLVWT. The results suggest that the extent to which the SNPs modify hypertrophy development in the current cohort is significantly influenced by the founder mutation context. The literature showed a marginal association of rs6464170 with colon cancer (Slattery *et al.*, 2010). However, none of the variants have been linked to hypertrophy development or evaluated on a functional level.

Statistically significant haplotype effects and significant differences in haplotype effects amongst the founder mutation groups, which did not reflect the significant SNP effects, were observed, therefore suggesting that the trait variance can be ascribed to the combined effects of variants contained within the respective haplotypes. The effect of the CACC haplotype was an estimated increase of 1.48 mm in mIVST. The effect of the TGGG haplotype was an estimated decrease of 2.03 mm in mLVWT. The effect of the CGCC haplotype was higher on LVM (42.6 g) in the R403W<sub>MYH7</sub> group relative to the A797T<sub>MYH7</sub> group. Also, its effect was higher in the R92W<sub>TNNT2</sub> group compared to the A797T<sub>MYH7</sub> group: 57.3 g for LVM, 4.4 mm for mIVST, 3.76 mm for mLVWT, 30.1 for the CWT score and 1.88 for PC1. The effect of the CGCG haplotype was lower in the R92W<sub>TNNT2</sub> group compared to the R403W<sub>MYH7</sub> group: 90 g for LVM, 7.6 mm for mIVST, 7.6mm for mLVWT, 92.3 for the CWT score and 5.77 for PC1. Furthermore, its effect was lower in the R92W<sub>TNNT2</sub> group relative to the A797T<sub>MYH7</sub> group: 1.72 mm for mPWT and 0.68 for PC1. The effect of the CGGC haplotype was lower on mIVST (7.3 mm) in the R92W<sub>TNNT2</sub> group than the A797T<sub>MYH7</sub> group. The effect of the TAGC haplotype was lower in the R403W<sub>MYH7</sub> group compared to the A797T<sub>MYH7</sub> group: 7.4 mm for mIVST and 7.18mm for mLVWT. The significant effects of haplotypes CGCC, CGCG, CGGC and TAGC are thus the result of the combined effects of variants contained within the respective haplotypes, which are further significantly influenced by the founder mutation context.

#### g) *PRKAG3*

Similar to *PRKAG1* and *PRKAG2* genes, *PRKAG3* encodes the  $\gamma 3$  non-catalytic, regulatory subunit of AMPK.

A significant haplotype effect was observed in the absence of significant SNP effects, suggesting that the effects may be due to the combined effects of variants contained within the haplotype. The

effect of the TT haplotype was seemingly cardioprotective as an estimated decrease of 13.4 g in LVM. The haplotype comprises rs1000935 and rs16859382 found to be in complete LD which each other ( $D' = 1.00$ ). Both SNPs are intronic and the relevant *in silico* predictions were performed to determine the potential effects thereof on mRNA splicing (<http://www.ncbi.nlm.nih.gov/SNP>, SNPbrowser<sup>TM</sup> v.4.0.1). However, Netgene2 comparisons did not reveal any differences in splice signal motifs amongst the two alleles (Brunak *et al.*, 1991; Hebsgaard *et al.*, 1996).

The results suggest that the alleles interact to modify hypertrophy development by altering mRNA splicing (or an as yet unknown mechanism for rs16859382) or that they are in LD with interacting effect alleles. According to the SNPbrowser<sup>TM</sup> v.4.0.1 software, a total of four coding, non-synonymous variants are in LD with the investigated SNPs namely rs34720726 (GCT → GTT; A482V), rs33985460 (CGG → TGG; R340W), rs35050588 (CTG → GTG; L153V) and rs692243 (CCA → GCA; P71A). The effects of the amino acid substitutions on the function of relevant proteins were predicted using the SIFT algorithm and all, but one substitution was predicted to be tolerated (Kumar *et al.*, 2009). The rs33985460 missense mutation is characterised as a change from the basic polar Arginine (Arg) to the neutral, slightly polar Tryptophan (Trp) (CGG → TGG; R340W) which may affect the tertiary protein structure and so protein interactions. The afore-described SNP and mutations have to date not been characterized functionally or implicated in the development of disease.

#### 4.6 Optimal selection

We identified a set of six variants that together explained most of the variation in hypertrophy in the current cohort. We estimated that an individual carrying all of the risk alleles for these variants would have a 5.7 higher PC1 measure compared to an individual with none of the risk alleles. However, neither of these individuals existed in our study group. The highest number of risk alleles carried by a single individual in the current cohort was eleven, observed for a single NC individual, whose mLVT of >12mm placed him in a clinically affected category within an HCM family in the absence of knowledge of his mutation status. Second to this, a total of ten risk alleles were observed in each of five MC individuals. The average effect per allele on PC1 was 0.475 for our set of polymorphisms; an MC individual harbouring ten risk alleles is therefore predicted to have a PC1 4.75 points higher.

## 4.7 Future studies

The current explorative study forms part of a larger research effort aimed at identifying genetic modifiers of hypertrophy in HCM within a South African cohort. It succeeded in identifying a modifying role, in many instances for the first time, for each of the candidate genes investigated with the exception of *PRKAG1*. It is, therefore clear that sarcomeric genes and genes relating to myocardial energetics influence the development of hypertrophy within the present study population and it may also do so in other HCM and hypertrophy cohorts. Table 4.1 provides a priority list of genes for future studies under the following headings: number of associations between multiple SNPs and a trait, number of haplotype and trait associations and number of SNP/haplotype associations with multiple SNPs. Each 'x' corresponds to an association identified per criteria. We chose to group and prioritize the results in this way so as to ascertain the degree to which individual genes are involved in hypertrophy development i.e. whether they showed fairly consistent effects with significant results for all four of the tests of association performed or marginal effects with significance in only some instances. For example, a gene that showed significant associations for all tests should be prioritized above a gene that indicated a single significant single SNP result with only one trait.

**Table 4.1 Priority list of genes for future studies**

Candidate gene	Number of associations between multiple SNPs and a trait	Number of haplotype and trait associations	Number of SNP/haplotype associations with multiple traits
<b>Thin filament components</b>			
<i>ACTC1</i>	-	xx	-
<i>TNNT2</i>	-	xxxx	x
<i>TNNI3</i>	-	xxxx	x
<i>TPM1</i>	xxx	xxxxxxxxxxxxx	xxxx
<i>ACTN3</i>	-	x	-
<b>Thick filament components</b>			
<i>MYL3</i>	-	xxxxxx	xx
<i>MYH7</i>	-	xx	xx
<i>MYL2</i>	-	xx	xx
<b>Intermediate filament component</b>			
<i>MYBPC3</i>	x	xxxxxxx	xx

Candidate gene	Number of associations between multiple SNPs and a trait	Number of haplotype and trait associations	Number of SNP/haplotype associations with multiple traits
<b>Fatty acid metabolism components</b>			
<i>CD36</i>	-	xxxxxxx	xxx
<i>CPT1B</i>	-	xxxxxxxxx	xx
<i>PPARA</i>	-	xxxxxxxxx	xx
<i>PPARG</i>	-	xxxxxxxxxxx	xxx
<i>PGCIA</i>	-	xxxxxxxxx	xx
<b>Glucose metabolism components</b>			
<i>ALDOA</i>	-	xx	x
<i>PFKM</i>	-	xxxxxxxxxxx	xxxxxxx
<i>PDK4</i>	-	xxxxx	xx
<b>Creatine kinase energy shuttle components</b>			
<i>CKM</i>	-	xxxxxxxxxxx	xxxx
<i>CKB</i>	-	xxx	-
<b>Cellular energy homeostasis</b>			
<i>PRKAA1</i>	xxx	xx	xx
<i>PRKAA2</i>	-	x	-
<i>PRKAB1</i>	-	xxx	-
<i>PRKAB2</i>	-	-	-
<i>PRKAG1</i>	-	-	-
<i>PRKAG2</i>	xxxxx	xxxxxxxxxxxxxxxxx	xxxxx
<i>PRKAG3</i>	-	x	-

**Abbreviations:** *ACTC1*-Actin, alpha, cardiac muscle 1; *ACTN3*-Actinin, alpha 3; *ALDOA*-Aldolase A, fructose-bisphosphate; *CD36*-CD36 antigen, thrombospondin receptor; *CKB*-Creatine kinase, brain; *CKM*-Creatine kinase, muscle; *CTP1B*- Carnitine palmitoyltransferase 1B, muscle; *MYBPC3*-Myosin binding protein C, cardiac; *MYH7*-Myosin heavy chain 7, cardiac muscle, beta; *MYL2*-Myosin light chain 2, regulatory cardiac, slow; *MYL3*-Myosin light chain 3, alkali, ventricular, skeletal slow; *PDK4*-Pyruvate dehydrogenase kinase, isozyme 4; *PFKM*-Phosphofructokinase, muscle; *SNP*-single nucleotide polymorphism; *TNNI3*-Troponin I type 3, cardiac; *TNNT2*-Troponin T type 2, cardiac; *TPMI*-Tropomyosin 1; *PPARA*-Peroxisome proliferator-activated receptor alpha; *PPARG*-Peroxisome proliferator-activated receptor gamma; *PGCIA*-Peroxisome proliferator-activated receptor gamma, coactivator 1 alpha; *PRKAA1*-Protein kinase, AMP-activated, alpha 1 catalytic subunit; *PRKAA2*-Protein kinase, AMP-activated, alpha 2 catalytic subunit; *PRKAB1*-Protein kinase, AMP-activated, beta 1 non-catalytic subunit; *PRKAB2*-Protein kinase, AMP-activated, beta 2 non-catalytic subunit; *PRKAG1*-Protein kinase, AMP-activated, gamma 1 non-catalytic subunit; *PRKAG2*-Protein kinase, AMP-activated gamma 2 non-catalytic subunit; *PRKAG3*-Protein kinase, AMP-activated, gamma 3 non-catalytic subunit

The modifying capacity of the single SNPs and haplotypes that indicated significant effects should now be corroborated by means of association studies in larger study populations from different origins. In addition, the single SNPs and coding non-synonymous variants with which they are in LD should be prioritised for functional studies based on their predicted functional significance.

Such investigations should, where relevant (i.e. in the presence of significant differences in effect amongst the founder mutation groups), extend to the evaluation of SNP effect in combination with individual founder mutations, that is as proposed, the influence of compensatory mechanisms secondary to the effect of the causal mutations. According to the SNPbrowser™ v.4.0.1 software, all SNPs in LD with the investigated variants were limited to either intronic or coding sequences. However, the possibility that the significantly associated variants could be in LD with SNPs in the promoter and/or other regulatory sequences cannot be excluded and may become apparent with the continuous updating of current LD maps. Functional evaluations with respect to significant haplotype effects are most complicated as it reflects the combined effects of variants contained within the respective haplotypes i.e. it may include any and all alleles within the haplotype. Again, the variants within the haplotype (and coding non-synonymous variants of predicted functional consequence with which they are in LD) should be prioritised based on proposed functional significance and further investigated in combination with the aim of elucidating the exact effect loci and their precise interrelations on a molecular level. These investigations too should, where applicable, explore the influence of founder mutation and haplotype interaction.

A number of the intronic variants which were evaluated *in silico*, which indicated differences with respect to the recognition of splicing motifs upon comparison of their respective alleles, thereby suggesting that they affect mRNA splicing. There is value in subjecting these variants to further *in silico* evaluations aimed at predicting their eventual effects at protein level. However, the bioinformatic tools currently available for splicing predictions have a number of limitations. Thomassen et al. (2012) describe these shortcomings as a need to improve the sensitivity and specificity with which the likelihood of disrupted splicing is predicted, specifically for variants located outside the acceptor and donor AG and GT sequences; as well as poor prediction of alternatively used mechanisms, particularly with respect to cryptic splice sites (Thomassen *et al.*, 2012). It is, therefore necessary to perform these predictions in conjunction with RNA-based assays. Such analyses were beyond the scope of the current study.

It is important to note that the probands in this study were previously subjected to mutation screening for HCM-causal mutations in the MYBPC3, MYH7, TNNT2 and TNNI3 genes, but carried only one of the founder mutations. The potential, therefore exists that the probands or family members may carry HCM-causing mutations in causal genes other than those screened for. Also, family members may harbour causal mutations in the genes screened that are not present in the



proband. However, it may be considered unlikely given that the probands are typically worst affected and, therefore, in all probability carry the strongest risk allele(s). The exception would be when a family member carries an HCM-causing mutation and the effects thereof are masked by a protective modifier allele(s). Short of screening the entire cohort, future studies should address this issue by subjecting the most severely affected mutation carriers to mutation screening for those HCM-causing genes included in the current study. If, upon screening, additional mutations are identified, family members should undergo relevant screening to determine their carrier-status.

As described in Section 1.2.1, *TNNC* is an HCM susceptibility gene and we therefore considered it as candidate modifier of hypertrophy development. However, according to the SNPbrowser<sup>TM</sup> v.4.0.1 software none of the *TNNC* SNPs characterised, to date, met our SNP selection criteria; i.e., the software indicated the presence of only one TaqMan validated SNP, rs2070914, which had an insufficient heterozygosity value (equal to 0 in both the YRI and CEU populations) for use in statistical analysis of transmission disequilibrium. Screening of our cohort for mutations in the *TNNC* gene is currently being performed as part of a novel study in our laboratory. The gene could therefore be revisited as a potential modifier pending the outcome of the aforementioned study and/or the continuous updating of LD maps.

As mentioned, amongst others, significant results were identified for the *CKM* and *PDK4* genes. It is thus of interest to evaluate whether genotypes correlate with the relevant enzyme concentrations and/or activity levels. The recruitment of patients for blood sample collection, which would allow for determination of their relevant CK and pyruvate measures, is currently being performed. However, this is an ongoing effort as patient recall is challenging. In addition, these tests are not currently done in our laboratory and blood assays are performed by commercial pathology laboratories at considerable cost. This aspect of the study will, therefore, be concluded as a future aim.

## 4.8 Conclusion

The study, performed as a hypothesis-generating investigation, identified sarcomeric modifiers of hypertrophy within a South African cohort of HCM families. The extent of the identified modifying effects can be described as substantial considering that overt hypertrophy is defined as an mLVWT of 35 mm or more in adults and that the diagnostic cut-off value in HCM pedigrees is an mLVWT

of 11 mm. For example, the smallest of the effects is a 0.24 mm decrease in the mPWT measure (after adjusting for all the relevant confounders), owing to the T-allele of the rs7260463 *CKM* variant. Therefore, the heart of a G/G homozygous individual will be nearly 0.5 mm thicker relative to that of a T/T homozygous individual, if all other factors are equal. This effect size may appear modest, but it should be considered within the context of complex disease that is the cumulative and synergistic result of many smaller effects. In contrast, the largest significant difference in effect pertaining to the LVM measure was seen for the *CKM* gene haplotype TTGA. It indicated a 120.3 g lower effect on LVM in R92W<sub>TNNT2</sub> group compared to the R403W<sub>MYH7</sub> group. This example clearly illustrates the sizeable variation in the risk of developing LVH owing to the compound effect of the modifier and the individual founder mutations.

As discussed, the therapeutic correction of primary HCM-causing mutations is challenging. The significant results observed for sarcomeric genes may, for the moment, improve only the understanding of genotype/phenotype relationships and potentially patient risk stratification and choice of treatment, e.g. whether the risk-profile of a given patient warrants implantation of an ICD or whether drug intervention would be sufficient. The significant results observed for the genes relating to myocardial energetics may also hold promise for metabolic modulation of disease. However, much functional research, as described in the foregoing future studies section, is required.

## THESIS REFERENCES

[http://www.genedx.com/site/hypertrophic\\_cardiomyopathy\\_and\\_its\\_genetics](http://www.genedx.com/site/hypertrophic_cardiomyopathy_and_its_genetics)

[http://www.biologycorner.com/APbiology/cellular/notes\\_cellular\\_respiration.html](http://www.biologycorner.com/APbiology/cellular/notes_cellular_respiration.html)

<http://www.asecho.org/quidelines.php>

[http://www.med.yale.edu/.../aortic\\_regurgitation.html](http://www.med.yale.edu/.../aortic_regurgitation.html)

<http://www.pubmed.gov>

<http://www.genecards.org/cgi-bin/carddisp.pl?gene=ACTN3&search=actn3>

<http://www.ncbi.nlm.nih.gov/SNP>

<http://www.elmhurst.edu/~chm/vchembook/561aminostructure.html>

[www3.appliedbiosystems.com/cms/groups/mcb\\_marketing/documents/generaldocuments/cms\\_040597.pdf](http://www3.appliedbiosystems.com/cms/groups/mcb_marketing/documents/generaldocuments/cms_040597.pdf)

Abecasis GR, Cardon LR, & Cookson WO (2000). A general test of association for quantitative traits in nuclear families. *Am J Hum Genet* **66**, 279-292.

Abozguia K, Elliott P, McKenna W, Phan TT, Nallur-Shivu G, Ahmed I, Maher AR, Kaur K, Taylor J, Henning A, Ashrafian H, Watkins H, & Frenneaux M (2010). Metabolic modulator perhexiline corrects energy deficiency and improves exercise capacity in symptomatic hypertrophic cardiomyopathy. *Circulation* **122**, 1562-1569.

Abraham MR, Selivanov VA, Hodgson DM, Pucar D, Zingman LV, Wieringa B, Dzeja PP, Alekseev AE, & Terzic A (2002). Coupling of cell energetics with membrane metabolic sensing. Integrative signaling through creatine kinase phosphotransfer disrupted by M-CK gene knock-out. *J Biol Chem* **277**, 24427-24434.

Adams TD, Yanowitz FG, Fisher AG, Ridges JD, Nelson AG, Hagan AD, Williams RR, & Hunt SC (1985). Heritability of cardiac size: an echocardiographic and electrocardiographic study of monozygotic and dizygotic twins. *Circulation* **71**, 39-44.

Akey J, Jin L, & Xiong M (2001). Haplotypes vs single marker linkage disequilibrium tests: what do we gain? *Eur J Hum Genet* **9**, 291-300.

Alcalai R, Seidman JG, & Seidman CE (2008). Genetic basis of hypertrophic cardiomyopathy: from bench to the clinics. *J Cardiovasc Electrophysiol* **19**, 104-110.

Alexander DH, Novembre J, & Lange K (2009). Fast model-based estimation of ancestry in unrelated individuals. *Genome Res* **19**, 1655-1664.

Alves ML, Gaffin RD, & Wolska BM (2010). Rescue of familial cardiomyopathies by modifications at the level of sarcomere and Ca<sup>2+</sup> fluxes. *J Mol Cell Cardiol* **48**, 834-842.

An D, Kewalramani G, Qi D, Pulinilkunnil T, Ghosh S, Abrahani A, Wambolt R, Allard M, Innis SM, & Rodrigues B (2005). beta-Agonist stimulation produces changes in cardiac AMPK and coronary lumen LPL only during increased workload. *Am J Physiol Endocrinol Metab* **288**, E1120-E1127.

Anan R, Greve G, Thierfelder L, Watkins H, McKenna WJ, Solomon S, Vecchio C, Shono H, Nakao S, Tanaka H, & . (1994). Prognostic implications of novel beta cardiac myosin heavy chain gene mutations that cause familial hypertrophic cardiomyopathy. *J Clin Invest* **93**, 280-285.

Andersen PS, Havndrup O, Bundgaard H, Moolman-Smook JC, Larsen LA, Mogensen J, Brink PA, Borglum AD, Corfield VA, Kjeldsen K, Vuust J, & Christiansen M (2001). Myosin light chain mutations in familial hypertrophic cardiomyopathy: phenotypic presentation and frequency in Danish and South African populations. *J Med Genet* **38**, E43.

Andersen PS, Hedley PL, Page SP, Syrris P, Moolman-Smook JC, McKenna WJ, Elliott PM, & Christiansen M (2012). A Novel Myosin Essential Light Chain Mutation Causes Hypertrophic Cardiomyopathy with Late Onset and Low Expressivity. *Biochemistry Research International* **2012**.

Anderson PA, Greig A, Mark TM, Malouf NN, Oakeley AE, Ungerleider RM, Allen PD, & Kay BK (1995). Molecular basis of human cardiac troponin T isoforms expressed in the developing, adult, and failing heart. *Circ Res* **76**, 681-686.

Arad M, Maron BJ, Gorham JM, Johnson WH, Jr., Saul JP, Perez-Atayde AR, Spirito P, Wright GB, Kanter RJ, Seidman CE, & Seidman JG (2005). Glycogen storage diseases presenting as hypertrophic cardiomyopathy. *N Engl J Med* **352**, 362-372.

Arany Z, Novikov M, Chin S, Ma Y, Rosenzweig A, & Spiegelman BM (2006). Transverse aortic constriction leads to accelerated heart failure in mice lacking PPAR-gamma coactivator 1alpha. *Proc Natl Acad Sci U S A* **103**, 10086-10091.

Aras O & Dilsizian V (2007). The role and regulation of CD36 for fatty acid imaging of the heart: implications in diabetes mellitus and chronic kidney disease. *J Nucl Cardiol* **14**, S110-S117.

Ardlie KG, Kruglyak L, & Seielstad M (2002). Patterns of linkage disequilibrium in the human genome. *Nat Rev Genet* **3**, 299-309.

Asaka M, Nagase K, & Alpert E (1983). Biochemical and clinical studies of aldolase isozymes in human cancer. *Isozymes Curr Top Biol Med Res* **11**, 183-195.

Asakawa M, Takano H, Nagai T, Uozumi H, Hasegawa H, Kubota N, Saito T, Masuda Y, Kadowaki T, & Komuro I (2002). Peroxisome proliferator-activated receptor gamma plays a critical role in inhibition of cardiac hypertrophy in vitro and in vivo. *Circulation* **105**, 1240-1246.

Ashby B, Frieden C, & Bischoff R (1979). Immunofluorescent and histochemical localization of AMP deaminase in skeletal muscle. *J Cell Biol* **81**, 361-373.

Ashrafian H, McKenna WJ, & Watkins H (2011). Disease pathways and novel therapeutic targets in hypertrophic cardiomyopathy. *Circ Res* **109**, 86-96.

Ashrafian H, Redwood C, Blair E, & Watkins H (2003). Hypertrophic cardiomyopathy: a paradigm for myocardial energy depletion. *Trends Genet* **19**, 263-268.

Atkinson B & Therneau T (2008). Kinship: mixed-effects Cox models, sparse matrices, and modeling data from large pedigrees. *R package Version 1.1.1*.

Au Y (2004). The muscle ultrastructure: a structural perspective of the sarcomere. *Cell Mol Life Sci* **61**, 3016-3033.

Baars HF, Smagt JJ, & Doevendans P (2010). *Clinical Cardiogenetics* Springer.

Barger PM, Brandt JM, Leone TC, Weinheimer CJ, & Kelly DP (2000). Deactivation of peroxisome proliferator-activated receptor-alpha during cardiac hypertrophic growth. *J Clin Invest* **105**, 1723-1730.

Barrett JC, Fry B, Maller J, & Daly MJ (2005). Haploview: analysis and visualization of LD and haplotype maps. *Bioinformatics* **21**, 263-265.

Barroso I, Gurnell M, Crowley VE, Agostini M, Schwabe JW, Soos MA, Maslen GL, Williams TD, Lewis H, Schafer AJ, Chatterjee VK, & O'Rahilly S (1999). Dominant negative mutations in human PPARgamma associated with severe insulin resistance, diabetes mellitus and hypertension. *Nature* **402**, 880-883.

Bauml MA & Underwood DA (2010). Left ventricular hypertrophy: an overlooked cardiovascular risk factor. *Cleve Clin J Med* **77**, 381-387.

Berman Y & North KN (2010). A gene for speed: the emerging role of alpha-actinin-3 in muscle metabolism. *Physiology (Bethesda)* **25**, 250-259.

Bertola LD, Ott EB, Griepsma S, Vonk FJ, & Bagowski CP (2008). Developmental expression of the alpha-skeletal actin gene. *BMC Evol Biol* **8**, 166.

Berul CI, McConnell BK, Wakimoto H, Moskowitz IP, Maguire CT, Semsarian C, Vargas MM, Gehrman J, Seidman CE, & Seidman JG (2001). Ventricular arrhythmia vulnerability in cardiomyopathic mice with homozygous mutant Myosin-binding protein C gene. *Circulation* **104**, 2734-2739.

- Bessman SP & Geiger PJ (1981). Transport of energy in muscle: the phosphorylcreatine shuttle. *Science* **211**, 448-452.
- Biesiadecki BJ & Jin JP (2002). Exon skipping in cardiac troponin T of turkeys with inherited dilated cardiomyopathy. *J Biol Chem* **277**, 18459-18468.
- Biesiadecki BJ, Schneider KL, Yu ZB, Chong SM, & Jin JP (2004). An R111C polymorphism in wild turkey cardiac troponin I accompanying the dilated cardiomyopathy-related abnormal splicing variant of cardiac troponin T with potentially compensatory effects. *J Biol Chem* **279**, 13825-13832.
- Blair E, Price SJ, Baty CJ, Ostman-Smith I, & Watkins H (2001a). Mutations in cis can confound genotype-phenotype correlations in hypertrophic cardiomyopathy. *J Med Genet* **38**, 385-388.
- Blair E, Redwood C, Ashrafian H, Oliveira M, Broxholme J, Kerr B, Salmon A, Ostman-Smith I, & Watkins H (2001b). Mutations in the gamma(2) subunit of AMP-activated protein kinase cause familial hypertrophic cardiomyopathy: evidence for the central role of energy compromise in disease pathogenesis. *Hum Mol Genet* **10**, 1215-1220.
- Blair E, Redwood C, de Jesus OM, Moolman-Smook JC, Brink P, Corfield VA, Ostman-Smith I, & Watkins H (2002). Mutations of the light meromyosin domain of the beta-myosin heavy chain rod in hypertrophic cardiomyopathy. *Circ Res* **90**, 263-269.
- Bonne G, Carrier L, Richard P, Hainque B, & Schwartz K (1998). Familial hypertrophic cardiomyopathy: from mutations to functional defects. *Circ Res* **83**, 580-593.
- Bos JM, Ommen SR, & Ackerman MJ (2007). Genetics of hypertrophic cardiomyopathy: one, two, or more diseases? *Curr Opin Cardiol* **22**, 193-199.
- Bos JM, Towbin JA, & Ackerman MJ (2009). Diagnostic, prognostic, and therapeutic implications of genetic testing for hypertrophic cardiomyopathy. *J Am Coll Cardiol* **54**, 201-211.
- Bosse Y, Pascot A, Dumont M, Brochu M, Prud'homme D, Bergeron J, Despres JP, & Vohl MC (2002). Influences of the PPAR alpha-L162V polymorphism on plasma HDL(2)-cholesterol response of abdominally obese men treated with gemfibrozil. *Genet Med* **4**, 311-315.
- Bowker-Kinley MM, Davis WI, Wu P, Harris RA, & Popov KM (1998). Evidence for existence of tissue-specific regulation of the mammalian pyruvate dehydrogenase complex. *Biochem J* **329** ( Pt 1), 191-196.
- Bray NJ, Buckland PR, Owen MJ, & O'Donovan MC (2003). Cis-acting variation in the expression of a high proportion of genes in human brain. *Hum Genet* **113**, 149-153.
- Brunak S, Engelbrecht J, & Knudsen S (1991). Prediction of human mRNA donor and acceptor sites from the DNA sequence. *J Mol Biol* **220**, 49-65.

- Cambronero F, Marin F, Roldan V, Hernandez-Romero D, Valdes M, & Lip GY (2009). Biomarkers of pathophysiology in hypertrophic cardiomyopathy: implications for clinical management and prognosis. *Eur Heart J* **30**, 139-151.
- Campbell H & Rudan I (2002). Interpretation of genetic association studies in complex disease. *Pharmacogenomics J* **2**, 349-360.
- Cardon LR & Bell JI (2001). Association study designs for complex diseases. *Nat Rev Genet* **2**, 91-99.
- Cardon LR & Palmer LJ (2003). Population stratification and spurious allelic association. *Lancet* **361**, 598-604.
- Carrier L, Bonne G, Bahrend E, Yu B, Richard P, Niel F, Hainque B, Cruaud C, Gary F, Labeit S, Bouhour JB, Dubourg O, Desnos M, Hagege AA, Trent RJ, Komajda M, Fiszman M, & Schwartz K (1997). Organization and sequence of human cardiac myosin binding protein C gene (MYBPC3) and identification of mutations predicted to produce truncated proteins in familial hypertrophic cardiomyopathy. *Circ Res* **80**, 427-434.
- Carstens N. The role of renin-angiotensin-aldosterone system (RAAS) genes in the development of hypertrophy in hypertrophic cardiomyopathy (HCM). 2009. University of Stellenbosch.  
Ref Type: Thesis/Dissertation
- Chapelle JP (1999). Cardiac troponin I and troponin T: recent players in the field of myocardial markers. *Clin Chem Lab Med* **37**, 11-20.
- Chen SH, Li YM, Yu CH, & Jiang LL (2007). [The association of Val227Ala polymorphism of the peroxisome proliferator activated receptor alpha (PPAR alpha) gene with non-alcoholic fatty liver disease]. *Zhonghua Gan Zang Bing Za Zhi* **15**, 64-65.
- Chen SN, Rodriguez G, Czernuszewicz G, Jin UH, Jin J, & Marian AJ (2010). Abstract 21194: TRIM63, Encoding MuRF1, is a Novel Gene for Human Hypertrophic Cardiomyopathy. *Circulation* **122**, A21194.
- Chung MW, Tsoutsman T, & Semsarian C (2003). Hypertrophic cardiomyopathy: from gene defect to clinical disease. *Cell Res* **13**, 9-20.
- Clark KA, McElhinny AS, Beckerle MC, & Gregorio CC (2002). Striated muscle cytoarchitecture: an intricate web of form and function. *Annu Rev Cell Dev Biol* **18**, 637-706.
- Colhoun HM, McKeigue PM, & Davey SG (2003). Problems of reporting genetic associations with complex outcomes. *Lancet* **361**, 865-872.
- Collins A, Lau W, & De La Vega FM (2004). Mapping genes for common diseases: the case for genetic (LD) maps. *Hum Hered* **58**, 2-9.

- Colson BA, Locher MR, Bekyarova T, Patel JR, Fitzsimons DP, Irving TC, & Moss RL (2010). Differential roles of regulatory light chain and myosin binding protein-C phosphorylations in the modulation of cardiac force development. *J Physiol* **588**, 981-993.
- Corfield VA, Moolman JC, Martell R, & Brink PA (1993). Polymerase chain reaction-based detection of MN blood group-specific sequences in the human genome. *Transfusion* **33**, 119-124.
- Cresci S (2007). Pharmacogenetics of the PPAR genes and cardiovascular disease. *Pharmacogenomics* **8**, 1581-1595.
- Crilley JG, Boehm EA, Blair E, Rajagopalan B, Blamire AM, Styles P, McKenna WJ, Ostman-Smith I, Clarke K, & Watkins H (2003). Hypertrophic cardiomyopathy due to sarcomeric gene mutations is characterized by impaired energy metabolism irrespective of the degree of hypertrophy. *J Am Coll Cardiol* **41**, 1776-1782.
- Crute BE, Seefeld K, Gamble J, Kemp BE, & Witters LA (1998). Functional domains of the alpha1 catalytic subunit of the AMP-activated protein kinase. *J Biol Chem* **273**, 35347-35354.
- Da Poian AT, El-Bacha T, & Luz MR (2010). Nutrient Utilization in Humans: Metabolism Pathways. *Nature Education* **3**, 11.
- Dahlof B, Devereux RB, Kjeldsen SE, Julius S, Beevers G, de FU, Fyhrquist F, Ibsen H, Kristiansson K, Lederballe-Pedersen O, Lindholm LH, Nieminen MS, Omvik P, Oparil S, & Wedel H (2002). Cardiovascular morbidity and mortality in the Losartan Intervention For Endpoint reduction in hypertension study (LIFE): a randomised trial against atenolol. *Lancet* **359**, 995-1003.
- Dalloz F, Osinska H, & Robbins J (2001). [Genetically modified animal models in cardiovascular research]. *Rev Esp Cardiol* **54**, 764-789.
- Daly MJ, Rioux JD, Schaffner SF, Hudson TJ, & Lander ES (2001). High-resolution haplotype structure in the human genome. *Nat Genet* **29**, 229-232.
- Dausse E, Komajda M, Fetler L, Dubourg O, Dufour C, Carrier L, Wisniewsky C, Bercovici J, Hengstenberg C, al-Mahdawi S, & . (1993). Familial hypertrophic cardiomyopathy. Microsatellite haplotyping and identification of a hot spot for mutations in the beta-myosin heavy chain gene. *J Clin Invest* **92**, 2807-2813.
- Davies SP, Hawley SA, Woods A, Carling D, Haystead TA, & Hardie DG (1994). Purification of the AMP-activated protein kinase on ATP-gamma-sepharose and analysis of its subunit structure. *Eur J Biochem* **223**, 351-357.
- Daw EW, Lu Y, Marian AJ, & Shete S (2008). Identifying modifier loci in existing genome scan data. *Ann Hum Genet* **72**, 670-675.



- de Bakker PI, Burtt NP, Graham RR, Guiducci C, Yelensky R, Drake JA, Bersaglieri T, Penney KL, Butler J, Young S, Onofrio RC, Lyon HN, Stram DO, Haiman CA, Freedman ML, Zhu X, Cooper R, Groop L, Kolonel LN, Henderson BE, Daly MJ, Hirschhorn JN, & Altshuler D (2006). Transferability of tag SNPs in genetic association studies in multiple populations. *Nat Genet* **38**, 1298-1303.
- De La Vega FM (2007). Selecting single-nucleotide polymorphisms for association studies with SNPbrowser software. *Methods Mol Biol* **376**, 177-193.
- De La Vega FM, Isaac HI, & Scafe CR (2006). A tool for selecting SNPs for association studies based on observed linkage disequilibrium patterns. *Pac Symp Biocomput* 487-498.
- de Wit E, Delport W, Rugamika CE, Meintjes A, Moller M, van Helden PD, Seoighe C, & Hoal EG (2010). Genome-wide analysis of the structure of the South African Coloured Population in the Western Cape. *Hum Genet* **128**, 145-153.
- Debold EP, Schmitt JP, Patlak JB, Beck SE, Moore JR, Seidman JG, Seidman C, & Warshaw DM (2007). Hypertrophic and dilated cardiomyopathy mutations differentially affect the molecular force generation of mouse alpha-cardiac myosin in the laser trap assay. *Am J Physiol Heart Circ Physiol* **293**, H284-H291.
- Demo EM, Skrzynia C, & Baxter S (2009). Genetic counseling and testing for hypertrophic cardiomyopathy: the pediatric perspective. *J Cardiovasc Transl Res* **2**, 500-507.
- Desvergne B & Wahli W (1999). Peroxisome proliferator-activated receptors: nuclear control of metabolism. *Endocr Rev* **20**, 649-688.
- Devereux RB, Wachtell K, Gerds E, Boman K, Nieminen MS, Papademetriou V, Rokkedal J, Harris K, Aurup P, & Dahlöf B (2004). Prognostic significance of left ventricular mass change during treatment of hypertension. *JAMA* **292**, 2350-2356.
- Dhandapany PS, Sadayappan S, Xue Y, Powell GT, Rani DS, Nallari P, Rai TS, Khullar M, Soares P, Bahl A, Tharkan JM, Vaideeswar P, Rathinavel A, Narasimhan C, Ayapati DR, Ayub Q, Mehdi SQ, Oppenheimer S, Richards MB, Price AL, Patterson N, Reich D, Singh L, Tyler-Smith C, & Thangaraj K (2009). A common MYBPC3 (cardiac myosin binding protein C) variant associated with cardiomyopathies in South Asia. *Nat Genet* **41**, 187-191.
- Dolinsky VW & Dyck JR (2006). Role of AMP-activated protein kinase in healthy and diseased hearts. *Am J Physiol Heart Circ Physiol* **291**, H2557-H2569.
- Doring F, Onur S, Kurbitz C, Boulay MR, Perusse L, Rankinen T, Rauramaa R, Wolfarth B, & Bouchard C (2011). Single nucleotide polymorphisms in the myostatin (MSTN) and muscle creatine kinase (CKM) genes are not associated with elite endurance performance. *Scand J Med Sci Sports* **21**, 841-845.
- dos Remedios CG, Chhabra D, Kekic M, Dedova IV, Tsubakihara M, Berry DA, & Nosworthy NJ (2003). Actin binding proteins: regulation of cytoskeletal microfilaments. *Physiol Rev* **83**, 433-473.

- Duan SZ, Ivashchenko CY, Russell MW, Milstone DS, & Mortensen RM (2005). Cardiomyocyte-specific knockout and agonist of peroxisome proliferator-activated receptor-gamma both induce cardiac hypertrophy in mice. *Circ Res* **97**, 372-379.
- Dunaway GA, Kasten TP, Sebo T, & Trapp R (1988a). Analysis of the phosphofructokinase subunits and isoenzymes in human tissues. *Biochem J* **251**, 677-683.
- Dunaway GA, Kasten TP, Sebo T, & Trapp R (1988b). Analysis of the phosphofructokinase subunits and isoenzymes in human tissues. *Biochem J* **251**, 677-683.
- Dyck JR & Lopaschuk GD (2006). AMPK alterations in cardiac physiology and pathology: enemy or ally? *J Physiol* **574**, 95-112.
- Epstein ND, Cohn GM, Cyran F, & Fananapazir L (1992). Differences in clinical expression of hypertrophic cardiomyopathy associated with two distinct mutations in the beta-myosin heavy chain gene. A 908Leu----Val mutation and a 403Arg----Gln mutation. *Circulation* **86**, 345-352.
- Erdmann J, Daehmlow S, Wischke S, Senyuva M, Werner U, Raible J, Tanis N, Dyachenko S, Hummel M, Hetzer R, & Regitz-Zagrosek V (2003). Mutation spectrum in a large cohort of unrelated consecutive patients with hypertrophic cardiomyopathy. *Clin Genet* **64**, 339-349.
- Fananapazir L & Epstein ND (1994). Genotype-phenotype correlations in hypertrophic cardiomyopathy. Insights provided by comparisons of kindreds with distinct and identical beta-myosin heavy chain gene mutations. *Circulation* **89**, 22-32.
- Fatkin D, Christe ME, Aristizabal O, McConnell BK, Srinivasan S, Schoen FJ, Seidman CE, Turnbull DH, & Seidman JG (1999). Neonatal cardiomyopathy in mice homozygous for the Arg403Gln mutation in the alpha cardiac myosin heavy chain gene. *J Clin Invest* **103**, 147-153.
- Feige JN, Gelman L, Michalik L, Desvergne B, & Wahli W (2006). From molecular action to physiological outputs: peroxisome proliferator-activated receptors are nuclear receptors at the crossroads of key cellular functions. *Prog Lipid Res* **45**, 120-159.
- Ferrantini C, Belus A, Piroddi N, Scellini B, Tesi C, & Poggesi C (2009). Mechanical and energetic consequences of HCM-causing mutations. *J Cardiovasc Transl Res* **2**, 441-451.
- Filatov VL, Katrukha AG, Bulargina TV, & Gusev NB (1999). Troponin: structure, properties, and mechanism of functioning. *Biochemistry (Mosc )* **64**, 969-985.
- Finck BN (2007). The PPAR regulatory system in cardiac physiology and disease. *Cardiovasc Res* **73**, 269-277.

Finck BN, Lehman JJ, Leone TC, Welch MJ, Bennett MJ, Kovacs A, Han X, Gross RW, Kozak R, Lopaschuk GD, & Kelly DP (2002). The cardiac phenotype induced by PPARalpha overexpression mimics that caused by diabetes mellitus. *J Clin Invest* **109**, 121-130.

Flashman E, Redwood C, Moolman-Smook J, & Watkins H (2004). Cardiac myosin binding protein C: its role in physiology and disease. *Circ Res* **94**, 1279-1289.

Flavigny J, Richard P, Isnard R, Carrier L, Charron P, Bonne G, Forissier JF, Desnos M, Dubourg O, Komajda M, Schwartz K, & Hainque B (1998). Identification of two novel mutations in the ventricular regulatory myosin light chain gene (MYL2) associated with familial and classical forms of hypertrophic cardiomyopathy. *J Mol Med (Berl)* **76**, 208-214.

Fleg JL & Strait J (2012). Age-associated changes in cardiovascular structure and function: a fertile milieu for future disease. *Heart Fail Rev* **17**, 545-554.

Fokstuen S, Munoz A, Melacini P, Iliceto S, Perrot A, Ozcelik C, Jeanrenaud X, Rieubland C, Farr M, Faber L, Sigwart U, Mach F, Lerch R, Antonarakis SE, & Blouin JL (2011). Rapid detection of genetic variants in hypertrophic cardiomyopathy by custom DNA resequencing array in clinical practice. *J Med Genet* **48**, 572-576.

Fowler SJ, Napolitano C, & Priori SG (2009). The genetics of cardiomyopathy: genotyping and genetic counseling. *Curr Treat Options Cardiovasc Med* **11**, 433-446.

Freydina NA, Shpagina MD, & Podlubnaya ZA (1986). Localization of binding sites of F-protein (phosphofructokinase) on the myosin molecule. *J Muscle Res Cell Motil* **7**, 481-490.

Friedrich FW, Bausero P, Sun Y, Treszl A, Kramer E, Juhr D, Richard P, Wegscheider K, Schwartz K, Brito D, Arbustini E, Waldenstrom A, Isnard R, Komajda M, Eschenhagen T, & Carrier L (2009). A new polymorphism in human calmodulin III gene promoter is a potential modifier gene for familial hypertrophic cardiomyopathy. *Eur Heart J* **30**, 1648-1655.

Furst DO, Vinkemeier U, & Weber K (1992). Mammalian skeletal muscle C-protein: purification from bovine muscle, binding to titin and the characterization of a full-length human cDNA. *J Cell Sci* **102 ( Pt 4)**, 769-778.

Gabr RE, El-Sharkawy AM, Schar M, Weiss RG, & Bottomley PA (2011). High-energy phosphate transfer in human muscle: diffusion of phosphocreatine. *Am J Physiol Cell Physiol* **301**, C234-C241.

Gabriel SB, Schaffner SF, Nguyen H, Moore JM, Roy J, Blumenstiel B, Higgins J, Defelice M, Lochner A, Faggart M, Liu-Cordero SN, Rotimi C, Adeyemo A, Cooper R, Ward R, Lander ES, Daly MJ, & Altshuler D (2002). The structure of haplotype blocks in the human genome. *Science* **296**, 2225-2229.

Garcia M, Pujol A, Ruzo A, Riu E, Ruberte J, Arbos A, Serafin A, Albella B, Feliu JE, & Bosch F (2009). Phosphofructo-1-kinase deficiency leads to a severe cardiac and hematological disorder in addition to skeletal muscle glycolysis. *PLoS Genet* **5**, e1000615.

- Geisterfer-Lowrance AA, Kass S, Tanigawa G, Vosberg HP, McKenna W, Seidman CE, & Seidman JG (1990). A molecular basis for familial hypertrophic cardiomyopathy: a beta cardiac myosin heavy chain gene missense mutation. *Cell* **62**, 999-1006.
- Genin E, Feingold J, & Clerget-Darpoux F (2008). Identifying modifier genes of monogenic disease: strategies and difficulties. *Hum Genet* **124**, 357-368.
- Girolami F, Ho CY, Semsarian C, Baldi M, Will ML, Baldini K, Torricelli F, Yeates L, Cecchi F, Ackerman MJ, & Olivetto I (2010). Clinical features and outcome of hypertrophic cardiomyopathy associated with triple sarcomere protein gene mutations. *J Am Coll Cardiol* **55**, 1444-1453.
- Goldfarb LG, Petersen RB, Tabaton M, Brown P, LeBlanc AC, Montagna P, Cortelli P, Julien J, Vital C, Pendelbury WW, & . (1992). Fatal familial insomnia and familial Creutzfeldt-Jakob disease: disease phenotype determined by a DNA polymorphism. *Science* **258**, 806-808.
- Goldstein DB (2001). Islands of linkage disequilibrium. *Nat Genet* **29**, 109-111.
- Gordon D & Finch SJ (2005). Factors affecting statistical power in the detection of genetic association. *J Clin Invest* **115**, 1408-1418.
- Greenberg MJ, Kazmierczak K, Szczesna-Cordary D, & Moore JR (2010). Cardiomyopathy-linked myosin regulatory light chain mutations disrupt myosin strain-dependent biochemistry. *Proc Natl Acad Sci U S A* **107**, 17403-17408.
- Gunning P, O'Neill G, & Hardeman E (2008). Tropomyosin-based regulation of the actin cytoskeleton in time and space. *Physiol Rev* **88**, 1-35.
- Gwinn DM, Shackelford DB, Egan DF, Mihaylova MM, Mery A, Vasquez DS, Turk BE, & Shaw RJ (2008). AMPK phosphorylation of raptor mediates a metabolic checkpoint. *Mol Cell* **30**, 214-226.
- Hajri T, Ibrahimi A, Coburn CT, Knapp FF, Jr., Kurtz T, Pravenec M, & Abumrad NA (2001). Defective fatty acid uptake in the spontaneously hypertensive rat is a primary determinant of altered glucose metabolism, hyperinsulinemia, and myocardial hypertrophy. *J Biol Chem* **276**, 23661-23666.
- Hall D, Mayosi BM, Rahman TJ, Avery PJ, Watkins HC, & Keavney B (2011). Common variation in the CD36 (fatty acid translocase) gene is associated with left-ventricular mass. *J Hypertens* **29**, 690-695.
- Hance JE, Fu SY, Watkins SC, Beggs AH, & Michalak M (1999). alpha-actinin-2 is a new component of the dystrophin-glycoprotein complex. *Arch Biochem Biophys* **365**, 216-222.
- Handschin C & Spiegelman BM (2008). The role of exercise and PGC1alpha in inflammation and chronic disease. *Nature* **454**, 463-469.

- Hardie DG & Carling D (1997). The AMP-activated protein kinase--fuel gauge of the mammalian cell? *Eur J Biochem* **246**, 259-273.
- Hardie DG, Carling D, & Carlson M (1998). The AMP-activated/SNF1 protein kinase subfamily: metabolic sensors of the eukaryotic cell? *Annu Rev Biochem* **67**, 821-855.
- Hardie DG & Pan DA (2002). Regulation of fatty acid synthesis and oxidation by the AMP-activated protein kinase. *Biochem Soc Trans* **30**, 1064-1070.
- Hardie DG, Scott JW, Pan DA, & Hudson ER (2003). Management of cellular energy by the AMP-activated protein kinase system. *FEBS Lett* **546**, 113-120.
- Harmon CM & Abumrad NA (1993). Binding of sulfosuccinimidyl fatty acids to adipocyte membrane proteins: isolation and amino-terminal sequence of an 88-kD protein implicated in transport of long-chain fatty acids. *J Membr Biol* **133**, 43-49.
- Harris SP, Lyons RG, & Bezold KL (2011). In the thick of it: HCM-causing mutations in myosin binding proteins of the thick filament. *Circ Res* **108**, 751-764.
- Harvey PA & Leinwand LA (2011). The cell biology of disease: cellular mechanisms of cardiomyopathy. *J Cell Biol* **194**, 355-365.
- Hawley SA, Davison M, Woods A, Davies SP, Beri RK, Carling D, & Hardie DG (1996). Characterization of the AMP-activated protein kinase kinase from rat liver and identification of threonine 172 as the major site at which it phosphorylates AMP-activated protein kinase. *J Biol Chem* **271**, 27879-27887.
- He H, Javadpour MM, Latif F, Tardiff JC, & Ingwall JS (2007). R-92L and R-92W mutations in cardiac troponin T lead to distinct energetic phenotypes in intact mouse hearts. *Biophys J* **93**, 1834-1844.
- Hebsgaard SM, Korning PG, Tolstrup N, Engelbrecht J, Rouze P, & Brunak S (1996). Splice site prediction in Arabidopsis thaliana pre-mRNA by combining local and global sequence information. *Nucleic Acids Res* **24**, 3439-3452.
- Hefti MA, Harder BA, Eppenberger HM, & Schaub MC (1997). Signaling pathways in cardiac myocyte hypertrophy. *J Mol Cell Cardiol* **29**, 2873-2892.
- Hernandez OM, Jones M, Guzman G, & Szczesna-Cordary D (2007). Myosin essential light chain in health and disease. *Am J Physiol Heart Circ Physiol* **292**, H1643-H1654.
- Hershberger RE (2010). A glimpse into multigene rare variant genetics: triple mutations in hypertrophic cardiomyopathy. *J Am Coll Cardiol* **55**, 1454-1455.

- Heward JM, Brand OJ, Barrett JC, Carr-Smith JD, Franklyn JA, & Gough SC (2007). Association of PTPN22 haplotypes with Graves' disease. *J Clin Endocrinol Metab* **92**, 685-690.
- Ho CY (2009). Hypertrophic cardiomyopathy: preclinical and early phenotype. *J Cardiovasc Transl Res* **2**, 462-470.
- Ho CY (2010a). Genetics and clinical destiny: improving care in hypertrophic cardiomyopathy. *Circulation* **122**, 2430-2440.
- Ho CY (2010b). Hypertrophic cardiomyopathy. *Heart Fail Clin* **6**, 141-159.
- Ho CY, Lever HM, DeSanctis R, Farver CF, Seidman JG, & Seidman CE (2000). Homozygous mutation in cardiac troponin T: implications for hypertrophic cardiomyopathy. *Circulation* **102**, 1950-1955.
- Horman S, Browne G, Krause U, Patel J, Vertommen D, Bertrand L, Lavoine A, Hue L, Proud C, & Rider M (2002). Activation of AMP-activated protein kinase leads to the phosphorylation of elongation factor 2 and an inhibition of protein synthesis. *Curr Biol* **12**, 1419-1423.
- Hornemann T, Stolz M, & Wallimann T (2000). Isoenzyme-specific interaction of muscle-type creatine kinase with the sarcomeric M-line is mediated by NH(2)-terminal lysine charge-clamps. *J Cell Biol* **149**, 1225-1234.
- Horowitz JD, Chirkov YY, Kennedy JA, & Sverdlov AL (2010). Modulation of myocardial metabolism: an emerging therapeutic principle. *Curr Opin Cardiol* **25**, 329-334.
- Hougs L, Havndrup O, Bundgaard H, Kober L, Vuust J, Larsen LA, Christiansen M, & Andersen PS (2005). One third of Danish hypertrophic cardiomyopathy patients with MYH7 mutations have mutations [corrected] in MYH7 rod region. *Eur J Hum Genet* **13**, 161-165.
- Houten SM, Chegary M, Te BH, Wijnen WJ, Glatz JF, Luiken JJ, Wijburg FA, & Wanders RJ (2009). Pyruvate dehydrogenase kinase 4 expression is synergistically induced by AMP-activated protein kinase and fatty acids. *Cell Mol Life Sci* **66**, 1283-1294.
- Hue L & Rider MH (1987). Role of fructose 2,6-bisphosphate in the control of glycolysis in mammalian tissues. *Biochem J* **245**, 313-324.
- Huss JM & Kelly DP (2005). Mitochondrial energy metabolism in heart failure: a question of balance. *J Clin Invest* **115**, 547-555.
- Ingles J, Doolan A, Chiu C, Seidman J, Seidman C, & Semsarian C (2005). Compound and double mutations in patients with hypertrophic cardiomyopathy: implications for genetic testing and counselling. *J Med Genet* **42**, e59.

Innes BA, McLaughlin MG, Kapuscinski MK, Jacob HJ, & Harrap SB (1998). Independent genetic susceptibility to cardiac hypertrophy in inherited hypertension. *Hypertension* **31**, 741-746.

Inoki K, Zhu T, & Guan KL (2003). TSC2 mediates cellular energy response to control cell growth and survival. *Cell* **115**, 577-590.

Iseli TJ, Walter M, van Denderen BJ, Katsis F, Witters LA, Kemp BE, Michell BJ, & Stapleton D (2005). AMP-activated protein kinase beta subunit tethers alpha and gamma subunits via its C-terminal sequence (186-270). *J Biol Chem* **280**, 13395-13400.

Jagatheesan G, Rajan S, Schulz EM, Ahmed RP, Petrashevskaya N, Schwartz A, Boivin GP, Arteaga GM, Wang T, Wang YG, Ashraf M, Liggett SB, Lorenz J, Solaro RJ, & Wieczorek DF (2009). An internal domain of beta-tropomyosin increases myofilament Ca(2+) sensitivity. *Am J Physiol Heart Circ Physiol* **297**, H181-H190.

Jameel MN & Zhang J (2009). Myocardial energetics in left ventricular hypertrophy. *Curr Cardiol Rev* **5**, 243-250.

Jarvik GP, Hatsukami TS, Carlson C, Richter RJ, Jampsa R, Brophy VH, Margolin S, Rieder M, Nickerson D, Schellenberg GD, Heagerty PJ, & Furlong CE (2003). Paraoxonase activity, but not haplotype utilizing the linkage disequilibrium structure, predicts vascular disease. *Arterioscler Thromb Vasc Biol* **23**, 1465-1471.

Javadpour MM, Tardiff JC, Pinz I, & Ingwall JS (2003). Decreased energetics in murine hearts bearing the R92Q mutation in cardiac troponin T. *J Clin Invest* **112**, 768-775.

Jentarra GM, Rice SG, Olfers S, Saffen D, & Narayanan V (2011). Evidence for population variation in TSC1 and TSC2 gene expression. *BMC Med Genet* **12**, 29.

Jeschke B, Uhl K, Weist B, Schroder D, Meitinger T, Dohlemann C, & Vosberg HP (1998). A high risk phenotype of hypertrophic cardiomyopathy associated with a compound genotype of two mutated beta-myosin heavy chain genes. *Hum Genet* **102**, 299-304.

Jiang C, Ting AT, & Seed B (1998). PPAR-gamma agonists inhibit production of monocyte inflammatory cytokines. *Nature* **391**, 82-86.

Johnson GC, Esposito L, Barratt BJ, Smith AN, Heward J, Di GG, Ueda H, Cordell HJ, Eaves IA, Dudbridge F, Twells RC, Payne F, Hughes W, Nutland S, Stevens H, Carr P, Tuomilehto-Wolf E, Tuomilehto J, Gough SC, Clayton DG, & Todd JA (2001). Haplotype tagging for the identification of common disease genes. *Nat Genet* **29**, 233-237.

Jung WI, Sieverding L, Breuer J, Hoess T, Widmaier S, Schmidt O, Bunse M, van EF, Apitz J, Lutz O, & Dietze GJ (1998). <sup>31</sup>P NMR spectroscopy detects metabolic abnormalities in asymptomatic patients with hypertrophic cardiomyopathy. *Circulation* **97**, 2536-2542.

- Kabaeva ZT, Perrot A, Wolter B, Dietz R, Cardim N, Correia JM, Schulte HD, Aldashev AA, Mirrakhimov MM, & Osterziel KJ (2002). Systematic analysis of the regulatory and essential myosin light chain genes: genetic variants and mutations in hypertrophic cardiomyopathy. *Eur J Hum Genet* **10**, 741-748.
- Kaludercic N, Reggiani C, & Paolocci N (2009). Genes, geography and geometry: the "critical mass" in hypertrophic cardiomyopathy. *J Mol Diagn* **11**, 12-16.
- Kannel WB, Gordon T, Castelli WP, & Margolis JR (1970). Electrocardiographic left ventricular hypertrophy and risk of coronary heart disease. The Framingham study. *Ann Intern Med* **72**, 813-822.
- Kannel WB & Schatzkin A (1985). Sudden death: lessons from subsets in population studies. *J Am Coll Cardiol* **5**, 141B-149B.
- Keren A, Syrris P, & McKenna WJ (2008). Hypertrophic cardiomyopathy: the genetic determinants of clinical disease expression. *Nat Clin Pract Cardiovasc Med* **5**, 158-168.
- Kimura A, Harada H, Park JE, Nishi H, Satoh M, Takahashi M, Hiroi S, Sasaoka T, Ohbuchi N, Nakamura T, Koyanagi T, Hwang TH, Choo JA, Chung KS, Hasegawa A, Nagai R, Okazaki O, Nakamura H, Matsuzaki M, Sakamoto T, Toshima H, Koga Y, Imaizumi T, & Sasazuki T (1997). Mutations in the cardiac troponin I gene associated with hypertrophic cardiomyopathy. *Nat Genet* **16**, 379-382.
- Kodde IF, van der SJ, Smolenski RT, & de Jong JW (2007). Metabolic and genetic regulation of cardiac energy substrate preference. *Comp Biochem Physiol A Mol Integr Physiol* **146**, 26-39.
- Koeck T, Levison B, Hazen SL, Crabb JW, Stuehr DJ, & Aulak KS (2004). Tyrosine nitration impairs mammalian aldolase A activity. *Mol Cell Proteomics* **3**, 548-557.
- Kolwicz SC, Jr. & Tian R (2009). Metabolic therapy at the crossroad: how to optimize myocardial substrate utilization? *Trends Cardiovasc Med* **19**, 201-207.
- Konno T, Chang S, Seidman JG, & Seidman CE (2010). Genetics of hypertrophic cardiomyopathy. *Curr Opin Cardiol*.
- Koren MJ, Devereux RB, Casale PN, Savage DD, & Laragh JH (1991). Relation of left ventricular mass and geometry to morbidity and mortality in uncomplicated essential hypertension. *Ann Intern Med* **114**, 345-352.
- Kraft T, Hornemann T, Stolz M, Nier V, & Wallimann T (2000). Coupling of creatine kinase to glycolytic enzymes at the sarcomeric I-band of skeletal muscle: a biochemical study in situ. *J Muscle Res Cell Motil* **21**, 691-703.
- Kraja AT, Hunt SC, Rao DC, vila-Roman VG, Arnett DK, & Province MA (2011). Genetics of hypertension and cardiovascular disease and their interconnected pathways: lessons from large studies. *Curr Hypertens Rep* **13**, 46-54.



- Kramerova I, Kudryashova E, Wu B, Ottenheijm C, Granzier H, & Spencer MJ (2008). Novel role of calpain-3 in the triad-associated protein complex regulating calcium release in skeletal muscle. *Hum Mol Genet* **17**, 3271-3280.
- Kronert WA, Acebes A, Ferrus A, & Bernstein SI (1999). Specific myosin heavy chain mutations suppress troponin I defects in *Drosophila* muscles. *J Cell Biol* **144**, 989-1000.
- Kudo N, Barr AJ, Barr RL, Desai S, & Lopaschuk GD (1995). High rates of fatty acid oxidation during reperfusion of ischemic hearts are associated with a decrease in malonyl-CoA levels due to an increase in 5'-AMP-activated protein kinase inhibition of acetyl-CoA carboxylase. *J Biol Chem* **270**, 17513-17520.
- Kudo N, Gillespie JG, Kung L, Witters LA, Schulz R, Clanachan AS, & Lopaschuk GD (1996). Characterization of 5'AMP-activated protein kinase activity in the heart and its role in inhibiting acetyl-CoA carboxylase during reperfusion following ischemia. *Biochim Biophys Acta* **1301**, 67-75.
- Kumar P, Henikoff S, & Ng PC (2009). Predicting the effects of coding non-synonymous variants on protein function using the SIFT algorithm. *Nat Protoc* **4**, 1073-1081.
- Kuo TY, Lau W, & Collins AR (2007). LDMAP: the construction of high-resolution linkage disequilibrium maps of the human genome. *Methods Mol Biol* **376**, 47-57.
- Labeit S, Gautel M, Lakey A, & Trinick J (1992). Towards a molecular understanding of titin. *EMBO J* **11**, 1711-1716.
- Laing NG & Nowak KJ (2005). When contractile proteins go bad: the sarcomere and skeletal muscle disease. *Bioessays* **27**, 809-822.
- Lasky-Su J, Lyon HN, Emilsson V, Heid IM, Molony C, Raby BA, Lazarus R, Klanderma B, Soto-Quiros ME, Avila L, Silverman EK, Thorleifsson G, Thorsteinsdottir U, Kronenberg F, Vollmert C, Illig T, Fox CS, Levy D, Laird N, Ding X, McQueen MB, Butler J, Ardlie K, Papoutsakis C, Dedoussis G, O'Donnell CJ, Wichmann HE, Cledon JC, Schadt E, Hirschhorn J, Weiss ST, Stefansson K, & Lange C (2008). On the replication of genetic associations: timing can be everything! *Am J Hum Genet* **82**, 849-858.
- Lawson JW (1987). Hypertrophic cardiomyopathy: current views on etiology, pathophysiology, and management. *Am J Med Sci* **294**, 191-210.
- Lechin M, Quinones MA, Omran A, Hill R, Yu QT, Rakowski H, Wigle D, Liew CC, Sole M, Roberts R, & . (1995). Angiotensin-I converting enzyme genotypes and left ventricular hypertrophy in patients with hypertrophic cardiomyopathy. *Circulation* **92**, 1808-1812.
- Lehman JJ & Kelly DP (2002). Transcriptional activation of energy metabolic switches in the developing and hypertrophied heart. *Clin Exp Pharmacol Physiol* **29**, 339-345.

Lekanne Deprez RH, Muurling-Vlietman JJ, Hruda J, Baars MJ, Wijnaendts LC, Stolte-Dijkstra I, Alders M, & van Hagen JM (2006). Two cases of severe neonatal hypertrophic cardiomyopathy caused by compound heterozygous mutations in the MYBPC3 gene. *J Med Genet* **43**, 829-832.

Levy D, Anderson KM, Savage DD, Balkus SA, Kannel WB, & Castelli WP (1987). Risk of ventricular arrhythmias in left ventricular hypertrophy: the Framingham Heart Study. *Am J Cardiol* **60**, 560-565.

Levy D, Anderson KM, Savage DD, Kannel WB, Christiansen JC, & Castelli WP (1988). Echocardiographically detected left ventricular hypertrophy: prevalence and risk factors. The Framingham Heart Study. *Ann Intern Med* **108**, 7-13.

Levy D, Garrison RJ, Savage DD, Kannel WB, & Castelli WP (1990a). Prognostic implications of echocardiographically determined left ventricular mass in the Framingham Heart Study. *N Engl J Med* **322**, 1561-1566.

Levy D, Labib SB, Anderson KM, Christiansen JC, Kannel WB, & Castelli WP (1990b). Determinants of sensitivity and specificity of electrocardiographic criteria for left ventricular hypertrophy. *Circulation* **81**, 815-820.

Lodi R, Cooper JM, Bradley JL, Manners D, Styles P, Taylor DJ, & Schapira AH (1999). Deficit of in vivo mitochondrial ATP production in patients with Friedreich ataxia. *Proc Natl Acad Sci U S A* **96**, 11492-11495.

Lombardi R, Rodriguez G, Chen SN, Ripplinger CM, Li W, Chen J, Willerson JT, Betocchi S, Wickline SA, Efimov IR, & Marian AJ (2009). Resolution of established cardiac hypertrophy and fibrosis and prevention of systolic dysfunction in a transgenic rabbit model of human cardiomyopathy through thiol-sensitive mechanisms. *Circulation* **119**, 1398-1407.

Lopaschuk GD, Ussher JR, Folmes CD, Jaswal JS, & Stanley WC (2010). Myocardial fatty acid metabolism in health and disease. *Physiol Rev* **90**, 207-258.

Lossie J, Ushakov DS, Ferenczi MA, Werner S, Keller S, Haase H, & Morano I (2012). Mutations of ventricular essential myosin light chain disturb myosin binding and sarcomeric sorting. *Cardiovasc Res* **93**, 390-396.

Loubser O, Marais AD, Kotze MJ, Godenir N, Thiart R, Scholtz CL, de Villiers JN, Hillermann R, Firth JC, Weich HF, Maritz F, Jones S, & van der Westhuyzen DR (1999). Founder mutations in the LDL receptor gene contribute significantly to the familial hypercholesterolemia phenotype in the indigenous South African population of mixed ancestry. *Clin Genet* **55**, 340-345.

Lucas DT, Aryal P, Szweda LI, Koch WJ, & Leinwand LA (2003). Alterations in mitochondrial function in a mouse model of hypertrophic cardiomyopathy. *Am J Physiol Heart Circ Physiol* **284**, H575-H583.

- Luedde M, Fogel U, Knorr M, Grundt C, Hippe HJ, Brors B, Frank D, Haselmann U, Antony C, Voelkers M, Schrader J, Most P, Lemmer B, Katus HA, & Frey N (2009). Decreased contractility due to energy deprivation in a transgenic rat model of hypertrophic cardiomyopathy. *J Mol Med* **87**, 411-422.
- Luiken JJ, Coort SL, Willems J, Coumans WA, Bonen A, van d, V, & Glatz JF (2003). Contraction-induced fatty acid translocase/CD36 translocation in rat cardiac myocytes is mediated through AMP-activated protein kinase signaling. *Diabetes* **52**, 1627-1634.
- Luiken JJ, Niessen HE, Coort SL, Hoebbers N, Coumans WA, Schwenk RW, Bonen A, & Glatz JF (2009). Etomoxir-induced partial carnitine palmitoyltransferase-I (CPT-I) inhibition in vivo does not alter cardiac long-chain fatty acid uptake and oxidation rates. *Biochem J* **419**, 447-455.
- Luo J, Wu S, Liu J, Li Y, Yang H, Kim T, Zhelyabovska O, Ding G, Zhou Y, Yang Y, & Yang Q (2010). Conditional PPARgamma knockout from cardiomyocytes of adult mice impairs myocardial fatty acid utilization and cardiac function. *Am J Transl Res* **3**, 61-72.
- Lutucuta S, Tsybouleva N, Ishiyama M, Defreitas G, Wei L, Carabello B, & Marian AJ (2004). Induction and reversal of cardiac phenotype of human hypertrophic cardiomyopathy mutation cardiac troponin T-Q92 in switch on-switch off bigenic mice. *J Am Coll Cardiol* **44**, 2221-2230.
- Lyczkowski DA, Conant KD, Pulsifer MB, Jarrett DY, Grant PE, Kwiatkowski DJ, & Thiele EA (2007). Intrafamilial phenotypic variability in tuberous sclerosis complex. *J Child Neurol* **22**, 1348-1355.
- Maass AH, Ikeda K, Oberdorf-Maass S, Maier SK, & Leinwand LA (2004). Hypertrophy, fibrosis, and sudden cardiac death in response to pathological stimuli in mice with mutations in cardiac troponin T. *Circulation* **110**, 2102-2109.
- Macarthur DG & North KN (2004). A gene for speed? The evolution and function of alpha-actinin-3. *Bioessays* **26**, 786-795.
- Mamczur P, Dus D, & Dzugaj A (2007). Colocalization of aldolase and FBPase in cytoplasm and nucleus of cardiomyocytes. *Cell Biol Int* **31**, 1122-1130.
- Maniatis N, Collins A, Xu CF, McCarthy LC, Hewett DR, Tapper W, Ennis S, Ke X, & Morton NE (2002). The first linkage disequilibrium (LD) maps: delineation of hot and cold blocks by diplotype analysis. *Proc Natl Acad Sci U S A* **99**, 2228-2233.
- Maniatis N, Morton NE, Gibson J, Xu CF, Hosking LK, & Collins A (2005). The optimal measure of linkage disequilibrium reduces error in association mapping of affection status. *Hum Mol Genet* **14**, 145-153.
- Marian AJ (2002). Modifier genes for hypertrophic cardiomyopathy. *Curr Opin Cardiol* **17**, 242-252.
- Marian AJ (2009). Experimental therapies in hypertrophic cardiomyopathy. *J Cardiovasc Transl Res* **2**, 483-492.

- Marian AJ (2010). Hypertrophic cardiomyopathy: from genetics to treatment. *Eur J Clin Invest* **40**, 360-369.
- Marian AJ & Roberts R (1998). Molecular genetic basis of hypertrophic cardiomyopathy: genetic markers for sudden cardiac death. *J Cardiovasc Electrophysiol* **9**, 88-99.
- Marian AJ, Salek L, & Lutucuta S (2001). Molecular genetics and pathogenesis of hypertrophic cardiomyopathy. *Minerva Med* **92**, 435-451.
- Marian AJ, Senthil V, Chen SN, & Lombardi R (2006). Antifibrotic effects of antioxidant N-acetylcysteine in a mouse model of human hypertrophic cardiomyopathy mutation. *J Am Coll Cardiol* **47**, 827-834.
- Maron BJ (2002). Hypertrophic cardiomyopathy: a systematic review. *JAMA* **287**, 1308-1320.
- Maron BJ, Gardin JM, Flack JM, Gidding SS, Kurosaki TT, & Bild DE (1995). Prevalence of hypertrophic cardiomyopathy in a general population of young adults. Echocardiographic analysis of 4111 subjects in the CARDIA Study. Coronary Artery Risk Development in (Young) Adults. *Circulation* **92**, 785-789.
- Marsin AS, Bertrand L, Rider MH, Deprez J, Beauloye C, Vincent MF, Van den BG, Carling D, & Hue L (2000). Phosphorylation and activation of heart PFK-2 by AMPK has a role in the stimulation of glycolysis during ischaemia. *Curr Biol* **10**, 1247-1255.
- Mathew J, Sleight P, Lonn E, Johnstone D, Pogue J, Yi Q, Bosch J, Sussex B, Probstfield J, & Yusuf S (2001). Reduction of cardiovascular risk by regression of electrocardiographic markers of left ventricular hypertrophy by the angiotensin-converting enzyme inhibitor ramipril. *Circulation* **104**, 1615-1621.
- Mayosi BM, Keavney B, Watkins H, & Farrall M (2003). Measured haplotype analysis of the aldosterone synthase gene and heart size. *Eur J Hum Genet* **11**, 395-401.
- McDonagh TA, Gardner RS, Clark AL, & Dargie H (2011). *Oxford Textbook of Heart Failure* Oxford University Press.
- McGarry JD & Brown NF (1997). The mitochondrial carnitine palmitoyltransferase system. From concept to molecular analysis. *Eur J Biochem* **244**, 1-14.
- McVean G (2007). Linkage Disequilibrium, Recombination and Selection. In *Handbook of Statistical Genetics* pp. 909-944. John Wiley & Sons, Ltd.
- Medin M, Hermida-Prieto M, Monserrat L, Laredo R, Rodriguez-Rey JC, Fernandez X, & Castro-Beiras A (2007). Mutational screening of phospholamban gene in hypertrophic and idiopathic dilated cardiomyopathy and functional study of the PLN -42 C>G mutation. *Eur J Heart Fail* **9**, 37-43.

Mehrabi MR, Thalhammer T, Haslmayer P, Glogar HD, Wieselthaler G, Humpeler S, Marktl W, & Ekmekcioglu C (2002). The peroxisome proliferator-activated receptor gamma (PPARgamma) is highly expressed in human heart ventricles. *Biomed Pharmacother* **56**, 407-410.

Mengi SA & Dhalla NS (2004). Carnitine palmitoyltransferase-I, a new target for the treatment of heart failure: perspectives on a shift in myocardial metabolism as a therapeutic intervention. *Am J Cardiovasc Drugs* **4**, 201-209.

Merante F, Tein I, Benson L, & Robinson BH (1994). Maternally inherited hypertrophic cardiomyopathy due to a novel T-to-C transition at nucleotide 9997 in the mitochondrial tRNA(glycine) gene. *Am J Hum Genet* **55**, 437-446.

Messerli FH, Ventura HO, Elizardi DJ, Dunn FG, & Frohlich ED (1984). Hypertension and sudden death. Increased ventricular ectopic activity in left ventricular hypertrophy. *Am J Med* **77**, 18-22.

Mettikolla P, Calander N, Luchowski R, Gryczynski I, Gryczynski Z, Zhao J, Szczesna-Cordary D, & Borejdo J (2011). Cross-bridge kinetics in myofibrils containing familial hypertrophic cardiomyopathy R58Q mutation in the regulatory light chain of myosin. *J Theor Biol* **284**, 71-81.

Michels M. Hypertrophic Cardiomyopathy: Pathophysiology, Genetics and Invasive Treatment. 2011. [The Author] ; Erasmus University [Host].

Ref Type: Electronic Citation

Miyaoka K, Kuwasako T, Hirano K, Nozaki S, Yamashita S, & Matsuzawa Y (2001). CD36 deficiency associated with insulin resistance. *Lancet* **357**, 686-687.

Mogensen J, Klausen IC, Pedersen AK, Egeblad H, Bross P, Kruse TA, Gregersen N, Hansen PS, Baandrup U, & Borglum AD (1999). Alpha-cardiac actin is a novel disease gene in familial hypertrophic cardiomyopathy. *J Clin Invest* **103**, R39-R43.

Mohiddin SA, Begley DA, McLam E, Cardoso JP, Winkler JB, Sellers JR, & Fananapazir L (2003). Utility of genetic screening in hypertrophic cardiomyopathy: prevalence and significance of novel and double (homozygous and heterozygous) beta-myosin mutations. *Genet Test* **7**, 21-27.

Molkentin JD, Lu JR, Antos CL, Markham B, Richardson J, Robbins J, Grant SR, & Olson EN (1998). A calcineurin-dependent transcriptional pathway for cardiac hypertrophy. *Cell* **93**, 215-228.

Montagna P, Gambetti P, Cortelli P, & Lugaresi E (2003). Familial and sporadic fatal insomnia. *Lancet Neurol* **2**, 167-176.

Moolman JC, Corfield VA, Posen B, Ngumbela K, Seidman C, Brink PA, & Watkins H (1997). Sudden death due to troponin T mutations. *J Am Coll Cardiol* **29**, 549-555.

- Moon SS, Lee JE, Lee YS, Kim SW, Jeoung NH, Lee IK, & Kim JG (2012). Association of pyruvate dehydrogenase kinase 4 gene polymorphisms with type 2 diabetes and metabolic syndrome. *Diabetes Res Clin Pract* **95**, 230-236.
- Moss RL, Swinford AE, & Greaser ML (1983). Alterations in the Ca<sup>2+</sup> sensitivity of tension development by single skeletal muscle fibers at stretched lengths. *Biophys J* **43**, 115-119.
- Mukherjea P, Tong L, Seidman JG, Seidman CE, & Hitchcock-DeGregori SE (1999). Altered regulatory function of two familial hypertrophic cardiomyopathy troponin T mutants. *Biochemistry* **38**, 13296-13301.
- Musumeci O, Bruno C, Mongini T, Rodolico C, Aguenouz M, Barca E, Amati A, Cassandrini D, Serlenga L, Vita G, & Toscano A (2011). Clinical features and new molecular findings in muscle phosphofructokinase deficiency (GSD type VII). *Neuromuscul Disord*.
- Nabel EG (2003). Cardiovascular disease. *N Engl J Med* **349**, 60-72.
- Nahrendorf M, Spindler M, Hu K, Bauer L, Ritter O, Nordbeck P, Quaschnig T, Hiller KH, Wallis J, Ertl G, Bauer WR, & Neubauer S (2005). Creatine kinase knockout mice show left ventricular hypertrophy and dilatation, but unaltered remodeling post-myocardial infarction. *Cardiovasc Res* **65**, 419-427.
- Naimi B, Harrison A, Cummins M, Nongthomba U, Clark S, Canal I, Ferrus A, & Sparrow JC (2001). A tropomyosin-2 mutation suppresses a troponin I myopathy in *Drosophila*. *Mol Biol Cell* **12**, 1529-1539.
- Nakao S, Takenaka T, Maeda M, Kodama C, Tanaka A, Tahara M, Yoshida A, Kuriyama M, Hayashibe H, Sakuraba H, & . (1995). An atypical variant of Fabry's disease in men with left ventricular hypertrophy. *N Engl J Med* **333**, 288-293.
- Neitzel H (1986). A routine method for the establishment of permanent growing lymphoblastoid cell lines. *Hum Genet* **73**, 320-326.
- Newman MA & University of Pittsburgh (2008). *mTOR signaling pathway associated with skeletal muscle hypertrophy following resistance exercise training* University of Pittsburgh.
- Newton-Cheh C & Hirschhorn JN (2005). Genetic association studies of complex traits: design and analysis issues. *Mutat Res* **573**, 54-69.
- North KN & Beggs AH (1996). Deficiency of a skeletal muscle isoform of alpha-actinin (alpha-actinin-3) in merosin-positive congenital muscular dystrophy. *Neuromuscul Disord* **6**, 229-235.
- Offer G, Starr R, & Trinick J (1988). Phosphofructokinase: a component of the thick filament? *Adv Exp Med Biol* **226**, 61-73.

Okamoto F, Tanaka T, Sohmiya K, & Kawamura K (1998). CD36 abnormality and impaired myocardial long-chain fatty acid uptake in patients with hypertrophic cardiomyopathy. *Jpn Circ J* **62**, 499-504.

Okin PM, Devereux RB, Jern S, Kjeldsen SE, Julius S, & Dahlöf B (2000). Baseline characteristics in relation to electrocardiographic left ventricular hypertrophy in hypertensive patients: the Losartan intervention for endpoint reduction (LIFE) in hypertension study. The Life Study Investigators. *Hypertension* **36**, 766-773.

Okin PM, Devereux RB, Jern S, Kjeldsen SE, Julius S, Nieminen MS, Snapinn S, Harris KE, Aurup P, Edelman JM, Wedel H, Lindholm LH, & Dahlöf B (2004). Regression of electrocardiographic left ventricular hypertrophy during antihypertensive treatment and the prediction of major cardiovascular events. *JAMA* **292**, 2343-2349.

Oliveira SM, Ehtisham J, Redwood CS, Ostman-Smith I, Blair EM, & Watkins H (2003). Mutation analysis of AMP-activated protein kinase subunits in inherited cardiomyopathies: implications for kinase function and disease pathogenesis. *J Mol Cell Cardiol* **35**, 1251-1255.

Olson EN & Williams RS (2000). Remodeling muscles with calcineurin. *Bioessays* **22**, 510-519.

Palmiter KA, Tyska MJ, Haerberle JR, Alpert NR, Fananapazir L, & Warshaw DM (2000). R403Q and L908V mutant beta-cardiac myosin from patients with familial hypertrophic cardiomyopathy exhibit enhanced mechanical performance at the single molecule level. *J Muscle Res Cell Motil* **21**, 609-620.

Pang T, Xiong B, Li JY, Qiu BY, Jin GZ, Shen JK, & Li J (2007). Conserved alpha-helix acts as autoinhibitory sequence in AMP-activated protein kinase alpha subunits. *J Biol Chem* **282**, 495-506.

Paschou P, Drineas P, Lewis J, Nievergelt CM, Nickerson DA, Smith JD, Ridker PM, Chasman DI, Krauss RM, & Ziv E (2008). Tracing sub-structure in the European American population with PCA-informative markers. *PLoS Genet* **4**, e1000114.

Patel MS & Roche TE (1990). Molecular biology and biochemistry of pyruvate dehydrogenase complexes. *FASEB J* **4**, 3224-3233.

Patel R, Lim DS, Reddy D, Nagueh SF, Lutucuta S, Sole MJ, Zoghbi WA, Quinones MA, Roberts R, & Marian AJ (2000). Variants of trophic factors and expression of cardiac hypertrophy in patients with hypertrophic cardiomyopathy. *J Mol Cell Cardiol* **32**, 2369-2377.

Patel R, Nagueh SF, Tsybouleva N, Abdellatif M, Lutucuta S, Kopelen HA, Quinones MA, Zoghbi WA, Entman ML, Roberts R, & Marian AJ (2001). Simvastatin induces regression of cardiac hypertrophy and fibrosis and improves cardiac function in a transgenic rabbit model of human hypertrophic cardiomyopathy. *Circulation* **104**, 317-324.

Patil N, Berno AJ, Hinds DA, Barrett WA, Doshi JM, Hacker CR, Kautzer CR, Lee DH, Marjoribanks C, McDonough DP, Nguyen BT, Norris MC, Sheehan JB, Shen N, Stern D, Stokowski RP, Thomas DJ, Trulsson

MO, Vyas KR, Frazer KA, Fodor SP, & Cox DR (2001). Blocks of limited haplotype diversity revealed by high-resolution scanning of human chromosome 21. *Science* **294**, 1719-1723.

Pilia G, Chen WM, Scuteri A, Orru M, Albai G, Dei M, Lai S, Usala G, Lai M, Loi P, Mameli C, Vacca L, Deiana M, Olla N, Masala M, Cao A, Najjar SS, Terracciano A, Nedorezov T, Sharov A, Zonderman AB, Abecasis GR, Costa P, Lakatta E, & Schlessinger D (2006). Heritability of cardiovascular and personality traits in 6,148 Sardinians. *PLoS Genet* **2**, e132.

Pittman AM, Myers AJ, bou-Sleiman P, Fung HC, Kaleem M, Marlowe L, Duckworth J, Leung D, Williams D, Kilford L, Thomas N, Morris CM, Dickson D, Wood NW, Hardy J, Lees AJ, & de SR (2005). Linkage disequilibrium fine mapping and haplotype association analysis of the tau gene in progressive supranuclear palsy and corticobasal degeneration. *J Med Genet* **42**, 837-846.

Planavila A, Laguna JC, & Vazquez-Carrera M (2005). Nuclear factor-kappaB activation leads to down-regulation of fatty acid oxidation during cardiac hypertrophy. *J Biol Chem* **280**, 17464-17471.

Poetter K, Jiang H, Hassanzadeh S, Master SR, Chang A, Dalakas MC, Rayment I, Sellers JR, Fananapazir L, & Epstein ND (1996). Mutations in either the essential or regulatory light chains of myosin are associated with a rare myopathy in human heart and skeletal muscle. *Nat Genet* **13**, 63-69.

Polekhina G, Gupta A, Michell BJ, van DB, Murthy S, Feil SC, Jennings IG, Campbell DJ, Witters LA, Parker MW, Kemp BE, & Stapleton D (2003). AMPK beta subunit targets metabolic stress sensing to glycogen. *Curr Biol* **13**, 867-871.

Posen BM, Moolman JC, Corfield VA, & Brink PA (1995). Clinical and prognostic evaluation of familial hypertrophic cardiomyopathy in two South African families with different cardiac beta myosin heavy chain gene mutations. *Br Heart J* **74**, 40-46.

Prado A, Canal I, Barbas JA, Molloy J, & Ferrus A (1995). Functional recovery of troponin I in a *Drosophila* heldup mutant after a second site mutation. *Mol Biol Cell* **6**, 1433-1441.

Pravenec M, Churchill PC, Churchill MC, Viklicky O, Kazdova L, Aitman TJ, Petretto E, Hubner N, Wallace CA, Zimdahl H, Zidek V, Landa V, Dunbar J, Bidani A, Griffin K, Qi N, Maxova M, Kren V, Mlejnek P, Wang J, & Kurtz TW (2008). Identification of renal Cd36 as a determinant of blood pressure and risk for hypertension. *Nat Genet* **40**, 952-954.

Price AL, Zaitlen NA, Reich D, & Patterson N (2010). New approaches to population stratification in genome-wide association studies. *Nat Rev Genet* **11**, 459-463.

Puccio H & Koenig M (2000). Recent advances in the molecular pathogenesis of Friedreich ataxia. *Hum Mol Genet* **9**, 887-892.

Puigserver P, Wu Z, Park CW, Graves R, Wright M, & Spiegelman BM (1998). A cold-inducible coactivator of nuclear receptors linked to adaptive thermogenesis. *Cell* **92**, 829-839.



- Puntmann VO, Jahnke C, Gebker R, Schnackenburg B, Fox KF, Fleck E, & Paetsch I (2010). Usefulness of magnetic resonance imaging to distinguish hypertensive and hypertrophic cardiomyopathy. *Am J Cardiol* **106**, 1016-1022.
- Pyle WG & Solaro RJ (2004). At the crossroads of myocardial signaling: the role of Z-discs in intracellular signaling and cardiac function. *Circ Res* **94**, 296-305.
- Rakus D, Mamczur P, Gizak A, Dus D, & Dzugaj A (2003). Colocalization of muscle FBPase and muscle aldolase on both sides of the Z-line. *Biochem Biophys Res Commun* **311**, 294-299.
- Randle PJ (1986). Fuel selection in animals. *Biochem Soc Trans* **14**, 799-806.
- Rao DC & Gu CC (2008). *Genetic dissection of complex traits* Academic Press.
- Redwood CS, Moolman-Smook JC, & Watkins H (1999). Properties of mutant contractile proteins that cause hypertrophic cardiomyopathy. *Cardiovasc Res* **44**, 20-36.
- Reinhard W, Stark K, Sedlacek K, Fischer M, Baessler A, Neureuther K, Weber S, Kaess B, Wiedmann S, Mitsching S, Lieb W, Erdmann J, Meisinger C, Doering A, Tolle R, Jeron A, Riegger G, & Hengstenberg C (2008). Association between PPARalpha gene polymorphisms and myocardial infarction. *Clin Sci (Lond)* **115**, 301-308.
- Ren J, Pulakat L, Whaley-Connell A, & Sowers JR (2010). Mitochondrial biogenesis in the metabolic syndrome and cardiovascular disease. *J Mol Med* **88**, 993-1001.
- Richard P, Isnard R, Carrier L, Dubourg O, Donatien Y, Mathieu B, Bonne G, Gary F, Charron P, Hagege M, Komajda M, Schwartz K, & Hainque B (1999). Double heterozygosity for mutations in the beta-myosin heavy chain and in the cardiac myosin binding protein C genes in a family with hypertrophic cardiomyopathy. *J Med Genet* **36**, 542-545.
- Robitaille J, Brouillette C, Houde A, Lemieux S, Perusse L, Tchernof A, Gaudet D, & Vohl MC (2004). Association between the PPARalpha-L162V polymorphism and components of the metabolic syndrome. *J Hum Genet* **49**, 482-489.
- Roche TE, Baker JC, Yan X, Hiromasa Y, Gong X, Peng T, Dong J, Turkan A, & Kasten SA (2001). Distinct regulatory properties of pyruvate dehydrogenase kinase and phosphatase isoforms. *Prog Nucleic Acid Res Mol Biol* **70**, 33-75.
- Roman MJ, Okin PM, Kizer JR, Lee ET, Howard BV, & Devereux RB (2010). Relations of central and brachial blood pressure to left ventricular hypertrophy and geometry: the Strong Heart Study. *J Hypertens* **28**, 384-388.
- Rothman KJ (1990). No adjustments are needed for multiple comparisons. *Epidemiology* **1**, 43-46.

Rowe GC, Jiang A, & Arany Z (2010). PGC-1 coactivators in cardiac development and disease. *Circ Res* **107**, 825-838.

Russell RR, III, Bergeron R, Shulman GI, & Young LH (1999). Translocation of myocardial GLUT-4 and increased glucose uptake through activation of AMPK by AICAR. *Am J Physiol* **277**, H643-H649.

Rutter WJ (1964). Evolution of Aldolase. *Fed Proc* **23**, 1248-1257.

Saba MM, Ibrahim MM, & Rizk HH (2001). Gender and the relationship between resting heart rate and left ventricular geometry. *J Hypertens* **19**, 367-373.

Sack MN, Disch DL, Rockman HA, & Kelly DP (1997). A role for Sp and nuclear receptor transcription factors in a cardiac hypertrophic growth program. *Proc Natl Acad Sci U S A* **94**, 6438-6443.

Sakai S, Miyauchi T, Irukayama-Tomobe Y, Ogata T, Goto K, & Yamaguchi I (2002). Peroxisome proliferator-activated receptor-gamma activators inhibit endothelin-1-related cardiac hypertrophy in rats. *Clin Sci (Lond)* **103 Suppl 48**, 16S-20S.

Schaid DJ, Rowland CM, Tines DE, Jacobson RM, & Poland GA (2002). Score tests for association between traits and haplotypes when linkage phase is ambiguous. *Am J Hum Genet* **70**, 425-434.

Schaub MC, Hefti MA, Zuellig RA, & Morano I (1998). Modulation of contractility in human cardiac hypertrophy by myosin essential light chain isoforms. *Cardiovasc Res* **37**, 381-404.

Scheffold T, Waldmuller S, & Borisov K (2011). A case of familial hypertrophic cardiomyopathy emphasizes the importance of parallel screening of multiple disease genes. *Clin Res Cardiol*.

Schillaci G, Verdecchia P, Porcellati C, Cuccurullo O, Cosco C, & Perticone F (2000). Continuous relation between left ventricular mass and cardiovascular risk in essential hypertension. *Hypertension* **35**, 580-586.

Schiller NB, Shah PM, Crawford M, DeMaria A, Devereux R, Feigenbaum H, Gutgesell H, Reichek N, Sahn D, Schnittger I, & . (1989). Recommendations for quantitation of the left ventricle by two-dimensional echocardiography. American Society of Echocardiography Committee on Standards, Subcommittee on Quantitation of Two-Dimensional Echocardiograms. *J Am Soc Echocardiogr* **2**, 358-367.

Schunkert H, Hense HW, Holmer SR, Stender M, Perz S, Keil U, Lorell BH, & Riegger GA (1994). Association between a deletion polymorphism of the angiotensin-converting-enzyme gene and left ventricular hypertrophy. *N Engl J Med* **330**, 1634-1638.

Schwenk RW, Luiken JJ, Bonen A, & Glatz JF (2008). Regulation of sarcolemmal glucose and fatty acid transporters in cardiac disease. *Cardiovasc Res* **79**, 249-258.

- Scolletta S & Biagioli B (2010). Energetic myocardial metabolism and oxidative stress: let's make them our friends in the fight against heart failure. *Biomed Pharmacother* **64**, 203-207.
- Scott JW, Hawley SA, Green KA, Anis M, Stewart G, Scullion GA, Norman DG, & Hardie DG (2004). CBS domains form energy-sensing modules whose binding of adenosine ligands is disrupted by disease mutations. *J Clin Invest* **113**, 274-284.
- Sebkhi A, Zhao L, Lu L, Haley CS, Nunez DJ, & Wilkins MR (1999). Genetic determination of cardiac mass in normotensive rats: results from an F344xWKY cross. *Hypertension* **33**, 949-953.
- Seidman CE & Seidman JG (2011). Identifying sarcomere gene mutations in hypertrophic cardiomyopathy: a personal history. *Circ Res* **108**, 743-750.
- Seidman JG & Seidman C (2001). The genetic basis for cardiomyopathy: from mutation identification to mechanistic paradigms. *Cell* **104**, 557-567.
- Semsarian C, Healey MJ, Fatkin D, Giewat M, Duffy C, Seidman CE, & Seidman JG (2001). A polymorphic modifier gene alters the hypertrophic response in a murine model of familial hypertrophic cardiomyopathy. *J Mol Cell Cardiol* **33**, 2055-2060.
- Senthil V, Chen SN, Tsybouleva N, Halder T, Nagueh SF, Willerson JT, Roberts R, & Marian AJ (2005). Prevention of cardiac hypertrophy by atorvastatin in a transgenic rabbit model of human hypertrophic cardiomyopathy. *Circ Res* **97**, 285-292.
- Shastry BS (2007). SNPs in disease gene mapping, medicinal drug development and evolution. *J Hum Genet* **52**, 871-880.
- Sherwood L (2004). *Human physiology: from cells to systems* Thomson/Brooks/Cole.
- Sipola P, Magga J, Husso M, Jaaskelainen P, Peuhkurinen K, & Kuusisto J (2011). Cardiac MRI assessed left ventricular hypertrophy in differentiating hypertensive heart disease from hypertrophic cardiomyopathy attributable to a sarcomeric gene mutation. *Eur Radiol* **21**, 1383-1389.
- Slattery ML, Herrick JS, Lundgreen A, Fitzpatrick FA, Curtin K, & Wolff RK (2010). Genetic variation in a metabolic signaling pathway and colon and rectal cancer risk: mTOR, PTEN, STK11, RPKAA1, PRKAG2, TSC1, TSC2, PI3K and Akt1. *Carcinogenesis* **31**, 1604-1611.
- Sobel E & Lange K (1996). Descent graphs in pedigree analysis: applications to haplotyping, location scores, and marker-sharing statistics. *Am J Hum Genet* **58**, 1323-1337.
- Soor GS, Luk A, Ahn E, Abraham JR, Woo A, Ralph-Edwards A, & Butany J (2009). Hypertrophic cardiomyopathy: current understanding and treatment objectives. *J Clin Pathol* **62**, 226-235.

Soranzo N, Spector TD, Mangino M, Kuhnel B, Rendon A, Teumer A, Willenborg C, Wright B, Chen L, Li M, Salo P, Voight BF, Burns P, Laskowski RA, Xue Y, Menzel S, Altshuler D, Bradley JR, Bumpstead S, Burnett MS, Devaney J, Doring A, Elosua R, Epstein SE, Erber W, Falchi M, Garner SF, Ghorji MJ, Goodall AH, Gwilliam R, Hakonarson HH, Hall AS, Hammond N, Hengstenberg C, Illig T, Konig IR, Knouff CW, McPherson R, Melander O, Mooser V, Nauck M, Nieminen MS, O'Donnell CJ, Peltonen L, Potter SC, Prokisch H, Rader DJ, Rice CM, Roberts R, Salomaa V, Sambrook J, Schreiber S, Schunkert H, Schwartz SM, Serbanovic-Canic J, Sinisalo J, Siscovick DS, Stark K, Surakka I, Stephens J, Thompson JR, Volker U, Volzke H, Watkins NA, Wells GA, Wichmann HE, Van Heel DA, Tyler-Smith C, Thein SL, Kathiresan S, Perola M, Reilly MP, Stewart AF, Erdmann J, Samani NJ, Meisinger C, Greinacher A, Deloukas P, Ouwehand WH, & Gieger C (2009). A genome-wide meta-analysis identifies 22 loci associated with eight hematological parameters in the HaemGen consortium. *Nat Genet* **41**, 1182-1190.

Southam L, Rodriguez-Lopez J, Wilkins JM, Pombo-Suarez M, Snelling S, Gomez-Reino JJ, Chapman K, Gonzalez A, & Loughlin J (2007). An SNP in the 5'-UTR of GDF5 is associated with osteoarthritis susceptibility in Europeans and with in vivo differences in allelic expression in articular cartilage. *Hum Mol Genet* **16**, 2226-2232.

Spindler M, Saupe KW, Christe ME, Sweeney HL, Seidman CE, Seidman JG, & Ingwall JS (1998). Diastolic dysfunction and altered energetics in the alphaMHC403/+ mouse model of familial hypertrophic cardiomyopathy. *J Clin Invest* **101**, 1775-1783.

Spirito P & Maron BJ (1989). Relation between extent of left ventricular hypertrophy and age in hypertrophic cardiomyopathy. *J Am Coll Cardiol* **13**, 820-823.

Spirito P, Seidman CE, McKenna WJ, & Maron BJ (1997). The management of hypertrophic cardiomyopathy. *N Engl J Med* **336**, 775-785.

Squire JM (1997). Architecture and function in the muscle sarcomere. *Curr Opin Struct Biol* **7**, 247-257.

Steinberg GR & Kemp BE (2009). AMPK in Health and Disease. *Physiol Rev* **89**, 1025-1078.

Swanepoel C. Investigating ligands of cardiac myosin binding protein C (cMyBPC) as potential regulators of contractility and modifiers of hypertrophy. 2010. University of Stellenbosch.  
Ref Type: Thesis/Dissertation

Swoboda KJ, Specht L, Jones HR, Shapiro F, DiMauro S, & Korson M (1997). Infantile phosphofructokinase deficiency with arthrogyposis: clinical benefit of a ketogenic diet. *J Pediatr* **131**, 932-934.

Taberner C, Polo JM, Sevillano MD, Munoz R, Berciano J, Cabello A, Baez B, Ricoy JR, Carpizo R, Figols J, Cuadrado N, & Claveria LE (2000). Fatal familial insomnia: clinical, neuropathological, and genetic description of a Spanish family. *J Neurol Neurosurg Psychiatry* **68**, 774-777.

Takano H, Nagai T, Asakawa M, Toyozaki T, Oka T, Komuro I, Saito T, & Masuda Y (2000). Peroxisome proliferator-activated receptor activators inhibit lipopolysaccharide-induced tumor necrosis factor-alpha expression in neonatal rat cardiac myocytes. *Circ Res* **87**, 596-602.

Takimoto E & Kass DA (2007). Role of oxidative stress in cardiac hypertrophy and remodeling. *Hypertension* **49**, 241-248.

Tardiff JC, Hewett TE, Palmer BM, Olsson C, Factor SM, Moore RL, Robbins J, & Leinwand LA (1999). Cardiac troponin T mutations result in allele-specific phenotypes in a mouse model for hypertrophic cardiomyopathy. *J Clin Invest* **104**, 469-481.

Tarui S, Giichi O, Ikura Y, Tanaka T, Suda M, & Nishikawa M (1965). Phosphofructokinase deficiency in skeletal muscle. A new type of glycogenosis. *Biochemical and Biophysical Research Communications* **19**, 517-523.

Taylor MR, Carniel E, & Mestroni L (2004). Familial hypertrophic cardiomyopathy: clinical features, molecular genetics and molecular genetic testing. *Expert Rev Mol Diagn* **4**, 99-113.

Theis JL, Bos JM, Bartleson VB, Will ML, Binder J, Vatta M, Towbin JA, Gersh BJ, Ommen SR, & Ackerman MJ (2006). Echocardiographic-determined septal morphology in Z-disc hypertrophic cardiomyopathy. *Biochem Biophys Res Commun* **351**, 896-902.

Thierfelder L, Watkins H, MacRae C, Lamas R, McKenna W, Vosberg HP, Seidman JG, & Seidman CE (1994). Alpha-tropomyosin and cardiac troponin T mutations cause familial hypertrophic cardiomyopathy: a disease of the sarcomere. *Cell* **77**, 701-712.

Thomassen M, Blanco A, Montagna M, Hansen TV, Pedersen IS, Gutierrez-Enriquez S, Menendez M, Fachal L, Santamarina M, Steffensen AY, Jonson L, Agata S, Whiley P, Tognazzo S, Tornero E, Jensen UB, Balmana J, Kruse TA, Goldgar DE, Lazaro C, Diez O, Spurdle AB, & Vega A (2012). Characterization of BRCA1 and BRCA2 splicing variants: a collaborative report by ENIGMA consortium members. *Breast Cancer Res Treat* **132**, 1009-1023.

Tsai HJ, Choudhry S, Naqvi M, Rodriguez-Cintron W, Burchard EG, & Ziv E (2005). Comparison of three methods to estimate genetic ancestry and control for stratification in genetic association studies among admixed populations. *Hum Genet* **118**, 424-433.

Tsoutsman T, Bagnall RD, & Semsarian C (2008a). Impact of multiple gene mutations in determining the severity of cardiomyopathy and heart failure. *Clin Exp Pharmacol Physiol* **35**, 1349-1357.

Tsoutsman T, Kelly M, Ng DC, Tan JE, Tu E, Lam L, Bogoyevitch MA, Seidman CE, Seidman JG, & Semsarian C (2008b). Severe heart failure and early mortality in a double-mutation mouse model of familial hypertrophic cardiomyopathy. *Circulation* **117**, 1820-1831.

Tsybouleva N, Zhang L, Chen S, Patel R, Lutucuta S, Nemoto S, Defreitas G, Entman M, Carabello BA, Roberts R, & Marian AJ (2004). Aldosterone, through novel signaling proteins, is a fundamental molecular bridge between the genetic defect and the cardiac phenotype of hypertrophic cardiomyopathy. *Circulation* **109**, 1284-1291.

Turcani M & Rupp H (1997). Etomoxir improves left ventricular performance of pressure-overloaded rat heart. *Circulation* **96**, 3681-3686.

Tuunanen H, Engblom E, Naum A, Nagren K, Hesse B, Airaksinen KE, Nuutila P, Iozzo P, Ukkonen H, Opie LH, & Knuuti J (2006). Free fatty acid depletion acutely decreases cardiac work and efficiency in cardiomyopathic heart failure. *Circulation* **114**, 2130-2137.

Tuunanen H, Kuusisto J, Toikka J, Jaaskelainen P, Marjamaki P, Peuhkurinen K, Viljanen T, Sipola P, Stolen KQ, Hannukainen J, Nuutila P, Laakso M, & Knuuti J (2007). Myocardial perfusion, oxidative metabolism, and free fatty acid uptake in patients with hypertrophic cardiomyopathy attributable to the Asp175Asn mutation in the alpha-tropomyosin gene: a positron emission tomography study. *J Nucl Cardiol* **14**, 354-365.

Tyska MJ, Hayes E, Giewat M, Seidman CE, Seidman JG, & Warshaw DM (2000). Single-molecule mechanics of R403Q cardiac myosin isolated from the mouse model of familial hypertrophic cardiomyopathy. *Circ Res* **86**, 737-744.

Ueno S, Ohki R, Hashimoto T, Takizawa T, Takeuchi K, Yamashita Y, Ota J, Choi YL, Wada T, Koinuma K, Yamamoto K, Ikeda U, Shimada K, & Mano H (2003). DNA microarray analysis of in vivo progression mechanism of heart failure. *Biochem Biophys Res Commun* **307**, 771-777.

Unno K, Isobe S, Izawa H, Cheng XW, Kobayashi M, Hirashiki A, Yamada T, Harada K, Ohshima S, Noda A, Nagata K, Kato K, Yokota M, & Murohara T (2009). Relation of functional and morphological changes in mitochondria to myocardial contractile and relaxation reserves in asymptomatic to mildly symptomatic patients with hypertrophic cardiomyopathy. *Eur Heart J* **30**, 1853-1862.

Ussher JR & Lopaschuk GD (2006). Clinical implications of energetic problems in cardiovascular disease. *Heart Metabolism* **32**, 9-17.

Uys GM. Investigations of the role of myomegalin in the phosphorylation of cardiac myosin binding protein C. 2010. University of Stellenbosch.  
Ref Type: Thesis/Dissertation

van der Leij FR, Cox KB, Jackson VN, Huijckman NC, Bartelds B, Kuipers JR, Dijkhuizen T, Terpstra P, Wood PA, Zammit VA, & Price NT (2002). Structural and functional genomics of the CPT1B gene for muscle-type carnitine palmitoyltransferase I in mammals. *J Biol Chem* **277**, 26994-27005.

Van Driest SL, Vasile VC, Ommen SR, Will ML, Tajik AJ, Gersh BJ, & Ackerman MJ (2004). Myosin binding protein C mutations and compound heterozygosity in hypertrophic cardiomyopathy. *J Am Coll Cardiol* **44**, 1903-1910.

van Slegtenhorst M, de HR, Hermans C, Nellist M, Janssen B, Verhoef S, Lindhout D, van den OA, Halley D, Young J, Burley M, Jeremiah S, Woodward K, Nahmias J, Fox M, Ekong R, Osborne J, Wolfe J, Povey S, Snell RG, Cheadle JP, Jones AC, Tachataki M, Ravine D, Sampson JR, Reeve MP, Richardson P, Wilmer F, Munro C, Hawkins TL, Sepp T, Ali JB, Ward S, Green AJ, Yates JR, Kwiatkowska J, Henske EP, Short

- MP, Haines JH, Jozwiak S, & Kwiatkowski DJ (1997). Identification of the tuberous sclerosis gene TSC1 on chromosome 9q34. *Science* **277**, 805-808.
- Verhaaren HA, Schieken RM, Mosteller M, Hewitt JK, Eaves LJ, & Nance WE (1991). Bivariate genetic analysis of left ventricular mass and weight in pubertal twins (the Medical College of Virginia twin study). *Am J Cardiol* **68**, 661-668.
- Viana R, Towler MC, Pan DA, Carling D, Viollet B, Hardie DG, & Sanz P (2007). A conserved sequence immediately N-terminal to the Bateman domains in AMP-activated protein kinase gamma subunits is required for the interaction with the beta subunits. *J Biol Chem* **282**, 16117-16125.
- Wang P, Zou Y, Fu C, Zhou X, & Hui R (2005). MYBPC3 polymorphism is a modifier for expression of cardiac hypertrophy in patients with hypertrophic cardiomyopathy. *Biochem Biophys Res Commun* **329**, 796-799.
- Watkins H, Ashrafian H, & Redwood C (2011). Inherited cardiomyopathies. *N Engl J Med* **364**, 1643-1656.
- Watkins H, Conner D, Thierfelder L, Jarcho JA, MacRae C, McKenna WJ, Maron BJ, Seidman JG, & Seidman CE (1995a). Mutations in the cardiac myosin binding protein-C gene on chromosome 11 cause familial hypertrophic cardiomyopathy. *Nat Genet* **11**, 434-437.
- Watkins H, McKenna WJ, Thierfelder L, Suk HJ, Anan R, O'Donoghue A, Spirito P, Matsumori A, Moravec CS, Seidman JG, & . (1995b). Mutations in the genes for cardiac troponin T and alpha-tropomyosin in hypertrophic cardiomyopathy. *N Engl J Med* **332**, 1058-1064.
- Watkins H, Rosenzweig A, Hwang DS, Levi T, McKenna W, Seidman CE, & Seidman JG (1992). Characteristics and prognostic implications of myosin missense mutations in familial hypertrophic cardiomyopathy. *N Engl J Med* **326**, 1108-1114.
- Watkins H, Seidman JG, & Seidman CE (1995c). Familial hypertrophic cardiomyopathy: a genetic model of cardiac hypertrophy. *Hum Mol Genet* **4 Spec No**, 1721-1727.
- Wei B, Gao J, Huang XP, & Jin JP (2010). Mutual rescues between two dominant negative mutations in cardiac troponin I and cardiac troponin T. *J Biol Chem* **285**, 27806-27816.
- Weigt C, Schoepper B, & Wegner A (1990). Tropomyosin-troponin complex stabilizes the pointed ends of actin filaments against polymerization and depolymerization. *FEBS Lett* **260**, 266-268.
- Wigginton JE & Abecasis GR (2005). PEDSTATS: descriptive statistics, graphics and quality assessment for gene mapping data. *Bioinformatics* **21**, 3445-3447.
- Wigle ED, Rakowski H, Kimball BP, & Williams WG (1995). Hypertrophic cardiomyopathy. Clinical spectrum and treatment. *Circulation* **92**, 1680-1692.

- Wilding JR, Joubert F, de AC, Fortin D, Novotova M, Veksler V, & Ventura-Clapier R (2006). Altered energy transfer from mitochondria to sarcoplasmic reticulum after cytoarchitectural perturbations in mice hearts. *J Physiol* **575**, 191-200.
- Willard HF & Ginsburg GS (2009). *Essentials of Genomic and Personalized Medicine* Academic.
- Winkelmann BR, Hoffmann MM, Nauck M, Kumar AM, Nandabalan K, Judson RS, Boehm BO, Tall AR, Ruano G, & Marz W (2003). Haplotypes of the cholesteryl ester transfer protein gene predict lipid-modifying response to statin therapy. *Pharmacogenomics J* **3**, 284-296.
- Wolf PA, D'Agostino RB, Belanger AJ, & Kannel WB (1991). Probability of stroke: a risk profile from the Framingham Study. *Stroke* **22**, 312-318.
- Wu B, Wang L, Liu Q, & Luo Q (2012). Myocardial contractile and metabolic properties of familial hypertrophic cardiomyopathy caused by cardiac troponin I gene mutations: a simulation study. *Exp Physiol* **97**, 155-169.
- Wu C, DeWan A, Hoh J, & Wang Z (2011). A comparison of association methods correcting for population stratification in case-control studies. *Ann Hum Genet* **75**, 418-427.
- Xu Q, Dewey S, Nguyen S, & Gomes AV (2010). Malignant and benign mutations in familial cardiomyopathies: insights into mutations linked to complex cardiovascular phenotypes. *J Mol Cell Cardiol* **48**, 899-909.
- Yamazaki N, Shinohara Y, Shima A, Yamanaka Y, & Terada H (1996). Isolation and characterization of cDNA and genomic clones encoding human muscle type carnitine palmitoyltransferase I. *Biochim Biophys Acta* **1307**, 157-161.
- Yang Q & Li Y (2007). Roles of PPARs on regulating myocardial energy and lipid homeostasis. *J Mol Med* **85**, 697-706.
- Young ME, Laws FA, Goodwin GW, & Taegtmeyer H (2001). Reactivation of peroxisome proliferator-activated receptor alpha is associated with contractile dysfunction in hypertrophied rat heart. *J Biol Chem* **276**, 44390-44395.
- Zamorano-Leon JJ, Modrego J, Mateos-Caceres PJ, Macaya C, Martin-Fernandez B, Miana M, de las HN, Cachofeiro V, Lahera V, & Lopez-Farre AJ (2010). A proteomic approach to determine changes in proteins involved in the myocardial metabolism in left ventricles of spontaneously hypertensive rats. *Cell Physiol Biochem* **25**, 347-358.
- Zhang K, Calabrese P, Nordborg M, & Sun F (2002). Haplotype block structure and its applications to association studies: power and study designs. *Am J Hum Genet* **71**, 1386-1394.



Zhang Q, Zhao S, Chen H, Liu X, Zhang L, & Li F (2009). Analysis of the codon use frequency of AMPK family genes from different species. *Mol Biol Rep* **36**, 513-519.

Zhao G, Jeoung NH, Burgess SC, Rosaaen-Stowe KA, Inagaki T, Latif S, Shelton JM, McAnally J, Bassel-Duby R, Harris RA, Richardson JA, & Kliewer SA (2008). Overexpression of pyruvate dehydrogenase kinase 4 in heart perturbs metabolism and exacerbates calcineurin-induced cardiomyopathy. *Am J Physiol Heart Circ Physiol* **294**, H936-H943.

Zhou G, Myers R, Li Y, Chen Y, Shen X, Fenyk-Melody J, Wu M, Ventre J, Doebber T, Fujii N, Musi N, Hirshman MF, Goodyear LJ, & Moller DE (2001). Role of AMP-activated protein kinase in mechanism of metformin action. *J Clin Invest* **108**, 1167-1174.

Zoghbi ME, Woodhead JL, Moss RL, & Craig R (2008). Three-dimensional structure of vertebrate cardiac muscle myosin filaments. *Proc Natl Acad Sci U S A* **105**, 2386-2390.

Zondervan KT & Cardon LR (2004). The complex interplay among factors that influence allelic association. *Nat Rev Genet* **5**, 89-100.

Zong H, Ren JM, Young LH, Pypaert M, Mu J, Birnbaum MJ, & Shulman GI (2002). AMP kinase is required for mitochondrial biogenesis in skeletal muscle in response to chronic energy deprivation. *Proc Natl Acad Sci U S A* **99**, 15983-15987.

Zot AS & Potter JD (1987). Structural aspects of troponin-tropomyosin regulation of skeletal muscle contraction. *Annu Rev Biophys Biophys Chem* **16**, 535-559.

**APPENDIX I****1. DNA EXTRACTION SOLUTIONS****Cell Lysis Buffer**

Sucrose	0.32M
Triton-X-100	1%
MgCl <sub>2</sub>	5mM
Tris-HCl (pH 8)	10mM
Add sterile water to a final volume of 1L	

**3M Sodium Acetate**

NaAc.3H <sub>2</sub> O	40.18g
Sterile water	50ml
Adjust the pH to 5.2 with glacial acetic acid and add sterile water to final volume of 100ml	

**Na-EDTA Solution**

NaCl	18.75ml of 4mM stock solution
EDTA	250ml of 100mM stock solution
Mix well	

**Phenol/Chloroform**

Phenol, saturated with 1X TE	50ml
Chloroform	48ml
8-Hydroxyquinoline	2ml
Mix well and store at 4°C	

**Chloroform/Octanol (24:1)**

Chloroform	96ml
Octanol	4ml
Mix well and store at 4°C	

**10X TE-buffer Stock Solution**

TrisOH	0.1M (pH 8)
EDTA	0.01M (pH 8)
Sterile water	
Mix well	

## 2. ELECTROPHORESIS STOCK SOLUTIONS

### 20X SB Stock Solution

di-Sodium tetraborate decahydrate 38.14g

Add sterile water to a final volume of 1 L

### 1X SB Solution

20X SB solution 50ml

Add sterile water to a final volume of 1 L

## 3. GELS

### 2% Agarose gel

Agarose 2g

SB Buffer (1X) 100ml

Microwave for 1 min on maximum power and add 5 $\mu$ l ethidium bromide (10mg/ml) when temperature of  $\pm 55^{\circ}\text{C}$  is reached

## 4. LOADING DYES

### Ethidium Bromide Stock (10mg/ml)

Ethidium bromide 500mg

Sterile water 50ml

Stir well on magnetic stirrer for 4h and store in dark container at 4 $^{\circ}\text{C}$

### Bromophenol Blue Loading Dye

Bromophenol Blue 0.1% (w/v)

Add sterile water to a final volume of 100ml. Store at 4 $^{\circ}\text{C}$